Defining Innate Immunity to *Clostridium difficile*

Presented by

Nazila Vajhi Jafari

A thesis submitted for the degree of

Doctor of Philosophy to

University College London

January 2012

Infectious Diseases and Microbiology Unit

Institute of Child Health

University College London

DECLARATION

I, Nazila Vajhi Jafari, confirm that the work presented in this thesis is my own. Where information has been derived from other sources, I confirm that this has been indicated in the thesis.

ABSTRACT

Clostridium difficile is a spore-forming anaerobic bacillus and a leading cause of nosocomial diarrhoea. *C. difficile* infection (CDI) occurs often following antibiotic treatment leading to alteration of the gut microbiota enabling *C. difficile* to thrive and cause a range of symptoms from asymptomatic carriage to severe diarrhoea, pseudomembranous colitis (PMC) and death. *C. difficile* virulence is associated with production of toxins (A, B and binary CDT) nonetheless this bacteria harbours an array of other virulence factors. The role of toxins has been well studied by utilising purified/recombinant toxins however it is unknown how the gastrointestinal mucosa responds to bacterial cell.

In the present study, *C. difficile*-mediated innate immunity response was investigated primarily utilising four different *C. difficile* strains including: R20291 a hypervirulent strain (A^+B^+, CDT^+), 630 a fully sequenced strain (A^+B^+) and variant strains M68 and CF5 (A^-B^+). Initial studies showed that under laboratory conditions all strains shared comparable survival and sporulation capacity (in an aerobic environment), whereas strains R20291, M68, and CF5 achieved similar growth kinetics.

Bacterial adherence to human intestinal epithelia cell (IEC) study revealed that strain R20291 adhered significantly to Caco-2 cells compared to other strains. Although an equivalent adherence level was noted with strains 630, M68 and CF5 but it did not correlate with downstream cellular responses. While R20291 was the most potent, 630 and M68 were found to be as cytotoxic, leading to significant cell apoptosis. Furthermore, these strains showed an extensive IEC tight junction disruption leading to paracellular permeability, detected as occludin redistribution, transepithelial electrical resistance (TEER) and FITC-dextran influx. In contrast, strain CF5 had the least effect on cell death, IEC barrier integrity and showed less Rac1 glucosylation when compared with strain M68. Although all four strains induced antimicrobial immunity and pro-inflammatory cytokines, CF5 mediated the least pro-inflammatory responses. Similar findings were also observed in an *ex vivo* model of infection utilising human colonic explants.

Noting the anaerobic nature of *C. difficile*, experiments conducted in an Ussing vertical chamber system showed significant increase in antimicrobial and pro-inflammatory responses and a rapid TEER loss.

C. difficile-mediated dendritic cell (DC) activation established in murine model system demonstrated up-regulation of co-stimulatory molecules leading to a predominant anti-inflammatory IL-10 secretion. Similar results were also detected with human monocyte-derived DCs. Despite a significant IL-10 expression in infected murine DCs, which is known to suppress IL-12 and IL-23 induction, it was detected that *C. difficile* may generate a cytokine milieu that favours dual Th1/Th17 immunity. Moreover, *C. difficile* strains triggered an ASC-containing inflammasome causing the activation of caspase-1 and release of mature IL-1β.

Utilising R20291 and 630 isogenic mutants the role of toxins in murine and human DC function was investigated observing DC activation and cytokine production in a toxin-dependent and independent manner. These findings indicated that multiple bacterial factors may play a role in initiating host innate immune responses to *C. difficile* infection.

ACKNOWLEDGEMENTS

Firstly, I would like to thank Dr. Mona Bajaj-Elliott my primary supervisor, for providing me with the opportunity to pursue research as part of her team and for her support and guidance. I also would like to thank my second supervisor, Dr. Elaine Allan for her help and advice.

I also thank Dr. Lisa Dawson and Dr. Richard Stabler for all their guidance and advice, Prof. Nigel Minton and Dr. Sarah Kuehne for providing me with *C. difficile* isogenic mutant strains and Dr. Bertrand Vernay for carrying out the time-lapse and confocal microscopy.

I am very grateful and appreciate all the help and support given to me throughout my studies by Lindsey, Marianne, Hannah, Holly, Anna, Mark, and Nayani. I also thank all other members of both 5th and 6th floor labs at ICH for making the long hours in the lab an enjoyable experience.

I would like to express my gratitude to everyone at Eastman Dental Institute for being very accommodating over the course of my project. I particularly thank Dr. Haitham Hussain for his invaluable help, and Kat and Mike for sharing their experiences of working with *C. difficile*.

Finally, I owe my deepest and foremost gratitude to my parents and my brother for their love and support, especially my mother and brother, who gave me endless support and encouragement after our sad loss. To my family, I dedicate this thesis. Last but not least, I thank Mohammad for sharing this journey with me and always being there when I needed.

TABLE OF CONTENTS

LIST OF FIGURES

LIST OF TABLES

PUBLICATIONS & ABSTRACTS

Abstracts: Poster Presentations

Human intestinal epithelial cell response(s) to *Clostridium difficile*.

Nazila V Jafari*[1], Elaine Allan[2], Lindsey A Edwards[1], Mona Bajaj-Elliott[1]. [1]Institute of Child Health, [2] Eastman Dental Institute. University College London, UK.

14th International Congress of Mucosal Immunology (ICMI 2009). July 5-9, 2009, Boston, USA.

Effect of *Clostridium difficile* on human intestine.

Nazila V Jafari*[1], Elaine Allan[2], Lindsey A Edwards[1], Kathleen A Dunlop[1], Mona Bajaj-Elliott[1]. [1]Institute of Child Health, University College London, UK, [2]Eastman Dental Institute, University College London UK.

6th ClosPath International Conference. 19-23 October, 2009, Rome, Italy.

Clostridium difficile Mediated Effects on Intestinal Epithelia.

Jafari, N.V.[1], Allan, E.[2], Vernay, B.[3], Stabler, R.A.[4], Wren, B.W.[4], Bajaj-Elliott, M.[1], [1,3]Institute of Child Health, University College London, London, UK., [2]Eastman Dental Institute, University College London, London, UK., [4]London School of Hygiene and Tropical Medicine, London, UK.

15th International Congress of Mucosal Immunology (ICMI 2011). July 5-9, 2011, Paris, France.

Abstracts: Oral Presentations

Understanding *Clostridium difficile* mediated disease pathogenesis.

Jafari, N.[1], Edwards, L.A.[1], Allan, E.[2], Bajaj-Elliott, M.[1], [1]Infectious Diseases and Microbiology Unit, Institute of Child Health, University College London, London, UK, [2]Division of Microbial Diseases, Eastman Dental Institute, University College London, London, UK.

2nd UEGF Teaching Activity on Basic Science. 16-18 July, 2010, Cambridge, UK.

Publications

Nazila V. Jafari, Elaine Allan, Mona Bajaj-Elliott, 2010.

Human Intestinal Epithelial Response(s) to Clostridium difficile. *Clostridium difficile* Methods and Protocols, Chapter 9.

P.Mullany, A.P. Roberts (eds.), London, Humana Press, pp. 135-146.

Jafari, N.V., Kuehne, S.A., Elawad, M., Bryant, C.E., Wren, B.W., Minton, N.P., Allan, E., Bajaj-Elliott, M.

Clostridium difficile modulates host innate immunity via toxin-dependent and independent mechanism(s). Manuscript in preparation.

Jafari, N.V., Dawson, L.F., Stabler, R.A., Wren, B.W., Allan, E., Bajaj-Elliott, M.

Differential host immunity response(s) to historic and recent *C. difficile* ribotype 017 strains. Manuscript in preparation.

Jafari, N.V., Wren, B.W., Allan, E., Bajaj-Elliott, M.

Anaerobic conditions enhance *C. difficile* mediated effects on human intestinal epithelial cells. Manuscript in preparation.

ABBREVIATIONS

Ab	Antibody
AID	Activation-induced cytidine deaminase
AIM2	Absent in melanoma 2
AJ	Adherens Junction
ANOVA	Analysis of variance
APC	Antigen Presenting Cell
APRIL	A proliferation-inducing ligand
APS	Ammonium persulfate
ASC	Apoptosis-associated speck-like protein containing a CARD domain
BAFF	B cell-activating factor of the TNF family
BCR	B Cell Receptor
BHI	Brain Heart Infusion
BMDC	Bone-marrow-derived Dendritic Cell
bp	base pair
BSA	Bovine Serum Albumin
CAR	Coxsackievirus and adenovirus receptor
CARD	Caspase activating and recruitment domains
CD40L	CD40 Ligand
CDI	*C. difficile* Infection
CDT	*C. difficile* Transferase
CFU	Colony Forming Unit
CFSE	Carboxyfluorescein Diacetate Succinimidyl Ester
CPE	Cytopathic Effect
CSR	Class-switch DNA recombination
DAPI	4',6-Diamidino-2-Phenylindole
DC	Dendritic Cell
DMSO	Dimethylsulphoxide

EBI3	Epstein-Barr virus induced gene 3
ECL	Enhanced chemiluminescence
EDTA	Ethylenediaminetetraacetic acid
ELISA	Enzyme Linked Immunosorbent Assay
ER	Endoplasmic Reticulum
F-actin	Filamentous actin
FACS	Fluorescence Activated Cell Sorter
FAE	Follicle-associated Epithelium
FCS	Foetal Calf Serum
FITC	Fluorescein Isothiocyanate
Foxp3	Forkhead box P3
g	Gram
g	Gravity
GALT	Gut-associated lymphoid tissue
GAPDH	Glyceraldehyde-3-Phosphate Dehydrogenase
GATA3	GATA-binding protein 3
GI	Gastrointestinal tract
GM-CSF	Granulocyte Macrophage Colony Stimulating Factor
Hprt	Hypoxanthine guanine phosphoribosyl transferase
HY	Hypervirulent
IECs	Intestinal Epithelial Cells
IFN	Interferon
Ig	Immunoglobulin
IL	Interleukin
IRF3	Interferon regulatory factor 3
IVOC	In vitro organ culture
JAM-A	Junctional Adhesion Molecule-A
Knockout	KO
LDH	Lactate dehydrogenase
LF	Lethal factor

LP	Lamina propria
LPS	Lipopolysaccharide
LRR	Leucine-rich receptors
mA	Milliamp
Mal	MyD88 adaptor like
MALT	Mucosal-associated lymphoid tissue
MAMP	Microbe-associated molecular pattern
MAPK	Mitogen-activated protein kinase
M cell	Microfold cell
MD-2	Myeloid differentiation protein 2
MFI	Median Fluorescence Intensity
MHC	Major Histocompatibility Complex
MLN	Mesentric lymph node
MOI	Multiplicity of infection
MW	Molecular weight
MyD88	Myeloid differentiation antigen 88
N	Normal
nFcR	Neonatal Fc receptor
NF-κB	Nuclear factor kappa B
NLR	Nod-like receptor
Nod	Nucleotide oligomerisation domain
OD	Optical density
p	Probability
PaLoc	Pathogenicity Locus
PAMP	Pathogen-associated molecular pattern
PBS	Phosphate-buffered saline
PCR	Polymerase Chain Reaction
PE	Phycoerythrin
PeCy5	Phycoerythrin-cyanine 5
PG	Peptidoglycan

PerCP	Peridinin Chlorophyll Protein
PFA	Paraformaldehyde
PFGE	Pulsed field gel electrophoresis
PI	Propidium Iodide
pIgR	Polymeric Ig receptor
PMA	Phorbol 12-myristate 13-acetate
PMC	Pseudomembranous Colitis
PP	Peyer's patche
PRR	Pattern recognition receptor
PS	Phosphatidylserine
REA	Restriction endonuclease analysis
RFLP	Restriction fragment length polymorphism
RIG-1	Retinoic acid inducible gene 1
RLR	RIG-1-like receptor
RORγt	Retinoic acid receptor related orphan receptor-γt
PVDF	Polyvinylidene fluoride
rpm	revolutions per minute
RT	Room temperature
RT-PCR	Reverse Transcription-Polymerase Chain Reaction
SDS-PAGE	Sodium Dodecyl Sulfate Polyacrylamide Gel Electrophoresis
SED	Sub-epithelial dome
sIgA	Secretory IgA
SLP	Surface Layer Protein
sPLA2	Secretory Phospholipase A2
STAT	Signal Transducer and Activator of Transcription
TACI	Transmembrane activator and calcium modulating cyclophilin-ligand interactor
TAE	Tris-Acetate-EDTA
T-bet	T-box expressed in T cell
TBS	Tris-buffered saline

TcdA	Toxin A
TcdB	Toxin B
TEER	Transepithelial Electrical Resistance
TEMED	*N*,*N*,*N*′,*N*′-Tetramethylethylenediamine
TGF-β	Transforming Growth Factor beta
Th	T helper
Th1	T helper type 1 cell
Th2	T helper type 2 cell
Th17	T helper type 17 cell
TICAM 1	Toll/IL-1 receptor domain containing adaptor molecule 1
TIR	Toll/IL-1 receptor
TIRAP	TIR domain containing protein
TJ	Tight junction
TLR	Toll-like receptor
TNF-α	Tumour Necrosis Factor alpha
TRAM	TRIF related adaptor molecule
Treg	T regulatory cell
TRIF	TIR domain containing adaptor protein inducing IFN-β
TSLP	Thymic stormal lymphopoietin
V	Volt
WT	Wild type
YPM	Yeast peptone media
ZO	Zonula occludin

Chapter 1

Introduction

1.1 *Clostridium difficile*

1.1.1 Introduction

The genus *Clostridium* is comprised of Gram-positive, spore-forming anaerobic rods. *Clostridium difficile*, originally named *Bacillus difficilis*, causes gastrointestinal (GI) infection and is a key cause of nosocomial illness worldwide. The bacterium was first identified in 1935 from the stools of healthy newborns (Bongaerts & Lyerly, 1994). The designated name related to the difficulties involved in its isolation and study. However, it was not until 1978 that it was identified as the primary cause of antibiotic-associated diarrhoea and pseudomembranous colitis (PMC) (Dodson & Borriello, 1996; Voth & Ballard, 2005).

C. difficile produces two large heat-labile exotoxins: toxin A (TcdA), an enterotoxin and toxin B (TcdB), a cytotoxin. TcdA and TcdB are among the largest bacterial toxins known to date and are joined by *Clostridium sordellii* lethal toxin (TcsL), haemorrhagic toxin (TcsH), and *Clostridium novyi* alpha toxin (Tcnα) to make up the large clostridial cytotoxins (LCTs) family (Just & Gerhard, 2004; Voth & Ballard, 2005). Toxin-producing clostridial species are associated with a range of diseases, including botulism (*C. botulinum*), tetanus (*C. tetani*), gas gangrene, food poisoning (*C. perfringens*), diarrhoea, and PMC (*C. difficile*) (Bruggemann, 2005).

In addition to TcdA and TcdB, two major virulence factors of *C. difficile*, a number of other putative virulence factors have been described including: a binary toxin (CDT) (Rupnik *et al.,* 2003a), endospores (Sebaihia *et al.,* 2006; Burns & Minton, 2011), surface layer proteins (SLP) (Calabi *et al.,* 2002; Wright *et al.,* 2005), fimbriae (Borriello *et al.,* 1990; Sebaihia *et al.,* 2006), and capsule (Borriello *et al.,* 1990; Davies & Borriello, 1990).

C. difficile infection (CDI) may result in a spectrum of disease, which can range from mild diarrhoea to life-threatening colitis (Dallal *et al.,* 2002; Johal *et al.,* 2004a). CDI often occurs following treatment with broad-spectrum antibiotics. In addition to morbidity and mortality, CDI is a burden on healthcare due to extended hospitalisation and increased cost (Ghantoji *et al.,* 2010). Once regarded as relatively rare occurrence, CDI has become a common noscomial infection, but it is not confined to the hospital environment only and community-acquired infection is on the rise (Dial *et al.,* 2005; Cartman *et al.,* 2010; Freeman *et al.,* 2010) and *C. difficile* is now also being recognised as an important cause of enteric disease in animals (Songer & Anderson, 2006; Rupnik, 2007). CDI continues to

increase in most developed countries especially with the emergence of more highly virulent strains causing increased disease severity, a rise in fatalities placing a large financial burden on healthcare systems worldwide (Goorhuis *et al.,* 2008; Kuehne *et al.,* 2011). The ease of spread of *C. difficile*, the fact that it is often resistant to antibiotics and often causes recurrent infections makes management and treatment of CDI problematic in healthcare facilities and signifies a need for an improved understanding of *C. difficile* pathogenesis.

1.1.2 *C. difficile* Virulence Factors

C. difficile produces a number of factors that contribute to its virulence. Some directly contribute to the pathology of the infection, while others enable *C. difficile* to colonise and initiate the pathology (Borriello, 1998). Not all strains are virulent and studies have been carried out to determine what accounts for the differing virulence between strains.

1.1.2.1 *C. difficile* Toxins

The major virulence factors of *C. difficile* are toxin A (TcdA; 308 kDa) and toxin B (TcdB; 270 kDa), two highly related UDP-glucosylating toxins. These two toxins share more than 60% amino acid sequence homology (Miura *et al.,* 2011). TcdA and TcdB consist of single, large polypeptide chain stabilised by disulfide bonds. Amino-termini in both toxins are highly conserved, are catalytic and function in the target cell cytoplasm by the same mechanism. The carboxy-terminus; however, includes a receptor binding domain, which differs between the two toxins (Keel & Songer, 2006).

***C. difficile* Pathogenicity Locus (PaLoc)**

The two toxin-encoding genes, *tcdA* and *tcdB*, respectively, are situated on the *C. difficile* chromosome in a 19.6 kb pathogenicity locus (PaLoc), along with three accessory genes *tcdR, tcdC* and *tcdE* (Kuehne *et al.,* 2010) (Figure 1.1). The two toxin genes, *tcdA* and *tcdB*, are transcribed in the same direction. The *tcdR* gene encodes an alternative sigma factor (TcdR), found upstream of *tcdB*, and is a positive regulator of *tcdA* and *tcdB* expression (Deneve *et al.,* 2009). It is responsive to environmental conditions and is increased during stationary phase of growth (Voth & Ballard, 2005). *tcdC* is found downstream of *tcdA* and it encodes an anti-sigma factor (TcdC) which represses toxin production by directly

interacting with TcdR and destabilising TcdR holoenzyme (Matamouros *et al.,* 2007). The third gene, *tcdE* encodes the TcdE protein, which has similarities to phage holing proteins (Tan *et al.,* 2001). It has been suggested that TcdE may be involved in toxin secretion (Dupuy *et al.,* 2008). *tcdC* is expressed during the exponential phase of growth while all the other genes are expressed during the late logarithmic and stationary phases (Matamouros *et al.,* 2007; Rupnik *et al.,* 2009). In addition to TcdR and TcdC, CodY a factor encoded outside the PaLoc, also participates in the regulation of toxin synthesis by monitoring the nutrient sufficiency of the environment. CodY proteins have the ability to repress genes (which are not needed in a nutrient sufficient environment) and to release the suppression under nutrient-limited conditions (Dineen *et al.,* 2007).

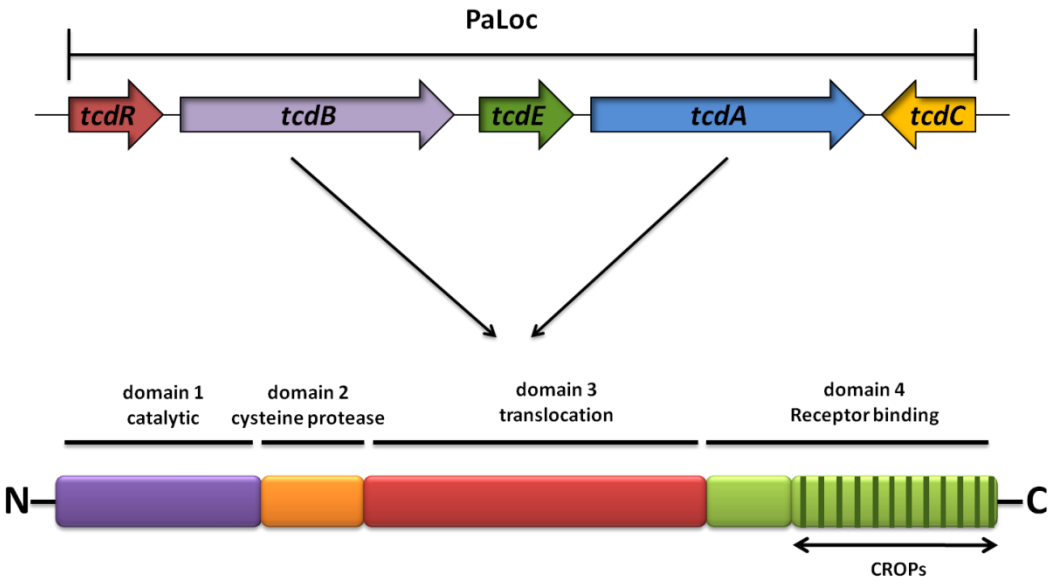

Figure 1.1. *C. difficile* PaLoc encodes the toxin A and B genes. Toxin genes *tcdA* are *tcdB* are situated on the *C. difficile* chromosome in a 19.6 kb pathogenicity locus (PaLoc), along with three accessory genes *tcdR, tcdE* and *tcdC*. Adapted from Voth & Ballard, 2005; Egerer *et al.,* 2007; and Albesa-Jove *et al.,* 2010.

Functional Domains of TcdA and TcdB

TcdA and TcdB are multidomain secreted proteins that contain specialised functional properties. The N-terminus of each protein has glucosyltransferase activity (the first 543 amino acids) and represents the biologically active part of the toxin. The middle part of the toxins is involved in translocation of the toxins into the host cell cytosol (Albesa-Jove *et al.,* 2010). The C-terminal domain has short combined repetitive oligopeptides (CROPs) required for receptor binding (Carroll & Barrtlett, 2010) (Figure 1.1). In animal models, the trisaccharide Gal1 (α1–3) Gal (β1–4) GlcNac is part of the host receptor for TcdA (Rupnik *et al.,* 2009). This carbohydrate is not present in humans; however, Na *et al.* identified glycoprotein 96 (gp96), which is expressed on human colonocyte apical membranes as well as in the cytoplasm as the main colonocyte receptor for TcdA (Na *et al.,* 2008). The function of the C-terminal part of TcdB is probably similar to that of TcdA; however, the receptor for *C. difficile* TcdB has not yet been identified (Jank & Aktories, 2008).

The C-terminal repetitive region of the secreted toxins binds to host cell receptors. The toxin-receptor complex is endocytosed and the toxin translocates to the early endosomes. The low pH in this compartment triggers conformational changes, which leads to toxin insertion into vesicle membranes via pore formation (Reineke *et al.,* 2007; Albesa-Jove *et al.,* 2010). As TcdA forms pores in artificial membrane at low pH, it was hypothesised that acidic endosome in living cells may also cause similar changes, a process that is accompanied by pore formation (Reineke *et al.,* 2007). In the case of TcdB it has been shown that the toxin is cleaved between leucine 543/glycine 544 at neutral pH generating a fragment of 63 kDa (catalytic domain), which reaches the cytosol, while a 207 kDa (ligand-translocation domain) fragment remains in the membrane fraction (Rupnik *et al.,* 2005). A later study proposed that other large clostridial cytotoxins share this autocatalytic process, which is dependent upon host cytosolic inositolphosphate cofactors. Host cell inositolhexaphosphate ($InsP_6$) induces aspartate protease-dependent autocatalytic cleavage, resulting in biologically active toxin (Reineke *et al.,* 2007). In contrast, Egerer *et al.* showed that autocleavage is essential for toxin activity, and that leucine 543 is the relevant cleavage site and a cysteine protease catalytic triad (cysteine 698, histidine 653, and aspartate 587) is involved in toxin processing (Egerer *et al.,* 2007).

Mechanism of Action

Following translocation into the cytosol, the toxins target the Ras superfamily of small GTPases (Rho, Rac, and Cdc42), modifying them through monoglucosylation of threonine 35/37 (Genth *et al.,* 2008). These small proteins are important in regulating several distinct signalling pathways including cytoskeletal rearrangements and cell growth. Glucosylation prevents the structural changes required for active conformation of Rho GTPases, thus significantly altering their function resulting in inhibition of cell division and membrane trafficking. On cultured intestinal epithelial cells (IECs), the cytotoxic effect is characterised by a reduction in transepithelial resistance (TEER), indicating a loss of IEC barrier function. Rho glucosylation results in the disappearance of polymerised filamentous actin (F-actin) causing cell rounding, termed cytopathic effect (CPE). The toxins also provoke mitochondrial damage that eventually proceeds to apoptosis (Just *et al.,* 1994 &1995; Genth *et al.,* 2006; Gerhard *et al.,* 2008; Miura *et al.,* 2011).

The apoptotic properties of *C. difficile* TcdA and TcdB are well known. These toxins induce apoptosis in IECs, neurons, endothelial cells and monocytes. The executioner caspase-3 is involved in TcdA-induced apoptosis; however, activation of another executioner, caspase-6 has also been described. Caspase-3 and 6 are activated by two initiator caspases, caspase-8 and caspase-9. Caspase-8 is the major driver of the extrinsic apoptotic pathway, which is activated via transmembrane death receptors such as the Fas receptor. Caspase-9, represents the intrinsic pathway, and is activated by an apoptosome, which is triggered by the release of cytochrome *c* from damaged mitochondria. Ultimately, procaspase-3 is cleaved by both caspases-8 and 9 mediated pathways causing apoptosis (Nottrott *et al.,* 2007; Gerhard *et al.,* 2008).

***C. difficile* Hypervirulent Strains**

In the last decade, the global incidence of CDI has increased dramatically in North America, Canada and Europe due to the emergence and spread of epidemic strains that predominantly belong to PCR ribotype 027 (based on comparison of PCR products patterns of the 16S-23S rRNA intergenic spacer region; Rupnik *et al.,* 2001). These strains are also characterised as toxinotype III [based on PCR restriction fragment length polymorphism (RFLP) analysis of *C. difficile* PaLoc; Rupnik *et al.,* 2001], North American pulsed field gel electrophoresis (PFGE) type 1 (NAP1) and restriction endonuclease analysis (REA) group BI (BI/NAP1/027) (Cartman *et al.,* 2010). Ribotype 027 strains are associated with more severe

disease, increased mortality, higher relapse rates and increased resistance to fluoroquinolone antibiotics (Stabler *et al.,* 2009).

C. difficile ribotype 027 strains produce 16 and 23 times more TcdA and TcdB respectively when compared to historic strains (Warny *et al.,* 2005). Ribotype 027 strains also produce a binary toxin (or *C. difficile* Transferase, CDT), which is proposed to enhance colonisation of *C. difficile* by triggering the formation of microtubule protrusion on cells of the GI epithelium (Schwan *et al.,* 2009). These strains also encode a variant *tcdC* repressor gene. Moreover, ribotype 027 strains harbour various deletions at the 3' end of the *tcdC* gene, resulting in truncated TcdC proteins. An 18 bp deletion in *tcdC* was initially suggested to be the cause of increased toxin production by the epidemic strains (Warny *et al.,* 2005), however, Spigaglia *et al.* detected 39- and 18- bp deletions in *tcdC* and showed that nonsense mutations in *tcdC* reduced TcdC protein (Spigaglia & Mastrantonio, 2002). Matamouros *et al.* demonstrated that a *tcdC* gene containing only the 18 bp in-frame deletion encodes a TcdC protein that is active both *in vivo* and *in vitro* (Matamouros *et al.,* 2007; Dupuy *et al.,* 2008). Additional mutations in *tcdC* have subsequently been described in toxin hyperproducing strains. In particular, a single base pair deletion at position 117 with the previously described 18 bp deletion causes a frameshift mutation and consequent truncation of *tcdC* (Curry *et al.,* 2007).

Toxin Variant Strains

The majority of *C. difficile* strains are A^+B^+ but a number of isolates have deletions in *tcdA*, resulting in a truncated form of the toxin, and produce only a functional toxin B (A^-B^+) (Voth & Ballard, 2005). Despite the known role of TcdA in disease pathogenesis, strains lacking TcdA have been recovered from patients with clinical disease and from outbreaks (Johnson *et al.,* 2003). These isolates are a rare cause of disease in the United States (0.2%) but constitute anywhere from 3% of all isolates in UK and France to as high as 39% in Japan, 56% in Israel to replacing completely A^+B^+ strains in Argentina (97.9%) (Drudy *et al.,* 2007). These variant *C. difficile* strains differ from the reference strain VPI 10463 in the length and restriction sites in toxin genes, as well as other regions of the PaLoc (Rupnik *et al.,* 2003b).

Earlier studies suggested that administration of pure TcdA alone to hamsters was sufficient to cause disease, whereas TcdB alone was not (Lyerly *et al.,* 1988). Interestingly, intragastric challenge of hamsters with TcdB can cause disease symptoms if prior damage to the mucosa has occurred through co-administrations of TcdA. Moreover, co-administration results in more severe disease symptoms leading to the notion that both toxins act

synergistically (Lyerly *et al.,* 1985). The isolation of variant strains which apparently produce no TcdA (A^-B^+ strains) presents a challenge to the established dogma that both toxins are required for disease.

The first A^-B^+ strain to be characterised was strain 8864 (toxinotype X) containing a 5.9 kb deletion in the 3' end of *tcdA* and *tcdC* preventing production of TcdA, as well as a 1.1 kb insertion in between *tcdA* and *tcdE* (Soehn *et al.,* 1998). It causes pathology in animal models however its virulence in humans remains undefined (Torres, 1991; Borriello *et al.,* 1992). Serogroup F strains (type strain 1470, toxinotype VIII also known as PCR ribotype 017) were the second A^-B^+ strain type that was identified with a 1.8 kb deletion in *tcdA*, and a mutation that introduces a stop codon at amino acid position 47 (von Eichel-Streiber *et al.,* 1999). These strains are frequently isolated from asymptomatic infants and lack pathogenicity in animals however, they have also been isolated from symptomatic and PMC patients and outbreaks (Delmee & Avesani, 1990; Depitre *et al.,* 1993; Rupnik *et al.,* 2003b). Toxinotype VIII appears to be the most clinically significant variant strain type causing four documented outbreaks, sporadic cases of diarrhoea and PMC (Drudy *et al.,* 2007). Analysis of TcdB-8864 and 1470 showed that these toxins are a hybrid between TcdB from reference strain VPI 10463 (A^+B^+) and *C. sordellii* lethal toxin (Chaves-Olarte *et al.,* 1999), while their receptor binding domain is 100% homologous with strain 10463, the enzymatic domain shares only 79% homology (Drudy *et al.,* 2007).

1.1.2.2 Other Virulence Factors

Although TcdA and TcdB are the major virulence factors in *C. difficile* associated disease, other factors undoubtedly contribute to virulence, particularly the initial colonisation process.

I. Binary Toxin

In addition to producing TcdA and TcdB, approximately 6% of *C. difficile* strains including ribotype 027 epidemic strains, produce a third toxin, known as *C. difficile* binary toxin (CDT). Whilst not absolutely required for virulence, CDT may enhance virulence (Cartman *et al.,* 2010; Carrol & Bartlett, 2010). CDT is a member of the clostridial binary toxins that include C2 toxin from *C. botulinum* types C and D, iota toxin from *C. perfringens* type E and *C. spiroforme* iota-like toxin. This toxin is an actin-specific ADP-ribosyltransferase consisting of two subunits; an enzymatic component CDTa (48 kDa) and a binding component CDTb (99

kDa) (Stubbs *et al.,* 2000; Rupnik *et al.,* 2003a). CDT is encoded by two genes, *cdtA* and *cdtB*, which are transcriptionally linked and are located on the *C. difficile* chromosome at a locus separate from the PaLoc named the CDT locus (CdtLoc), together with the regulatory gene, *cdtR* (Rupnik *et al.,* 2009). CDT production is tightly regulated by CdtR (Carter *et al.,* 2007).

CDT binds to target cells via CDTb and transports the enzymatic CDTa into the cytosol. CDTa ADP-ribosylates G-actin at arginine 177 thereby blocking actin polymerisation (Aktories *et al.,* 1986; Vandekerckhove *et al.,* 1987). ADP-ribosylated actin acts as a capping protein at barbed ends of actin filaments thus inhibiting elongation leading to depolymerisation of F-actin (Wegner & Aktories, 1988; Aktories & Wegner, 1992). Although the role of CDT in pathogenesis is unclear, new findings by Schwan *et al.* revealed that the actin ADP-ribosylating toxins, *C. difficile* CDT, *C. perfringens* iota toxin and *C. botulinum* C2 toxin can induce the formation of novel thin, dynamic, microtubules on the surface of IECs, leading to increased adherence of clostridia both in *in vitro* and *in vivo*. These protrusions increase the adherence of clostridia to IECs by ~5-fold *in vitro* and 4-fold in the mouse large intestine (Schwan *et al.,* 2009).

II. Endospores

Sporulation is initiated under conditions of nutrient limitation. Endospores, which are metabolically dormant cells, are formed following asymmetrical cell division. The internal cytoplasm is protected by thick concentric external layers, the spore coat and the cortex (Lawley *et al.,* 2009), they consequently are highly resistant to a variety of chemical agents, desiccation and extreme temperature conditions. These properties allow *C. difficile* to persist on surfaces causing contamination in healthcare settings. Ingestion of spores leads to infection or re-infection of co-habiting individuals (Rupnik *et al.,* 2009; Burns & Minton, 2011).

Upon reaching the GI tract's anaerobic environment, the ingested spores germinate to toxin-producing vegetative cells and, in susceptible individuals, cause diarrhoeal disease. Bile salts and glycine can act as co-germinants for *C. difficile* spores. In bile, glycine is conjugated to cholate. When glycocholate passes into the lower bowel, the glycyl group is deconjugated from cholate by the normal microbial flora. The products of deconjugation, cholate and glycine are sufficient to stimulate germination and outgrowth of *C. difficile* spores (Sorg & Sonenshein, 2008).

III. Surface Layer Proteins (SLPs)

C. difficile is surrounded by a paracrystalline array of protein(s) which lie external to the cell wall. This surface (S)-layer is composed of two proteins, derived from a single gene, *slpA* (Calabi *et al.,* 2001; Karjalainen *et al.,* 2001). The translated gene product undergoes two rounds of post-translational cleavage, firstly to remove the signal sequence following secretion, and then internal cleavage at position 355 releases the two mature SLPs; a high molecular weight SLP (HMW-SLP, 45 kDa) which is a cell wall binding protein attached to the underlying peptidoglycan moiety. The low molecular weight SLP (LMW-SLP, 36 kDa) localises to the external surface of the bacterium (Cerquetti *et al.,* 2000; Wright *et al.,* 2005; Fagan *et al.,* 2009). Recombinant HMW-SLP is able to adhere to human and mouse intestinal tissue whilst antibodies against it are able to block adherence of *C. difficile* to cultured cells (Calabi *et al.,* 2002).

Several other *C. difficile* proteins are implicated in attachment to IECs; these include the S-layer P36 and P47 adhesins proteins (Deneve *et al.,* 2009), a 66 kDa cell wall protein Cwp66 (Waligora *et al.,* 2001), Fbp68 a 68 kDa fibronectin binding protein (Hennequin *et al.,* 2003), the GroEL heat shock protein (Hennequin *et al.,* 2001), and Cwp84, a cysteine protease, which is involved in degradation of several extracellular matrix proteins (fibronectin, laminin and vitronectin) and may degrade host tissue to enhance the spread of infection (Janoir *et al.,* 2007).

IV. Flagellin

C. difficile is known to express peritrichous flagella. *C. difficile* flagella components, FliC (flagellin) and FliD (flagellar cap protein) may aid attachment to intestinal mucus. Flagellated strains adhere 10-fold greater than nonflagellated strains when tested in the mouse cecum (Tasteyre *et al.,* 2001). Glycosylation of the flagellin protein is required for its appropriate assembly and consequent motility; however, genomic microarray studies indicate that motility may not be required for virulence due to divergence in the flagellar sequences noted amongst the varying strains (Twine *et al.,* 2009).

V. Antibiotic Resistance

Antibiotic resistance is an important virulence factor of *C. difficile*, as the bacterium is resistant to most antibiotics. The development of resistance amongst isolates can be traced over time, particularly for widely used antibiotics such as cephalosporins and clindamycin (Delaney *et al.,* 2007). Antibiotic resistance genes in *C. difficile* is mostly transposon

mediated, with erythromycin resistance (*ermB*) carried on *Tn5398* (Hussain *et al.,* 2005; Sebaihia *et al.,* 2006), chloramphenicol resistance on *Tn4453* (Lyras *et al.,* 2004) and tetracycline resistance on *Tn5397* (Hussain *et al.,* 2005). The more recent isolates are sharing increased resistance to fluoroquinolones encompassing a large range of ribotypes and are spreading at an alarming rate (Spigaglia *et al.,* 2008).

Treatment with broad spectrum antibiotics leads to the disruption of the normal gut flora, which enable *C. difficile* to proliferate. Interestingly, re-colonisation of gut normal flora is prevented by *C. difficile*. This is due to production of *para*-cresol by the bacterium (Dawson *et al.,* 2008). *Para*-cresol is a phenolic compound, with bacteriostatic properties, produced via aminotransfer of tyrosine to *para*- hydroxyphenylacetic acid, which is then decarboxylated to *para*-cresol. Only *C. difficile* and *Lactobacillus* strains are able to produce *para*-cresol from tyrosine. Importantly, *C. difficile* itself is able to tolerate high concentrations of this compound, suggesting that this may provide a competitive advantage for *C. difficile* over other intestinal microflora, consequently contributing to the progression of CDI (Sebaihia *et al.,* 2006; Dawson *et al.,* 2009).

1.1.3 *C. difficile* Pathogenesis

C. difficile is spread via the faecal-oral route. The organism is ingested in vegetative or spore form. Spores survive the acidic environment of the stomach and germinate into the vegetative form, which can multiply and colonise the colon. Disturbance of the normal intestinal flora increases susceptibility to infection and pathology. The gut microbiota acts as a colonisation barrier, which protects against *C. difficile*. Antibiotic therapy alters the normal flora compromising the barrier (Bartlett, 2006). After colonisation, *C. difficile* releases TcdA and TcdB. Carbohydrate receptors for TcdA have been identified on the brush border of IECs. TcdA acts primarily on IECs causing inflammation, fluid and mucus secretion and tissue damage (Voth & Ballard, 2005) whereas TcdB shows broad cell tropism (Heinlen & Ballard, 2010). TcdA is responsible for the activation and recruitment of inflammatory mediators such as IL-6, IL-8 by IECs, and IL-1, IL-6, IL-8, TNF-α by human monocytes (Kachrimanidou & Malisiovas, 2011).

C. difficile glucosylating toxins catalyse the glucosylation of Rho- and or Ras-GTPases from UDP-glucose. TcdA and TcdB glucosylate Rho at threonine site 37, Rac and Cdc42 at threonine-35. By inactivating Rho proteins, glucosylating toxins induce cell rounding,

accompanied by a loss of actin stress fibres, re-organisation of the cortical actin, disruption of the intercellular junctions and subsequently an increase in cell barrier permeability (termed as CPE). In contrast, cytotoxic effect results in toxin-induced cell death. Concomitant with barrier function alteration and increased permeability, TcdA and TcdB disrupt apical and basal actin filaments with a subsequent disorganisation of tight junction proteins such as ZO-1, ZO-2, occludin, and claudin (Popoff & Geny, 2011) and eventually resulting in cell death. TcdA and TcdB are able to induce either type I programmed cell death (apoptosis) or type III programmed cell death (necrosis) (Genth *et al.,* 2008).

C. difficile does not invade the colonic mucosa and does not cause disease if no toxin is produced. Even in the presence of toxin, some people become carriers or develop mild self-limited diarrhoea while others develop severe colitis and may present several relapses of the disease. Clinical manifestation depends on the rapidity of the serum antibody response to the toxin (Fordtran, 2006). Up to 60% of healthy adults have detectable IgG and IgA against TcdA and TcdB and almost 70% of healthy newborns and infants aged up to 12 to 18 months become colonised with *C. difficile* while normal colonic flora is being established. Large amounts of toxins can be detected in their stools, although children rarely develop colitis. Most patients with acute infection do not exhibit an IgM response, but rather a secondary IgG response. It has been shown that the development of asymptomatic carriage is associated with the development of high titers of anti-TcdA antibodies, whereas low titers are correlated with the subsequent development of CDI and more severe disease, indicating the probable importance of humoral immunity in preventing disease (Heinlen & Ballard, 2010).

1.1.4 Risk Factors

Antibiotic exposure, advanced age and hospitalisation are three major risk factors for *C. difficile* infection. Prior exposure to antimicrobial agents is the most widely recognised and modifiable risk factor for CDI, despite infrequent cases of community-onset CDI without prior antibiotic treatment. Patients with CDI in a hospital setting are generally exposed to an antibiotic prior to acquiring the infection (Rupnik *et al.,* 2009). A recent study showed that 85% of CDI patients had received antibiotic therapy within 28 days prior to the onset of symptoms (Kachrimanidou & Malisiovas, 2011). Any antimicrobial agent with an antibacterial spectrum can cause CDI, but some carry a higher risk than others, e.g.

clindamycin followed by ampicillin or amoxicillin played a prominent role in the 1970s but were largely supplanted by cephalosporins in the 1980s, and more recently by fluoroquinolones (Bartlett, 2006; Rupnik *et al.,* 2009). Other major risk factors for CDI are advanced age (>65 years) and hospitalisation. Elderly patients with severe underlying illnesses and prolonged hospitalisation are particularly susceptible (Monaghan *et al.,* 2008; Kachrimanidou & Malisiovas, 2011).

Patients receiving immunosuppressive agents such as chemotherapeutic or immunosuppressant drugs are also vulnerable for developing CDI, in particular those who are not able to mount an effective IgG antibody response against *C. difficile* toxins. Other risk factors associated with CDI include treatment with proton-pump inhibitors, H_2 blockers, gastric acid suppression agents, and finally the presence of GI diseases such as inflammatory bowel disease (IBD) (Monaghan *et al.,* 2008; Rupnik *et al.,* 2009; Kachrimanidou & Malisiovas, 2011).

1.1.5 Treatment

Recommendations for CDI therapy vary, as they are based on the extent of disease severity and whether it is an initial or recurrent infection. Given the recognised role of antibiotic therapy in causing CDI, mild disease may be treated by withdrawing the inciting antibiotic. *C. difficile* has long been considered as a multiple antibiotic resistant organism (resistant to erythromycin, clindamycin, lincomycin, tetracycline, and chloramphenicol), mainly due to the large number of mobile genetic elements in the genome which harbour antibiotic resistant genes (Cartman *et al.,* 2010; Heinlen & Ballard, 2010; Kyne, 2010).

Currently only metronidazole and vancomycin provide an effective treatment. Whilst vancomycin has fewer side effects and is more effective, metronidazole has until now been preferred due to its lower price. Further, concerns over the increasing problem of vancomycin resistance in other bacteria have made vancomycin the last resort antibiotic. Metronidazole is becoming increasingly ineffective and there are reports of metronidazole resistant *C. difficile* strains. This is extremely worrying, as there are increasing reports of gene transfer examples between *Enterococcus spp.* and *Clostridium spp*. *Enterococcus faecicum* is the major source of vancomycin resistance gene *vanA*, and as this organism lives in the same niche as *C. difficile*, *vanA* transfer to *C. difficile* would appear to be just a matter of time, and if so there may be an emergence of metronidazole resistant strains

carrying *vanA*, the consequences would be fatal (Stoddart & Wilcox, 2002; Cartman *et al.,* 2010). Although metronidazole and vancomycin are effective at inhibiting *C. difficile* and treating symptoms, the use of these antibiotics does not allow for the re-establishment of gut normal flora. As a result up to 30% of patients will have recurrent CDI usually within 14 days of treatment termination and 50% of this group may have multiple recurrences. Between 20 and 50% of these recurrences are caused by new *C. difficile* strains, indicating re-infection rather than a relapse of the original infection (Kyne & Kelly, 2001; Rupnik *et al.,* 2009; Heinlen & Ballard, 2010; Kyne, 2010).

Other approaches are being investigated in the treatment of CDI, including the use of alternative antimicrobial agents, combination of antibiotics, toxin binding agents (a high molecular weight toxin binding polymer, GT160-246), probiotics, immunotherapy, phage-based approaches, and less acceptable but probably effective faecal transplantation; however, none of these approaches have yet achieved wide acceptance (Stoddart & Wilcox, 2002; Cartman *et al.,* 2010; Kyne, 2010).

1.1.6 Epidemiology

It is not clear whether CDI is due to existing *C. difficile* in the gut or exposure to an external source at the time of susceptibility, although in the vast majority of cases evidently the latter is responsible for the infection (Dodson & Borriello, 1996). Spread of the organism in health care settings is thought to be the result of ingestion of spores. Patients with CDI can be the main source of infection for others as a 20-40% rate of colonisation in hospitalised adults is seen compared with 2-3% in healthy adults (Heinlen & Ballard, 2010) although asymptomatic carriage may also play a role (Dodson & Borriello, 1996). *C. difficile* is uncommon among healthy adults in the general population; however, up to 50% of infants and approximately 20% of hospital patients who are culture positive for *C. difficile*, are asymptomatic carriers (Keel & Songer, 2006).

Vernacchio *et al.* (2006) detected *C. difficile* in the stool of healthy children at a similar rate to healthy adults (3.5%) and children with acute diarrhoea (Wilson, 2006). Kim *et al.* (2008) later demonstrated an increase in CDI incidence in hospitalised young children with the median age of 4 years. Importantly, the incidence in hospitalised children <1 year of age is also on the increase, indicating that *C. difficile* might be pathogenic in this group as well (Zilberberg *et al.,* 2008). More recent studies suggest that CDI in children may also be

acquired in the community (Baker *et al.,* 2010). Community-acquired CDI in adults has been reported sporadically for a number of years and is linked to the use of gastric acid-suppressing agents. It has been estimated that approximately 28% of all CDI cases are community-acquired (Heinlen & Ballard, 2010).

In 2002, an increase in severe CDI was reported by the University of Pittsburgh Medical Centre in the United States, which signalled the beginning of a continuous rise of CDI rate in Canada, US and Europe (Rupnik *et al.,* 2009). Hospitals in Canada began experiencing an epidemic of *C. difficile* associated disease, reporting about 14,000 nosocomial cases between 2003 and 2004. In 2005, disease rates increased at least five times greater than the historical average. The incidence of CDI in individuals over 65 years of age in just one hospital in Quebec increased from 102 in 1991-92 to 210 in 2002 and to 866 in 2003 per 100,000 people (Warny *et al.,* 2005). Strain typing revealed that ~82% of tested isolates were of ribotype 027, previously a minor ribotype in isolate collection (Cloud & Kelly, 2007).

Hospitals throughout the Unites States also reported increased numbers of severe cases of CDI due to ribotype 027 from 2001 to 2003, which continued through 2006 (O'Connor *et al.,* 2009). In 2006, CDI rates in US hospitals exceeded 300,000 cases per year and it is currently estimated that there are ~500,000 cases per year with 15,000 to 20,000 fatal cases (Rupnik *et al.,* 2009). In Europe only a few countries have the necessary systems to measure the CDI incidence and the associated death rates, and in some cases testing for *C. difficile* is not optimal. In 2002, the incidence of CDI in Germany increased from 1.7 to 3.8 cases per 100,000 to 14.8 in 2006 (Burckhardt *et al.,* 2008). In Spain, the incidence of diagnosed CDI in patients aged >65 years increased 3-fold between 1997 and 2005 (Soler *et al.,* 2008).

In 2003 the first outbreak due to *C. difficile* ribotype 027 was reported in the UK, followed by another outbreak in 2005 (HC, 2006). A total of 498 CDI cases with 172 deaths were caused by these two outbreaks (HC, 2006). Since the first outbreak, several outbreaks due to ribotype 027 strains have been documented in almost all UK health board regions (Buckley *et al.,* 2011). In UK, the voluntary reporting of positive stool samples (Health Protection Agency data) showed that CDI has been an increasing problem since the early 1990s. Whilst part of the increase is due to improved reporting, it is widely accepted that there has also been an increase in the number of cases (Monaghan *et al.,* 2008). In England, all the cases of CDI must be reported, and data made publicly available for each healthcare facility. In 2008 a national mandatory target was set to reduce the incidence of CDI by 30%

by 2010-11 (Duerden, 2011). Death involving CDI was decreased by 31% between 2009 and 2010 from 3,933 to 2,704. During 2006 to 2010, CDI rates were highest in men and women aged >85 at 2,186 and 2,194 per million respectively and *C. difficile* was involved in 1.1% of all deaths in England and Wales and less than 2% of all hospital deaths (www.statistics.gov.uk).

The increased rates of CDI have primarily been attributed to ribotype 027 strains but are not limited to this ribotype only. In different countries other ribotypes such as 001, 053 and 106 are associated with outbreaks and severe disease. PCR ribotype 078 (toxinotype V) has increased from 3% to 13% in several European countries (Rupnik *et al.,* 2009). In the Netherlands, patients infected with ribotype 078 are younger than those infected with ribotype 027 and more frequently have community associated disease. Ribotype 078 strains share features with ribotype 027 strains which include; genes encoding toxins A and B, binary toxin, and a variant *tcdC*. Significantly, the ribotype 078 strains isolated from humans are genetically related to isolates from pigs (Goorhuis *et al.,* 2008). It should be noted that in many countries, a different ribotype can predominate and present an equivalent threat in terms of disease severity, but be extremely rare elsewhere.

1.1.7 The Evolution of *C. difficile*

Although *C. difficile* was recognised as a pathogen only three decades ago, a number of PCR ribotypes have emerged causing outbreaks worldwide (Bartlett, 2006), with different ribotypes dominating a certain time and geographical region (Cheknis *et al.,* 2009). Four major clades of *C. difficile* isolates were revealed in a genomic comparison of 75 well-characterised *C. difficile* isolates to that of the genome-sequenced strain 630 (Stabler *et al.,* 2006). A hypervirulent (HY), a toxin A^-B^+ and two other clades with intermixed human and animal isolates (HA1 and HA2) were identified (Figure 1.2). The HY clade consisted of 20 PCR ribotype 027 strains, which formed a tight and distinct clade. A later study investigating the evolution of this highly virulent clone showed that one modern epidemic 027 strain (R20291, the strain responsible for an outbreak at Stoke Mandeville Hospital in 2006) has gained five genetic regions over the past two decades compared to the historic and non-epidemic ribotype 027 strain (CD196). Also 027 strains show considerable genetic differences compared to strain 630 and these changes correlate with observed phenotypic differences in motility, survival, antibiotic resistance and toxicity (Stabler *et al.,* 2009).

Image unavailable due to copyright restrictions

Figure 1.2. Phylogenetic comparison of clinical isolates and animal sources of *C. difficile* strains. Genomic comparisons of 75 *C. difficile* strains from diverse geographical locations comprising 21 hypervirulent, 13 A^+B^+, 14 A^-B^+, and 7 A^-B^- human isolates (black) and 7 bovine (green), 6 swine (red), 4 equine (light blue), and 3 murine isolates (blue) showed four major clades containing HY, A^-B^+, HA1, and HA2 (Stabler *et al.,* 2006).

The A^-B^+ clade formed a tight subclade of A^-B^+ strains; part of a larger clade including a subclade of A^-B^- strains and four animal isolates (Figure 1.2). As the hypervirulent and A^-B^+ isolates were clustered into two independent clades, Stabler *et al.* suggested a low genetic diversity and the wide geographical spread of these phylogenetic lineages. The HA1 and HA2 clades were distinct from the hypervirulent and toxin A^-B^+ strains. HA1 had mainly human isolates, while HA2 showed predominantly animal isolates; nevertheless, the comparative phylogenomic analysis in this study failed to distinguish any host specificity of the strains leading to the possibility of animals as a source of human infection (Stabler *et al.,* 2006).

C. difficile, as a genetically diverse species has evolved within the last 1.1 to 85 million years based on two independent dating methods (He *et al.,* 2010). Disease-associated isolates

(017s, 027s, and 078s) have emerged from multiple lineages, in addition to genetic modifications other elements may have contributed to the emergence of *C. difficile* as a major pathogen indicating independent evolution of virulence in these lineages. Interestingly, the population of the hypervirulent clade was identified to have expanded around the start of the century, a time corresponding to the first report of ribotype 027 hospital outbreaks (He *et al.,* 2010).

1.1.8 The Animal Models of *C. difficile* Infection

Many animal species have been investigated to identify an appropriate model of human CDI. Hamster (Price *et al.,* 1979), guinea pig (Knoop, 1979), rabbit (Alcantara *et al.,* 2001), pig (Steele *et al.,* 2010), rats and mice (Castagliuolo *et al.,* 1998; Chen *et al.,* 2008) have all been considered.

The hamster models is the most widely used model as CDI can be initiated by administration of a range of antibiotics followed by *C. difficile* exposure (Borriello *et al.,* 1988). They are particularly sensitive to *C. difficile* and die within 2-3 days of infection following rapid development of CDI (Lyerly *et al.,* 1985). The hamster model develops a fulminant colitis but does not demonstrate the spectrum of CDI seen in humans.

Animals such as mice and rats are not as readily susceptible to CDI as hamsters, however, their gnotobiotic counterparts can be colonised by *C. difficile* and consequently exhibit intestinal pathology. The disease in germ-free animals involves the colon, as observed in humans, while in hamsters *C. difficile* affects primarily the cecum and some parts of the ileum (Chen *et al.,* 2008).

Recently, the piglet model was established representing a reproducible model of acute or chronic CDI with characteristic PMC. CDI is common in swine, and in piglets causes enteritis during the first week of their life showing similar disease to humans (Steele *et al.,* 2010).

1.2 Host Immune Response

1.2.1 Innate GI Mucosal Response(s)

The GI tract is the site where the divergent needs of nutrient absorption and host defence collide. Nutrient absorption requires a thin large surface area, this however has the potential to compromise host defence. Many infectious diseases involve the gut and the gut protects itself by harbouring a large number of immune cells (MacDonald & Monteleone, 2005).

The GI mucosal immune system is the largest and most complex part of the immune system. It encounters more antigen than any other part of the body, yet it must be able to readily discriminate between invasive pathogens and the resident flora as well as harmless antigens, such as food proteins (Hecht, 1999). As most human pathogens enter the body through a mucosal surface, such as the GI tract, requirement of a prompt immune response is necessary to protect and prevent further spread of the encountered infection(s). By contrast, hypersensitivity responses against food antigens or commensal bacteria can lead to inflammatory disorders like celiac disease and Crohn's disease, respectively. Therefore, immunological tolerance of the GI mucosal immune system is vital for providing protection against external pathogens without reacting against itself (Weiner, 1994; Mowat, 2003).

The gut-associated lymphoid tissue (GALT) is the largest immune organ in the body and can be divided into effector sites and organised tissues. Effector site(s) consist of inductive lymphocytes that are scattered throughout the epithelium and the lamina propria (LP) of the mucosa. The organised tissues, responsible for the induction phase of the immune response are the Peyer's patches (PPs) and mesenteric lymph nodes (MLNs), as well as smaller and isolated lymphoid follicles. The lymphoid areas are separated from the intestinal lumen by a single layer of columnar epithelial cells, known as the follicle-associated epithelium (FAE), and a more diffuse area immediately beneath the epithelium, known as the sub-epithelial dome (SED) (Mowat, 2003; Spencer *et al.,* 2009; Weiner *et al.,* 2011). The FAE differs from the epithelium that covers the villus mucosa and the most notable feature of the FAE is the presence of microfold (M) cells. The FAE has lower levels of digestive enzymes, less pronounced brush border and is infiltrated by the large numbers of B cells, T cells, macrophages and dendritic cells (DCs) (Mowat, 2003) (Figure 1.3).

Image unavailable due to copyright restrictions

Figure 1.3. The intestinal mucosal immune system. A single layer of IEC provides a physical barrier that separates the intestinal lumen from the underlying LP. IECs are derived from stem cells and can differentiate into villous or colonic absorptive enterocytes, mucin producing goblet cells, enteroendocrine cells which secrete hormones, and Paneth cells at the base of the small intestine crypts. Beneath the IECs, the LP contains macrophages, DCs, B cells (especially IgA-producing plasma cells), and T cells. M cells are located in the specialised regions of the small intestine epithelium termed FAE overlying the PPs (Abreu, 2010).

M cells are specialised enterocytes that can be distinguished from the neighbouring IEC. Compared with absorptive enterocytes, M cells have less extensive apical brush border, a reduced glycocalyx and diminished expression of enzymes involved in absorption. Importantly, they have the capacity to rapidly transcytose antigens relatively intact and deliver them to antigen presenting cells (APCs) in the PPs and lymphoid cells consequently priming naive T and B cells to memory or effector cells. These cells migrate from the different lymph vessels of the GALT to the MLN and then through peripheral blood to other mucosal effector sites such as the LP. The FAE express Toll-like receptors (TLRs) and chemokines to attract antigen presenting sub-epithelial DC into the apical area of the PPs (Hershberg, 2002; Niedergang & Kweon, 2005; Wells *et al.,* 2011).

The GI tract is unique as it is the largest area of the body in constant contact with microorganisms. Virtually all entero-pathogens enter through the oral intake. In the oral cavity streptococci predominate in the resident flora. The majority of oral or food-borne bacteria are washed with saliva into the stomach, although the secreted gastric acid aims to promote sterility; however, *Helicobacter pylori* are resident in the gastric mucosa of many individuals. Digestion and absorption of nutrients continues in the small intestine (duodenum, jejunum, proximal ileum) which is relatively sterile. The last section of the GI tract is the large intestine (cecum, colon, rectum) harbouring an extensive number of resident bacterial flora consisting of different species of anaerobic and aerobic bacteria (Cunliffe & Mahida, 2004).

1.2.1.1 Intestinal Epithelium

The intestinal surface covers an area of approximately 250 m^2 and is lined by a single layer of columnar IEC that forms a barrier between the intestinal lumen and host connective tissue. IECs are in continuous contact with the gut microflora, consisting of 10^{14} microorganisms exceeding by 10-fold the total ensemble of human cells, belonging to >500 different bacterial species. The gut has been identified as one of the most densely populated habitats known in biology (Guarner & Malagelada, 2003; Sears, 2005; Pastorelli *et al.,* 2008).

1.2.1.2 Intestinal Epithelium Barrier Structure and Function

The formidable task of differentiating between pathogens and commensal microflora and eliciting the appropriate action is the responsibility of IECs and the underlying mucosal immune system. IECs form a monolayer that acts as an impermeable barrier to microbes; hence its regulation is critical in restricting access and preventing hyperactivity of the intestine (Mumy & McCormick, 2005).

The epithelium of the small intestine forms an adjacent two-dimensional sheet composed of four main epithelial cell types: absorptive enterocytes, mucin secreting goblet cells, hormones secreting enteroendocrine cells and antimicrobial peptide secreting Paneth cells, which are derived from stem cells (Figure 1.3). Following their origin from stem cells located near the crypt base, the epithelial cells (apart from Paneth cells) differentiate as

they migrate up the villus tip in 4-7 days. They are subsequently shed by apoptosis upon reaching the villus tip. In contrast to the other epithelial cell types, Paneth cells are long-lived, residing at the crypt base for approximately 20 days. There are also M cells that play a central role in sampling antigenic molecules and microorganisms and their delivery to the underlying mucosal-associated lymphoid tissue (MALT) (Cunliffe & Mahida, 2004; Colbere-Garapin *et al.,* 2007). The surface epithelium of the colon lacks villi, and Paneth cells are absent, therefore the stem cells reside directly at the crypt base occupying the bottom two-third of colonic crypts, whereas differentiated cells constitute the top third and the surface epithelium (Raedtke & Clevers, 2005).

Two main lineages of differentiated cell types are recognised within the intestinal epithelium: the enterocyte of the absorptive lineage and the secretory lineage, which encompasses goblet cells, the enteroendocrine cell, and the Paneth cells. Absorptive cells are more abundant in the small intestine and are responsible for secreting hydrolases and absorbing nutrients. Number of mucous secreting goblet cells increases from proximal (small intestine) to distal (colon and rectum). Enteroendocrine lineage cells represent a small proportion (<1%) of the IEC compartment and can be subdivided further on the basis of variety of hormones they secret including serotonin, substance P and secretin. Paneth cells exist only in the small intestine and reside at the crypt base. They secret antimicrobial peptides such as cryptidins (termed defensins in humans) and lysozyme to control the microbial content of the intestine (Raedtke & Clevers, 2005; Barker *et al.,* 2008). The intestinal epithelium in addition to forming a physical barrier composed of cell membranes and interspersed tight junctions, achieves further reinforcement of its barrier function through a chemical antimicrobial shield.

I. Physical Barrier

a) Tight junctions

The primary responsibility of the IEC is to act as a barrier and prevent the passage of harmful intraluminal entities and at the same time function as a selective filter, allowing the translocation of essential dietary nutrients, electrolytes, and water from the intestinal lumen. The IEC mediates selective permeability through two major routes; transcellular (transepithelial) and paracellular pathways. Transcellular permeability is associated with solute transport through the IEC and is regulated by selective transporters for amino acids, electrolytes, sugars, and short chain fatty acids. Paracellular permeability is defined as

transport in the space between IEC and is regulated via a series of intercellular junctions, known collectively as the epithelial junctional complex (Groschwitz & Hogan, 2009).

The epithelial junctional complex is subdivided into tight junctions (TJs), adherens junctions (AJs), and desmosomes. TJs are typically located at the apical end of the basolateral membrane forming an apical ring, whereas AJs and desmosomes are located more within the basolateral membrane and thought to be more important in the mechanical linkage of adjacent cells. The TJs, on the other hand, are responsible for sealing the intracellular space and regulating selective paracellular ionic solute transport. Both TJ and AJ are linked intracellularly to the actin cytoskeleton often seen co-localised with junctions to form a belt-like ring of filaments encircling the cell border, referred to as perijunctional actin, contrarily desmosomes are linked to intermediate filaments. TJ and AJ are also important in the regulation of cellular proliferation, polarisation, and differentiation (Groschwitz & Hogan, 2009; Terry *et al.,* 2010).

AJs also known as zonula adherens are formed by interactions between transmembrane proteins, intracellular adaptor proteins and the cytoskeleton. The majority of AJs are structured by cadherin-catenin interactions. E-cadherin, a calcium-dependent adhesion molecule, is a type I transmembrane protein composed of an intracellular C-terminus and an extracellular N-terminus. The extracellular domain interacts with the E-cadherin of the neighbouring cell promoting cell-cell adhesion. The intracellular domain contains a catenin-binding domain that interacts directly with p120 catenin and β-catenin. In turn, β-catenin binds to α-catenin 1, which regulates local actin assembly and contributes to development of the perijunctional actinomyosin ring. AJs are required for assembly of TJs, which seals the paracellular space (Groschwitz & Hogan, 2009; Turner, 2009).

The TJ complex is composed of transmembrane proteins linked to a network of adaptor proteins that form a cytoplasmic plaque, and regulatory molecules that include kinases. The transmembrane proteins mediate cell-cell adhesion and form the paracellular barrier. The adaptor proteins (such as; zonula occludens 1 (ZO-1), ZO-2, ZO-3) link transmembrane proteins to the cytoskeleton acting as scaffolds for recruitment of various signalling proteins. TJs contain two main types of transmembrane components; tetra-span and single-span transmembrane proteins. The tetra-span proteins include occludin, tricellulin, and the claudins. The single-span proteins associated with TJs are the junctional adhesion molecules (JAMs) and its related proteins coxsackievirus and adenovirus receptors (CAR) (Balda & Matter, 2008; Guttman & Finlay, 2009; Turner, 2009; Terry *et al.,* 2010). Expression of AJ

and TJ proteins are regulated by phosphorylation, which can either promote TJ formation and barrier function or alternatively cause TJ protein re-distribution and complex de-stabilisation (Groschwitz & Hogan, 2009).

Interaction between *C. difficile* TcdA and TcdB leads to disruption of IEC barrier function due to enhanced paracellular permeability (Riegler *et al.,* 1995; Sutton *et al.,* 2008). Toxins cause disorganisation of apical and basal F-actin resulting in dissociation of occludin and ZO-1 from TJ. *C. difficile* toxins inactivate Rho protein family members, therefore toxin-mediated TJ dysfunction and cytoskeletal rearrangement may result from inactivation of Rho, which is an essential regulator of filamentous actin (Hecht *et al.,* 1988; Nusrat *et al.,* 2001; Chen *et al.,* 2002).

II. Chemical Barrier

a) Mucins

The IEC physical barrier is reinforced by a membrane-anchored glycoprotein network called glycocalyx which is formed by the secretion and apical attachment of a heavily glycosylated mucin-rich layer (Artis, 2008). Mucins are highly complex glycoproteins that range from 200 to 2,000 kDa. The GI mucosal surface coated by a hydrated mucus gel creates a physical-chemical barrier that prevents large particles including microbes from directly contacting the IEC (Hecht, 1999; Turner, 2009).

b) IgA

Secretory immunoglobulin A (sIgA) is triggered by presentation of commensal antigens to B cells in GALT by intestinal DCs. In the gut lumen, IgA is continuously produced in large amounts (>5 g per day), binding predominantly to commensal bacteria and to dietary antigens (Kraehenbuhl & Corbett, 2004). IgA production will be discussed further in section 1.2.2.2.

c) Antimicrobial peptides (AMPs)

Defensins are small (2-6 kDa), arginine-rich, cationic peptides with broad spectrum antimicrobial activity. Defensins contain six conserved cysteine residues, which form three intramolecular disulfide bonds and a β-sheet structure. Cationic charge and the hydrophobic structure allow them to interact with the anionic elements (e.g. LPS) of the prokaryotic membrane, thereby entering and creating pores, causing cell lysis. On the basis

of the arrangement and spacing of the disulfide bonds, defensins are divided into two major groups; α- and β-defensins. In humans and mice, both groups are encoded by a cluster of genes on chromosome 8. They are synthesised as pre-propeptides and are post-translationally processed into mature and active peptides (Cunliffe & Mahida, 2004; Eckman, 2005).

α-Defensins

Six α-defensins have been identified in humans; these comprise four neutrophil defensisns (HNP1, -2, -3, -4) and two Paneth cell defensins (HD-5, -6). In addition to the α-defensin family in humans and mice (termed cryptdins), Paneth cells also express antimicrobial proteins such as lysozyme and secretory phospholipase A2 (sPLA2). Paneth cells play a role in maintaining the relative sterility of the lumen and/or protecting stem cells (Hecht, 1999; Cunliffe & Mahida, 2004; Cederlund *et al.,* 2011).

HNP-1-3 are potential inhibitors of bacterial toxins. HNP-1 inhibits the protease activity of lethal factor (LF) from *Bacillus anthracis*, and HNP-1-3 protects mice from intoxication (Kim *et al.,* 2005). HNP-1 has a neutralising effect on the mono-ADP-ribosyltransferase activity of diphtheria toxin and *Pseudomonas* exotoxin A (Kim *et al.,* 2006a). Recently, Giesemann *et al.* showed that HNP-1, HNP-3, and HD-5 can inhibit *C. difficile* TcdB by blocking its catalytic activity. The specificity of α-defensins in inhibiting TcdB activity was shown as hBD-1 (β-defensin) and cathelicidin LL-37 have no effect on glucosyltransferase activity of TcdB. Additionally, the inhibitory effect of α-defensins is TcdB specific, as under the same experimental conditions, TcdA activity is not affected (Giesemann *et al.,* 2008).

β-Defensins

Compared with α-defensins, members of the β-defensin subfamily (hBD-1 and hBD-2) are more widely expressed throughout the GI tract. In contrast to hBD-1, hBD-2 is not expressed constitutively by IEC, but is strongly induced in inflamed or infected tissue, particularly in patients with Ulcerative colitis. Two other members of β-defensins, hBD-3 and hBD-4 are found in colonic epithelium with higher expression in crypt compared with surface cells, however, like hBD-2, show strong inducibility by microbial and inflammatory stimuli (Hecht, 1999; Eckman, 2005).

Cathelicidins

The cathelicidin family of AMPs is not as widespread in nature as the defensin family, suggesting a more recent ancestry. Cathelicidins are cationic in which cathelin, a highly conserved N-terminal domain is linked to a C-terminal peptide with antimicrobial activity. Humans have one cathelicidin gene that encodes the pre-proprotein LL-37/human cationic protein 18 kDa (hCAP18). LL-37/hCAP18 is expressed in neutrophils, mast cells, and epithelial cells. This protein is produced in GI tract constitutively in differentiated surface and upper crypt IEC in the colon, but not in the deeper regions of the colonic crypt or IEC of the small intestine (Eckman, 2005; Cederlund *et al.,* 2011).

1.2.1.3 Pattern Recognition Receptors (PRRs)

The gut epithelium itself is able to sense commensal bacteria and pathogens directly; however, integral to this are the pattern recognition receptors (PRRs), which recognise conserved molecular structures known as pathogen-associated molecular patterns (PAMPs) and activate pro-inflammatory pathways alerting the host to microbial presence (MacDonald & Monteleone, 2005). As conserved structures are also present on non-pathogenic microorganisms (commensals), the term microbe-associated molecular patterns (MAMPs) is increasingly being used (Wells *et al.,* 2011). DCs are also known to efficiently acquire antigens by extending their dendrites into the gut lumen and directly sample and detect the luminal micro-environment by PRRs (Artis, 2008). Three major classes of PRRs studied to date are; Toll-like receptors (TLRs), Retinoic acid inducible gene I (RIG-I)-like receptors (RLRs), and nucleotide oligomerisation domain (NOD) -like receptors (NLRs) (Kawai & Akira, 2010; Wells *et al.,* 2011).

The ubiquitously expressed RLRs (RIG-I, Mda5 and LGP2) are cytoplasmic proteins that recognise viral RNAs and signal through the adaptor molecule IPS-1, inducing innate antiviral responses, including the activation of type I interferon (IFN) (Kawai & Akira, 2010). NLRs represent a large family of PRRs that recognise microbial molecules in the host cytosol. Most NLRs have three domains structure consisting of a variable amino-terminal domain, a centrally located Nod domain, and carboxy-terminal leucine-rich repeats (LRRs) domain that detect PAMPs. Nod1 and Nod2 were the first NLRs to be identified. Both have been identified as intracellular peptidoglycan (PG) receptors, which recognise different moieties of PG. Nod2 detects muramyl dipeptide (MDP) found in nearly all Gram-positive

and Gram-negative bacteria, whereas Nod1 recognises peptidoglycan fragments containing γ-D-glutamyl-*meso*diaminopimelic acid (DAP), from most Gram-negative and certain Gram-positive bacteria. Nod1 and Nod2 both possess a caspase activating and recruitment domain (CARD) at their amino-termini, a single CARD domain in Nod1 and two tandem CARD domains in Nod2, followed by a nucleotide binding domain and a series of LRRs (Kelly & Conway, 2005). Several NLRs, including NLRC4 (or IPAF), NLRP1 and NLRP3 (or NALP3) are involved in responding to various stimuli to form the inflammasome complex, which promote the release of IL-1β and IL-18 via caspase-1 (Franchi *et al.,* 2009). NLR proteins trigger a number of signalling transduction cascades including the pro-inflammatory and anti-apoptotic NF-κB (via Nod1 and Nod2), caspase-1 inflammasome (via NLRC4, NLRP3, and NLRP1) and apoptotic/pyroptotic cell death (via NLRP1 and NLRP3) (Bergsbaken *et al.,* 2009; Philpott & Girardin, 2010). Nod1 deficient mice are more susceptible to *C. difficile* infection than Nod2 deficient mice (Hasegawa *et al.,* 2011). $Nod1^{-/-}$ mice show impaired neutrophil recruitment and clearance of the bacteria consequently triggering pro-inflammatory responses and in particular IL-1β, suggesting a protective role of Nod1 against *C. difficile* infection. This data is intriguing as why PG of *C. difficile*, a Gram-positive bacterium is not being recognised by Nod2 remains to be answered.

TLRs are type I transmembrane receptors that share a high homology to the Toll receptors originally identified in *Drosophila melanogaster*. TLRs are structurally characterised by extracellular LRRs at the N-terminal domain, followed by a single transmembrane domain and an intracellular Toll/IL-1 receptor (TIR) signalling domain at the C-terminus (Mumy & McCormick, 2005). The TIR domain has no role in molecular recognition; however, it is required for interactions with TIR containing adaptor proteins, via direct TIR-TIR association. TLRs are activated following direct recognition of a wide range of MAMPs. Following ligand recognition by the LRR domain, the TIR domains transactivate leading to recruitment of the adaptor proteins and cell activation. Hence, TLRs expressed at the apical membrane of gut IECs have the ability to detect MAMPs present in the gut lumen and initiate intracellular responses (Kelly & Conway, 2005). TLRs recognise multiple MAMPs, including lipopolysaccharide (LPS) detected by TLR4, bacterial lipoproteins, lipoteichoic acids and PG by TLR2, flagellin by TLR5, unmethylated microbial CpG DNA and viruses by TLR9, double-stranded RNA by TLR3 and single-stranded viral RNA recognised by TLR7 (Iwasaki & Medzhitov, 2004). Depending on their cellular localisation, TLRs are largely divided into two subgroups. One group is composed of TLR1, TLR2,TLR4, TLR5, TLR6 and TLR11, which are expressed on cell surfaces and the second group (TLR3, TLR7, TLR8 and

TLR9) are expressed exclusively in intracellular vesicles such as early and late endosomes where they detect incoming nucleic acids (Kawai & Akira, 2010). TLRs can form complexes with various members to confer a further degree of specificity. TLR2 generally forms heterodimers with TLR1 or TLR6. TLR2-TLR1 heterodimer recognises triacylated lipopeptides from Gram-negative bacteria, whereas the TLR2-TLR6 heterodimer recognises diacylated lipopetides from Gram-positive bacteria and *Mycoplasma spp*. TLR4 forms a complex with MD-2 (myeloid differentiation protein 2), additional proteins such as CD14 and LPS-binding protein complex are also involved in forming the LPS binding (Netea *et al.,* 2004; Kawai & Akira, 2010).

Following receptor ligation, TLRs recruit cytoplasmic adaptor proteins to its TIR domain. One of the main mechanism(s) of differential downstream signalling is the selective recruitment of different adaptor proteins. All adaptors possess a conserved TIR domain which ligates via TIR-TIR interactions. Myeloid differentiation antigen 88 (MyD88) is a central adaptor required by all TLRs except TLR3, and activates NF-κB and mitogen-activated protein kinases (MAPKs) to induce host innate immune responses. MyD88 is directly recruited by most TLRs however TLR2 and TLR4 can also recruit an adaptor called MyD88 adaptor like (Mal) or TIR domain containing protein (TIRAP). Another TIR domain containing adaptor protein inducing IFN-β (TRIF), also known as Toll/IL-1 receptor domain containing adaptor molecule 1 (TICAM1), acts as an additional adaptor for TLR3 and TLR4 signalling (Netea *et al.,* 2004; Blasius & Beutler, 2010; Li *et al.,* 2010). TLR4 recruits TIRAP at the plasma membrane and subsequently facilitates the recruitment of MyD88 to trigger the initial activation of NF-κB and/or MAPK. TLR4 displays MyD88-independent signalling by recruiting TRIF and forming a signalling complex with TRIF related adaptor molecule (TRAM), also known as TICAM2, which serves as a bridging adaptor to initiate the TRIF-dependent pathway that leads to IRF3 (Interferon regulatory factor 3) activation as well as the late-phase activation of NF-κB and MAPK and consequently induction of type I interferon and inflammatory cytokines (Kawai & Akira, 2010; Kelly & Conway, 2005; Li *et al.,* 2010).

Taken all together, the host innate immune system has evolved to detect microbial presence via signature motif recognising receptors that lead to an array of signalling events which culminate in early host defence and simultaneously activate the adaptive immune system for future encounters.

1.2.2 Acquired Mucosal Immune Response

The GI mucosal immune system consists of multiple cell types. The IECs are the first layer of defence lining the luminal surface of the GI tract, while DCs interlinked among the intestinal cells, are capable of sampling the luminal contents and presenting antigens to T cells in the lamina propria and lymphoid follicles. In the small intestine, specialised M cells residing in the FAE above the PPs transport antigens via transcytosis to the PPs, where APCs process and present them to naive lymphocytes (Abreu *et al.,* 2005). DCs are the most effective APC involved in this process, bridging the innate and acquired immunity. TLRs expressed on the surface of different DC subsets in PPs leads to differential responses, subsequently initiating an appropriate T and B cell-mediated immunity (Iwasaki & Medzhitov, 2004; Netea *et al.,* 2004).

DCs are continuously produced from haematopoietic stem cells within the bone marrow and can be divided into subsets according to surface marker expression, specialised function(s) and tissue distribution. Human and mouse DCs are different both in their ontogeny and function. In humans, two types of DC have been described; myeloid and plasmacytoid. While all murine DCs express CD11c integrin, they can be subdivided into three classes according to their surface markers and location including; CD8α, CD4 and B220/Gr1 (Rescigno, 2002; Ardavin, 2003). Immature DCs are found in all peripheral tissues where they efficiently capture foreign and self antigens, whereas mature DCs are primarily found in lymphoid tissues (Banchereau & Steinman, 1998). Immature DCs exposed to microbial products, mature and migrate to the T cell area of secondary lymphoid organs such as MLNs, where they activate naive T cells. Activation and maturation of DCs occurs upon recognition of phylogenetically conserved MAMPs, by expression of PRRs such as TLRs, C-type lectins, and mannose receptors. DCs also express the NLR receptor family which include nucleotide-binding oligomerisation domain proteins NOD1 and NOD2 (Niess & Reinecker, 2006). Immature DCs begin a maturation program in response to antigen which induces their migration to lymphoid organs. Ultimately, mature DCs present the antigenic peptides in the context of the major histocompatibility complex (MHC) molecules and express the co-stimulatory molecules, leading to secretion of cytokines that will aid activation of antigen-specific T cells (Niedergang & kweon, 2005).

1.2.2.1 T cells

$CD4^+$ T cells are central to host adaptive immune responses. Naive $CD4^+$ T cells differentiate into a range of T helper (Th) cells, which are classified on the basis of their cytokine profile and related to the function of the specific T cell subset. Th1 cells produce interferon-γ (IFN-γ) and interleukin-2 (IL-2) and their development is controlled by transcriptional factor T-bet (T-box expressed in T cells). Th1 cells also provide help to $CD8^+$ T cells and macrophages to kill cells infected with viruses and intracellular pathogens (Szabo *et al.,* 2000; Malefyt, 2009). Th2 cells function via; IL-4, IL-5, IL-10, IL-13 and IL-25. The key regulator of Th2 commitment is the transcription factor GATA3 (GATA-binding protein 3). Th2 cells provide help to B cells leading to their activation and differentiation into secretory immunoglobulin producing cells. Th2 cells eliminate extracellular bacteria and regulate B cell class switching to IgE through IL-4 (Paul & Zhu, 2010). IL-5 and IL-13 play a pivotal role in recruiting eosinophils, a cell type crucial for parasite elimination.

In recent years additional T cell subsets including Regulatory T cells (Treg), Th17, and Th9 cells have been identified. Several types of Treg cells have been described on the basis of their origin, generation, and mechanism of action. Two main subsets are: naturally arising $CD25^+CD4^+$ Tregs, which express the transcription factor forkhead box p3 (Foxp3) and inducible Tregs, which develop in the periphery from $CD4^+$ T cells exposed to various signal such as regulatory cytokines or APCs conditioned by bacterial products. Inducible Tregs include populations of T regulatory 1 (Tr1), which secrete IL-10; transforming growth factor (TGF)-β producing cells; and inducible $Foxp3^+$ Tregs. Both Tregs (natural or inducible) have the capacity to control the intensity of effector responses (Belkaid & Tarbell, 2009; Campbell & Koch, 2011). T cell subsets that produce IL-17A, IL-17F, IL-22, and CCL20 are designated Th17. Combination of IL-6 and TGF-β acts in concert to differentiate naive $CD4^+$ T cells to Th17, interestingly in the absence of IL-6, Tregs can be generated *in vitro*, proposing an intriguing link between Th17 and Tregs. The orphan nuclear receptor RORγt (retinoic acid receptor related orphan receptor-γt) is the key lineage defining transcription factor for Th17 cells, downstream signalling for Th17 differentiation depends on Stat3 (signal transducers and activators 3) activation. IL-17 is important in the host defence against extracellular bacteria such as *Klebsiella pneumoniae*, *Bacteroides fragilis* and against fungi like *Candida albicans*; however, pathogens such as *Borrelia burgdorferi*, which stimulates IL-17 expression causes development of autoimmunity (Stockinger & Veldhoen, 2007, Stockinger *et al.,* 2007). Combination of TGF-β and IL-4 induce the differentiation of

naive murine $CD4^+$ T cells into a unique IL-9 producing Th9 subset. Both human and murine Th9 cells do not co-express cytokines that are characteristics of other Th subsets; however, in contrast to murine, IL-10 is not expressed by human Th9 cells. Although the exact function of this subset of effector Th cells has yet to be defined, it has been proposed that Th9 cells may provide additional help for mast cells through the production of IL-9 (Malefyt, 2009; Ma *et al.,* 2010).

In the presence of appropriate signals, naive T cells can differentiate into any of the distinct T cell subsets. IL-12, a heterodimeric cytokine composed of p35 and p40 subunits, is a key inducer and growth factor for polarised Th1 responses and moreover promotes survival, differentiation, and gene expression of Th1 cells. An IL-12 family member, IL-23 shares the p40 subunit of IL-12. IL-23 is a heterodimer composed of p40 and a unique subunit p19, this cytokine plays an important role in maintaining Th17 effector function whilst another IL-12 family member IL-27 composed of; p35-related protein p28 and a p40-related protein EBI3 (Epstein-Barr virus induced gene 3), is involved in early initiation of Th1 responses antagonising development of Th17 cells (Brombacher *et al.,* 2003; Reiner, 2007; Stockinger & Veldoen, 2007; Malefyt, 2009). All three IL-12 family members are produced by DCs in response to stimuli. This family is central to the nature of the downstream T cell immune outcome and several novel therapies for autoimmune diseases including rheumatoid arthritis (RA) and inflammatory bowel disease (IBD) are targeting the IL-12 family.

Several studies have shown that *C. difficile* toxins can interact with T cells directly or indirectly via monocytes. T cell apoptosis following exposure to TcdA suggests a direct interaction between T cells and the toxin, which is concomitant with reduced T cell proliferation and suppressed mucosal immune response (Mahida *et al.,* 1998). On the other hand, toxins are found to markedly reduce the capacity of toxin treated-monocytes to stimulate T cell proliferation implying that *C. difficile* toxins interact only with monocytes (Daubener *et al.,* 1988). Additionally, T and B cells are shown to be relatively more resistant to *C. difficile* toxins compared to the innate immune cells (monocytes/macrophages and IECs), suggesting that antibody-mediated protection by the adaptive immune system may be of major importance during exposure of the host to high concentrations of *C. difficile* toxins (Solomon *et al.,* 2005).

1.2.2.2 B cells

B lineage cells are the central mediators of humoral immunity and critical component(s) of the adaptive responses. B cell activation is initiated following antigen recognition via the B cell receptor (BCR), resulting in B cell proliferation and differentiation. Activated B cells differentiate to form either plasma cells, which are capable of secreting antibody or memory cells that provide long-lasting protection against secondary infection (Harwood & Batista, 2010). Antibodies released by effector B cells and plasma cells provide the first line of protection at mucosal surfaces. In the GI tract the vast majority of mucosal cells secrete IgA and to a lesser extent IgM but no IgG, whereas the respiratory and urogenital tracts contain equal amounts of IgA and IgG and some IgM. In humans, the respiratory tract also contains IgD. Both IgA and IgM interact with the polymeric Ig receptor (pIgR), an antibody transporter expressed on the basolateral surface of IEC. After binding to pIgR, IgA and IgM dimers translocate to the IEC surface, thus generating secretory IgA (sIgA) and sIgM. IgG antibody gains access to respiratory and urogenital secretions through two mechanisms; specifically via an antibody transporter known as nFcR (neonatal Fc receptor), and a nonspecific mechanism. IgD enters respiratory secretions through an unknown mechanism (Cerutti *et al.,* 2011a).

In the GI tract, sIgA plays multiple protective roles include: entrapping dietary antigens and microorganisms in mucus, down-modulating the expression of pro-inflammatory bacterial epitopes on commensal bacteria, blocking microbial components attachment to the epithelia and facilitating intra-epithelial neutralisation of incoming pathogens and microbial inflammatory products. Furthermore, IgA dimers secreted locally by plasma cells remove microorganisms that have breached the epithelial barrier either by transporting them back to the lumen or by promoting their clearance via an IgA receptor expressed by DCs, neutrophils, and other phagocytes (Cerutti & Rescigno, 2008). B cells express IgA antibody responses via two different pathways: low affinity IgA production from extra-follicular B cells (peritoneal B-1 cells and splenic marginal zone B cells) in a T cells-independent (TI) fashion, and high affinity IgA production from follicular B cells (also called B-2 cells) in a T cell-dependent manner (TD). Antigens that trigger TI pathway do not require $CD4^+$ Th cells to activate B cells, and include microbial TLR ligands (type-1) and microbial polysaccharides with repetitive structure (type-2) (Cerutti *et al.,* 2011b). Most antigens initiate mucosal IgA responses through a TD reaction that occur in mucosal lymphoid follicles such as, intestinal PP and MLN via the expression of a B cell specific enzyme [activation-induced cytidine

deaminase (AID)] that is required for diversification of Ig genes through class-switch DNA recombination (CSR). Also PPs are rich in TGF-β, a potent IgA-inducing factor. TGF-β associates with CD40 ligand (CD40L), a tumor necrosis factor (TNF) family member expressed by $CD4^+$ T cell and triggers IgA CSR to generate antigen-specific IgA^+ B cells. PPs also contain IL-4, IL-6 and IL-10 facilitating the expansion of IgA-expressing B cells. In T cell-rich regions of the PP, a migrated antigen-loaded DC can initiate a polarised Th2 response. Requirement of this response is ''conditioning'' of DCs by IEC through thymic stormal lymphopoietin (TSLP). TSLP, an IL-7 like cytokine, stimulates IL-10 production from DCs, an IgA-inducing cytokine and inhibits the generation of proinflammatory Th1 cells releasing IFN-γ by blocking DC production of IL-12, which is essential to initiate Th1 responses (Cerutti & Rescigno, 2008; Cerutti *et al.,* 2011a). As the conventional TD pathway requires a longer time (5-7 days) to initiate protective antibody responses, the intestinal mucosa has developed a faster TI pathway that generates IgA response to TLR activation. DC and IEC recognise microbial components and respond by releasing B cell-activating factor of the TNF family (BAFF) and a proliferation-inducing ligand (APRIL). BAFF and APRIL, B cell-stimulating factors are structurally and functionally related to CD40L and deliver CD40-independent IgA CSR-inducing signals via transmembrane activator and calcium modulating cyclophilin-ligand interactor (TACI). An important property of this receptor is establishing a close cooperation with B cell-intrinsic signals from TLRs (Cerutti & Rescigno, 2008; Cerutti *et al.,* 2011a; Cerutti *et al.,* 2011b).

Studies have demonstrated that colonic biopsies from patients with CDI have significantly fewer mucosal macrophages and B plasma cells, which was mainly due to reduction in IgA producing cells. It has been hypothesised that individuals with low numbers of IgA producing cells show severe mucosal inflammation following acquired initial infection. Patients with a single episode have significantly higher serum IgG and faecal IgA antitoxin A antibody titre than patients with recurrent CDI (Warny *et al.,* 1994; Johal *et al.,* 2004b). High serum IgG antibody levels against TcdA correlates strongly with asymptomatic carriage of *C. difficile*, while colonised patients with low IgG antibody levels have increased risk of *C. difficile* diarrhoea. Additionally, patients with a single episode of *C. difficile* diarrhoea have significantly higher concentration of serum IgM and IgG anti-TcdA, by day 3 and day 12 of disease onset, when compared to patients with relapsing CDI (Kyne *et al.,* 2000; Kyne *et al.,* 2001). High IgM antibody response to *C. difficile* SLPs markedly reduces the risk of recurrent CDI (Drudy *et al.,* 2004).

AIMS & HYPOTHESIS

In this thesis it was hypothesised that both bacterial virulence and host factors contribute to *Clostridium difficile* mediated pathogenesis. This study addressed the following aims:

- Microbial characterisation of *C. difficile* strains and their cytotoxic effects on human IECs (Chapter 3).
- *In vitro* and *ex vivo* innate immunity response(s) of human intestinal epithelia to *C. difficile* infection (Chapter 4).
- The role of TLRs in *C. difficile* recognition (Chapter 5).
- *C. difficile*-mediated murine and human DC activation and *C. difficile*-stimulated BMDC effects on T cell proliferation (Chapter 6).
- Effect of *C. difficile* toxins on murine and human DC activation (Chapter 7).

Chapter 2

Materials and Methods

2.1 Bacterial Culture

2.1.1 Bacterial Strains and Growth Conditions

C. difficile strains were cultured on Brain Heart Infusion (BHI) Agar (Oxoid, Basingstoke, UK) or pre-equilibrated BHI broth (Oxoid) containing *C. difficile* selective supplement (Oxoid) and 0.05% cysteine (Sigma-Aldrich, Poole, UK). BHI agar was supplemented with 5% difibrinated horse blood (Oxoid). All bacterial cultures were grown in an anaerobic chamber (Don Whitley Scientific, Shipley, UK) in an atmosphere of 10% CO_2, 10% H_2, and 80% N_2 at 37 °C. *C. difficile* strains used throughout this study are described at Table 2.1.

2.1.2 Bacterial Stock Culture Preparation

Bacterial stocks of *C. difficile* strains were maintained by suspending bacterial cell suspension or isolated colonies in either 30% glycerol or microbank (Pro-Lab, Neston, UK) and stored at -70 °C. The cultures were resuscitated by removing a loopful of glycerol stock or a single bead from microbank to inoculate a BHI agar plate. Plates were incubated in the anaerobic atmosphere at 37 °C for 48 h. To prepare bacterial broth culture, 15 ml pre-equilibrated BHI broth was inoculated with a single colony. Cultures were grown anaerobically shaking at 50 rpm until stationary phase was achieved.

Bacterial strains	Produced toxins	Ribotype	Reference/Source
027	A^+B^+, CDT^+	027	P. Mullany, Eastman Dental Institute, UCL
R20291	A^+B^+, CDT^+	027	Stoke Mandeville Hospital, UK , 2006
R20291 *tcdA*	A^-B^+, CDT^+	027	N. Minton, University of Nottingham, UK
R20291 *tcdB*	A^+B^-, CDT^+	027	
R20291 *cdtA*	A^+B^+, $CDTa^-$	027	
R20291 *cdtB*	A^+B^+, $CDTb^-$	027	
630	A^+B^+	012	Sebaihia *et al.,* 2006
630 Δerm	A^+B^+	012	Hussain *et al.,* 2005
630 Δerm *tcdA*	A^-B^+	012	Kuehne *et al.,* 2010
630 Δerm *tcdB*	A^+B^-	012	
630 Δerm *tcdA tcdB*	A^-B^-	012	
M68	A^-B^+	017	Stabler *et al.,* 2006
CF5	A^-B^+	017	
CF2	A^-B^+	017	R. Stabler, London School of Hygiene and Tropical Medicine, London, UK
CF3	A^-B^+	017	
CD586	A^-B^+	017	Lewisham isolates
CD816	A^-B^+	017	R. Stabler, London School of Hygiene and Tropical Medicine, London, UK
CD636	A^-B^+	017	
CD37	A^-B^-	undetermined	P. Mullany, Eastman Dental Institute, UCL Wust & Hardegger, 1983

Table 2.1. List of *C. difficile* strains employed in this study. Strains were selected from three different ribotypes including; 027 (hypervirulent), 012 (epidemic), and 017 (A^-B^+) strains. Strains 027, R20291, 630, 630 Δerm and CD37 were kindly given by Prof. Mullany and R20291 and 630 Δerm toxin mutant strains were kindly provided by Prof. Minton. Ribotype 017 strains were a kind gift from Dr. Stabler.

2.1.3 *C. difficile* Growth Kinetics

To establish *C. difficile* strain growth curves, a starter exponential phase culture was prepared by inoculating three single colonies into 10 ml pre-warmed BHI broth (shaking at 50 rpm) in the anaerobic workstation at 37°C. When an optical density at 600 nm (OD_{600}) of 0.3-0.4 was reached, cultures were diluted 1:10 in 15 ml of pre-equilibrated BHI broth in a 25 cm^2 cell culture flask (Nunc, Roskilde, Denmark) and grown shaking at 50 rpm (Dawson *et al.,* 2008). OD_{600} was measured by spectrophotometer (Pharmacia Biotech, Ultrospec 2000 UV/visible) at intervals of 1 h to monitor bacterial growth. Colony forming unit (cfu) counts were determined at 0.5, 1.00, and 1.5 OD_{600} by 10-fold serially diluted bacterial cultures in Dulbecco's Phosphate-Buffered Saline (PBS) (Invitrogen/Gibco, Paisley, UK). Dilutions were plated on blood agar base (Oxoid) supplemented with 7% difibrinated horse blood. Plates were incubated in the anaerobic chamber for 48 h. The number of colonies were counted and presented as cfu/ml.

2.1.4 *C. difficile* Survival under Aerobic Conditions

Since majority of the co-culture experiments presented in this thesis were performed in an aerobic environment (5% CO_2) it was imperative to examine *C. difficile* tolerance to oxygen. Pre-warmed BHI broths were inoculated with a single bacterial colony. Bacterial cultures were grown in the anaerobic chamber at 37 °C till stationary phase was achieved. Then stationary phase bacterial cultures were exposed to aerobic conditions (5% CO_2). Bacterial survival was enumerated by cfu counting over time.

2.1.5 *C. difficile* Sporulation

Sporulation of *C. difficile* strains were examined by using yeast peptone medium (YPM) and BHI media. YPM consisted of; 16.00 g peptone (Sigma-Aldrich), 10.00 g yeast (Sigma-aldrich), and 5 g NaCl/L of H_2O_2. Medium was autoclaved at 121 °C for 15 min. Pre-warmed YPM and BHI were inoculated with a colony of *C. difficile* and grown anaerobically at 37 °C for 10 days. A portion of bacterial culture was diluted 1:1 with either PBS or ethanol (to kill vegetative cells) for 1 h. Total number of bacteria (vegetative and spore) was enumerated in PBS-treated cultures and number of spores were determined by cfu counting in ethanol-

treated cultures. The remaining bacterial cultures were incubated aerobically (5% CO_2) at 37 °C to monitor spore formation. Spores were enumerated at 8 h post-exposure to oxygen.

The generated spores were stained by the Wirtz-Conklin staining method (Hamouda *et al.,* 2002; Ochsner *et al.,* 2009). The spore suspension was fixed on a glass slide with a Bunsen flame then stained with 5% Malachite Green (Sigma-Aldrich). Slides were heated for 5 min ensuring that the dye remained hot (but not boiling) then rinsed with water and counterstained with 0.5% Safranin-O (Sigma-Aldrich) for 1 min. After drying, the slides were examined for endospores by light microscopy (20x Leica GMBH, QImaging digital camera). Spores were stained in bright green/blue and vegetative cells in pink.

2.1.6 *C. difficile* Toxin Gene Detection

To detect *C. difficile* toxin genes, three colonies of each bacterial strain (grown on a BHI agar plate) were resuspended directly in 15 µl of Lyse-N-Go (Thermo Scientific, Northumberland, UK) PCR reagent. Table 2.2 outlines the thermal cycle programme that was performed to lyse the cells and release the total DNA.

Cycle #	Temperature (°C)	Time
1	65	30 sec
2	8	30 sec
3	65	90 sec
4	97	180 sec
5	8	60 sec
6	65	180 sec
7	97	60 sec
8	65	60 sec
9	80	hold

Table 2.2. Thermal cycle programme to release the total DNA.

Template nucleic acid (5 µl) was added to a PCR mixture [total 50 µl; 5 µl 10x ThermoPol Buffer, 2 µl Nucleotide Solution Mix (final concentration of 200 uM each dNTP), 1 µl (5000 u/ml) Taq DNA Polymerase, 200 pmoles of each primer (Tables 2.3), and H_2O up to 50 µl (New England Biolabs, Herts, UK)]. Reactions were subjected to 25 cycles of 95 °C for 30 sec, 54 °C for 90 sec and 72 °C for 2 min. PCR products were separated on a 1% agarose gel (Invitrogen/Gibco) in 1x Tris-Acetate-EDTA buffer (TAE) (Sigma-Aldrich). 1kb ladder (New England Biolabs) was used as DNA molecular weight (MW) marker.

Tables 2.3 describe the primers, which used to amplify regions of *tcdA* and *tcdB*, and binary toxin genes.

	Forward	**Reverse**
tcdA	5'-GAGGATCCGGCGATATAGATAATAAAG-'3	5'-CTGGATCCAAGGTAAGATGAGTATAC-'3
tcdB	5'- CAGGATCCATCTATGAGTCAAGAC-'3	5'- CTAAGCTTGGTATACCTGCTG-'3
cdtB	5'-CTTAATGCAAGTAAATACTGAG-'3	5'-AACGGATCTCTTGCT TCAGTC-'3
BIN 5/6	5'-AATATTGGGAGGGAGAATAAATG-'3	5'-TGTATTTTCATTGTTTCTCCTCC-'3
BIN 7/8	5'- ATTGTTGATGCAACATTGATACC-'3	5'-AATATATAT TGTATTGAGGGGAC-'3

Table 2.3. List of primers to amplify regions of *tcdA*, *tcdB* and binary toxin genes. *tcdA* and *tcdB* primers were in-house design. A specific region of *cdtB* gene was amplified using *cdtB* primer (forward position, *cdtB* 368-389; reverse position, *cdtB* 878-858) (Stubbs *et al*., 2000). *BIN5/6* and *BIN7/8* primers were utilised to amplify the entire *cdtA* and *cdtB* genes respectively (Spigaglia *et al.,* 2002).

2.1.7 *C. difficile* Toxin Detection by Western Blotting

Bacterial cultures grown to stationary phase were centrifuged at 2500 rpm for 15 min. Protein concentration was determined in bacterial pellets and supernatants by performing a Bradford assay (Sigma-Aldrich) per manufacture's instruction. Briefly, 1 part of the samples (blank, protein standards, and bacterial proteins) were mixed with 30 parts of the Bradford Reagent. Protein standard was prepared by serially diluting 1 mg/ml Bovine Serum Albumin (BSA, Sigma-Aldrich) with distilled water. The absorbance was measured at 595 nm (FLUOstar OPTIMA, BMG LABTECH GmbH, Germany). Protein concentration was determined by comparison of the bacterial proteins to the standard curve created using BSA.

Samples in laemmli buffer (Table 2.4) were boiled at 95-100 °C for 5 min and subjected to 6% SDS-PAGE (6% resolving and 4% stacking, Table 2.5) in a Mini-Protean® 3 Cell unit (BioRad Laboratories, Hemel Hempstead, UK). Table 2.6 describes buffers used in this procedure.

2x Laemmli Buffer	
0.5M Tris-HCl (pH 6.8)	2.5 ml
10% SDS	4 ml
Glycerol	2 ml
0.1% Bromophenol blue	0.5 ml
β-mercaptoethanol	2.5-5%
MilliQ water	1 ml
Total volume	10 ml

Table 2.4. Composition of 2x Laemmli buffer.

	6% Resolving Gel	**4% Stacking Gel**
MilliQ water	5.3 ml	7.2 ml
Gel buffer	2.6 ml	1.35 ml
30% Acrylamide	2 ml	1.33 ml
APS	100 µl	100 µl
TEMED	10 µl	10 µl
Total volume	10 ml	10 ml

Table 2.5. Composition of 6% Tris SDS gels.

Resolving Gel Buffer		**Stacking Gel Buffer**	
Tris 10% SDS MilliQ water pH	18.2 g 4 ml 100 ml 8.8	Tris 10% SDS MilliQ water pH	6.6 g 4 ml 100 ml 6.3
10x Gel Running Buffer		**10x Transfer buffer**	
Tris Glycine SDS MilliQ water pH	30.3 g 144.1 g 10 g 1 L 8.3	Tris Glycine MilliQ water	30.27 g 144.1g 1 L

Table 2.6. List of buffers used for SDS-PAGE and western blotting.

5 µl of SeeBlue® Plus2 Pre-Stained Standard (Invitrogen, Paisley, UK) was included to determine the MW and as a visual check for transfer efficiency. Gels were electrophoresed at 110 V (BioRad PowerPac 3000, BioRad Laboratories) for 5 h at 4 °C. Proteins were transferred to a nitrocellulose membrane (Amersham Hybond ECL membrane, GE Healthcare, Little Chalfont, England) using a wet transfer system (BioRad Laboratories) at 400 mA for 90 min at 4 °C. Post-transfer, non-specific binding was blocked by incubating the membrane in the blocking buffer [5% dried skimmed milk (Marvel, UK) in 0.1% Tween 20 (Sigma-Aldrich)-PBS] overnight at 4 °C on a shaker. This was followed by a single wash with 0.1% Tween 20-PBS for 5 min, the membrane was incubated with primary goat anti-TcdA or anti-TcdB antibody (kindly provided by Prof. Brendan Wren, London School of Hygiene and Tropical Medicine; 1:1000), in blocking buffer overnight at 4 °C on a shaker.

Membrane was washed 3x with 0.1% Tween 20-PBS for 5 min each, the blot was incubated with secondary antibody (Polyclonal rabbit anti-goat Ig/HRP; Dako, Denmark; 1:2000) overnight at 4 °C on a shaker. Blots were washed 3x with 0.1% Tween 20-PBS for 10 min. Toxins were detected using an enhanced chemiluminescence (ECL) reaction (Amersham ECL Western blotting detection reagent, GE Healthcare) followed by autoradiography film (Film CL-Xposure, Thermo Scientific, Loughborough, UK). The membranes were developed with an automated X-ray film developer (Autorad).

2.1.8 *C. difficile* Toxin Cytotoxicity Assay

C. difficile strains were grown to stationary phase in BHI broth. Bacterial cultures were centrifuged and supernatants filter sterilised (0.22 µm filter; Millipore, UK). Human colonic epithelial cell-line HT-29, and African green monkey kidney cells, Vero (see section 2.2.1) cells were seeded at a concentration of $1.5x10^5$ and $0.5x10^6$/ml. Semi-confluent HT-29 and confluent Vero cells were co-cultured with 2-fold serially diluted bacterial supernatants. Morphological changes 8 h post-infection were observed by microscopy. The cytopathic effect (CPE) was determined by comparing infected cells to uninfected control cells scoring each dilution on a scale from 0 to +4. A Nickon TMS inverted phase contrast microscope was used to visualised the cells at 40X magnification.

2.1.9 Analysis of Rac1 Glucosylation and Inflammasome Activation

2.1.9.1 Rac1 Glucosylation

A human ileocecal epithelial cell-line, Caco-2 (see section 2.2) was infected with strains CF5 and M68 bacterial culture and Caco-2 Rac1 glucosylation was investigated by western blotting. Cells were seeded at a concentration of $5x10^4$/ml and grown to form a monolayer. Cells were infected with stationary phase bacterial cultures at an MOI of 250 for 8 h.

2.1.9.2 Inflammasome Activation

Pro- and activated caspase-1 and pro- and mature IL-1β were detected in *C. difficile* infected murine bone-marrow-derived dendritic cells (BMDCs) (see section 2.3).

Cells were washed once with ice-cold PBS then lysed using ice-cold lysis buffer (Table 2.7) for 15 min. Cell suspensions were centrifuged (4 °C, 20 min, 12000 rpm). Supernatants were aspirated and subjected to 15% SDS-PAGE. 10 µl of ColorPlus PreStained Protein Ladder (New England, BioLabs) was used as MW marker. Gels were electrophoresed at 110 V for 1.5 h. Proteins were transferred to a PVDF transfer membrane (Amersham Hybond^{TM}-P, GE Healthcare) using a wet transfer system at 400 mA for 45 min. Blots were blocked by incubation in blocking buffer overnight at 4 °C on a shaker. This was followed by a single

wash with 0.1% Tween 20-PBS for 5 min, the membrane was incubated with primary antibody (Table 2.8) in blocking buffer overnight at 4 °C on a shaker.

Membrane was washed 3x with 0.1% Tween 20-PBS for 5 min and incubated with secondary antibody (Polyclonal rabbit anti-mouse Ig/HRP; Dako, Denmark; 1:2000 or Polyclonal goat anti-rabbit Ig/HRP; Dako; 1:2000) overnight at 4 °C on a shaker. Blots were washed 3x with 0.1% Tween 20-PBS for 10 min/wash prior to ECL detection. Rac1 was quantified densitometrically (BioRad ChemiDoc XRS, Bio-Rad Quantity One 1-D Analysis software, Hertfordshire, UK).

To detect β-actin, membranes were stripped using stripping buffer (Table 2.7) heated at 50 °C for 30 min. Blots were washed with 0.1% Tween 20-PBS and incubated in blocking buffer overnight at 4 °C on a shaker. Membranes were washed and incubated with primary rabbit β-actin monoclonal antibody (Cell Signaling Technology, Danvers, USA; 1:1000), in blocking buffer overnight at 4 °C on a shaker. Blots were incubated with secondary antibody (Polyclonal goat anti-rabbit Ig/HRP; Dako; 1:2000) overnight at 4 °C on a shaker subsequently membranes were washed and detected for β-actin.

Lysis Buffer		**Stripping Buffer**	
1.5M Tris	333 µl	0.5M Tris-HCl	5 ml
1% Triton X-100	100 µl	10% SDS	8 ml
0.5M NaCl	3 ml	β- mercaptoethanol	280 µl
pH	8.0	MilliQ water	Up to 40 ml
MilliQ water	Up to 10 ml		

Table 2.7. Composition of lysis and stripping buffers. Lysis buffer were supplemented with a protease inhibitor cocktail tablet (Roche, Burgess Hill, UK).

Primary antibody	MW	Dilution
Mouse anti-Rac1 (clone 102)	21 kDa	1:1000
Caspase-1 p10 (M-20): sc-514 Polyclonal rabbit anti mouse	prodomain: 10 kDa precursor: 45 kDa	1:500
IL-1β (H-153): sc-7884 Polyclonal rabbit anti human	mature: 17 kDa precursor: 31 kDa	1:500

Table 2.8. Antibodies used to detect Rac1, caspase-1 and IL-1β. Rac1 antibody was from BD Biosciences, USA. Both caspase-1 and IL-1 β antibodies were from Santa Cruz Biotechnology, inc., USA.

2.2 Mammalian Cell Culture

2.2.1 Mammalian Cell-lines

Caco-2 (American Type Culture Collection, HTB-37) and HT-29 (ATCC, HTB-38) human intestinal epithelial cell-lines and Vero (ATCC, CCL-81) African green monkey kidney cells were grown in Dulbecco's Modified Eagle Medium with GlutaMAX- I (DMEM) (Invitrogen/Gibco). T84 (ATCC, CCL-248) a human colonic carcinoma cell-line was grown in Dulbecco's Modified Eagle's Medium Nutrient Mixture F-12 HAM (Sigma-Aldrich). All media were supplemented with 10% fetal calf serum (FCS, Invitrogen/Gibco), 1% L-glutamine (Invitrogen/Gibco), 1% penicillin-streptomycin solution (Invitrogen/Gibco), and 1% non-essential amino acids (Invitrogen/Gibco). This media is referred as ''complete'' media. Cultures were maintained at 37 °C in 5% CO_2. Confluent cell-lines were routinely passaged by briefly rinsing with PBS (Invitrogen/Gibco) before detaching cells with 3 ml of trypsin-EDTA (Invitrogen/Gibco) for 2-3 min. This was followed by the addition of 10 ml complete DMEM. Cells were centrifuged (2000 g, 5 min) and pellets were resuspended in 10 ml of complete media. Subsequently, cells were subcultivated at a ratio of 1:5 to 1:10 as required. The T84 cell pellet was resuspended in 10 ml of complete DMEM F-12 Ham then subcultivated at a ratio of 1:2 to 1:4.

2.2.2 Lactate Dehydrogenase (LDH) Release Assay

Caco-2 monolayers and semi-confluent HT-29 cells were incubated with stationary phase bacterial cultures at an MOI of 10, 100, and 1000 for 8 h and 24 h. Co-culture supernatants were analysed for LDH release using Cytoscan-LDH Cytotoxicity assay kit (GBiosciences, St Louis, USA) according to manufacturer's instruction. Briefly, supernatants were centrifuged to remove particulates then 50 µl were transferred into 96-well flat bottom plates (Nunc). The reconstituted substrate mix was prepared as instructed and 50 µl of solution was added to each well. Plates were covered with foil and incubated at 37 °C for 20 min. 50 µl of Stop Solution was added to each well and absorbance was recorded at 490 nm (FLUOstar Optima). Cytotoxicity percentage was calculated as follows:

% Cytotoxicity= Experimental (OD_{490}) - Negative control (OD_{490}) / Maximum LDH release (OD_{490}) x 100

2.2.3 Ethidium Homodimer Uptake Assay

Human IEC death in response to *C. difficile* infection was evaluated by the ethidium homodimer uptake method using the Live/Dead viability/cytotoxicity kit (Invitrogen). Caco-2 cells were grown on Poly-L-lysine (Sigma-Aldrich) coated coverslips then monolayers were infected with stationary phase bacteria at an MOI of 250 for 8 h at 37 °C in 5% CO_2. 200 µl of the combined Live/Dead assay reagents (2 µM calcein-AM, 4 µM EthD-1) was added and incubated for 30 min at room temperature (RT). Following incubation, coverslips were mounted on the microscope slide and sealed. Labelled cells were observed under the fluorescence microscope (100x Leica DMLB).

2.2.4 Annexin-V & Propidium Iodide (PI) Staining

Caco-2 monolayers were infected with bacterial culture at an MOI of 250. At 6 h post-infection cells were washed with PBS and detached with acutase (PAA Laboratories GmbH, Austria). Cells were transferred into a tube and centrifuged at 200 g for 5 min. Cell pellets were resuspended in 100 µl of Annexin-V-FLUOS (Roche) labelling solution containing 20 µl Annexin-V-Fluos labelling reagent in 1 ml incubation buffer and 20 µl Propidium iodide solution. Cell suspension was incubated 10-15 min at RT then analysed by flow cytometry.

2.2.5 *C. difficile* Adherence Assay

Prior to co-culture, bacteria were labelled with Fluorescein isothiocyanate (FITC; Sigma-Aldrich). Saturated solution of FITC was prepared in PBS then filter sterlised. Bacterial cultures were diluted with FITC solution at ratio of 1:1 and incubated at 37 °C for 10 min. Solution mix was centrifuged (12000 rpm, 2 min) and supernatant aspirated. The labelled bacterial pellet was washed 3x with PBS. To detect efficiency of the labelling procedure, labelled and unlabelled bacteria were washed with PBS and then fixed in 4% Paraformaldehyde (4% PFA was dissolved in PBS by heating at 65 °C for 45 min, aliquots were stored at -20 °C) for 10-15 min at RT. Bacteria were washed and resuspended in FACS wash buffer (PBS, 1% FCS and 0.1% sodium azide) prior to analysis by flow cytometry.

FITC-labelled bacteria were co-cultured with Caco-2 monolayers at an MOI of 250. At 6 h post-infection cells were washed, detached by acutase and centrifuged at 2000 rpm for 5

min. Cell pellets were washed twice with PBS then fixed in 4% PFA. Cells were resuspended in FACS wash buffer and analysed by flow cytometry and analysed using FlowJo software (Tree Star).

2.2.6 Confocal Imaging

To detect degree of *C. difficile* adhesion/invasion to IEC, confocal imaging was utilised. Caco-2 monolayers were infected with FITC-labelled bacteria at an MOI of 250 for 8 h. Co-cultures were examined by epifluorescence on an inverted LSM710 confocal system mounted on an AxioObserver Z1 microscope (Carl Zeiss Ltd, UK). The images were captured with a LD LCI Plan-Apochromat 25x NA 0.8 water immersion DIC objective (Carl Zeiss Ltd). The FITC and Cell Mask Orange (Invitrogen) dyes were sequentially excited with a 488 nm Argon laser and a 561 nm diode. The emitted light detection range was automatically setup by the Smart setup module of the ZEN2009 software to avoid bleed-through between emission spectra (Carl Zeiss Ltd). The optical section thickness was set to 3.4 µm and z-stack images were acquired with 1.7 µm spacing between optical slices. The image files were exported into ImageJ (Rasband, W.S., ImageJ, U. S. National Institutes of Health, Bethesda, Maryland, USA, http://rsb.info.nih.gov/ij/, 1997-2009) where the orthogonal slices were created.

2.2.7 Time-lapse Microscopy

C. difficile mediated disruption of IEC integrity was investigated by live microscopy. Caco-2 cells were grown on a 14 mm, 12-well glass bottom culture plate (Mat Tek, Ashland, USA) then infected with FITC-labelled *C. difficile* strains. Co-cultures were monitored by time-lapse microscopy over 12 h in 15 min intervals.

Cells were examined by epifluorescence and transmitted light on an inverted Axiovert 135 microscope (Carl Zeiss Ltd) equipped with a temperature-controlled environmental chamber. The images were captured with a x32 LD A-Plan (NA 0.4) phase contrast objective (Carl Zeiss Ltd) using a C4742-80 ORCA-ER digital camera (Hamamatsu Photonics Ltd, UK) controlled by the Volocity software (Improvision, UK). Fluorescent Images of FITC-labelled bacteria and a phase contrast picture of the field of view were taken before the phase

contrast time lapse was recorded at a frame rate of 1 frame/15 min. The time-lapse files were exported into ImageJ (W. Rasband, NIH) where they were processed.

Confocal and time-lapse microscopy were performed by Dr B. Vernay, Light Microscopy Facility, Institute of Child Health.

2.2.8 Gene Expression Analysis

2.2.8.1 RNA Extraction

Control uninfected and infected cells were washed with PBS. Cells were lysed by adding 1 ml of TRIzol (Invitrogen). Lysed cells were transferred to a sterile 1.5 ml microcentrifuge tube. 200 µl of chloroform (Sigma-Aldrich) was added and the mix vortexed for 15 sec, incubated at RT for 3 min then centrifuged at 12000 rpm for 15 min at 4 °C. The top aqueous layer was transferred to a fresh sterile tube containing 500 µl isopropanol (Sigma-Aldrich) and vortexed. The mixture was incubated at RT for 10 min before centrifuging at 12000 rpm for 10 min at 4 °C. The pellet was washed with 1 ml 75% nuclease free ethanol (Sigma-Aldrich) and removed by centrifugation (7500 rpm for 5 min at 4°C). The total RNA was measured by NanoDrop® ND 1000 spectrophotometer (NanoDrop Technologies, USA). The pellet was resuspended in 50 µl of RNA Storage solution (Ambion, Warrington, UK) and stored at -70 °C.

2.2.8.2 cDNA Synthesis

The following components were added to a nuclease free microcentrifuge tube:

Oligo $(dT)_{12-18}$ (500 µg/ml) (Invitrogen)	1 µl
5 µg total RNA (Invitrogen)	x µl
10 mM dNTP Mix (Invitrogen)	1 µl
Sterile nuclease free water (Severn Biotech Ltd, Kidderminster, UK),	to 12µl

The mixture was heated to 65 °C for 5 min to promote binding between oligo dT and polyA tail of mRNA molecules, and rapidly transferred on ice. Subsequently, the following reagents were added to the contents of the tube:

5x First-Strand Buffer (Invitrogen)	4 µl
0.1 M DTT (Invitrogen)	2 µl
RNaseOUT™	1 µl

The contents of the tubes were mixed gently and incubated at 25 °C for 2 min. 1 µl of SuperScript™ II RT (Invitrogen) was added and mixed by pipetting, next incubated at 42 °C for 50 min. The reaction was inactivated by heating at 70 °C for 15 min.

2.2.8.3 Reverse Transcription Polymerase Chain Reaction (RT-PCR)

The obtained cDNA was used as a template for PCR amplification.

The following reagents were added to a microcentrifuge tube and mixed:

BIOMIX™ RED (Bioline, London, UK)	12.5 µl
Nuclease free water (Severn Biotech Ltd)	9.5-10.5 µl
10 µM Forward primer (Sigma-Genosys, Pampisford, UK)	1 µl
10 µM Reverse primer	1 µl
cDNA	1-2 µl

The amplification profile consisted of denaturation at 94 °C for 90 sec, annealing at 58 °C for 90 sec, and extension at 72 °C for 90 sec for 40 cycles. The sequence-specific primers were used, the expected PCR product size are listed in Table 2.9.

mRNA product	5’ primer	3’ primer	PCR size (bp)
IL-8	ATGACTTCCAAGCTGGCCGTGGCT	TCTCAGCCCTCTTCAAAAACTTCTC	289
IL-6	ATGAACTCCTTCTCCACAAGCGC	GAAGAGCCCTCAGGCTGGACTG	628
TNF-α	CGGGACGTGGAGCTGGCCGAGGAG	CACCAGCTGGTTATCTCTCAGCTC	355
IL-1α	GTCTCTGAATCAGAAATCCTTCTATC	CATGTCAAATTTCACTGCTTCATCC	420
IL-1β	AAACAGATGAAGTGCTCCTTCCAGG	TGGAGAACACCACTTGTTGCTCCA	388
hBD-1	TTGTCTGAGATGGCCTCAGGTAAC	ATACTTCAAAAGCAATTTTCCTTTAT	253
hBD-2	CCAGCCATCAGCCATGAGGGTCTTG	CATGTCGCACGTCTCTGATGAGGGAGG	276
IL-18	GCTGCTGAACCAGTAGAAGACAATTGC	CCTTGATGTTATCAGGAGGATTC	384
Caspase-1	AACCCAGCTATGCCCACATCCTCA	CAGATTTTGTAGCAGCATTGTCATGC	230
GAPDH	CTACTGGCGCTGGCAAGGCTGT	GCCATGAGGTCCACCACCCTGCTG	359

Table 2.9. List of primers used for RT-PCR. The oligonucleotide primers and PCR product size. [IL-8, IL-6, TNF-α, IL-1α, IL-1β (Jung *et al*., 1995)] [hBD-1, hBD-2, GAPDH (Zaalouk *et al*., 2004)], IL-18 & caspase-1 were in-house design.

2.2.8.4 Gel-Electrophoresis

PCR products were separated on a 2% agarose gel (Invitrogen) in 1x Tris-Borate-EDTA buffer (Sigma-Aldrich) at 50 V. Band intensities were quantified by densitometry (BioRad ChemiDoc XRS, Bio-Rad Quantity One 1-D Analysis software). Gene expression was normalised to the housekeeping gene glyceraldehyde-3-phosphate dehydrogenase (GAPDH).

2.2.9 Enzyme-linked Immunosorbent Assay (ELISA)

Cytokine protein secretion was measured by ELISA according to manufacturer’s instructions (eBioscience®, Hatfield, UK). Briefly, 96-well ELISA plates were coated with 100 µl/well of capture antibody diluted in coating buffer. Plates were sealed and incubated overnight at 4 °C then washed 5x with 250 µl/well wash buffer (0.05% Tween 20-PBS) allowing time for soaking (~1 min) during each wash step to increase the effectiveness of the washes. 100 µl of 1x assay diluent was used to block non-specific binding. Plates were incubated at RT for 1 h then washed. Using 1x assay diluent, 2-fold serial dilutions of the standard was prepared,

50 µl of the standard was added to each well in order to generate a standard curve. 50 µl of samples were added and plates were covered and incubated at 4 °C overnight then washed. 50 µl of detection antibody (in assay diluent) was added and plates were sealed and incubated at RT for 1 h followed by washing. 50 µl of Avidin-HRP (in assay diluent) was added and plates were incubated at RT for 30 min. Wells were washed with wash buffer for 1 to 2 min prior to aspiration. 50 µl of substrate solution (Tetramethylbenzidine Substrate Solution) was added at RT for 15 min. Finally 50 µl stop solution (2N H_2SO_4) was added to each well and absorbance was read at 450 nm by Multiskan Ascent ELISA reader (Thermo Electron Corporation, UK).

2.2.10 Occludin Immunofluorescence

T84 cells were seeded on glass coverslips at a density of $5x10^5$/ml and were grown to confluence. Cells were infected with bacterial cultures at an MOI of 250 for 8 h. To enhance occludin staining, cells were pre-extracted in buffer containing 10 mM Hepes (pH 7.1), 0.2% Triton X-100, 100 mM KCL, 3 mM $MgCl_2$, 1 mM $CaCl_2$, and 200 mM sucrose for 2 min on ice. Following pre-extraction, monolayers were fixed in 4% PFA for 15 min at RT. PFA was removed by 3 washes with 1% BSA/PBS. Subsequently, monolayers were permeabilised in 0.1% TritonX-100 (Sigma-Aldrich) in 1% BSA/PBS at RT for 30 min followed by blocking with 5% goat serum (Sigma-Aldrich) in 1% BSA/PBS for 1 h. Monolayers were incubated with 4 µg/ml rabbit anti-Occludin (Zymed, Invitrogen) antibody overnight at 4 °C. Cells were washed 3x with 1% BSA/PBS (total 45 min). Cells were incubated with Alexa Flour 488 goat anti-rabbit IgG secondary antibody (Invitrogen), diluted 1:500 in 1% BSA/PBS for 1 h in the dark at RT, followed by a single wash for 15 min in the dark. Coverslips were mounted on slides with Vectashield mounting medium with 4',6-diamidino-2-phenylindole (DAPI) (Vector, Peterborough, UK) and visualised using a fluorescence microscope (Leica DMLB, CoolSNAP-Pro_{cf} camera).

2.2.11 Measurement of Transepithelial Electrical Resistance (TEER)

Barrier function of T84 monolayers were assessed by measurement of TEER and increased permeability to FITC-dextran.

Prior to bacterial co-culture, 12 mm polyester membrane transwell inserts (Corning, New York, USA) were coated with collagen from rat tail (Sigma-Aldrich). Collagen was diluted in 60% ethanol and membranes were coated at 10 µg/cm^2 volume. Collagen-coated membranes were equilibrated with culture media DMEM F-12 HAM for 30 min. T84 cells were grown on collagen-coated membranes at 37 °C, 5% CO_2. When monolayers showed TEER of ~1500 Ω x cm^2 indicating establishment of epithelial barrier function, infection was performed and TEER was measured over 24 h using an epithelial Volt-Ohm meter voltmeter (World Precision Instruments Ltd, Stevenage, UK).

2.2.12 *In vitro* Permeability

Epithelial permeability was measured by applying FITC-conjugated dextran (4 kDa, 0.2 mg/ml, Sigma-Aldrich) to the apical compartment of transwell inserts. Aliquots from basolateral chambers were collected for assessment. FITC associated fluorescence was measured by FLUOstar Optima plate-reader after excitation at 488 nm and detection at 520 nm.

2.2.13 Ussing Vertical Diffusion Chamber System

T84 cells were grown on a 12mm snapwell inserts (tissue culture treated polyester membrane) supported by a detachable ring (Corning). The TEER was monitored until resistance reached ~1500 Ω x cm^2. Snapwell inserts with polarised cells were mounted between two half chambers of a vertical diffusion chamber (Harvard Apparatus, Kent, UK). Both side chambers were filled with non-supplemented DMEM F-12 HAM and bacteria (MOI of 250) was added to the apical side (Figure 2.1). The apical chamber was diffused with an anaerobic gas mixture (10% CO_2, 10% H_2, and 80% N_2, BOC, UK) and the basolateral compartment with 5% CO_2 (BOC). 8 h post-experiment, supernatants were collected and concentrated to 1 ml using Amicon Ultra 3K centrifugal filter device (Millipore) for cytokine analysis. TEER was measured in a time-dependent manner.

Figure 2.1. Anaerobic infection in vertical diffusion chamber system. This figure is adapted from Schuller & Phillips, 2010.

2.2.14 *In vitro* Organ Culture (IVOC)

Intestinal biopsies were obtained, with fully informed parental consent, from paediatric patients (12-30 individuals, mean age of 10) during routine endoscopy for intestinal disorders. Tissues taken from normal area were microscopically examined. Tissue samples oriented mucosal surface upward were placed on sterile foam supports in 12-well plates. The foams were saturated with IVOC media consisting of complete DMEM media supplemented at ratio of 1:1 with NCTC-135 medium (Sigma-Aldrich). Media levels were adjusted to just reach tissue level on the foam but not to immerse it (Hicks *et al.,* 1996). The explants were inoculated with $5x10^8$ *C. difficile* bacteria at 37 °C in 5% CO_2 humidified incubator for 3-6 h.

2.2.15 Transfected HEK293 Cells

HEK293 cells were grown in DMEM supplemented with 10% FCS, 1% penicillin-streptomycin solution, and 100 µg/ml Normocin (Source BioScience LifeSciences, Nottingham, UK). HEK293 transfected cells with TLR2/1, TLR2/6, TLR5, and TLR9 were grown in DMEM supplemented with 10% FCS, 1% penicillin-streptomycin solution, 100 µg/ml Normocin, and 10 µg/ml Blasticidin S (Source BioScience LifeSciences, Nottingham, UK). Blasticidin S was

replaced with 510 µg/ml Puromycin in ordered to grow TLR2-CD14, TLR4-CD14, and CD14 cells (TLR-transfected-HEK293 cells were kindly provided by Dr. David Guiliano, Department of Immunology and Molecular Pathology, UCL).

Cells were seeded in duplicates at a density of $3.5X10^4$/ml in a 96-well plate and grown for 24 h. Prior to infection, media was replaced with fresh DMEM and 20% non-heat-inactivated FCS without antibiotics. Cells were co-cultured with bacterial cultures at an MOI of 10 for 8 h. TNF-α (125 ng/ml) was used as a positive control for all cell-lines in addition to specific ligands for each TLR (Table 2.10). Supernatants were collected and IL-8 induction (indicator of TLR-mediated NF-κB activation) was measured by ELISA.

TLR Ligands	**Concentration**
TLR2: HKLM	$1x10^8$ cells/ml
TLR2/6: FSL-1	500 ng/ml
TLR2/1: Pam3CSK4	1 µg/ml
TLR4: *E. coli K 12* LPS	500 ng/ml
TLR5: *S. typhimurium* Flagellin	5 µg/ml
TLR9: ODN2006 (type B)	50 µM

Table 2.10. Human TLRs agonist used in this study. Human TLR1-9 agonist kit was from InvivoGen, San Diego, USA.

2.3 Dendritic Cell Culture

2.3.1 Murine Bone-marrow-derived DCs (BMDCs)

Femurs and tibias of C57BL/6 wild-type (WT) or Nod2, Ipaf, Nlrp3, and ASC knockout (KO) mice (6-12 weeks old, KO mice were kindly provided by Dr. Clare Bryant, Department of Veterinary Medicine, University of Cambridge) were separated and the surrounding muscles were removed by scissors. Intact bones were washed with PBS, 2% FCS, and 10 µg/ml gentamycin (Sigma-Aldrich) solution. Both ends were cut and bone-marrow was flashed with PBS, FCS, gentamycin solution. Bone-marrow was resuspended gently with pipette to break the clusters then centrifuged at 1600 g for 7 min. The cells were depleted of red blood cells using 1 ml/pair of legs red blood cell lysing buffer (Sigma-Aldrich) for 5 min. Cells were washed twice with PBS and centrifuged at 1600 g for 7 min. Cells were resuspended in 50 ml/pair of legs Iscove's Modified Dulbecco's Medium (IMDM) (Invitrogen) containing 50 µl 2-Mercaptoethanol (Invitrogen), 50 µl gentamycin, and 100 µl of recombinant mouse Granulocyte Macrophage-Colony Stimulating Factor (GM-CSF) (Invitrogen). Cells were cultured in 6-well plates and incubated at 37 °C. Cells were fed every 2 days. On day 7, cells were harvested by collecting non-adherent cells and detaching adherent cells with 2 mM EDTA-PBS (EDTA from Ambion). Cells were washed twice with PBS then resuspended in complete RPMI without antibiotics and seeded at a density of $1x10^6$/ml.

2.3.2 Human Monocyte-derived DCs

Blood samples were obtained from healthy donors, collected in a sterile tube containing 10 U/ml heparin (CP Pharmaceuticals Ltd, Wrexham, UK). Blood samples were diluted with an equal volume of Roswell Park Memorial Institute (RPMI) 1640 (Invitrogen). Subsequently, blood-RPMI mix was layered delicately over Lymphoprep™ (AXIS-SHIELD, Oslo, Norway) at a ratio of 2:1 and centrifuged at 800 g for 20 min. Peripheral blood mononuclear cells (PBMC) layer was carefully removed by pipetting, cells were washed with RPMI supplemented with 10% FCS, 1% L-glutamine , and 1% penicillin-streptomycin solution.

$CD14^+$ monocytes were separated by magnetic separation method using MACS column and MACS Separator (Mini MACS) per manufacturer's instructions. Briefly, after centrifugation

of PBMC, pellets were resuspended in MACS buffer (PBS, 2 mM EDTA, and 0.1% BSA; filter sterilised) then centrifuged at 300 g for 10 min. Supernatants were removed completely and pellets resuspended in 80 µl of MACS buffer/10^7 cells and 20 µl of CD14 MicroBeads (Miltenyi Biotec GmbH, Germany) then mixed and incubated at 4 °C for 30 min. Cells were washed with MACS buffer and centrifuged at 300 g for 10 min next resuspended in 5 ml MACS buffer.

MACS column was placed in the magnetic field of the Mini MACS Separator and washed with 3 ml MACS buffer then 5 ml cell suspension was applied to the column. Unlabelled cells that passed through the column were collected and column was washed twice with 3 ml of MACS buffer. Column was removed from the separator and 5 ml of MACS buffer was added to the column. Labelled cells were collected using the plunger to flush out the cells. Cells were washed with complete RPMI and centrifuged at 300 g for 10 min. $CD14^+$ monocytes were resuspended in complete media supplemented with 50 ng/ml recombinant human IL-4 and 100 ng/ml recombinant human GM-CSF (both from R & D Systems, Minneapolis, USA). Cells were cultured in a 6-well plate and incubated at 37 °C for 5-7 days to generate DCs.

2.3.3 Dendritic Cell Maturation

Dendritic cells were seeded at a density of $1x10^6$/ml and infected with bacterial culture at an MOI of 10. 8 h post-infection, cells were collected and centrifuged at 1600 rpm, 4 °C for 7 min. Supernatants were removed and cell pellets washed with 1 ml FACS wash (PBS, 1% FCS and 0.1% sodium azide) and centrifuged. Pellets were resuspended in 200 µl of blocking buffer (PBS, 10% FCS, 0.02% sodium azide) with rat anti-mouse CD16/CD32 (Mouse BD Fc Block™) (1: 1000) (BD Pharmingen™, BD Biosciences, USA). Cells were incubated for 10-15 min on ice and centrifuged at 2000 rpm for 5 min at 4 °C. Antibodies utilised (Table 2.11) were prepared in blocking buffer and 50 µl of antibody solution was added to cell pellet and mixed by pipetting. Cells were incubated on ice for 30-45 min then centrifuged. Pellets were washed twice with FACS wash buffer and fixed with 4% PFA for 20 min. Cells were washed and pellets resuspended in 100 µl PBS and analysed by flow cytometry.

Antibody	Clone	Dilution
Anti-Mouse CD80 PE-Cy5	16-10A1	1:300
Anti-Mouse CD86 FITC	GL1	1:400
Anti-Mouse MHC Class II FITC	14-4-4S	1:400
Anti-Mouse CD40 PE	1C10	1:40

Table 2.11. Antibodies used for detecting maturation markers. All antibodies were from eBioscience.

2.3.4 Real-time Polymerase Chain Reaction (PCR)

RNA was extracted from co-cultured cells as described in section 2.2.8.1. Extracted RNA was DNase treated to remove contaminating DNA using the TURBO DNA-*free*™ Kit (Ambion). 10x TURBO DNase Buffer (0.1 volume) and 1 µl of TURBO DNase was added to the RNA, mixed gently and incubated at 37 °C for 20-30 min. DNase Inactivation Reagent was resuspended and 0.1 volume was added and incubated at RT for 2 min mixing occasionally. The mix was centrifuged at 10000 g for 1.5 min and the RNA transferred into a fresh tube. cDNA was prepared by using the High-Capacity cDNA Reverse Transcription Kit (Applied Biosystems, USA). 2x Reverse Transcription master mix was prepared (20 µl of reaction/sample) on ice by adding the reaction mix components (Table 2.12) and mixed gently. The cDNA reverse transcription reaction was prepared by pipetting 10 µl of 2x master mix and 10 µl of RNA sample into a microcentrifuge tube. The tubes were sealed and briefly centrifuged then loaded to the thermal cycler and heated at 25 °C for 10 min, 37 °C for 120 min, 85 °C for 5 min, then cooled to 4 °C.

cDNA Reaction Mix	Volume
10x Reverse Transcription Buffer	2.0 µl
25x dNTP Mix (100 mM)	0.8 µl
10x Reverse Transcription Random Primers	2.0 µl
MultiScribe™ Reverse Transcriptase	1.0 µl
RNase Inhibitor	1.0 µl
Nuclease-free H_2O	3.2 µl
Total per Reaction	10.0 µl

Table 2.12. List of cDNA master mix components.

2.3.4.1 SYBR Green-based Gene Expression Analysis

Real-time PCR master mix was prepared by dispensing reagents (Table 2.13) into a 0.1 ml PCR tube (Qiagen, Crawley, UK). 1 µl of 5 µM working solution of each forward and reverse primer was also included (Table 2.14). Next, 2 µl of cDNA template was added to the master mix making the total reaction volume 20 µl. Tubes were briefly centrifuged then loaded on the Real-time Rotary Analyser (Rotor-Gene 6000, Corbett Life Science, Cambridge, England). The thermal reaction was: Hold at 95 °C for 10 min; 40 cycles of 95 °C for 15 sec, 58 °C for 30 sec, and 72 °C for 30 sec; Melt 70 °C to 95 °C, rising 1 °C, wait for 90 sec per melt and 5 sec for each step.

Reagent	Volume
2x JumpStart *Taq* Ready Mix	10 µl
Primers	2 µl
MilliQ water	6 µl
Total Volume	18 µl

Table 2.13. Master mix components for real-time PCR. SYBR® Green JumpStart™ Taq ReadyMix™ was from Sigma-Aldrich.

	Forward Primer	Reverse Primer
IL-12 p35	5'-CCTCAGTTTGGCCAGGGTC-3'	5'-CAGGTTTCGGGACTGGCTAAG-3'
IL-12 p40	5'-GGAAGCACGGCAGCAGAATA-3'	5'-AACTTGAGGGAGAAGTAGGAAT-3'
IL-27 p28	5′-TTCCCAATGTTTCCCTGACTTT-3′	5′-AAGTGTGGTAGCGAGGAAGCA-3′
IL-27 EBI3	5′-TGAAACAGCTCTCGTGGCTCTA-3′	5′-GCCACGGGATACCGAGAA-3′
IL-10	5′-GGTTGCCAAGCCTTATCGGA-3′	5′-ACCTGCTCCACTGCCTTGCT-3′
IL-6	5′-GTTCTCTGGGAAATCGTGGA-3′	5′- TGTACTCCAGGTAGCTATGG-3′
IL-1β	5′-CCAAAAGATGAAGGGCTGCT-3′	5′- AGAAGGTGCTCATGTCCTCA-3′
GAPDH	5′-CCTGGAGAAACCTGCCAAGTATG-3′	5′- AGAGTGGGAGTTGCTGTTGAA-3′

Table 2.14. List of primers used in SYBR Green-based real-time PCR. Primers were from Eurofins MEG Operon, Ebersberg, Germany.

2.3.4.2 TaqMan Probe-based Gene Expression Analysis

PCR master mix component (Table 2.15) was pipetted in duplicate for each sample into a nuclease-free 0.1 ml PCR tube (Qiagen) 4 µl of cDNA template was added and mixed gently. Tubes were briefly centrifuged then loaded on the Real-time Rotary Analyser (Rotor-Gene 6000) and the following thermal cycle was performed: Hold at 95 °C for 10 min; 45 cycles of 95 °C for 15 sec and 60 °C for 60 sec.

PCR Reaction Mix	Volume
20x TaqMan® Gene Expression Assay[1]	1.0 µl
2x TaqMan® Gene Expression Master Mix	10.0 µl
RNase-free water	5.0 µl
Total Volume	20 µl

Table 2.15. TaqMan probe-based PCR reaction mix component. All the reagents were from Applied Biosystems. [1]Gene expression assay was performed for IL23a, alpha subunit p19 and Hprt (hypoxanthine guanine phosphoribosyl transferase).

2.3.5 T Cell Proliferation Assay

2.3.5.1 T Cell Proliferation of Splenocytes

$1x10^6$/ml BMDC from WT mice were stimulated with PFA fixed *C. difficile* strains at an MOI of 50 for 24 h. In these experiments LPS- (Lipopolysaccharides from *Escherichia coli* 0111:B4, Sigma-Aldrich) was used as a positive control.

Splenocytes were harvested from WT mice by mashing a spleen and passing the contents through a cell strainer (70 µm, BD Falcon, BD Biosciences). Cells were washed with PBS and centrifuged at 1600 g for 7 min. Red blood cells were depleted using 1 ml of red blood cell lysing buffer for 5 min. Cells were washed twice with PBS and centrifuged. Pellets were resuspended in complete RPMI and incubated at 37 °C for 2-3 h.

Harvested splenocytes were washed in PBS and resuspended at $0.5x10^6$/ml in PBS. Cells were labelled with CFSE [5-(and 6)-Carboxyfluorescein diacetate succinimidyl ester] (eBioscience) to a final concentration of 10 µM and incubated at 37 °C for 8-10 min. Cells were washed twice with PBS/FCS and resuspended in complete RPMI containing 50 µl 2-Mercaptoethanol and 50 µl gentamycin. Dynabeads® Mouse T-Activator CD3/CD28 was added to CFSE-labelled splenocytes at a bead-to-cell ratio of 1:5 then co-cultured with *C. difficile*-stimulated BMDCs in a 96-well plate in a DC-to-splenocyte ratio of 1:10. Co-cultures were incubated at 37 °C for 72-96 h. Cells were co-stained with anti-mouse CD4 PE-Cy5 (dilution 1:160) (eBioscience) as described in section 2.3.3 and analysed at 48, 72, and 96 h by flow cytometry gated on $CD4^+$ cells.

2.3.5.2 Naive $CD4^+$ T Cell Proliferation

Naive $CD4^+$ T cells were isolated from spleen of OT-II transgenic mice (kindly provided by Dr. David Escors, Division of Infection and Immunity, UCL) using MagCellect* Mouse Naïve $CD4^+$ T Cell Isolation Kit (R & D Systems, Inc.). 5 ml of 1x MagCellect Buffer/$10x10^7$ cells was prepared by mixing 0.5 ml of MagCellect 10x Buffer with 4.5 ml PBS and stored on ice. Splenocytes were suspended in cold 1x MagCellect Buffer at a cell density of $10x\ 10^7$/ml. Cells were transferred into a 5 ml polystyrene tube and 100 µl of MagCellect Mouse Naïve $CD4^+$ T Cell Biotinylated Antibody Cocktail was added, mixture was gently mixed and incubated at 4 °C for 15 min. Next, 125 µl of MagCellect Streptavidin Ferrofluid was added to the cell-antibody suspension, mixed gently and incubated at 4 °C for 15 min. 1x MagCellect Buffer was added to the cell suspension to bring the volume of the reaction to 2 ml. The tube was placed in the MagCellect Magnet and incubated for 6 min at RT. The desired cells in the suspension was recovered by aspirating the reaction supernatant while the tube was still in the magnet and transferred into a fresh tube.

Isolated naive $CD4^+$ T cells were labelled with CFSE and subsequently co-cultured with *C. difficile*-stimulated BMDCs in the presence of $OVA_{323-339}$ peptide (Abgent, Inc., San Diego, USA) at a concentration of 1:1000 containing 10 units/ml recombinant mouse IL-2 (Invitrogen) and incubated at 37 °C. Cells were co-stained with anti-mouse CD4 PE-Cy5 (dilution 1:160) (eBioscience) and analysed at 48, 72, and 96 h by flow cytometry gated on $CD4^+$ T cells.

2.3.6 Intracellular Cytokine Staining

BMDCs stimulated with PFA-fixed *C. difficile* co-cultured with T cells were analysed for cytokine 96 h post-incubation. Cells were pelleted then resuspended in complete RPMI in the presence of 50 ng/ml Phorbol 12-myristate 13-acetate (PMA), 500 ng/ml ionomycin, and 5 μg/ml brefeldin A (all from Sigma-Aldrich) and incubated at 37 °C for 5 h.

Cells were harvested by centrifugation at 2000 rpm for 5 min at 4 °C then stained as described in section 2.3.3 with anti-mouse CD4 PE antibody (dilution 1:200) (eBioscience). Following cells surface staining, PFA fixed cells were washed twice with perm buffer (FACS wash buffer containing 0.1% saponin) then resuspended in 50 μl of anti-mouse IFN-γ PerCP-Cy5.5 (dilution 1:100) and anti-mouse IL-17A FITC (dilution 1:200) (eBioscience) in perm wash and incubated on ice for 20 min. cells were washed twice with perm wash then resuspended in FACS wash buffer and analysed by flow cytometry.

2.4 Statistical Analysis

Data were analysed using GraphPad Prism version 5.00 (San Diego, USA). Non parametric *t*-test (Mann-Whitney) was performed to compare groups in non-parametric data. Grouped analyses was achieved by two-way ANOVA and Bonferroni post-test to compare replicate means by row and compare each column to all the other columns. Data considered significant if only probability was $p<0.05$.

Chapter 3

Clostridium difficile-Intestinal Epithelial Cell Interactions (I)

3.1 Introduction

In recent years *C. difficile* infection (CDI) has emerged as the leading cause of healthcare diarrhoea in the developed world. CDI continues to rise due to the rapid emergence and transcontinental spread of highly virulent *C. difficile* strains of PCR ribotypes 027 and 078 (Dawson *et al.,* 2009). Historically most *C. difficile* strains were clindamycin resistant however, the emergence and spread of PCR ribotype 027 strains with acquired resistance to fluoroquinolone antibiotics is a new feature that was not present in historic strains of the same genotype (Rupnik *et al.,* 2009).

C. difficile strain 630, an epidemic PCR ribotype 012 was the first to be genome sequenced (Sebaihia *et al.,* 2006). This strain was isolated in 1982 from a patient with PMC produces both TcdA and TcdB (A^+B^+). Several *C. difficile* strains have now been sequenced (Welcome Trust Sanger Institute, UK), these include strain R20291 from the hypervirulent clade (Stabler *et al.,* 2009). This strain, which was isolated in 2006 during an outbreak at Stoke Mandeville Hospital, is a PCR ribotype 027. It releases a third toxin termed binary toxin (CDT) as well as TcdA and TcdB (A^+B^+, CDT^+). In addition to strain R20291, the Sanger Institute is currently sequencing two other *C. difficile* strains, CF5 and M68 from the A^-B^+ clade, which are respectively historic and recent representatives of PCR ribotype 017 (He *et al.,* 2010). CF5 was isolated in Belgium in 1995 from an asymptomatic patient, while M68 was isolated in 2006 during an outbreak in Ireland (Stabler *et al.,* 2006).

Despite advances made in understanding of *C. difficile* microbial pathogenesis, very little information is available on the interaction and contribution of *C. difficile* itself with the human host. Focus of the present study was therefore to improve our current limited understanding of *C. difficile*-mediated disease pathogenesis.

3.2 Microbiological Characterisation of *C. difficile* Strains under Investigation

As *C. difficile* isogenic mutants have only recently become available (Lyras *et al.,* 2009), this study initially opted to explore the effect of *C. difficile* virulence factors on the host by employing four different strains which included: R20291, 630, M68 and CF5. It was hypothesised that comparing and contrasting host responses to the selected array of strains may clarify toxin-specific mechanism(s) involved in host-pathogen interactions. Prior to commencing co-culture studies it was pertinent to investigate the microbiological features of the strains employed.

3.2.1 *C. difficile* Growth Kinetics

The *in vitro* growth kinetics of the bacterial strains was determined. This was necessary to ensure that the bacteria were studied in the late exponential/early stationary growth phase when the culture is in a vegetative state, and to establish the optimal range of multiplicity of infection (MOI) for co-culture experiments.

Growth curves of *C. difficile* strains R20291, 630, M68, and CF5 are shown in Figure 3.1. Bacterial cultures were grown to exponential phase by inoculating pre-equilibrated BHI broth with three single colonies. Secondary pre-equilibrated BHI broths were inoculated with primary exponential phase cultures to obtain OD_{600} nm of 0.01. All strains exhibited a short lag phase and there was no significant difference between the strains in the first two hours of growth. R20291, M68, and CF5 had similar growth rates reaching mid-logarithmic phase at ~3 h and entered stationary phase 4-5 h post-inoculation. In contrast, although strain 630 grew at a similar rate to the other strains in the first 2 h, its growth was slower thereafter, reaching mid-logarithmic at 4 h and stationary phase at 8 h. Viable counts were performed at three time points corresponding to OD_{600} readings of 0.5, 1.00, and 1.5 (Table 3.1) to determine the bacterial generation/doubling time and also to determine the MOI at OD_{600} of 1.5 or once bacteria reached to its stationary phase.

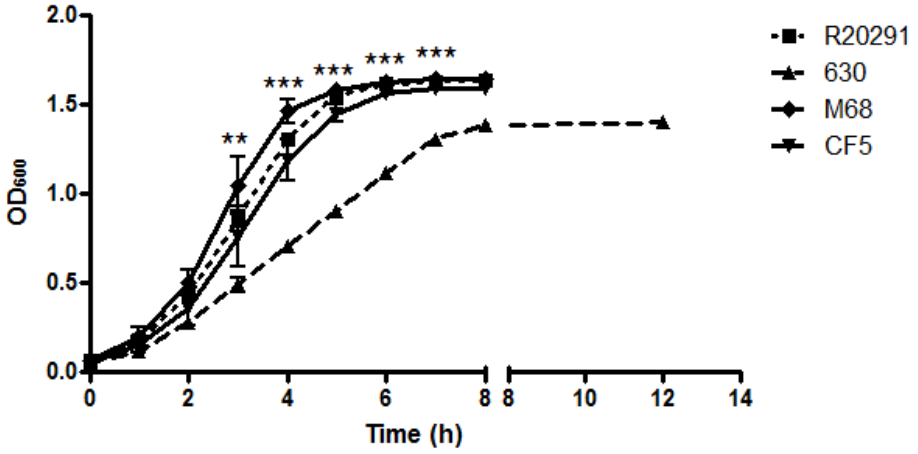

Figure 3.1. *C. difficile* strains exhibit differential growth kinetics. *C. difficile* strains were inoculated into BHI broth and growth rates monitored by optical density at 600nm. Statistically, there was no significant difference between the growth rates of R20291, M68, and CF5 however 630 showed a significantly slower rate of growth compared to the other strains between 3-7 h post-inoculation. Data presented as the mean ± SEM, n=3. $^{*}p<0.05$, $^{**}p<0.01$, $^{***}p<0.001$ (ANOVA with Bonferroni post-test) represent significant inter-strain difference.

Strains	CFU/ml(OD_{600}=0.5)	CFU/ml(OD_{600}=1.0)	CFU/ml(OD_{600}=1.5)
R20291	2.9×10^8 $\pm 5.7 \times 10^7$	5.8×10^8 $\pm 2.3 \times 10^7$	7.0×10^8 $\pm 1.0 \times 10^8$
630	1.5×10^8 $\pm 6.1 \times 10^7$	5.6×10^8 $\pm 6.2 \times 10^7$	6.1×10^8 $\pm 8.8 \times 10^6$
M68	2.4×10^8 $\pm 3.4 \times 10^7$	5.7×10^8 $\pm 1.2 \times 10^8$	6.4×10^8 $\pm 1.1 \times 10^8$
CF5	3.6×10^8 $\pm 3.7 \times 10^7$	5.5×10^8 $\pm 1.4 \times 10^8$	7.3×10^8 $\pm 8.7 \times 10^7$

Table 3.1. *C. difficile* strains undergo slow growth. Viable counts were performed at OD_{600} of 0.5, 1.00, and 1.5 and the generation times were found to be 15-22 min (fastest being R20291 and slowest 630). Using the viable counts at OD_{600}= 1.5, the relative MOI required in the co-culture studies was determined for each strain. Data represent mean ± SEM of three independent experiments.

3.2.2 *C. difficile* Survival under Aerobic Condition(s)

As *C. difficile* is an obligate anaerobe, exposing the bacteria to aerobic co-culture conditions of 5% CO_2 is likely to result in bacterial death during the time-course of the experiment. As the host responses measured are therefore likely to be in response to both live and dead bacteria, it was imperative to investigate any potential variation between the strains in the rate of cell death in response to oxygen.

BHI broth was inoculated with bacterial colonies and grown to stationary phase. Then, the stationary phase bacterial cultures were exposed to aerobic conditions and bacterial survival was enumerated over time by viable counting (Figure 3.2). *C. difficile* strains showed no significant difference in degree of cell death over the 8 h time-course. Furthermore, no significant inter-strain difference in viable counts was observed amongst the strains.

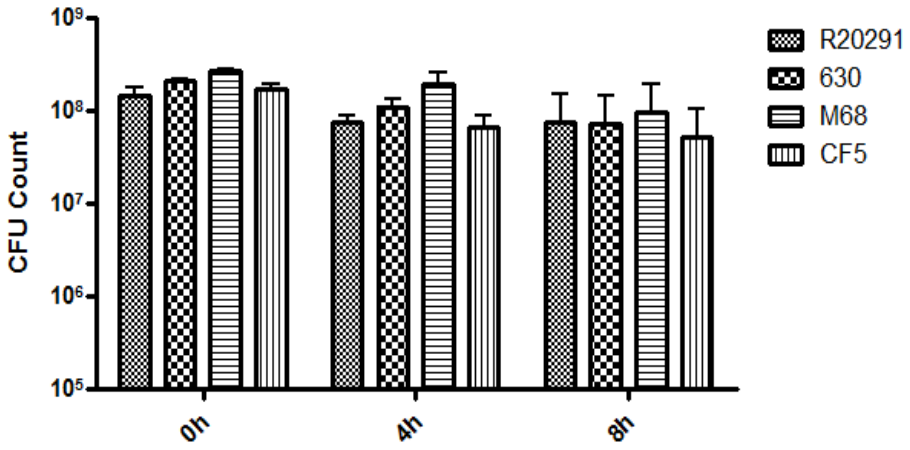

Figure 3.2. *C. difficile* strains show similar survival trend. Bacterial cultures were grown to stationary phase and subsequently they were exposed to aerobic conditions. Strains survival was determined in a time-dependent manner by CFU quantification. Data represent mean ± SEM (ANOVA with Bonferroni post-test), n=4.

3.2.3 *C. difficile* Sporulation

C. difficile produces endospores as a means to survive in hostile and/or unfavourable environments (Paredes *et al.,* 2005) but will germinate in the presence of specific effectors, termed germinants (Burns *et al.,* 2010). As exposure to oxygen during co-culture experiments can be considered a ''stress'' signal, it was necessary to investigate the rate of spore formation by each of the four strains under aerobic conditions.

Sporulation ability was examined using yeast peptone media (YPM), a medium described by Akerlund *et al.* for inducing *C. difficile* sporulation (Akerlund *et al.,* 2006 & 2008), and BHI medium. Anaerobically grown bacterial cultures were subjected to aerobic conditions and spore formation was enumerated by viable counting (Figure 3.3). Spores generated in YPM were visualised under a light microscope by the Wirtz-Conklin staining method (5% Malachite Green/ 0.5% Safranin) (Hamouda *et al.,* 2002; Ochsner *et al.,* 2009) endospores appeared bright green/blue and vegetative cells were pink (Figure 3.4, arrowheads).

Spore formation was undetectable in cultivated BHI cultures; however, all four strains sporulated to a similar degree in inoculated YPM media (Figure 3.3).

Collectively, Figures 3.1-3.3 indicated that strains R20291, M68, and CF5 exhibited similar microbiological properties. In comparison, strain 630 shared comparable sporulation and survival under aerobic conditions but showed slower growth kinetics.

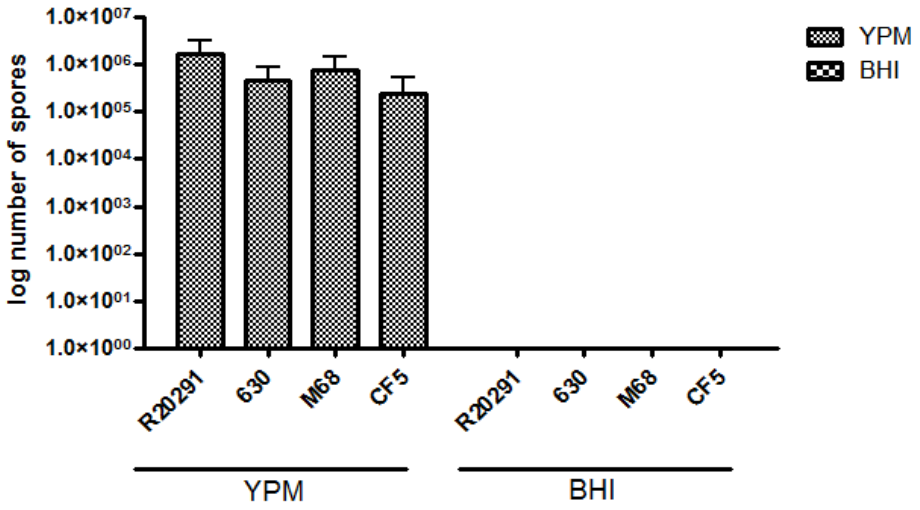

Figure 3.3. *C. difficile* strains sporulate equally in yeast peptone media. *C. difficile* strains were grown anaerobically in YPM or BHI media for 10 days, then they were exposed to oxygen for 8 h and spore-formation was enumerated after ethanol-killing of vegetative cells. Data represent mean ± SEM (ANOVA with Bonferroni post-test), n=3.

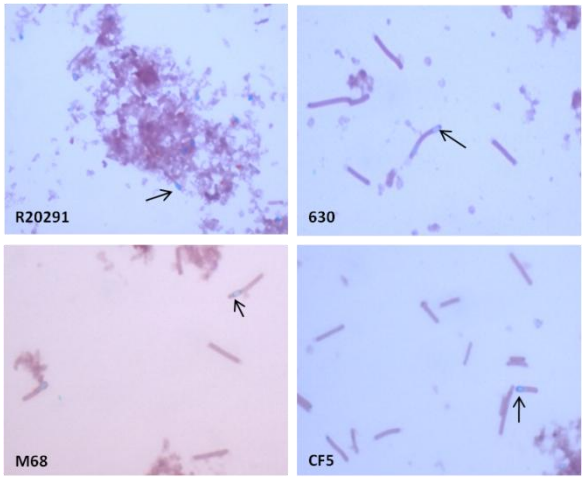

Figure 3.4. *C. difficile* strains sporulate in yeast peptone media. Generated spore suspensions were stained with 5% malachite green and 0.5% safranin O and visualised microscopically (20x Leica GMBH, QImaging digital camera). Endospores with no germination stained greenish-blue (arrowheads), whilst outgrown bacteria stained in pink.

3.3 Characterisation of *C. difficile* Toxins

C. difficile secretes two well characterised glucosyltransferase toxins, TcdA and TcdB. The genes encoding TcdA and TcdB, accompanied with three regulatory genes (*tcdC, tcdE, tcdR*), are located on the 19.6 kb PaLoc (Kuehne *et al.,* 2011). Additionally, ~6% of *C. difficile* isolates (Dawson *et al.,* 2009), and in particular strains of ribotype 027 produce a third toxin (CDT). This toxin is encoded on a separate region of the chromosome comprising the two components of CDT (*cdtA* & *cdtB*) and a regulatory gene (*cdtR*) (Carter *et al.,* 2007).

Some *C. difficile* strains have deletions in the sequences of one or more genes in the PaLoc compared with the sequence of the reference strain VPI 10463. The most well known and studied representatives of variant *C. difficile* strains are the A^-B^+ strains. These strains mostly belong to toxinotype VIII and are characterised by a 1.8 kb deletion within repetitive regions of *tcdA* gene, and a mutation which introduces a stop codon at amino acid position 47, consequently affecting production of TcdA (Rupnik *et al.,* 2003b).

3.3.1 *C. difficile* Toxin Gene Detection

Although all four strains under investigation have been characterised previously (Stabler *et al.,* 2006), it was important to confirm the presence of *tcdA, tcdB, cdtA,* and *cdtB* genes prior to study. Presence of the various toxin genes was verified by PCR (Figure 3.5). Strain CD37 a non-toxigenic strain was used as a negative control in *C. difficile* toxin gene detection.

TcdA gene (*tcdA*) was detected in strains R20291 and 630 as well as strains M68 and CF5 as a 519 bp fragment (Figure 3.5 a). This data was expected since A^-B^+ strains from toxinotype VIII do possess the *tcdA* gene even though they have lost the capacity for TcdA protein production. An 1121 bp fragment corresponding with *tcdB* gene was seen in all strains (Figure 3.5 b). To detect *cdtA* and *cdtB* genes, three different primer sets were used, *cdtB* primer to amplify a specific region of the *cdtB* gene, and *BIN5/6* and *BIN7/8* primers to amplify the entire *cdtA* and *cdtB* genes respectively (Figure 3.5 c). A 489 bp product was detected in R20291 corresponding with the *cdtB* gene, a 1452 bp and a 2413 bp fragment was identified in the whole amplified regions of *cdtA* and *cdtB* confirming the presence of these genes in R20291. As expected no bands were observed in the remaining strains.

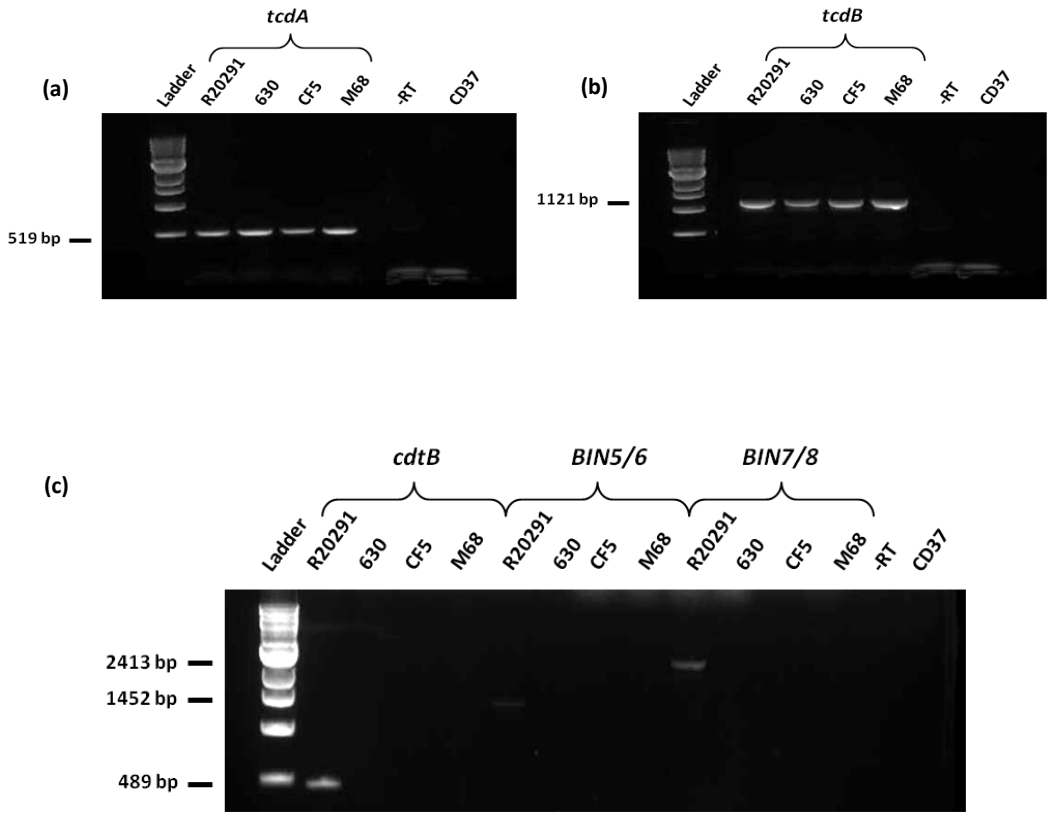

Figure 3.5. Confirmation of *tcdA, tcdB, cdtA* and *cdtB* genes in *C. difficile* strains. *C. difficile* strains were screened for toxin A, B, and CDT genes. Presence of toxin A (a) and B genes (b) was confirmed in the all strains. Using three different sets of primers existence of binary toxin genes were investigated and were detected only in strain R20291 (c). CD37 is a non-toxigenic strain.

3.3.2 *C. difficile* Toxin Protein Detection

Subsequent to verification of the toxins genes in all four strains, it was necessary to confirm the secretion of the toxins. Expression of CDT could not be studied as no specific antibody was available.

Bacterial cultures were grown to stationary phase and centrifuged. Bacterial pellet (10^8 cells) and supernatant (100 µg total protein) were subjected to 6% SDS-PAGE and toxin protein detected by western blotting (Figure 3.6).

TcdA protein was detected in bacterial cells (Figure 3.6 a) and supernatants (Figure 3.6 b) of strains R20291 and 630, confirming the production of TcdA by these strains. Interestingly, both strains expressed similar amounts of TcdA. In contrast, no detectable TcdA protein was noticed for strains CF5 and M68 in either compartment (Figures 3.6 a & b).

Presence of TcdB was detected in R20291, 630, and CF5 bacterial pellets (Figure 3.6 c) and in the supernatants of strains R20291 and CF5 (Figure 3.6 d). Strain CF5 produced more TcdB protein compared to the rest of the strains. Secretion of TcdB was not detected in bacterial pellet or supernatant of strain M68 with the employed antibody (Figures 3.6 c & d). Consequently, protein concentration was increased 10-fold in order to assist the detection of TcdB in strain M68. TcdB secretion was detected in the bacterial pellet (10^9) of all four strains (Figure 3.6 e) confirming that M68 indeed does produce TcdB.

In summary, *tcdA* and *tcdB* were present in all four strains, whilst binary toxin gene was identified only in strain R20291 (Figure 3.5). A comparable expression of TcdA was detected in strains R20291 and 630, while CF5 and M68 showed no detectable levels. It was also observed that *C. difficile* strains released TcdB protein to varying levels, with strain CF5 exhibiting significant expression of TcdB followed by R20291, 630, and M68 (Figure 3.6).

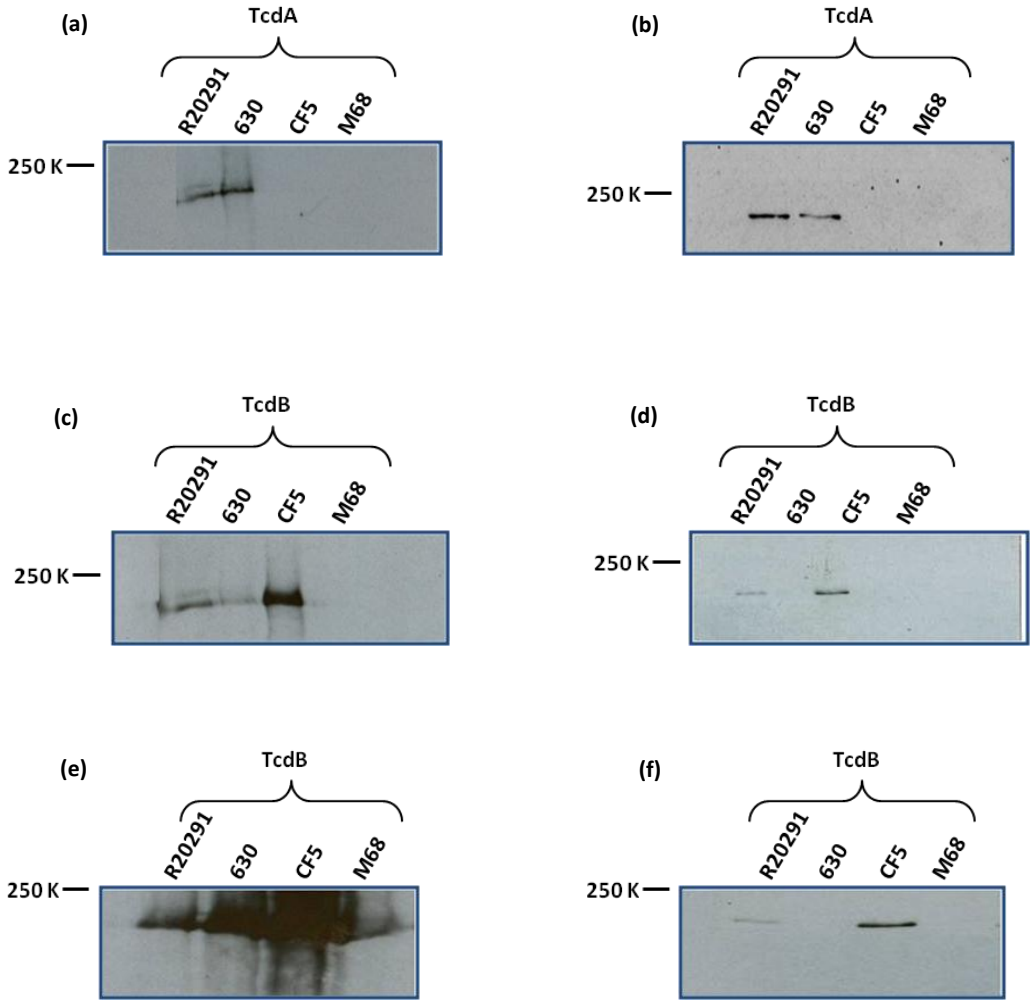

Figure 3.6. Varying expression of TcdA and TcdB in *C. difficile* strains. Bacterial pellet (10^8) and supernatant (100 µg total protein) were subjected to 6% SDS-PAGE. TcdA was detected in bacterial pellets (a) and supernatants (b). Using toxin B antibody, TcdB protein was detected in bacterial pellets of strains R20291, 630, and CF5 (c) and in bacterial supernatants of strains R20291 and CF5 (d). Presence of TcdB protein was investigated further in a concentration-dependent manner. TcdB expression was observed in bacterial pellets (10^9) of all four strains (e) but only strains R20291 and CF5 showed production of TcdB in bacterial supernatants (f).

3.4 *C. difficile*-mediated Effects on Human Intestinal Epithelial Cells (IECs)

The first host cell that *C. difficile* interacts with are the IECs of the colon. To determine the bacterial mediated effects on human IEC, two well characterised cell-lines; Caco-2, human ileocecal epithelial cells and HT-29, human colonic epithelial cells were employed. Host IEC responses to *C. difficile* hypervirulent strain R20291 (A^+B^+, CDT^+), strain 630 (A^+B^+), and A^-B^+ strains (M68 and CF5) were investigated. In early experiments, cell-lines were infected with bacteria at three MOIs (10, 100, and 1000), and cell viability was examined at 8 and 24 h post-infection. These experiments were conducted to establish the optimum MOI and time-course of infection for subsequent studies.

3.4.1 Cytotoxic Effect of *C. difficile* on Human IEC

The *C. difficile*-induced effect on IEC membrane integrity was assessed by measurement of the extracellular release of the cytosolic enzyme, lactate dehydrogenase (LDH), which is released following cell death.

Caco-2 (Figures 3.7 a & b) and HT-29 (Figures 3.7 c & d) were infected with the four *C. difficile* strains at an MOI 100 (Figures 3.7 a & c) and 1000 (Figures 3.7 b & d) for 8 and 24 h. Uninfected control Caco-2 cells showed a basal cell death of ~10-12%. Infection with MOI of 100 resulted in a modest increase in cytotoxicity at 8 h with R20291 causing the most (~20%) toxicity. By 24 h however, infection with strains R20291, 630, and M68 resulted in 80-90% cell death. At this time-point, CF5 mediated ~40% cytotoxicity, which was significantly less compared to other strains ($p<0.001$) (Figure 3.7 a).

In comparison, when experiments were conducted at an MOI of 1000, R20291, 630, and M68 induced significant cell death at 8 h post-infection (≤50%), while CF5 showed the least cytotoxicity (<20%). Nonetheless, 24 h post-infection, CF5 at this MOI caused ≥90% cell death as seen for the other three strains (Figure 3.7 b). These studies indicated that MOI of 1000 and 24 h post-infection time-point were not optimal to study host-pathogen interactions. Therefore, future experiments were conducted utilising an MOI of 100-500, whilst generally terminating higher MOI experiments at earlier time-points.

Similar infections were also conducted in HT-29 cells (Figures 3.7 c & d). Interestingly, the basal cytotoxicity of uninfected control cells were ~15-25%; higher than that observed for Caco-2 cells (Figure 3.7 a & b). This basal rate increased to ~30% at 8 h and 50-65% at 24 h upon infection with *C. difficile* strains at an MOI of 100, with no significant difference noted between the tested strains (Figure 3.7 c). Again, an increase in MOI (1000) led to a significant cytotoxicity response (Figure 3.7 d). CF5 yielded less cytotoxicity compared to the other three strains at 8 h, while at 24 h all the strains caused similar (85-95%) cell death.

Results from above (Figure 3.7), suggested that R20291, 630, and M68 have the ability to induce cell death to a similar extent, in contrast CF5 at early time-points of infection showed a modest toxic effect on the two IEC lines tested.

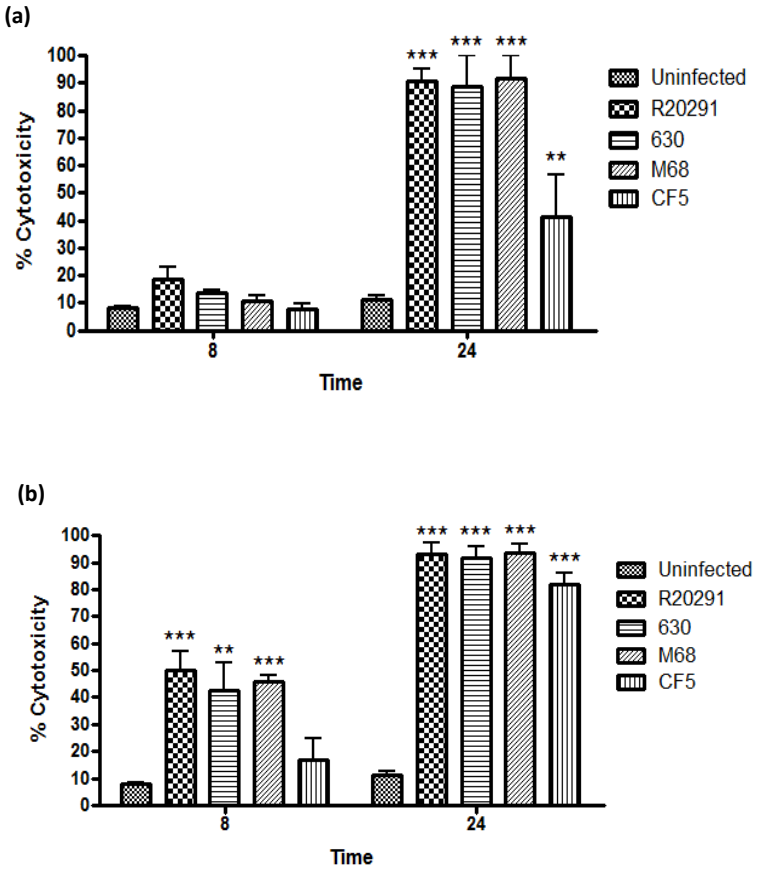

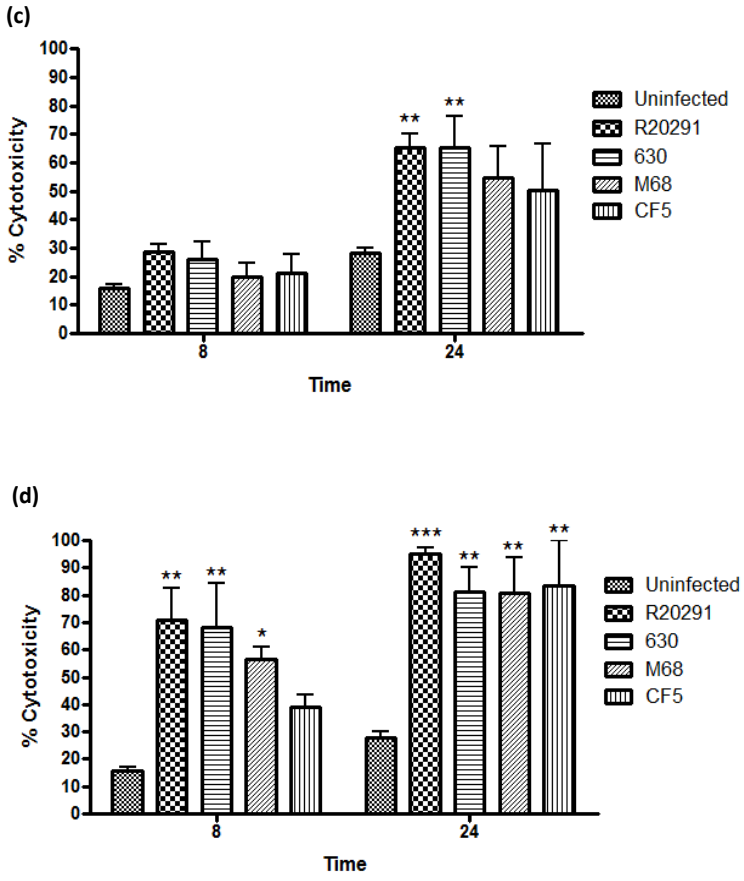

Figure 3.7. Lactate dehyrogenase (LDH) release by Caco-2 and HT-29 cell-lines exposed to *C. difficile*. Caco-2 monolayers were co-cultured with *C. difficile* strains at an MOI of 100 (a) and 1000 (b) and LDH release was measured at 8 and 24 h post-infection. Similarly, HT-29 cells were infected with *C. difficile* strains at an MOI of 100 (c) and 1000 (d) and cytotoxicity was measured at 8 and 24 h. Data are means ± SEM for n=5 experiments. $^{*}p<0.05$, $^{**}p<0.01$, and $^{***}p<0.001$ (ANOVA with Bonferroni post-test) represent significant difference from uninfected cells.

3.4.2 *C. difficile* Toxin Cytotoxicity

The functional properties of the toxins were examined by cytotoxicity assays utilising HT-29 and Vero (African green monkey kidney cell) cell-lines. HT-29 and Vero cells are susceptible to both TcdA and TcdB; however, HT-29 cells are known to be more sensitive to TcdA and Vero cells more sensitive to TcdB (Torres *et al.,* 1992). In these series of experiments, a non-toxigenic strain, CD37, was used as a negative control.

Semi-confluent HT-29 cells were co-cultured with filter-sterilised supernatants of stationary phase bacterial culture at an MOI of 500 and structural changes were observed microscopically at 8 h post-infection (Figure 3.8 a). No morphological changes compared to uninfected control cells were observed in cells infected with strain CD37. 8 h post-infection, cell alteration was noticeably visible in R20291 infected cells (Figure 3.8 a, arrowheads); while an intermediate cell rounding was initiated in cells infected with strains 630 and M68. No morphological change was observed in cells infected with strain CF5 (Figure 3.8 a). The cytopathic effect (CPE) of TcdA on HT-29 cells was quantified by infecting cells with 2-fold dilutions of filter-sterilised bacterial supernatants (Figure 3.8 b). A minimum cytotoxic activity was detected in uninfected control cells and cells infected with non-toxigenic strain CD37. R20291 showed the highest cytotoxicity compared to uninfected cells, while strains 630 and M68 exhibited an intermediate toxicity. The least cell intoxication was caused by strain CF5 (Figure 3.8 b).

Similar co-cultures were conducted using Vero cells to examine TcdB cytotoxicity (Figure 3.9). Confluent Vero cell monolayers were infected with filter-sterilised supernatants of stationary phase bacterial culture at an MOI of 500, and cell rounding observed 8 h post-infection (Figure 3.9 a). Cell monolayers cultured with the non-toxigenic strain CD37 showed no morphological changes compared to uninfected control cells. Considerable cell rounding was observed in cells infected with R20291 at 2 h. 8 h post-infection, cells incubated with strains 630 and M68 were rounded, but no significant change was detected in the cells infected with strain CF5 (Figure 3.9 a). The cytopathic effect of TcdB on Vero cells was also quantified by co-culturing cells with 2-fold dilutions of filter-sterilised bacterial supernatants (Figure 3.9 b). A minimum cytotoxic activity was detected in uninfected control cells and cells infected with CD37. Strains R20291, 630, and M68 caused similar cytotoxicity and showed very significant cell intoxication compared to uninfected control cells. Strain CF5 exhibited the least cell toxicity (Figure 3.9 b).

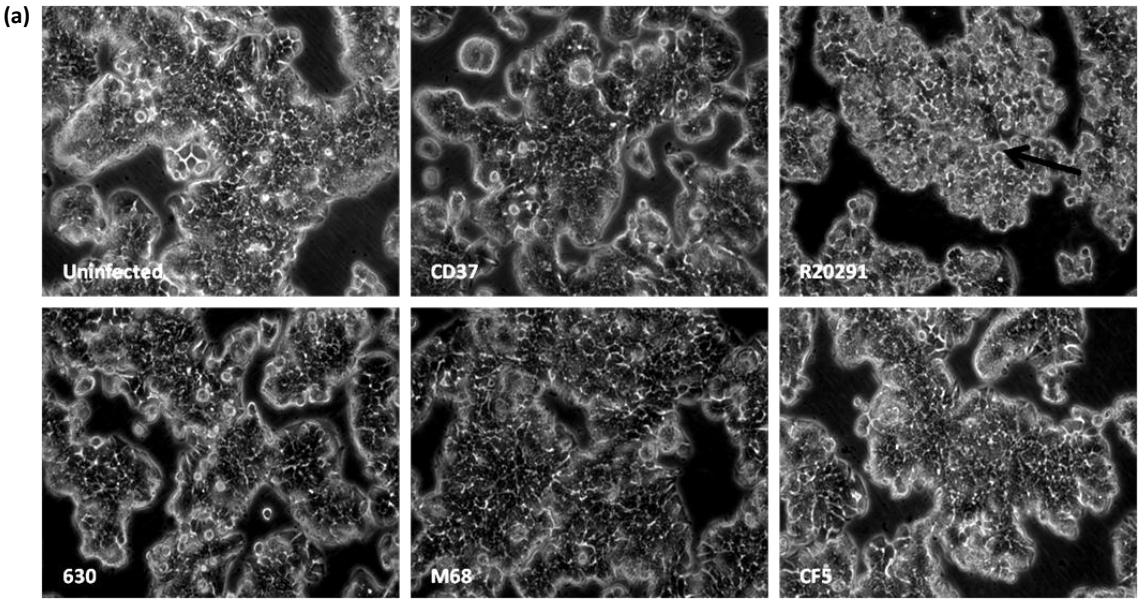

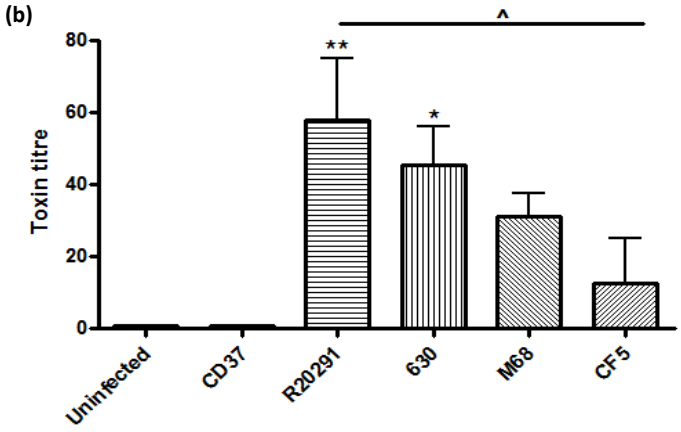

Figure 3.8. Strain R20291 exerts potent and early cytotoxic effect on HT-29 cells. Sub-confluent HT-29 cells were co-cultured with *C. difficile* supernatants at an MOI of 500. Cell morphological changes were observed microscopically (20x, Leica DFC320) at 8 h post-infection. Strain R20291 caused a significant cell rounding (arrow), whilst intermediate cell changes were observed with strains 630 and M68. Strain CF5 caused no cell morphological alteration (a). 2-fold dilutions of bacterial supernatants were used in HT-29 cell cytotoxicity assay in which the end-point titre of each dilution series was scored at 8 h post-infection. Data is presented as the mean ± SEM, n=3. $^{*}p<0.05$, $^{**}p<0.01$ compared to uninfected control, and $^{\wedge}p<0.05$ represents significant inter-strain difference (b). CD37 is a non-toxigenic strain. *P* values were obtained using ANOVA with Bonferroni post-test analysis.

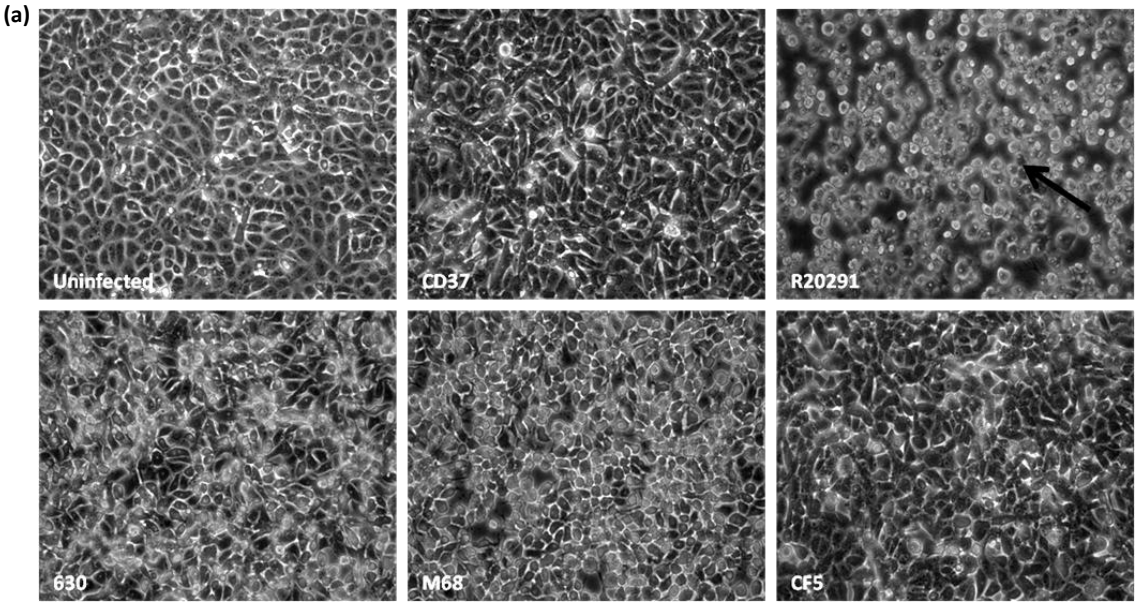

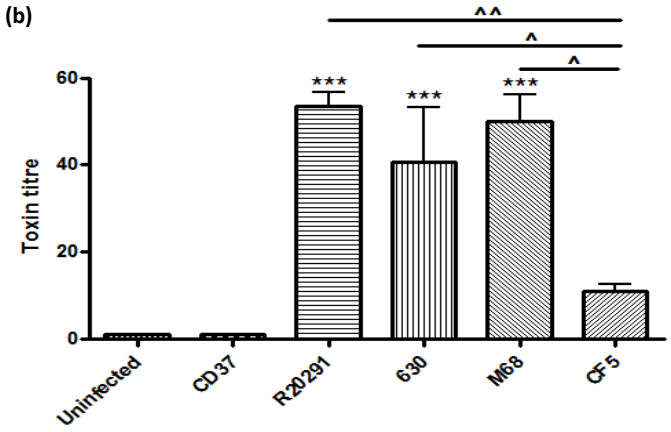

Figure 3.9. Strains R20291, 630 and M68 cause similar cell rounding in Vero cells. Confluent Vero cell monolayers were co-cultured with bacterial supernatants at an MOI of 500. Morphological changes were observed microscopically at 8 h post-infection. R20291 caused a complete cell rounding (arrow). A significant cell morphological change was observed with strains 630 and M68, while CF5 caused the least cell alteration (a). 2-fold dilutions of bacterial supernatants were used in Vero cell cytotoxicity assay in which the end-point titre of each dilution series was scored at 8 h post-infection. Data is presented as the mean ± SEM, n=3. $^{***}p<0.001$ compared to uninfected control, and $^{\wedge}p<0.05$, $^{\wedge\wedge}p<0.01$ represent significant inter-strain difference (b). CD37 is a non-toxigenic strain. *P* values were obtained using ANOVA with Bonferroni post-test analysis.

3.4.3 *C. difficile*-induced Apoptosis in Human IEC

It has been documented that *C. difficile* toxins target and disrupt the function of host Rho GTPases family members including Rho, Rac, and Cdc42. Rho GTPases are involved in actin cytoskeleton regulation and their inactivation leads to dysregulation of the cytoskeletal structure causing disruption of actin-associated apical junctional complex and subsequent cell death (Genth *et al.,* 2006; Genth *et al.,* 2008; Popoff & Geny, 2011).

Several studies have already shown that *C. difficile* induces apoptosis in human primary IECs and in cell-lines. TcdA and TcdB induce apoptosis by a mechanism dependent on inactivation of Rho, activation of caspase-3, -8, and -9 and Bid, and mitochondrial damage followed by cytochrome *c* release (Fiorentini *et al.,* 1998; Brito *et al.,* 2002; Matarrese *et al.,* 2007; Nottrott *et al.,* 2007; Gerhard *et al.,* 2008). In the following experiments, the role of *C. difficile* strains in causing cell death was investigated by utilising two well known methods.

3.4.3.1 Ethidium Homodimer Uptake Assay

Dead cells were marked and identified by using ethidium homodimer, a red fluorescence since their compromised membranes were permeable to this high affinity nucleic acid stain. Caco-2 monolayers were infected with *C. difficile* strains bacterial culture at an MOI of 250 and cell death was evaluated at 4 h and 8 h post-infection by quantifying number of cells marked by red fluorescence (Figures 3.10 & 3.11).

Uninfected control cells showed <10% cell death at 4 h and 8 h. Upon infection, the number of dead cells at 4 h increased to 20% with strains R20291 and M68 causing similar rates of cell death and CF5 showing no significant increase compared to uninfected cells (Figure 3.11). At 8 h, the number of marked cells increased further. More than 30% of infected cells with R20291 were dead, while strains 630 and M68 caused similar rates of cell death (~25-30%). Strain CF5 showed the lowest rate of cell death ~15% at 8 h, which was not significantly higher than the number of dead cells at 4 h infection. On the other hand, cell death rate caused by R20291 at 8 h was significantly increased compared to cell death at 4 h ($p<0.001$). Similar results were also observed with strains 630 and M68 ($p<0.05$).

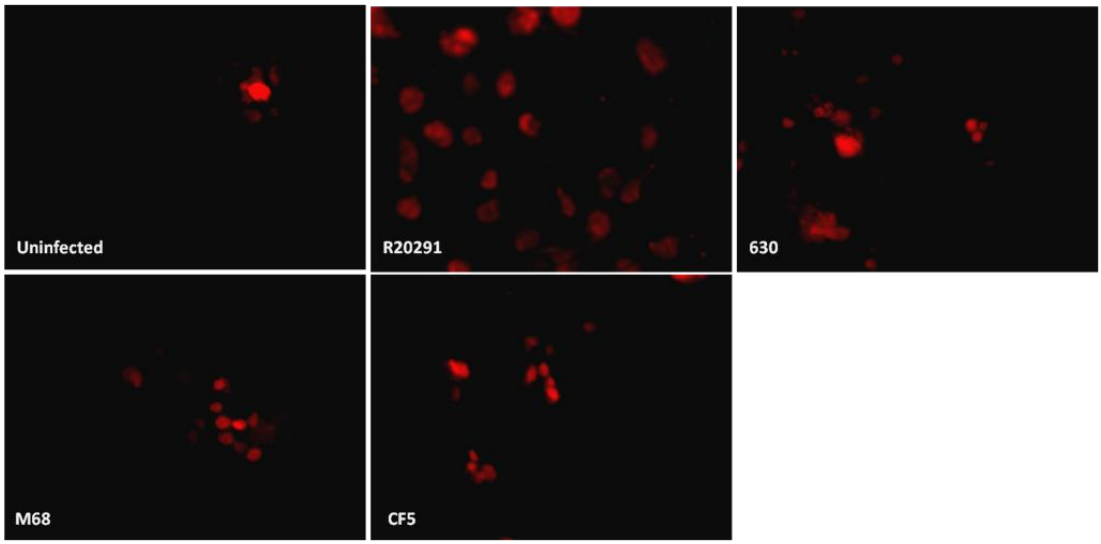

Figure 3.10. *C. difficile*-induced cell death in infected Caco-2 cells. Caco-2 cell monolayers were infected with *C. difficile* bacterial cultures at an MOI of 250 and cell death was evaluated by the ethidium homodimer uptake method. Dead cells were marked by red fluorescence stain. Data is representative of three individual experiments.

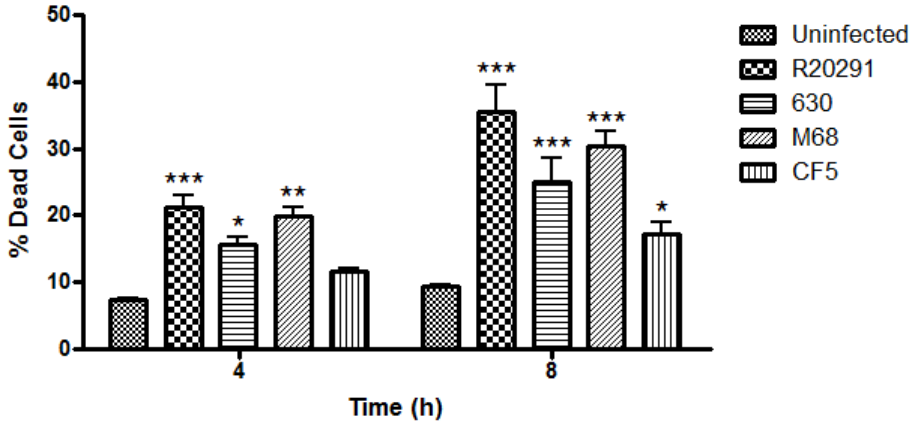

Figure 3.11. Increase in cell death caused by *C. difficile* infection is time dependent. Dead cells were counted from a minimum of five separate fields at 4 h and 8 h post-infection and presented as a percentage of the total number of cells in the corresponding field. Results are presented as mean value ± SEM, n=3. $^{*}p<0.05$, $^{**}p<0.01$ and $^{***}p<0.001$ (ANOVA with Bonferroni post-test) represent significant difference from uninfected cells.

3.4.3.2 Detection of *C. difficile*-induced Apoptosis by Annexin-V & Propidium Iodide

C. difficile-mediated apoptosis in IECs was investigated by employing annexin-V and propidium iodide (PI) staining. During the early stages of apoptosis, translocation of phosphatidylserine (PS) from the inner side of the plasma membrane to the outer layer leads to exposure of PS at the surface of the cell. Annexin-V has a high affinity for PS and since necrotic cells also expose PS, PI was utilised as a DNA stain to distinguish necrotic cells.

Caco-2 monolayers were co-cultured with *C. difficile* cultures at an MOI of 250; at 6 h post-infection, cells were stained with Annexin-V and PI prior to analysis by flow cytometry (Figure 3.12). Apoptotic cells were positive for Annaxin-V only (lower-right quadrant) and necrotic or late apoptotic cells were positive for both Annexin-V and PI (upper-right quadrant), while the viable cells were negative for both Annexin-V and PI (lower-left quadrant) (Figure 3.12 a). Less than 2% of uninfected control cells were apoptotic. Cells infected with R20291, 630, and M68 showed a similar number of apoptotic cells, whilst cell apoptosis caused by strain CF5 (<5%) was not significantly higher than that in the uninfected control (Figure 3.12 b). Cells which were positive for both Annexin-V and PI were considered necrotic cells. In uninfected control cells <1.5% of cells were necrotic. A similar number of necrotic cells was detected in infected Caco-2 cells with strains R20291, 630, and M68 (~5%) and CF5 showed 3% cell necrosis (Figure 3.12 b).

Overall, strains R20291, 630, and M68 caused significant increase in cell apoptosis and necrosis compared to strain CF5; interestingly, the number of apoptotic cells caused by each strain was not significantly higher than necrotic cells. The above data showed that strains R20291, 630, and M68 caused a significant number of cell death, early apoptosis or late apoptosis (necrosis), whilst CF5 infection resulted in significantly less cell death.

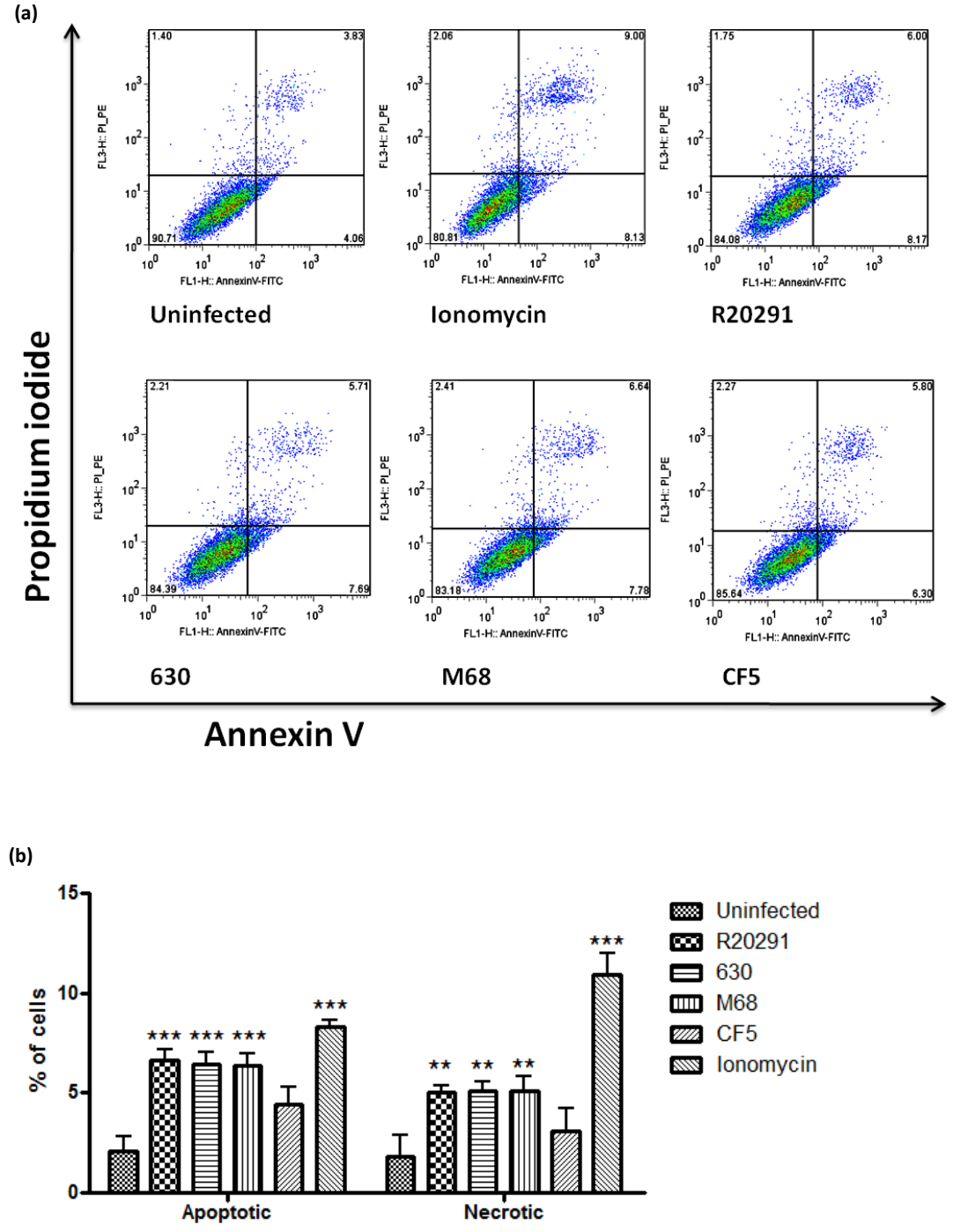

Figure 3.12. *C. difficile* causes apoptosis and necrosis in infected Caco-2 cells. Caco-2 monolayers were co-cultured with *C. difficile* strains at an MOI of 250. Cells were stained using Annexin-V and PI at 6 h post-infection and analysed by flow cytometry. 2 µM Ionomycin (an apoptotic inducer) was used as a positive control. Data is representative of three independent experiments (a). Number of apoptotic/necrotic cells were quantified and presented as a percentage. $^{**}p<0.01$ and $^{***}p<0.001$ (ANOVA with Bonferroni post-test) represent significant difference from uninfected cells (b).

3.4.4 Effect of *C. difficile* Adherence on Human IEC

Adherence to the IEC is a prerequisite for colonisation by many GI pathogens (Eckmann *et al.,* 1995; Kagnoff & Eckmann, 1997). To colonise mucosal surfaces, bacteria commonly interact with glycan structures of the host glycocalyx via bacterial adhesins such as fimbriae or pili, various outer membrane proteins and cell wall components (Moran *et al.,* 2011).

Colonisation of the GI tract by *C. difficile* is essential to its pathogenesis, which requires bacterial adherence to the mucosa. Drudy *et al.* 2001, showed adherence of *C. difficile* to human small and colonic IECs and in cell-lines utilising fluorochrome-labelled *C. difficile*. Several studies have shown binding of *C. difficile* to cultured cell-lines and GI tissues, and data suggests multiple adhesion mechanism(s) involving several bacterial surface layer proteins (Eveillard *et al.,* 1993; Calabi *et al.,* 2002; Cerquetti *et al.,* 2002).

To detect and quantify bacterial adherence to IEC, *C. difficile* strains were labelled with fluorescein isothiocyanate (FITC). Efficiency of the labelling procedure was tested (Figure 3.13) prior to co-culture with Caco-2 monolayers at an MOI of 250. 6 h post-infection, cells were detached and analysed (Figure 3.14 a), adherence was expressed as change in median fluorescent intensity (MFI) (Figures 3.14 b).

A minimum MFI value (~5) was detected in uninfected control cells and similar value was also observed in Caco-2 cells infected with unlabelled bacteria (Figures 3.14 b). Compared to uninfected control cells, all four strains adhered significantly to Caco-2 cells; however, strain R20291 showed increased adherence (MFI ~150) compared to the rest of the strains. A similar level of adherence (MFI ~100) was observed in strains 630, M68, and CF5 (Figure 3.14 b).

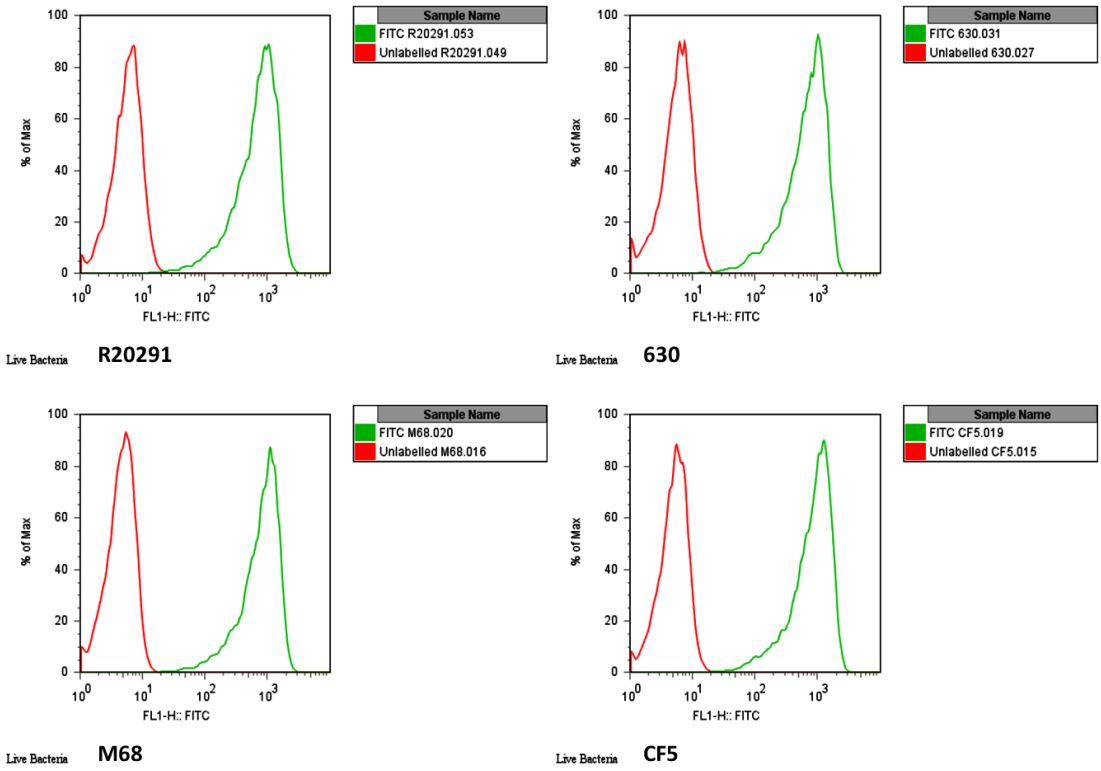

Figure 3.13. *C. difficile* strains show similar distribution of unlabelled and FITC-labelled bacteria. The FITC-labelling of the bacteria was seen as a shift of the bacteria along the FL1 axis in the histogram display mode, showing unlabelled (left peak) and FITC-labelled *C. difficile* (right peak). The fluorescence signal of the labelled population showed no overlap with unlabelled population indicating that the whole population was labelled. This data is representative of three individual experiments.

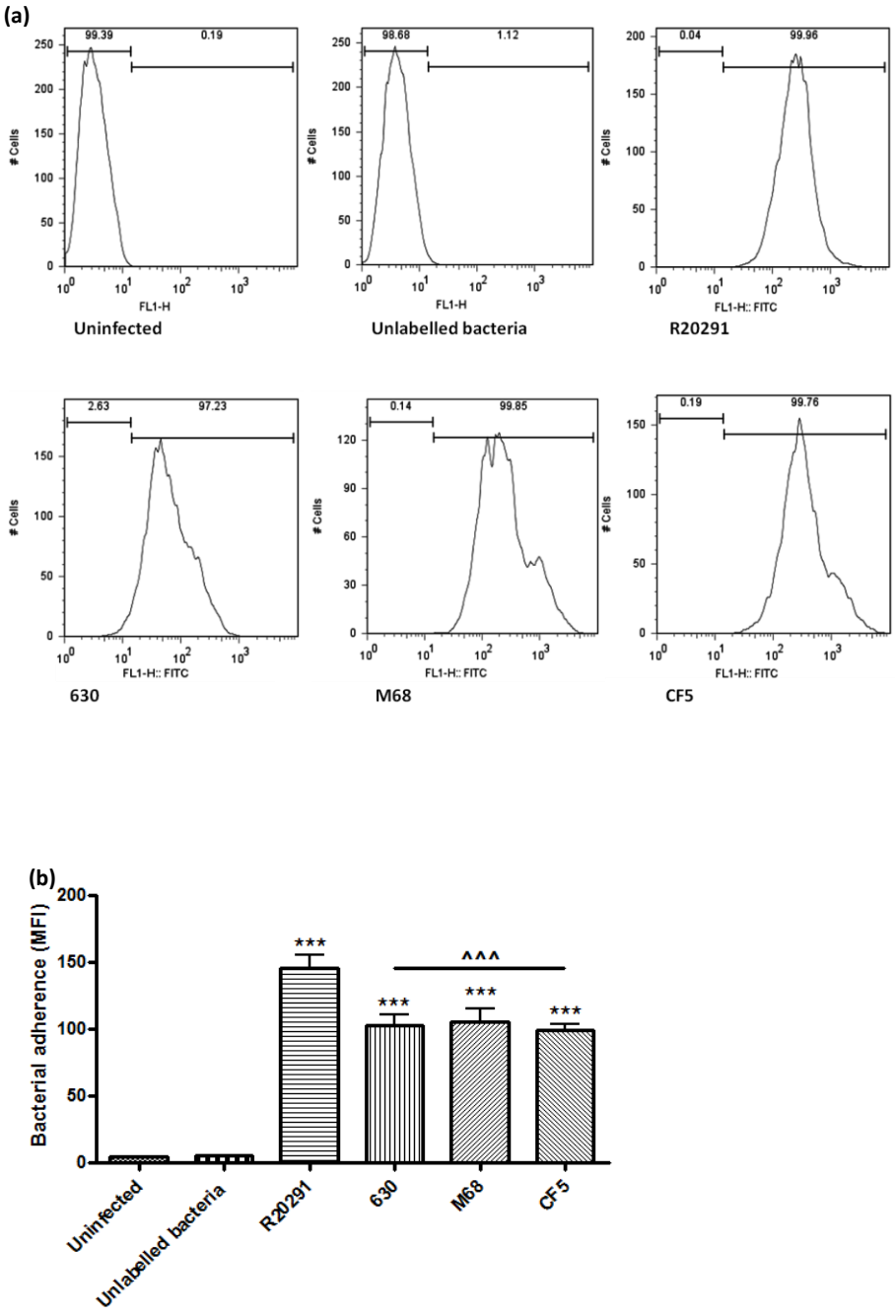

Figure 3.14. *C. difficile* strains adhere significantly to Caco-2 cells. FITC-labelled bacteria were co-incubated with Caco-2 cells at an MOI of 250. Flow cytometric analysis of Caco-2 cells alone and after incubation with FITC-labelled *C. difficile* showed bacterial association as a shift of adhered bacteria to Caco-2 cells along the FL1 axis in the histogram display. This data is representative of three separate experiments (a). Results were quantified and presented as change in MFI. Data represent mean ± SEM, n=3. $^{***}p<0.001$ represents significant difference from uninfected cells, and $^{\wedge\wedge\wedge}p<0.001$ represents significant inter-strain difference (b). *P* values were obtained using ANOVA with Bonferroni post-test.

Furthermore, invasion of IEC by *C. difficile* was assessed by acquiring confocal images. In figure 3.15, FITC-labelled CF5, the least toxic strain was co-cultured with Caco-2 monolayer at an MOI of 250. The optical images, taken at 8 h post-infection were displayed in three orthogonal projections [xy top left corner (a), xz down panel (b), yz right panel (c)] to distinguish between extracellular and internalised bacteria. Orthogonal views showed bacteria in close contact with apical surface of Caco-2 cells, further screening revealed no evidence of bacterial invasion.

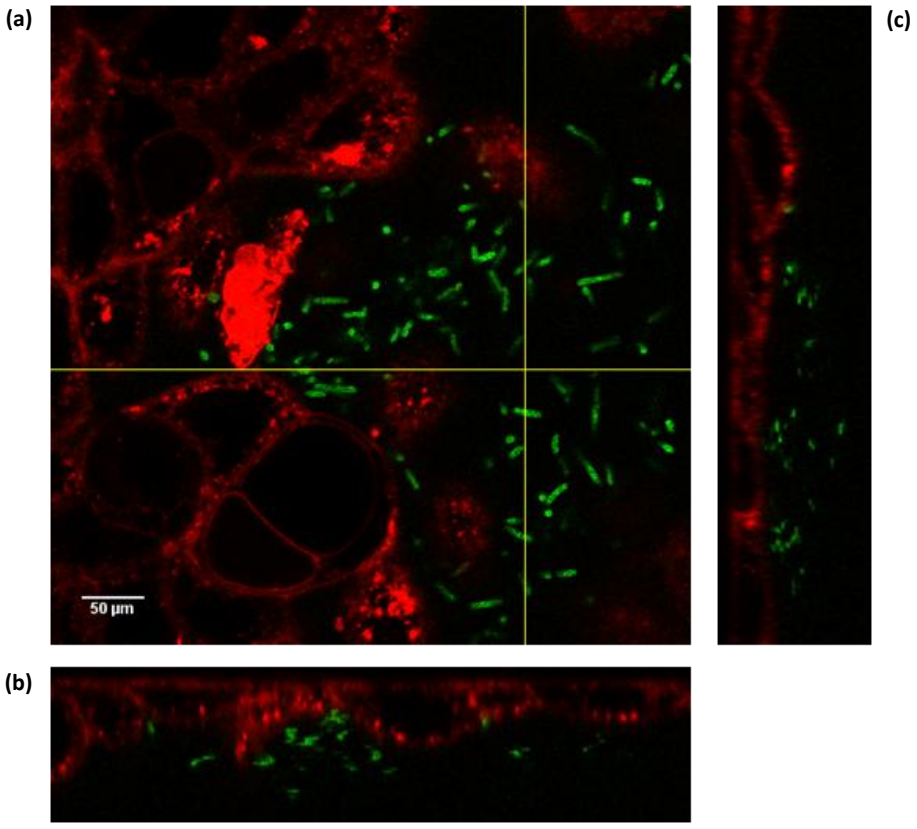

Figure 3.15. *C. difficile* is an extracellular bacterium. Caco-2 cells (stained with cell mask orange) were infected with strain CF5 (FITC-labelled) and examined by confocal microscopy at 8 h post-infection. Images were displayed in three xy (a), xz (b), and yz (c) orthogonal views. xz and yz projections showed bacteria in apical surface of Caco-2 monolayer. Images were taken by Dr. B. Vernay, UCL, ICH.

C. difficile association with IEC leads to time-dependent disruption of the epithelial monolayer. These cellular events were also followed. FITC-labelled *C. difficile* strains were co-cultured with Caco-2 monolayers and disruption of cell monolayer was monitored by time-lapse microscopy up to 12 h in 15 min intervals (Figure 3.16). An intact monolayer was observed in uninfected control cells at 12 h post-infection. Significant monolayer integrity disturbance was observed in infected cells with strains R20291, 630, and M68. On the other hand, cell monolayer infected with strain CF5 remained undamaged (Figure 3.16).

In summary, *C. difficile* strains exhibited a significant adherence to Caco-2 cells. However, despite similar adherence levels exhibited by strains 630, M68, and CF5, differential morphological changes were detected observing the least cell monolayer disruption by strain CF5.

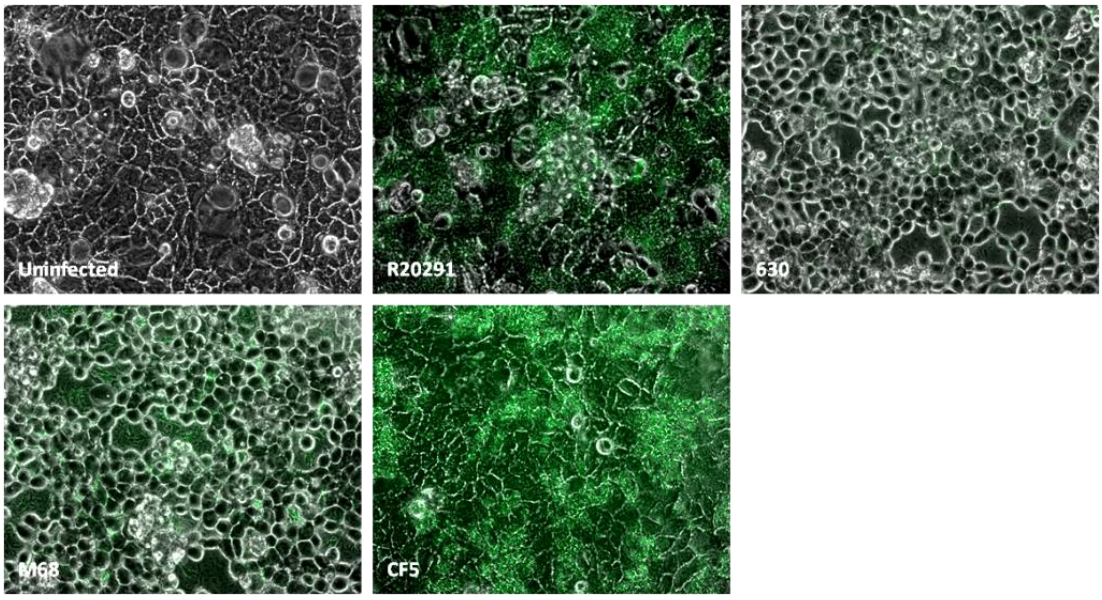

Figure 3.16. Monolayer disruption occurs following bacterial adherence. Caco-2 monolayers were co-cultured with FITC-labelled *C. difficile* strains at an MOI of 250. Morphological changes were visualised by time-lapse microscopy. Caco-2 monolayers infected with strains R20291, 630, and M68 showed substantial cell damages at 12 h post-infection comparing to uninfected control cells. In contrast, cell monolayer infected with CF5 maintained its integrity (32x phase contrast objective, Carl Zeiss Ltd). Images were taken by Dr. B. Vernay, UCL, ICH.

3.5 Characterisation of TcdB from Strains CF5 and M68

Both CF5 and M68 belong to ribotype 017 and carry the A^-B^+ phenotype. Despite both releasing TcdB (Figure 3.6), CF5 displayed a significant reduction in its potential cell cytotoxicity when compared to the strain M68 (Figures 3.8 & 3.9).

It is well-established that *C. difficile* TcdA and TcdB target the Rho subfamily of small GTPases and modify it via glucosylation leading to inactivation of Rho, Rac, and Cdc42 proteins and causing cytoskeletal changes. Treatment of different mammalian cell-lines with TcdB results in decreased levels of cellular Rac1 protein (Chaves-Olarte *et al.,* 2003; Genth *et al.,* 2006). Anti-Rac1 antibody (clone 102) interacts specifically with non-glucosylated Rac1, thus greater glucosylation leads to less binding, an indicator for the extent of Rac1 glucosylation. It was hypothesised that TcdB from strains CF5 and M68 cause differential Rac1 glucosylation leading to variation in their cytotoxic potential.

3.5.1 Mono- glucosylation of Rac by TcdB from Strains CF5 and M68

To establish whether TcdB from CF5 and M68 differ in its potential to modulate IEC Rac1 glucosylation, a co-culture study was conducted employing Caco-2 cells. Confluent monolayers were infected with bacterial cultures at an MOI of 250, then analysed at 8 h post-infection for Rac1 glucosylation (Figure 3.17 a). Rac1 was quantified densitometrically (Figure 3.17 b).

Uninfected control cells showed a spontaneous high expression of Rac1 (Figure 3.17). Both CF5 and M68 treated cells showed reduced levels of Rac1 compared to uninfected cells, whilst strain M68 caused a very significant decrease of Rac1 (Figure 3.17 a & b). Moreover, M68 infected cells exhibited a significant loss of Rac1 when compared with CF5 ($p<0.01$) indicating a considerable Rac1 glucosylation. The same samples were also examined for β-actin (45 kDa) to confirm equal loading (Figure 3.17 a).

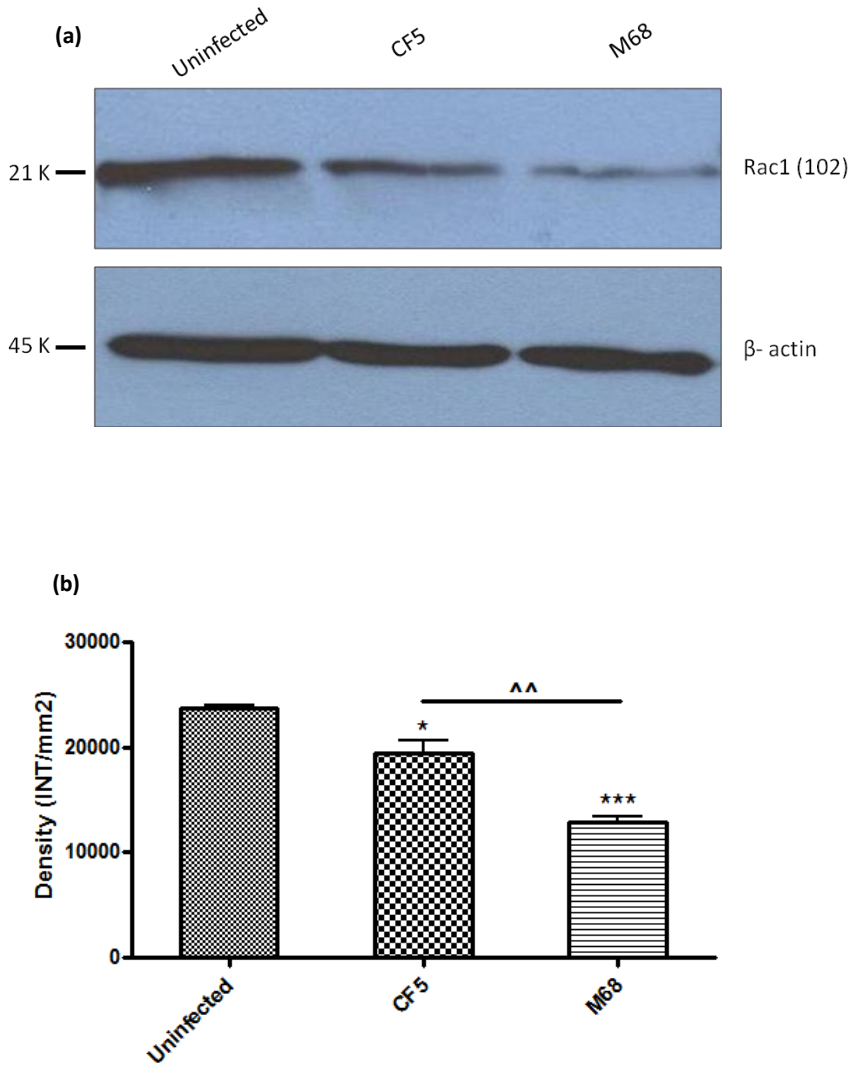

Figure 3.17. CF5 and M68 infection leads to differential Rac1 glucosylation in Caco-2 cells. Caco-2 cells were infected with CF5 and M68 bacterial cultures at an MOI of 250. At 8 h cell lysates were subjected to 15% SDS-PAGE followed by western blotting. Rac1 and β-actin levels were analysed with appropriate antibodies (a). Rac1 was quantified by densitometry (Bio-Rad ChemiDoc XRS) (b). Data represent the mean ± SEM, n=3. $^{*}p<0.05$ and $^{***}p<0.001$ compared to uninfected control, and $^{\wedge\wedge}p<0.01$ represents an inter-strain comparison. *P* values were obtained using ANOVA with Bonferroni post-test analysis.

3.6 Conclusions

Clostridium difficile is an anaerobic, spore-forming bacterium that has been recognised as the causative agent of CDI (Bartlett *et al.,* 1978; George *et al.,* 1978). CDI occurs following antibiotic-mediated disruption of the normal gut microbiota, which enables *C. difficile* to proliferate and cause symptoms ranging from asymptomatic carriage to severe diarrhoea, PMC and death. TcdA and TcdB are major virulence factors of *C. difficile* but this bacterium harbours an array of other virulence factors as well. The majority of studies on *C. difficile* so far have focused on using purified/recombinant toxins and the role of the bacterium itself in initiating disease has been overlooked. Therefore, the objective of this study was to elucidate early interactions between whole bacteria and the IEC. Understanding of early events may help in improving future diagnostics and therapeutics to this life-threatening infection.

In the current study, initial optimisation was conducted employing four different *C. difficile* strains due to lack of isogenic mutants at the commencement of this project. These included strain R20291 from the hypervirulent clade, a fully sequenced strain 630 (A^+B^+), and variant *C. difficile* strains CF5 and M68 (A^-B^+), which are historic and recent representatives of PCR ribotype 017, respectively (Stabler *et al.,* 2006). Prior to co-culture studies, *C. difficile* strains were characterised microbiologically and their capacity of toxin production was determined. The cytotoxic effect of *C. difficile* on human IEC was investigated by measuring LDH release, and the rate of infection-induced apoptosis and necrosis. Also the degree of bacterial adherence and subsequent effects on IEC monolayer disruption were investigated.

Similar growth kinetics were observed for strains R20291, M68, and CF5 reaching stationary phase at 4-5 h, while 630 showed slower growth, achieving stationary phase at 8 h post-inoculation. Strain 630 slow growth also corresponded with a longer doubling time (~22min) compared to the other strains (≥15 min). As *C. difficile* strains express toxins during the late logarithmic and stationary phases of growth (Voth & Ballard, 2005), MOI was determined by viable counting once each strain reached its stationary phase (OD_{600} of 1.5). Similar trend of cell death was observed with all four strains up to 8 h. Additionally, bacterial exposure to an aerobic environment can trigger spore formation. Sporulation is initiated under harsh or adverse environment leading to formation of metabolically dormant but highly resistant spores (Sorg & Sonenshein, 2008). It has been shown that *C. difficile* spore germinates in BHI media (Paredes-Sabja *et al.,* 2008) therefore, YPM, a

sporulation medium was employed to compare and contrast the spore formation. No sporulation was detected in BHI, whilst under the same conditions up to $1x10^6$/ml spores were observed in YPM also it was noted that all four strains sporulated to similar levels. Taken all together, it was hypothesised that during co-culture studies since *C. difficile* strains were grown in BHI, bacterial exposure to aerobic conditions led to bacterial death not sporulation.

Previous studies have shown that *C. difficile* can adhere to various cell-lines including Caco-2 and Vero cells *in vitro* and to mice caecal mucus *in vivo* (Karjalainen *et al.,* 1994; Cerquetti *et al.,* 2002). *C. difficile* strains adhered significantly to Caco-2 cells compared to uninfected control cells ($p<0.001$) however, R20291 exhibited greater adherence compared to the rest of the strains ($p<0.001$). To date a number of *C. difficile* virulence factors involved in adherence to IEC have been identified. *C. difficile* SLPs facilitate adhesion to cultured cell-lines and *ex vivo* human GI tissues (Calabi *et al.,* 2002). SLPs consist of two subunits; HMW and LMW. Extensive SLP sequence variation has been observed between different *C. difficile* strains, particularly in the LMW which lies external to the HMW on the bacterial cell surface (Wright *et al.,* 2005; Fagan *et al.,* 2009; Deneve *et al.,* 2009). This inter-strain variability might explain the differential adherence capacity observed between R20291 and the other strains. Further on this note, strain R20291 produces binary toxin and CDT can increase *C. difficile* adherence to IEC *in vitro* and *in vivo* (Schwan *et al.,* 2009).

At present, the role of individual toxins to IEC adherence remains undefined. The experiments conducted here however do highlight some potential features of *C. difficile* TcdA and TcdB function. Strains R20291 and 630 produced similar amounts of TcdA, in contrast the amount of TcdB produced by the various strains showed marked variation, in particular strain CF5 showed considerably more TcdB production than that observed with the other strains. This data can be interpreted as either a feature of the antibody employed, which resulted in better recognition of strain CF5 TcdB or that this strain does indeed produce higher level of TcdB. Further investigations utilising other toxin-specific antibodies are required to confirm which suggestion may hold.

Strains R20291, 630, and M68 caused cell toxicity to a similar extent, while CF5 showed a modest cytotoxicity at early time-points of infection. This was confirmed with ethidium homodimer uptake assay and Annexin-V/PI staining. Furthermore, cytotoxicity assays utilising HT-29 and Vero cells, which are known to be respectively more sensitive to TcdA and TcdB showed significant toxicity with R20291 infected HT-29 cells, and strains 630 and

M68 showed an intermediate level however, the difference was not statistically significant. If we hypothesise (based on Figure 3.6) that TcdA and TcdB from strains R20291 and 630 are equipotent then the trend for greater toxicity by the R20291 could be assigned to the presence of CDT. These suggestions at present remain assumptions as the lack of reagents impeded us from studying these aspects of host-pathogen crosstalk. An emerging theme from the data presented was that strain CF5 was the least toxic strain in all assays tested.

TcdA between strains R20291 and 630 exhibit 98% identity while enzymatic region of TcdB are 96% identical, C-terminal region in contrast shows the highest degree of sequence variation exhibiting only 88% identity (Lanis *et al.,* 2010). As strains M68 and CF5 sequences have not yet been completed, the comparison between the four strains in order to identify the sequence variation was not possible, however sequence differences should allow us to further dissect functional differences between the TcdB from the two strains. This is worth pursuing as studies have shown that toxins of some *C. difficile* strains and in particular TcdB have inherent variability such as in their glucosylating enzymatic activity (Torres, 1991; Alfa *et al.,* 2000; Chaves-Olarte *et al.,* 2003; Stabler *et al.,* 2008), therefore, the inactivation of Rac1, which is glucosylated by all clostridial toxins (Genth *et al.,* 2006) was investigated. Interestingly, significantly reduced levels of Rac1 were detected in cells infected with strain M68 compared to CF5, indicating greater Rac1 glucosylation by M68.

To improve our current limited understanding of TcdB structure and function, we proceeded with large-scale TcdB protein purification from M68 and CF5 bacterial cells. Cells from a 72h culture were harvested then separated on 6% SDS PAGE (data not shown, n=1). Appropriate band size products were cut and subjected to mass spectrometric analysis (Dr. Kevin Mills & Dr. Wendy Haywood; ICH/Biological mass spectrometry Centre). Detected protein sequences were identified using www.uniprot.org a protein database by aligning against *C. difficile* TcdB protein sequence (Figure 3.18). The preliminary data recovered 57 peptides from CF5 (Figure 3.18 a) and 33 peptides were identified in M68 (Figure 3.18 b) however, so far no amino acid difference or modification has been found. It needs to be noted that these studies are currently under investigation.

3.6.1 Summary

Taken all together, the work in this chapter demonstrated that:

- Strains R20291, M68 and CF5 showed similar microbiological properties, while 630 shared comparable sporulation kinetics and survival under aerobic conditions.
- Strain R20291 exhibited a very significant adherence to Caco-2 cells compared to other strains.
- Strains R20291, 630 and M68 exhibited similar cytotoxicity and cell death, whilst CF5 showed the least effect.
- Strain M68 significantly glucosylated Rac1 compared to CF5.

(a)

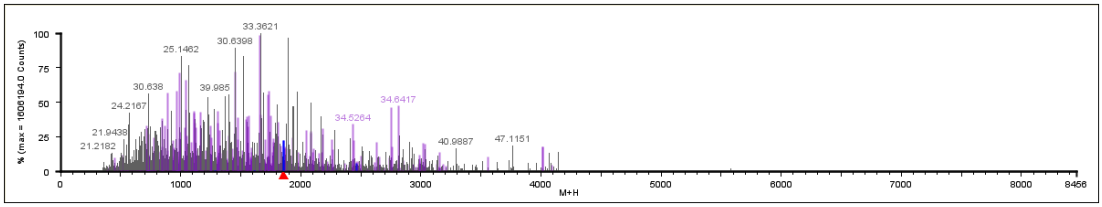

P18177 Coverage Map

1	MSLVNRKQLE	KMANVRFRTQ	EDEYVAILDA	LEEYHNMSEN	TVVEKYLKLK
51	DINSLTDIYI	DTYKKSGRNK	ALKKFKEYLV	TEVLELKNNN	LTPVEKNLHF
101	VWIGGQINDT	AINYINQWKD	VNSDYNVNVF	YDSNAFLINT	LKKTVVESAI
151	NDTLESFREN	LNDPRFDYNK	FFRKRMEIIY	DKQKNFINYY	KAQREENPEL
201	IIDDIVKTYL	SNEYSKEIDE	LNTYIEESLN	KITQNSGNDV	RNFEEFKNGE
251	SFNLYEQELV	ERWNLAAASD	ILRISALKEI	GGMYLDVDML	PGIQPDLFES
301	IEKPSSVTVD	FWEMTKLEAI	MKYKEYIPEY	TSEHFDMLDE	EVQSSFESVL
351	ASKSDKSEIF	SSLGDMEASP	LEVKIAFNSK	GIINQGLISV	KDSYCSNLIV
401	KQIENRYKIL	NNSLNPAISE	DNDFNTTTNT	FIDSIMAEAN	ADNGRFMMEL
451	GKYLRVGFFP	DVKTTINLSG	PEAYAAAYQD	LLMFKEGSMN	IHLIEADLRN
501	FEISKTNISQ	STEQEMASLW	SFDDARAKAQ	FEEYKRNYFE	GSLGEDDNLD
551	FSQNIVVDKE	YLLEKISSLA	RSSERGYIHY	IVQLQGDKIS	YEAACNLFAK
601	TPYDSVLFQK	NIEDSEIAYY	YNPGDGEIQE	IDKYKIPSII	SDRPKIKLTF
651	IGHGKDEFNT	DIFAGFDVDS	LSTEIEAAID	LAKEDISPKS	IEINLLGCNM
701	FSYSINVEET	YPGKLLLKVK	DKISELMPSI	SQDSIIVSAN	QYEVRINSEG
751	RRELLDHSGE	WINKEESIIK	DISSKEYISF	NPKENKITVK	SKNLPELSTL
801	LQEIRNNSNS	SDIELEEKVM	LTECEINVIS	NIDTQIVEER	IEEAKNLTSD
851	SINYIKDEFK	LIESISDALC	DLKQQNELED	SHFISFEDIS	ETDEGFSIRF
901	INKETGESIF	VETEKTIFSE	YANHITEEIS	KIKGTIFDTV	NGKLVKKVNL
951	DTTHEVNTLN	AAFFIQSLIE	YNSSKESLSN	LSVAMKVQVY	AQLFSTGLNT
1001	ITDAAKVVEL	VSTALDETID	LLPTLSEGLP	IIATIIDGVS	LGAAIKELSE
1051	TSDPLLRQEI	EAKIGIMAVN	LTTATTAIIT	SSLGIASGFS	ILLVPLAGIS
1101	AGIPSLVNNE	LVLRDKATKV	VDYFKHVSLV	ETEGVFTLLD	DKIMMPQDDL
1151	VISEIDFNNN	SIVLGKCEIW	RMEGGSGHTV	TDDIDHFFSA	PSITYREPHL
1201	SIYDVLEVQK	EELDLSKDLM	VLPNAPNRVF	AWETGWTPGL	RSLENDGTKL
1251	LDRIRDNYEG	EFYWRYFAFI	ADALITTLKP	RYEDTNIRIN	LDSNTRSFIV
1301	PIITTEYIRE	KLSYSFYGSG	GTYALSLSQY	NMGINIELSE	SDVWIIDVDN
1351	VVRDVTIESD	KIKKGDLIEG	ILSTLSIEEN	KIILNSHEIN	FSGEVNGSNG
1401	FVSLTFSILE	GINAIIEVDL	LSKSYKLLIS	GELKILMLNS	NHIQQKIDYI
1451	GFNSELQKNI	PYSFVDSEGK	ENGFINGSTK	EGLFVSELPD	VVLISKVYMD
1501	DSKPSFGYYS	NNLKDVKVIT	KDNVNILTGY	YLKDDIKISL	SLTLQDEKTI
1551	KLNSVHLDES	GVAEILKFMN	RKGNTNTSDS	LMSFLESMNI	KSIFVNFLQS
1601	NIKFILDANF	IISGTTSIGQ	FEFICDENDN	IQPYFIKFNT	LETNYTLYVG
1651	NRQNMIVEPN	YDLDDSGDIS	STVINFSQKY	LYGIDSCVNK	VVISPNIYTD
1701	EINITPVYET	NNTYPEVIVL	DANYINEKIN	VNINDLSIRY	VWSNDGNDFI
1751	LMSTSEENKV	SQVKIRFVNV	FKDKTLANKL	SFNFSDKQDV	PVSEIILSFT
1801	PSYYEDGLIG	YDLGLVSLYN	EKFYINNFGM	MVSGLIYIND	SLYYFKPPVN
1851	NLITGFVTVG	DDKYYFNPIN	GGAASIGETI	IDDKNYYFNQ	SGVLQTGVFS
1901	TEDGFKYFAP	ANTLDENLEG	EAIDFTGKLI	IDENIYYFDD	NYRGAVEWKE
1951	LDGEMHYFSP	ETGKAFKGLN	QIGDYKYYFN	SDGVMQKGFV	SINDNKHYFD
2001	DSGVMKVGYT	EIDGKHFYFA	ENGEMQIGVF	NTEDGFKYFA	HHNEDLGNEE
2051	GEEISYSGIL	NFNNKIYYFD	DSFTAVVGWK	DLEDGSKYYF	DEDTAEAYIG
2101	LSLINDGQYY	FNDDGIMQVG	FVTINDKVFY	FSDSGIIESG	VQNIDDNYFY
2151	IDDNGIVQIG	VFDTSDGYKY	FAPANTVNDN	IYGQAVEYSG	LVRVGEDVYY
2201	FGETYTIETG	WIYDMENESD	KYYFNPETKK	ACKGINLIDD	IKYYFDEKGI
2251	MRTGLISFEN	NNYYFNENGE	MQFGYINIED	KMFYFGEDGV	MQIGVFNTPD
2301	GFKYFAHQNT	LDENFEGESI	NYTGWLDLDE	KRYYFTDEYI	AATGSVIIDG
2351	EEYYFDPDTA	QLVISE			

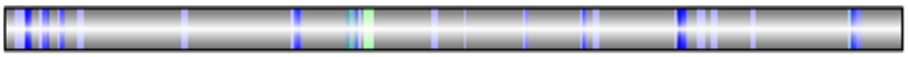

Key:

Regions of the protein sequence that match peptides are highlighted in colour, according to the key below

Matched to a peptide

Matched to a partial peptide

Matched to a modified peptide

Matched to a partial modified peptide

Highlights are transparent, so that regions where peptides overlap are visible on the coverage map. E.g. an overlap between a standard peptide and a modified peptide would appear as shown:

Accession	Entry	Description	mW (Da)	pI (pH)	PLGS Score	Peptides	Theoretical Peptides	Coverage (%)	Digest Peptides	Modified Peptides
TOXB - CLODI	P18177	Toxin B OS Clostridium difficile GN toxB PE 1 SV 3	269541	4.218	45.6396	57	178	19.273	50	2

(b)

P18177 Coverage Map

1	MSLVNRKQLE	KMANVRFRTQ	EDEYVAILDA	LEEYHNMSEN	TVVEKYLKLK
51	DINSLTDIYI	DTYKKSGRNK	ALKKFKEYLV	TEVLELKNNN	LTPVEKNLHF
101	VWIGGQINDT	AINYINQWKD	VNSDYNVNVF	YDSNAFLINT	LKKTVVESAI
151	NDTLESFREN	LNDPRFDYNK	FFRKRMEIIY	DKQKNFINYY	KAQREENPEL
201	IIDDIVKTYL	SNEYSKEIDE	LNTYIEESLN	KITQNSGNDV	RNFEEFKNGE
251	SFNLYEQELV	ERWNLAAASD	ILRISALKEI	GGMYLDVDML	PGIQPDLFES
301	IEKPSSVTVD	FWEMTKLEAI	MKYKEYIPEY	TSEHFDMLDE	EVQSSFESVL
351	ASKSDKSEIF	SSLGDMEASP	LEVKIAFNSK	GIINQGLISV	KDSYCSNLIV
401	KQIENRYKIL	NNSLNPAISE	DNDFNTTTNT	FIDSIMAEAN	ADNGRFMMEL
451	GKYLRVGFFP	DVKTTINLSG	PEAYAAAYQD	LLMFKEGSMN	IHLIEADLRN
501	FEISKTNISQ	STEQEMASLW	SFDDARAKAQ	FEEYKRNYFE	GSLGEDDNLD
551	FSQNIVVDKE	YLLEKISSLA	RSSERGYIHY	IVQLQGDKIS	YEAACNLFAK
601	TPYDSVLFQK	NIEDSEIAYY	YNPGDGEIQE	IDKYKIPSII	SDRPKIKLTF
651	IGHGKDEFNT	DIFAGFDVDS	LSTEIEAAID	LAKEDISPKS	IEINLLGCNM
701	FSYSINVEET	YPGKLLLKVK	DKISELMPSI	SQDSIIVSAN	QYEVRINSEG
751	RRELLDHSGE	WINKEESIIK	DISSKEYISF	NPKENKITVK	SKNLPELSTL
801	LQEIRNNSNS	SDIELEEKVM	LTECEINVIS	NIDTQIVEER	IEEAKNLTSD
851	SINYIKDEFK	LIESISDALC	DLKQQNELED	SHFISFEDIS	ETDEGFSIRF
901	INKETGESIF	VETEKTIFSE	YANHITEEIS	KIKGTIFDTV	NGKLVKKVNL
951	DTTHEVNTLN	AAFFIQSLIE	YNSSKESLSN	LSVAMKVQVY	AQLFSTGLNT
1001	ITDAAKVVEL	VSTALDETID	LLPTLSEGLP	IIATIIDGVS	LGAAIKELSE
1051	TSDPLLRQEI	EAKIGIMAVN	LTTATTAIIT	SSLGIASGFS	ILLVPLAGIS
1101	AGIPSLVNNE	LVLRDKATKV	VDYFKHVSLV	ETEGVFTLLD	DKIMMPQDDL
1151	VISEIDFNNN	SIVLGKCEIW	RMEGGSGHTV	TDDIDHFFSA	PSITYREPHL
1201	SIYDVLEVQK	EELDLSKDLM	VLPNAPNRVF	AWETGWTPGL	RSLENDGTKL
1251	LDRIRDNYEG	EFYWRYFAFI	ADALITTLKP	RYEDTNIRIN	LDSNTRSFIV
1301	PIITTEYIRE	KLSYSFYGSG	GTYALSLSQY	NMGINIELSE	SDVWIIDVDN
1351	VVRDVTIESD	KIKKGDLIEG	ILSTLSIEEN	KIILNSHEIN	FSGEVNGSNG
1401	FVSLTFSILE	GINAIIEVDL	LSKSYKLLIS	GELKILMLNS	NHIQQKIDYI
1451	GFNSELQKNI	PYSFVDSEGK	ENGFINGSTK	EGLFVSELPD	VVLISKVYMD
1501	DSKPSFGYYS	NNLKDVKVIT	KDNVNILTGY	YLKDDIKISL	SLTLQDEKTI
1551	KLNSVHLDES	GVAEILKFMN	RKGNTNTSDS	LMSFLESMNI	KSIFVNFLQS
1601	NIKFILDANF	IISGTTSIGQ	FEFICDENDN	IQPYFIKFNT	LETNYTLYVG
1651	NRQNMIVEPN	YDLDDSGDIS	STVINFSQKY	LYGIDSCVNK	VVISPNIYTD
1701	EINITPVYET	NNTYPEVIVL	DANYINEKIN	VNINDLSIRY	VWSNDGNDFI
1751	LMSTSEENKV	SQVKIRFVNV	FKDKTLANKL	SFNFSDKQDV	PVSEIILSFT
1801	PSYYEDGLIG	YDLGLVSLYN	EKFYINNFGM	MVSGLIYIND	SLYYFKPPVN
1851	NLITGFVTVG	DDKYYFNPIN	GGAASIGETI	IDDKNYYFNQ	SGVLQTGVFS
1901	TEDGFKYFAP	ANTLDENLEG	EAIDFTGKLI	IDENIYYFDD	NYRGAVEWKE
1951	LDGEMHYFSP	ETGKAFKGLN	QIGDYKYYFN	SDGVMQKGFV	SINDNKHYFD
2001	DSGVMKVGYT	EIDGKHFYFA	ENGEMQIGVF	NTEDGFKYFA	HHNEDLGNEE
2051	GEEISYSGIL	NFNNKIYYFD	DSFTAVVGWK	DLEDGSKYYF	DEDTAEAYIG
2101	LSLINDGQYY	FNDDGIMQVG	FVTINDKVFY	FSDSGIIESG	VQNIDDNYFY
2151	IDDNGIVQIG	VFDTSDGYKY	FAPANTVNDN	IYGQAVEYSG	LVRVGEDVYY
2201	FGETYTIETG	WIYDMENESD	KYYFNPETKK	ACKGINLIDD	IKYYFDEKGI
2251	MRTGLISFEN	NNYYFNENGE	MQFGYINIED	KMFYFGEDGV	MQIGVFNTPD
2301	GFKYFAHQNT	LDENFEGESI	NYTGWLDLDE	KRYYFTDEYI	AATGSVIIDG
2351	EEYYFDPDTA	QLVISE			

Accession	Entry	Description	mW (Da)	pI (pH)	PLGS Score	Peptides	Theoretical Peptides	Coverage (%)
TOXB - CLODI	P18177	Toxin B OS Clostridium difficile GN toxB PE 1 SV 3	269541	4.218	26.3981	33	178	13.9053

Figure 3.18. TcdB released from CF5 and M68 share protein sequences. Crude toxin obtained from CF5 (a) and M68 (b) pellets were analysed by proteomics in order to identify any protein post-translational modifications.

Chapter 4

Clostridium difficile-Intestinal Epithelial Cell Interactions (II)

4.1 Introduction

The GI tract is lined by a single layer of IEC which provides a primary barrier separating the intestinal lumen from the underlying tissue. The intestinal epithelium not only has a physical protective role, which is reinforced by the presence of mucus, but also absorbs water, salt and nutrients, secretes hormones and antimicrobial peptides. Another important function of the IEC is executing a clear discrimination between pathogens and commensals and initiating innate immune responses, whilst it is constantly exposed to dietary, microbial antigens and an estimated 10^{14} commensal bacteria (Mowat, 2003; Colbere-Garapin *et al.,* 2007; Artis, 2008).

C. difficile is an important nosocomial pathogen mediating a spectrum of diseases ranging from mild diarrhoea to fatal colitis, most often in the context of current or recent treatment with antibiotics. Administration of antibiotics leads to alteration in the gut ecosystem and disruption of the normal microbiota. These changes create a niche that allows *C. difficile* to colonise the colon, overgrow, and release two exotoxins; TcdA and TcdB (Beaugerie & Petit, 2004; Mahida, 2004). Both toxins are pro-inflammatory and enterotoxic, causing production of IL-6 and IL-8 in the human intestine (Mahida *et al.,* 1996; Ng *et al.,* 2003; Savidge *et al.,* 2003) and IL-1, IL-6, IL-8, and TNF-α by human monocytes (Flegel *et al.,* 1991; Linevsky *et al.,* 1997; Jefferson *et al.,* 1999; Warny *et al.,* 2000).

The effect and the role of *C. difficile* toxins have been well characterised mainly by utilising purified toxins in animal models of infection (Pothoulakis *et al.,* 1994; Rocha *et al.,* 1997; Souza *et al.,* 1997; Castagliuolo *et al.,* 1998; Alcantara *et al.,* 2001) and *in vitro* studies (Riegler *et al.,* 1995; Branka *et al.,* 1997; Melo Filho *et al.,* 1997; Mahida *et al.,* 1998; Ishida *et al.,* 2004; Meyer *et al.,* 2007; Sutton *et al.,* 2008), or employing recombinant toxins (Sun *et al.,* 2009). Surprisingly, very little information is available on the effect of *C. difficile* itself on human IEC. Thus, the aim of this study was to investigate how GI mucosa responds to the bacterial cell itself and its secretory products.

4.2 *C. difficile*-mediated Host Innate Immune Response(s)

Intestinal epithelial cells in addition to providing a physical and biochemical barrier, express a wide range of PRRs that can recognise bacterial factors and subsequently execute regulation of immune responses in the intestinal microenvironment. *C. difficile* TcdA and TcdB have been shown to induce disruption of epithelial barrier function and expression of pro-inflammatory cytokines and it has been documented that both toxins can stimulate the expression of IL-8 in human IEC (Mahida *et al.,* 1996; Kim *et al.,* 2002; Johal *et al.,* 2004c; NA *et al.,* 2005). There is only one study to date that suggests differential host cytokine responses to different concentrations of toxin. Johal and colleagues found IL-8 expression in response to high concentrations of TcdA (≥ 100 ng/ml), while low concentrations (≤ 10 ng/ml) induce TGF-β, a protective cytokine (Johal *et al.,* 2004c). One has to take these studies with caution as toxin concentration during an on-going CDI is not known. At present, IEC innate immune responses to whole bacteria are unknown.

In this study, *C. difficile*-induced inflammatory response(s) was examined using human IECs including; Caco-2, HT-29, and human colonic cell-line T84. The initial study was conducted using *C. difficile* strains; 027, 630 and its erythromycin-sensitive derivative strain (630 Δerm) (A^+B^+), and CD37 (a non-toxigenic *C. difficile* strain) at an MOI of 50. Strain 630 Δerm is a deletion mutant that has been generated by continuous subculture and has lost its phenotypic resistance to erythromycin and clindamycin (Hussain *et al.,* 2005).

Later in the study, these series of experiments were concluded using R20291 (PCR-ribotype 027), 630 (A^+B^+), and M68 and CF5 (A^-B^+) strains in order to elucidate differential response of A^+B^+ strains versus A^-B^+ *C. difficile* strains at various doses of MOIs.

4.2.1 Human IEC IL-8 Response to *C. difficile* Infection

To study IEC IL-8 response to *C. difficile* infection, Caco-2 monolayers were infected with 027, 630, 630 Δerm, and CD37 bacterial cultures at an MOI of 50. IL-8 mRNA expression was determined in a time-dependent manner at 2, 4, 6, and 8 h post-infection by semi-quantitative RT-PCR (Figure 4.1 a). Gene expression was quantified by densitometery and normalised to GAPDH. Data is presented as fold induction (Figure 4.1 b).

Cells infected with *C. difficile* strains showed ≥ 3-fold increase in IL-8 mRNA expression at 2 h and 4 h, followed by a decline to ~1-fold at 6 h and 8 h post-infection. No significant inter-strain difference was observed at any examined time-points (Figure 4.1 b).

C. difficile-induced IL-8 mRNA expression was further investigated by infecting Caco-2 monolayers with bacterial cultures of strains R20291, 630, M68, and CF5 at an MOI of 100. Gene expression was determined at 4 h and 8 h post-infection by RT-PCR (Figure 4.1 c). Infections with *C. difficile* strains caused similar increase in IL-8 mRNA expression, showing an increase of up to 3-fold at 8 h post-infection (Figure 4.1 d).

Previous studies have shown the effect of *C. difficile* toxins on human IEC leading to IL-8 production; however, it is unknown whether intestinal epithelia respond differentially to whole bacteria and its components. In this study, IL-8 release from human IEC in response to bacterial culture (whole bacterial cell plus supernatant) was compared with whole bacterial cell, filter-sterilised supernatant (containing toxins and secretory products) and spore preparations at 8 h post-infection (Figure 4.1 e).

Basal IL-8 protein levels in uninfected Caco-2 cells were generally <5 pg/ml. Upon infection with bacterial cultures and whole bacterial cells, IL-8 secretion increased to 10-40 pg/ml and 10-60 pg/ml, respectively. Bacterial supernatants induced intermediate amounts <20 pg/ml while *C. difficile* spores increased IL-8 release between 5-30 pg/ml (Figure 4.1 e).

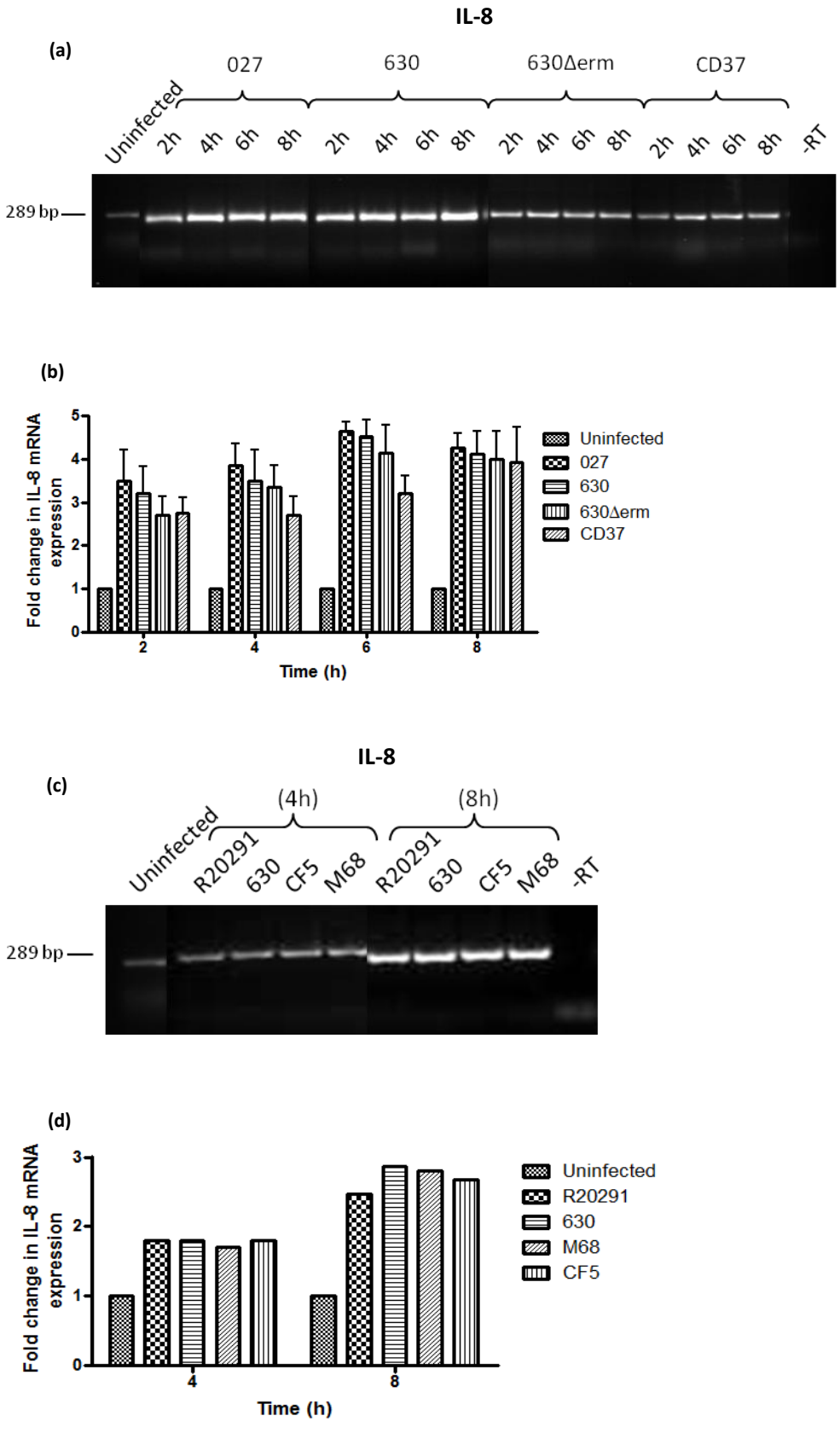
IL-8
(a)
027
630
630Δerm
CD37
Uninfected
2h
4h
6h
8h
-RT
289 bp
(b)
Fold change in IL-8 mRNA expression
Time (h)
Uninfected
027
630
630Δerm
CD37
IL-8
(c)
(4h)
(8h)
Uninfected
R20291
630
CF5
M68
-RT
289 bp
(d)
Fold change in IL-8 mRNA expression
Time (h)
Uninfected
R20291
630
M68
CF5

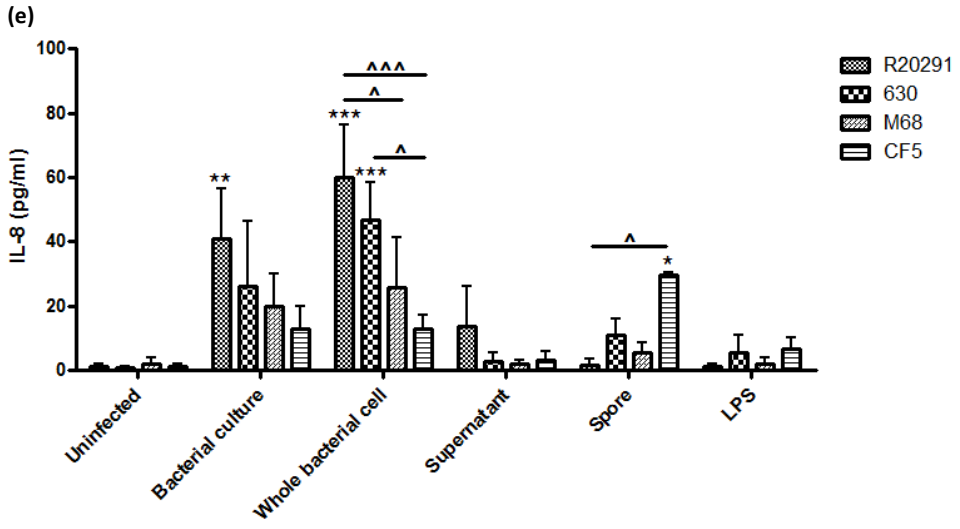

Figure 4.1. IL-8 gene and protein expression in response to *C. difficile* in Caco-2 cells. Caco-2 monolayers were infected with bacterial cultures at an MOI of 50 and IL-8 mRNA expression was quantified at specific time-points. Representative RT-PCR analysis at MOI 50 (a), data presented as fold change and represent mean ± SEM, n=3 (b). Representative RT-PCR analysis at MOI 100 (c), data presented as fold change and represent the average of two experiments (hence, no error bars given) (d). Induction of IL-8 in response to *C. difficile* bacterial culture, whole bacterial cell, supernatant, and spore (MOI of 500) was measured by ELISA at 8 h post-infection. LPS (1 µg/µl) was used as a reference stimulus. Data represent mean ± SEM, n=3. $^{*}p<0.05$, $^{**}p<0.01$ and $^{***}p<0.001$ represent significant difference from uninfected cells, and $^{\wedge}p<0.05$ and $^{\wedge\wedge\wedge}p<0.001$ represent significant inter-strain difference (e). *P* values were obtained using ANOVA with Bonferroni post-test analysis.

C. difficile-mediated IL-8 response was further investigated by conducting similar infections in HT-29 cells (Figure 4.2). HT-29 infected cells with 027, 630, 630 Δerm, and CD37 bacterial cultures showed ≤ 2-fold increase in IL-8 mRNA expression between 2 and 6 h post-infection. At 8 h, expression showed >2-fold increase. No significant difference in IL-8 response was detected amongst the strains (Figure 4.2 a & b). HT-29 cells infected with strains R20291, 630, M68, and CF5 exhibited >2-fold increase in IL-8 expression at 4 h. Similar IL-8 expression levels were also detected at 8 h post-infection, while no significant inter-strain difference was observed at either time-points (Figure 4.2 c & d).

Secretion of IL-8 protein was investigated by co-incubating HT-29 cells with bacterial cultures, whole bacterial cells, supernatants, and spores (Figure 4.2 e). Uninfected control cells showed <20 pg/ml IL-8, which were higher than that observed for uninfected Caco-2 cells (Figure 4.1 e). Bacterial cultures and whole bacterial cells caused marked induction of IL-8 (200-1500 pg/ml and 600-1400 pg/ml, respectively) interestingly, bacterial supernatants and spores resulted in <50 pg/ml IL-8 expression (Figure 4.2 e).

Collectively, *C. difficile* strains mediated 2 to 5-fold increase in IL-8 mRNA expression in Caco-2 and HT-29 cells, with the highest up-regulation generally detected between 6 and 8 h post-infection. Furthermore, A^-B^+ strains initiated similar IL-8 responses to A^+B^+ strains. This data also showed that *C. difficile* bacterial culture and whole cell bacteria mediated higher IL-8 induction compared to bacterial supernatants (containing secreted toxins) and spores. Importantly, HT-29 cells were much more responsive to *C. difficile* as measured by marked increase in IL-8 protein levels in comparison Caco-2 cells were significantly less responsive.

IL-8

(a)

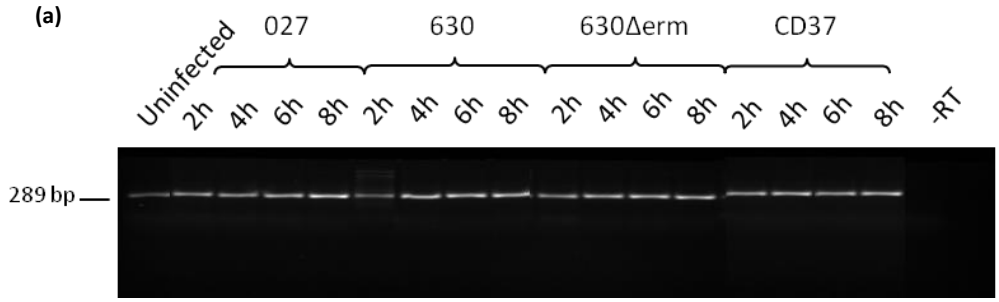
Uninfected
027
630
630Δerm
CD37
2h
4h
6h
8h
-RT
289 bp

(b)

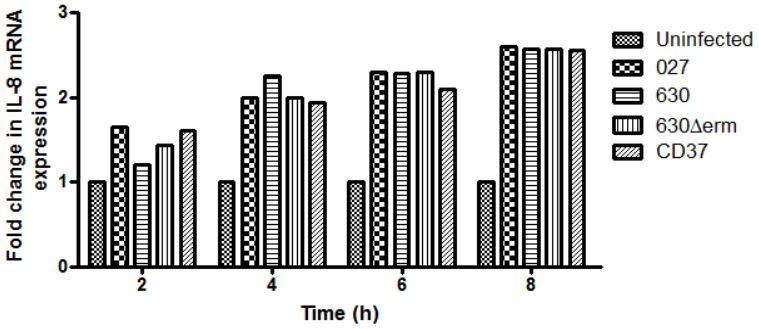
Fold change in IL-8 mRNA expression
Time (h)
Uninfected
027
630
630Δerm
CD37

IL-8

(c)

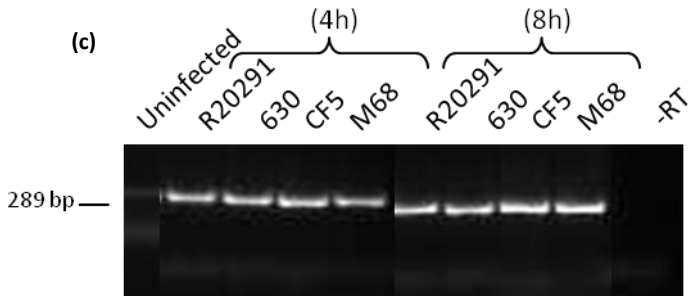
(4h)
(8h)
Uninfected
R20291
630
CF5
M68
-RT
289 bp

(d)

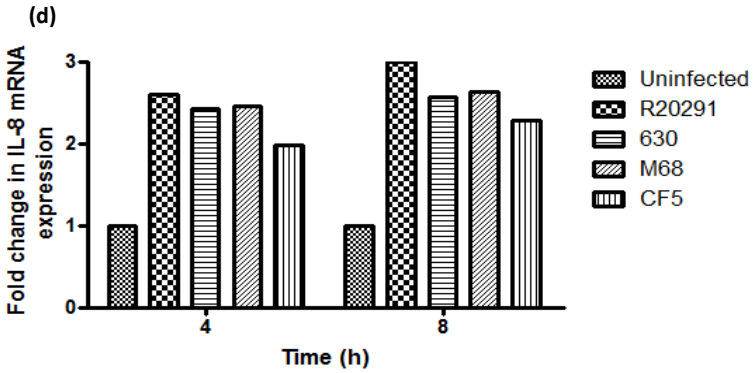
Fold change in IL-8 mRNA expression
Time (h)
Uninfected
R20291
630
M68
CF5

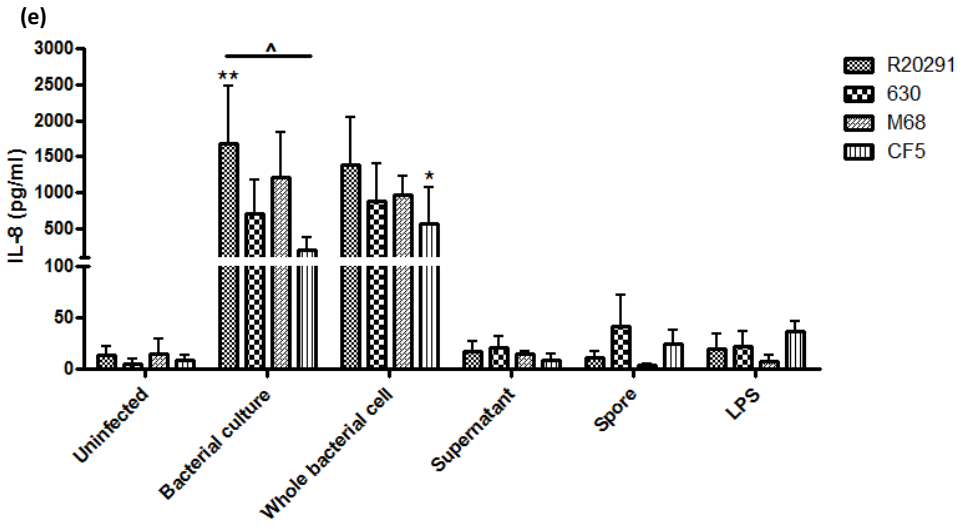

Figure 4.2. IL-8 induction in response to *C. difficile* in HT-29 cells. HT-29 cells were infected with bacterial cultures at an MOI of 50 and IL-8 mRNA expression was quantified at specific time-points. Representative RT-PCR analysis of IL-8 mRNA expression (a), data presented as fold change and represent the average of two experiments (hence, no error bars given) (b). Representative RT-PCR analysis of IL-8 mRNA expression at MOI 100 (c), data presented as fold change and represent the average of two experiments (hence, no error bars given) (d). Induction of IL-8 protein in response to *C. difficile* bacterial culture, whole bacterial cell, supernatant, and spore (MOI of 500) was measured by ELISA at 8 h post-infection. LPS (1 µg/µl) was used as a reference stimulus. Data represent mean ± SEM, n=3. $^{*}p<0.05$ and $^{**}p<0.01$ represent significant difference from uninfected cells, and $^{\wedge}p<0.05$ represents significant inter-strain difference (e). *P* values were obtained using ANOVA with Bonferroni post-test analysis.

4.2.2 *C. difficile*-mediated IL-6, TNF-α, hBD-2, and IL-1β Responses

To investigate IECs pro-inflammatory response(s) to *C. difficile*, Caco-2 monolayers were infected with 027, 630, 630 Δerm, and CD37 bacterial culture at an MOI of 50 and IL-6, TNF-α, hBD-2, and IL-1β mRNA expression was quantified as essentially described above for IL-8 (Figures 4.3-4.6 a).

Caco-2 infected cells showed 2-3-fold induction in IL-6 gene expression up to 6 h post-infection, with strain 027 exhibiting a trend for greater IL-6 up-regulation compared to the other strains (Figure 4.3 a).

In a separate series of experiments Caco-2 monolayers were co-cultured with strains R20291, 630, M68, and CF5 at an MOI of 100. Gene expression of IL-6 and IL-1β was determined at 4 and 8 h (Figures 4.3 & 4.6 b). In this series mRNA expression of TNF-α and hBD-2 was not measured. Infected Caco-2 cells showed a moderate IL-6 mRNA expression at 4 h post-infection, which increased to >2-fold at 8 h. No significant inter-strain difference was detected in modulating IL-6 expression (Figure 4.3 b). The IL-6 level was undetectable in uninfected control cells. Upon infection all four strains caused a very modest and similar increase to ~15 pg/ml (Figure 4.3 c).

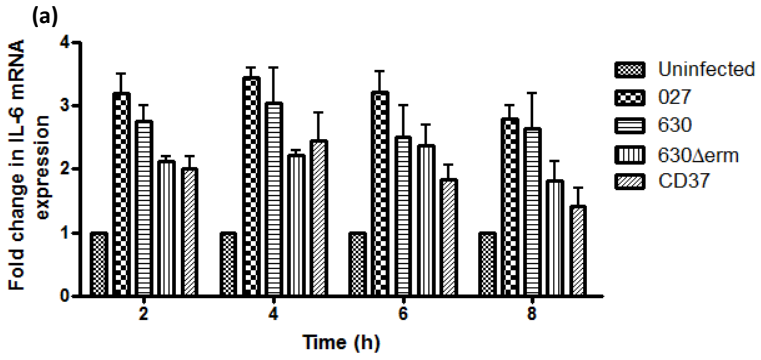

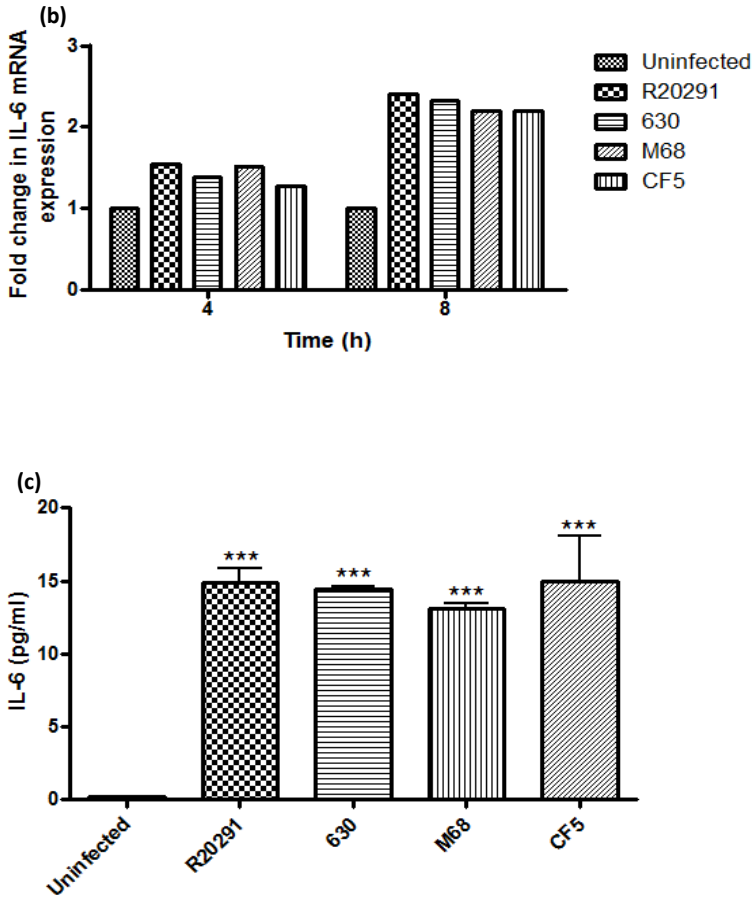

Figure 4.3. *C. difficile*-induced IL-6 mRNA and protein expression in Caco-2 cells. Caco-2 monolayers were infected with bacterial cultures at an MOI of 50. IL-6 mRNA expression was followed by RT-PCR and presented as fold change. Data represent mean ± SEM, n=3 (a). IL-6 expression in response to *C. difficile* strains (MOI 100). Data represent the average of two experiments (hence, no error bars given) (b); IL-6 protein expression was measured at 8 h post-infection. Data represent mean ± SEM, n=3. $^{***}p<0.001$ represents significant difference from uninfected cells (c). *P* values were obtained using ANOVA with Bonferroni post-test analysis.

Similar co-culture experiments were conducted to detect TNF-α gene and protein expression (Figure 4.4). Caco-2 cells infected with strains 027, 630, 630 Δerm, and CD37 showed an increase of ~3-4-fold in mRNA expression at 6 h post-infection with a decline at 8 h, all four strains exhibited similar TNF-α gene expression profile (~3-fold) (Figure 4.4 a).

When Caco-2 monolayers were co-cultured with bacterial cultures at an MOI of 100 and 500, TNF-α protein expression increased in a dose-dependent manner (Figure 4.4 b). TNF-α was undetectable in uninfected control cells, a modest response (<10 pg/ml) was detected at an MOI of 100, whilst MOI of 500 caused induction of >20-80 pg/ml (Figure 4.4 b).

Also, hBD-2 mRNA expression was followed during *C. difficile* infection. 2-4 h post-infection, a very modest (1-2-fold) increase was noted, with >2-3-fold increase at 8 h post-infection (Figure 4.5 a). hBD-2 protein level was quantified during infection with strains R20291, 630, M68, and CF5. hBD-2 remained undetectable in uninfected control cells. Strains R20291 and 630 caused induction to a similar extent (~100 pg/ml), while M68 elicited a more potent response (~150 pg/ml). Strain CF5 in contrast was less potent (80 pg/ml) (Figure 4.5 b).

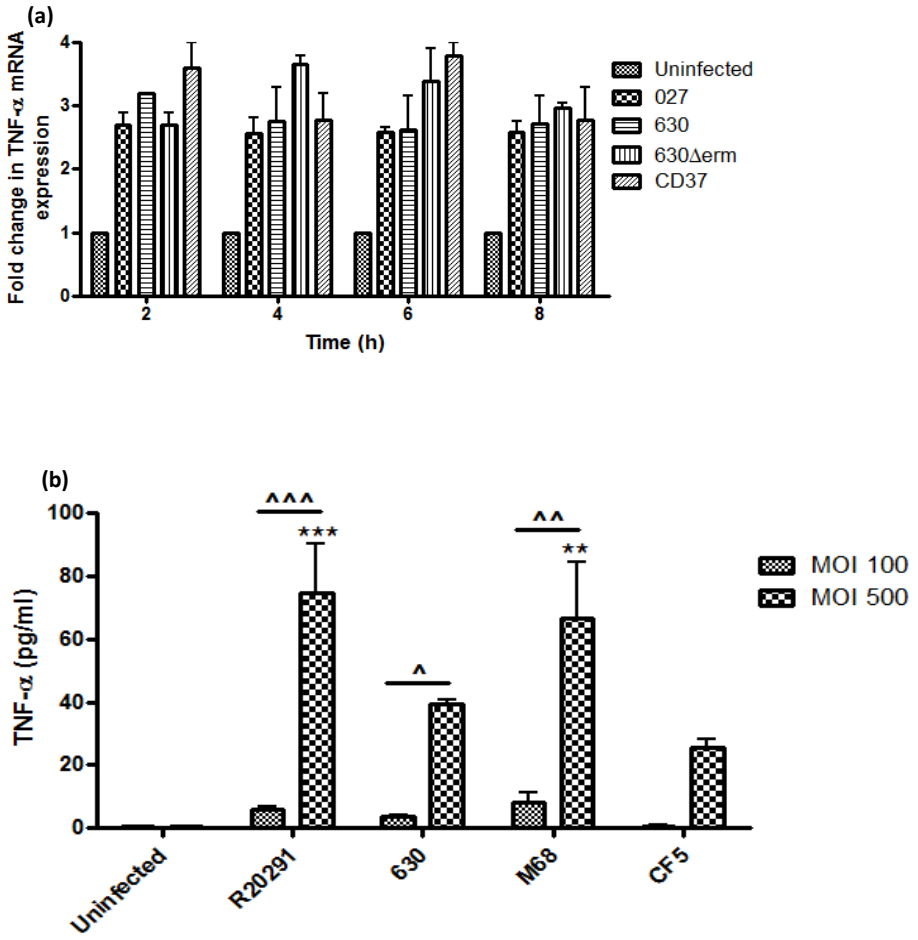

Figure 4.4. *C. difficile*-mediated TNF-α expression in Caco-2 cells. Caco-2 monolayers were infected with bacterial cultures at an MOI of 50. TNF-α mRNA expression was quantified and presented as fold change. Data represent mean ± SEM, n=3 (a). TNF-α protein expression was measured at 8 h post-infection (MOI of 100 and 500). Data represent mean ± SEM, n=3. $^{**}p<0.01$ and $^{***}p<0.001$ represent significant difference from uninfected cells, and $^{\wedge}p<0.05$, $^{\wedge\wedge}p<0.01$ and $^{\wedge\wedge\wedge}p<0.001$ represent significant inter-strain difference (b). *P* values were obtained using ANOVA with Bonferroni post-test analysis.

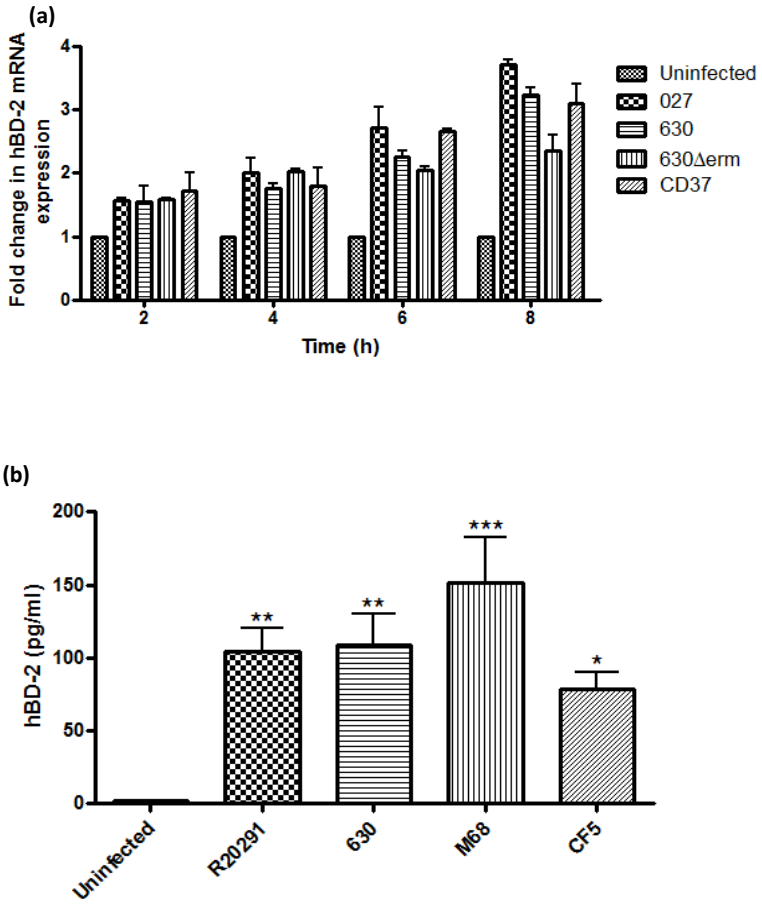

Figure 4.5. *C. difficile*-mediated hBD-2 induction in Caco-2 cells. Caco-2 monolayers were infected with bacterial cultures at an MOI of 50. Gene expression of hBD-2 was quantified and presented as fold change. Data represent mean ± SEM, n=3 (a). hBD-2 protein levels measured at 8 h post-infection (MOI 100). Data represent mean ± SEM, n=3. $^{*}p<0.05$, $^{**}p<0.01$ and $^{***}p<0.001$ represent significant difference from uninfected cells (b). *P* values were obtained using ANOVA with Bonferroni post-test analysis.

IL-1β mRNA expression was also measured (Figure 4.6). Caco-2 cells infected with 027, 630, 630 Δerm, and CD37 bacterial cultures showed ~3-4-fold increase in gene expression at 6 h post-infection, followed by a modest increase at 8 h. Strain CD37 caused the least change in IL-1β expression (Figure 4.6 a).

Strains R20291, 630, M68, and CF5 mediated a 2-fold increase in IL-1β mRNA expression at 4 h post-infection with a marginal increase at 8 h. R20291 infection exerted a potent effect on IL-1β, while strain CF5 was the least effective (Figure 4.6 b). IL-1β protein remained undetectable in infected Caco-2 cells.

Taken all together, this data suggested that *C. difficile* bacterial cultures caused 2 to 4-fold increase in gene expression of IL-6, TNF-α, hBD-2, and IL-1β, mainly between 4 and 8 h post-infection. *C. difficile*- induced TNF-α secretion in a dose-dependent manner, further significant antimicrobial hBD-2 induction was also noted. The lack of IL-1β protein in infected Caco-2 cells despite mRNA induction was an interesting observation.

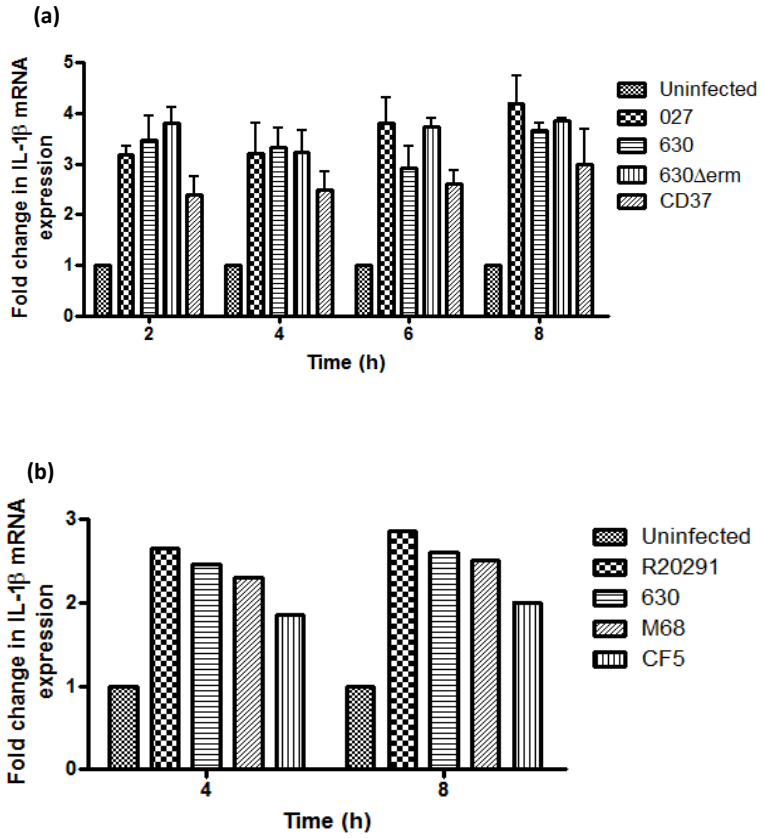

Figure 4.6. *C. difficile*-mediated IL-1β mRNA expression in Caco-2 cells. Caco-2 monolayers were infected with bacterial cultures at an MOI of 50. Gene expression of IL-1β was quantified at 2, 4, 6, and 8 h post-infection and presented as fold change. Data represent mean ± SEM, n=3 (a). IL-1β mRNA expression was measured at 4 h and 8 h post-infection (MOI 100). Data represent the average of two experiments (hence, no error bars given) (b). Data was analysed using ANOVA with Bonferroni post-test.

hBD-1 and IL-18 expression was also determined at 4 and 8 h post-infection (Figure 4.7). A modest <2-fold increase in hBD-1 mRNA expression was noted at 4 h reaching ~2-fold at 8 h post-infection (Figure 4.7 a). IL-18 mRNA showed no significant change at 4 h but expression elevated up to 2-fold at 8 h (Figure 4.7 b). Protein expression of hBD-1 and IL-18 were not measured.

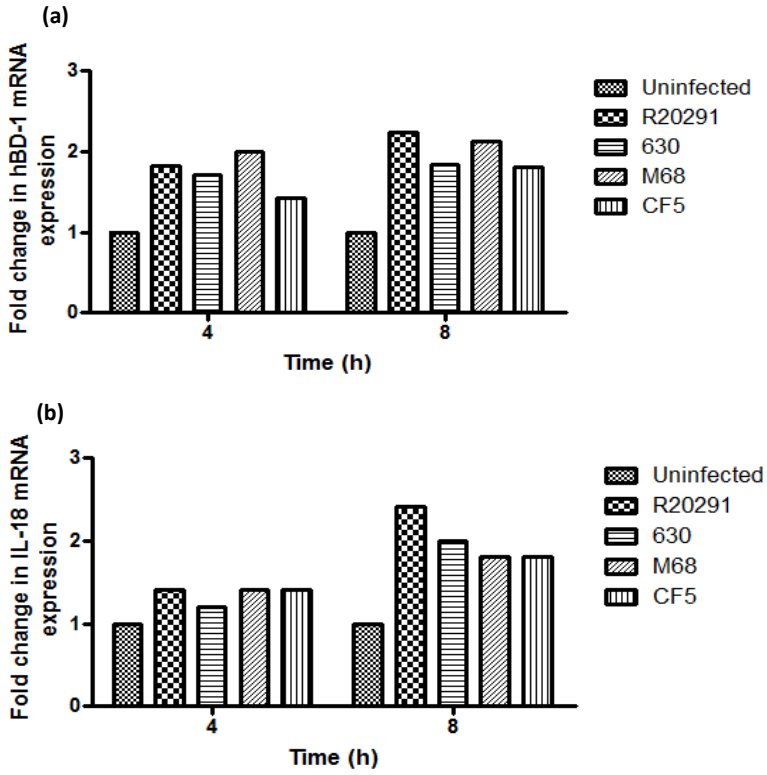

Figure 4.7. hBD-1 and IL-18 gene expression in response to *C. difficile* infection. Caco-2 monolayers were infected with bacterial cultures at an MOI of 100 and mRNA expression was quantified by RT-PCR. Gene expression of hBD-1 and IL-18 were presented as fold change. Data represent the average of two experiments (hence, no error bars given) and was analysed using ANOVA with Bonferroni post-test.

4.2.3 *C. difficile*-mediated Cytokine Expression in HT-29 Cells

C. difficile-mediated IEC cytokine response(s) were also studied in HT-29 cells. Experiments were essentially conducted as described above for Caco-2 cells.

C. difficile strains (027, 630, 630 Δerm and CD37) caused similar IL-6 expression, showing >2-fold mRNA up-regulation in the first 6 h of infection. At 8 h, expression increased slightly reaching ~3-fold (Figure 4.8 a). IL-1α showed no significant increase at 2 h, while exhibiting ~2-fold increase only at 6 h post-infection (Figure 4.8 b). IL-1β gene expression increased 2-fold at 6 and 8 h (Figure 4.8 c). hBD-1 increased nearly 1-fold 6 h post-infection, while reaching a ~3-fold increase at 8 h (Figure 4.8 d). *C. difficile* caused minimal enhancement of TNF-α expression at 2 and 4 h (Figure 4.8 e).

HT-29 cells were also infected with strains R20291, 630, M68, and CF5 at an MOI of 100. Infected cells showed >2 fold IL-1β gene expression at 4 h with a slight increase detected at 8 h post-infection (Figure 4.9 a). Approximately 2-fold hBD-1 gene expression was detected at 4 h, which remained unchanged at 8 h (Figure 4.9 b). *C. difficile* strains caused only a moderate increase of IL-18 gene expression (>1-2-fold) (Figure 4.9 c).

In summary, *C. difficile* strains caused 2 to 4-fold increase in inflammatory cytokine gene expression in both Caco-2 and HT-29 cell-lines. Importantly, the magnitude of inflammatory responses elicited to the presence of A^+B^+ and A^-B^+ strains were not significantly different.

(a)

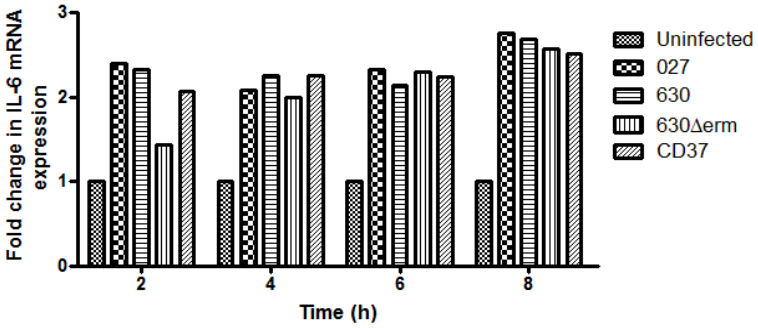
Fold change in IL-6 mRNA expression
0
1
2
3
2
4
6
8
Time (h)
Uninfected
027
630
630Δerm
CD37

(b)

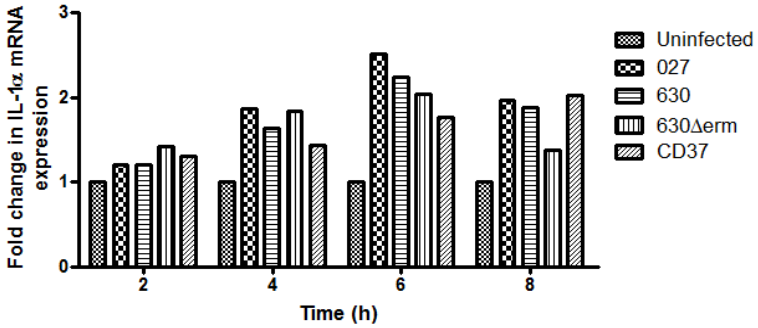
Fold change in IL-1α mRNA expression
0
1
2
3
2
4
6
8
Time (h)
Uninfected
027
630
630Δerm
CD37

(c)

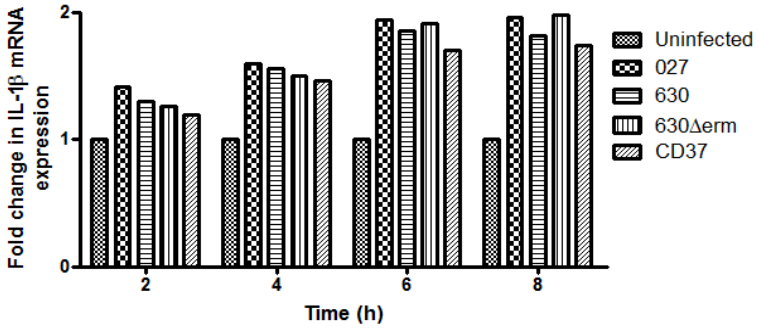
Fold change in IL-1β mRNA expression
0
1
2
2
4
6
8
Time (h)
Uninfected
027
630
630Δerm
CD37

(d)

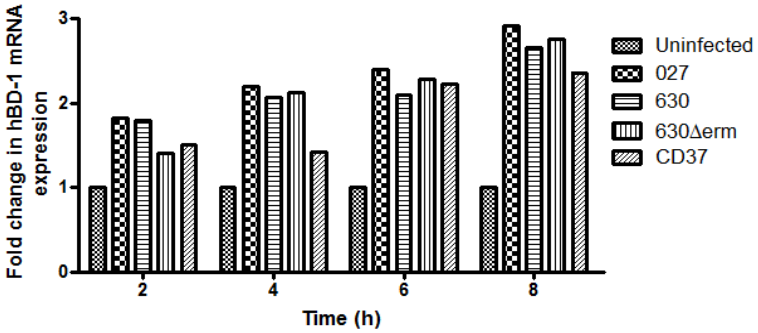
Fold change in hBD-1 mRNA expression
0
1
2
3
2
4
6
8
Time (h)
Uninfected
027
630
630Δerm
CD37

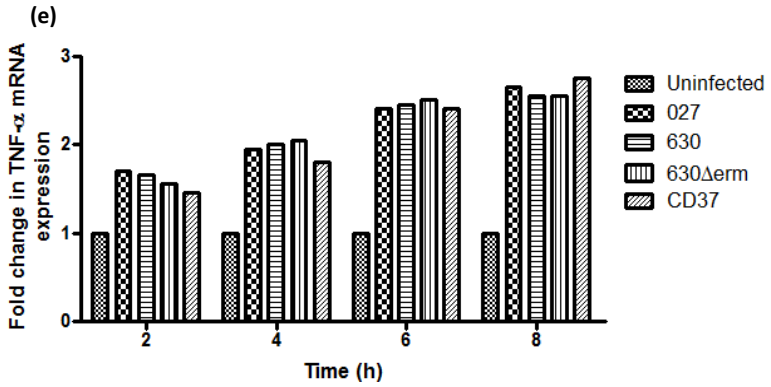

Figure 4.8. *C. difficile*-mediated cytokine mRNA expression in HT-29 cells. HT-29 cells were infected with *C. difficile* bacterial cultures at an MOI of 50. Fold change in IL-6 (a), IL-1α (b), IL-1β (c), hBD-1 (d), and TNF-α (e) mRNA expression was quantified by RT-PCR. Data represent the average of two experiments (hence, no error bars given) and was analysed using ANOVA with Bonferroni post-test.

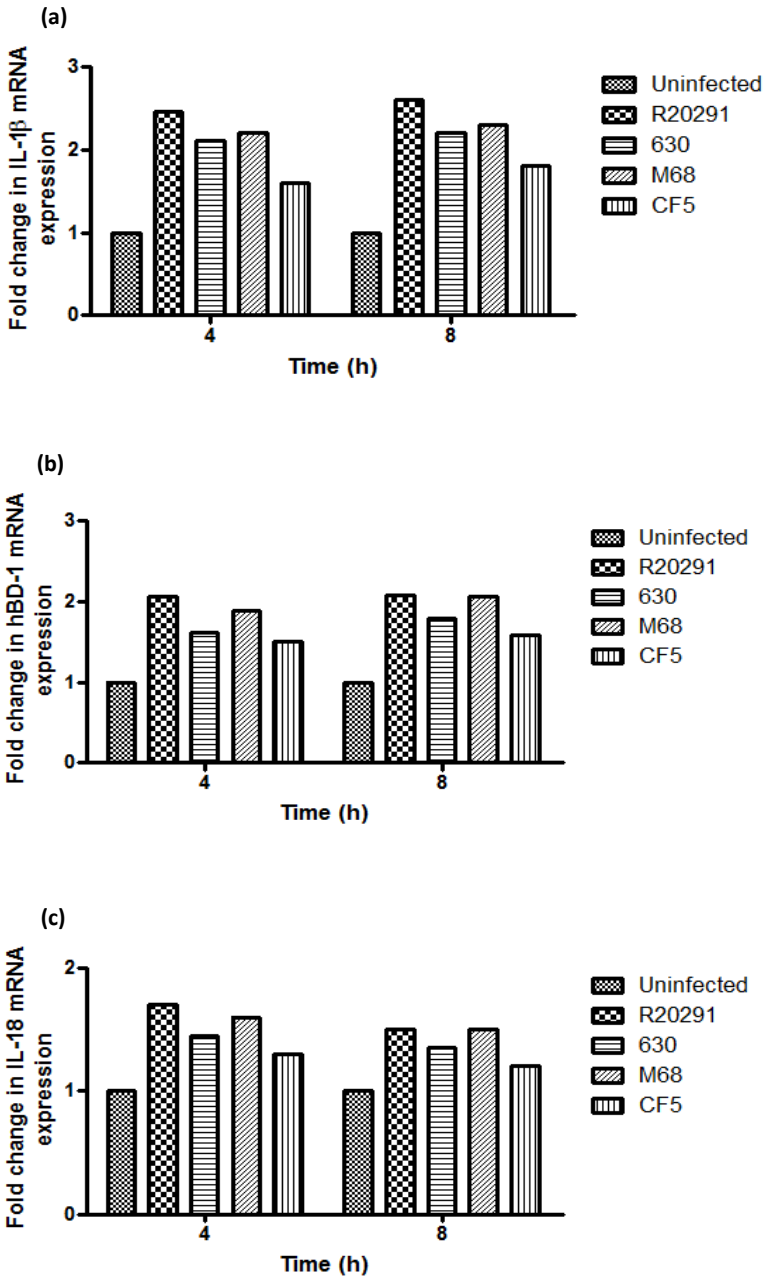

Figure 4.9. *C. difficile*-mediated effects on cytokine gene expression in HT-29 cells. HT-29 cells were infected with bacterial cultures at an MOI of 100. IL-1β (a), hBD-1 (b), and IL-18 (c) gene expression was measured and presented as fold induction. Data represent the average of two experiments (hence, no error bars given) and was analysed using ANOVA with Bonferroni post-test.

4.3 T84 Cell Cytokine Responses to *C. difficile* under Aerobic versus Anaerobic Conditions

Caco-2 and HT-29 cell-lines are routinely employed as model cell-lines to dissect host-pathogen interactions in the GI tract. The very modest effect of *C. difficile* on IEC cytokine response(s) described in the previous section was unexpected. Further, the aerobic conditions employed for the co-culture studies were sub-optimal as *C. difficile* is an anaerobic bacterium. To circumvent the various issues raised, the effect of *C. difficile* infection was investigated using well-characterised T84 cells. T84, a human colonic IEC grows to confluence as a monolayer and exhibits tight junctions (TJ). T84 cell is also the cell-line of choice to investigate IEC TJ biology plus the strongly-bonded cell layer allows IEC to polarise when grown on transwells/snapwell filter leading to spatial compartmentalisation, creating an apical and basolateral compartment. This experimental method when placed in an Ussing vertical chamber system allows the generation of an apical anaerobic and a basolateral aerobic environment, a more appropriate reflection of the colonic environment and therefore, a better model to study host-pathogen interactions.

T84 cells grown on transwell or snapwell were co-incubated with bacterial cultures at an MOI of 250 upon forming a monolayer. Supernatants were collected at 8 h post-infection to measure cytokine induction by ELISA (Figure 4.10).

A basal level of <20 pg/ml IL-8 was measured in uninfected control T84 cells. In aerobic co-culture (5% CO_2) *C. difficile* strains induced IL-8 protein (25-100 pg/ml), these levels increased further (60-250 pg/ml) when the same experiment was performed providing an anaerobic environment for bacteria (Figure 4.10 a). TNF-α levels were low in uninfected control cells (<10 pg/ml), upon infection under aerobic conditions, 25-80 pg/ml TNF-α was secreted by infected cells, while in an anaerobic co-culture induction increased to significantly higher amounts (90-450 pg/ml) (Figure 4.10 b). hBD-2 was undetectable in control cells, infection had minimal effect under aerobic conditions (<10 pg/ml) although the amounts were increased under an anaerobic environment (10-30 pg/ml) (Figure 4.10 c).

In summary, *C. difficile* strains mediated significantly greater inflammatory cytokine response(s) when host-pathogen crosstalk was allowed to occur under apically provided anaerobic conditions, environment optimal for the bacterium.

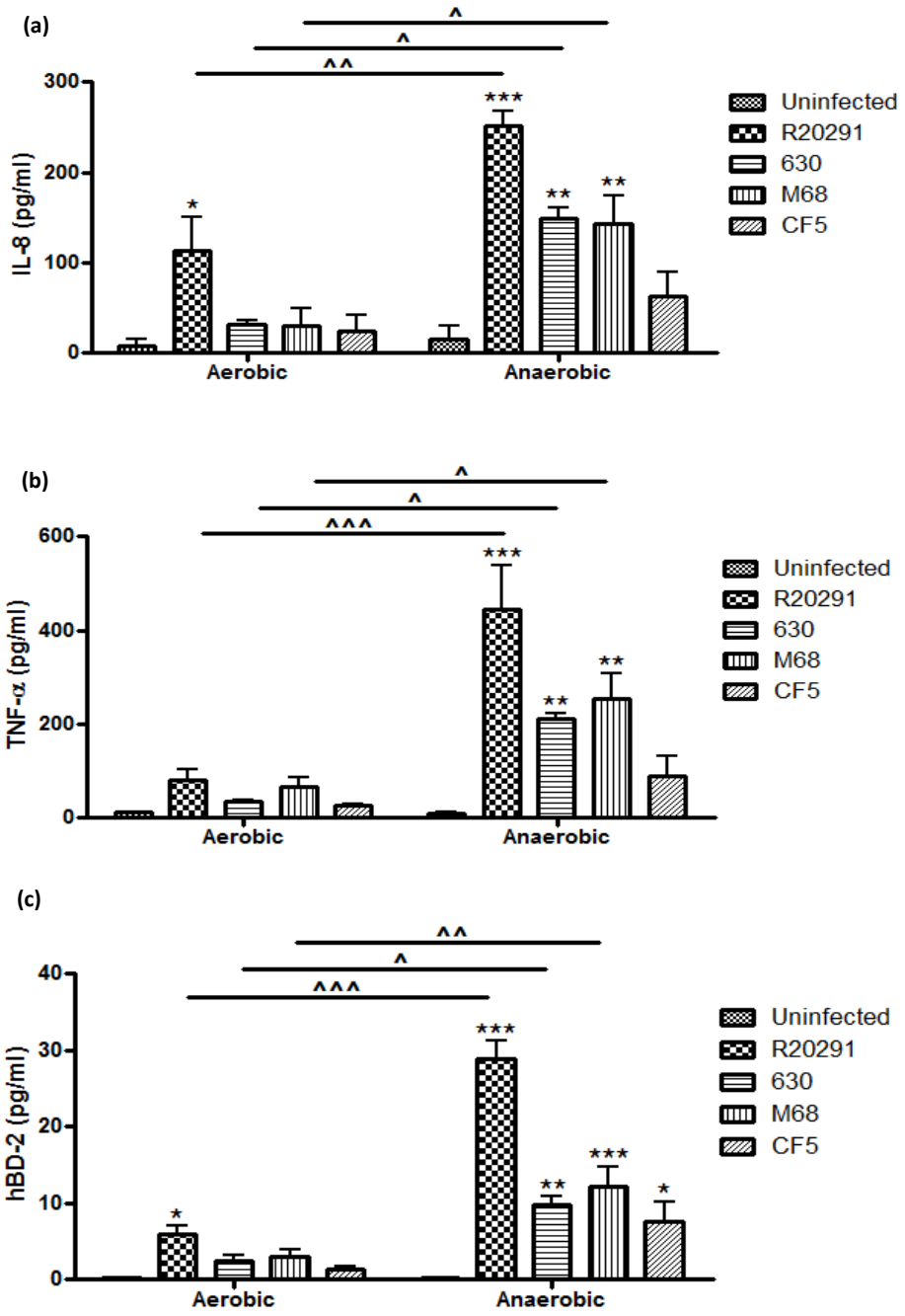

Figure 4.10. *C. difficile*-induced differential cytokine responses under aerobic and anaerobic conditions. T84 cells were co-cultured with bacterial culture (MOI 250) under aerobic or anaerobic conditions. IL-8 (a), TNF-α (b), and hBD-2 (c) proteins were quantified 8 h post-infection. Data represent mean ± SEM, n=3. $^{*}p<0.05$, $^{**}p<0.01$ and $^{***}p<0.001$ represent significant difference from uninfected cells, and $^{\wedge}p<0.05$, $^{\wedge\wedge}p<0.01$ and $^{\wedge\wedge\wedge}p<0.001$ represent significant difference in cytokine production under an aerobic versus anaerobic environment. *P* values were obtained using ANOVA with Bonferroni post-test analysis.

4.4 *C. difficile*-mediated Disruption of Human Intestinal Barrier Function

In the presence of intact cell layer, the epithelial barrier seal is established and maintained by the IEC (Turner, 2009). The epithelium permeability is regulated mainly by the presence of TJ complexes. TJs are composed of integral proteins including; occludin, claudins, and junctional adhesion molecule-A (JAM-A), which are located between individual composing cells (Pastorelli *et al.,* 2008). Occludin is a functional component of the paracellular barrier permeability and has a role in cellular defence. Occludin is expressed predominately at TJs in epithelial and endothelial cells. The C-terminus of occludin interacts with zonula occludens-1 protein (ZO-1) linking occludin to the actin cytoskeleton (Groschwitz *et al.,* 2009; Du *et al.,* 2010). Pathogens attack the intestinal barrier with various virulence factors directly by disruption and causing a decrease in transepithelial resistance or indirectly by phosphorylation/dephosphorylation of TJ proteins (Baumgart *et al.,* 2002). In addition to cell disruption, loss of adherens junctions results in ineffective epithelial cell polarisation and differentiation causing premature cell apoptosis (Turner, 2009).

Several studies have already shown *C. difficile* toxins-mediated effects on intestinal epithelial barrier function using purified toxins or bacterial supernatants (Riegler *et al.,* 1995; Alfa *et al.,* 2000; Nusrat *et al.,* 2001; Savidge *et al.,* 2003; Sutton *et al.,* 2008), however, it is yet to be defined whether whole cells of *C. difficile* play an additional role in disruption of TJs.

4.4.1 Occludin Re-distribution during *C. difficile* Infection

C. difficile-induced effect on IEC barrier function was investigated by following occludin expression during bacterial infection. As *C. difficile* leads to extensive actin cytoskeletal changes and cell rounding (Chapter 3), it was hypothesised that infection may mediate occludin redistribution during these cellular processes.

T84 monolayers were co-cultured with *C. difficile* bacterial cultures at an MOI of 250. Cells were immunostained for occludin and observed by fluorescence microscopy in a time-dependent manner (Figure 4.11). Occludin remained primarily confined to the membrane in uninfected control cells throughout the course of the experiment, on the other hand 8 h

post-infection, occludin had predominantly redistributed to an intracellular area with a corresponding decrease at the edge of epithelial cells. Extensive disruption of occludin was observed following infection with strains R20291, 630, and M68 (arrowheads in Figure 4.11). In contrast, minimal occludin redistribution was detected with CF5-infected monolayers compared to uninfected cells (Figure 4.11).

In parallel, cells infected with R20291, 630, and M68 showed significant barrier function disruption, whilst strain CF5 caused the least impact.

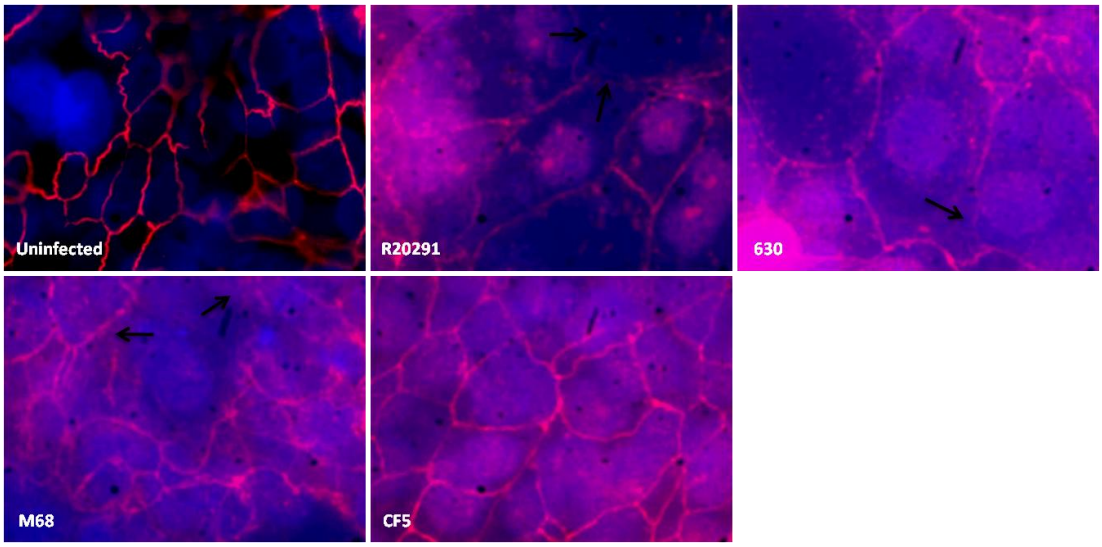

Figure 4.11. *C. difficile*-induced disruption of TJs in T84 cells leads to redistribution of occludin. T84 monolayers were infected with *C. difficile* bacterial cultures at an MOI of 250. At 8 h post-infection cells were stained for occludin and redistribution was observed by fluorescence microscopy (100x Leica DMLB). Data is representative of three independent experiments.

4.4.2 *C. difficile*-induced Transepithelial Electrical Resistance (TEER) Loss under Aerobic Conditions

C. difficile strains promote removal of occludin from TJs allowing its redistribution inside the IEC cytoplasm. Occludin redistribution induces destabilisation of the TJ complexes, leading to alteration of intestinal paracellular permeability. The effect of *C. difficile* on IEC permeability was assessed by measurement of transepithelial electrical resistance (TEER) and permeability to FITC-dextran.

T84 cells were grown on a permeable membrane prior to co-incubation with *C. difficile* cultures at an MOI of 250 under aerobic conditions. TEER changes were monitored over 24 h (Figure 4.12). Uninfected control cells exhibited a moderate decrease in TEER measurement during the experimental time. 2 h post-infection, cells infected with strains R20291, 630, and M68 showed a ~15% loss in TEER measurements. In contrast, strain CF5 caused decline in TEER at a slower rate showing a similar loss only after 4 h. Loss in TEER measurement continued at a steady rate. At 24 h, strains R20291, 630, and M68 infected cells showed a dramatic (~90%) loss in TEER compared to uninfected control cells, while strain CF5 showed ~60% TEER loss.

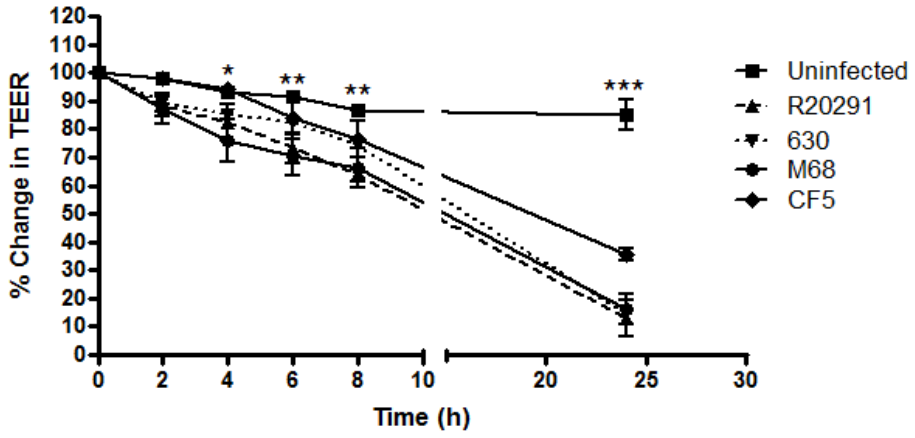

Figure 4.12. Time-dependent changes in IEC TEER during *C. difficile* infection. T84 monolayers were infected with bacterial cultures at an MOI of 250 in an aerobic environment. Change in TEER was monitored up to 24 h. Data represent mean ± SEM, n=3. $^{*}p<0.05$, $^{**}p<0.01$ and $^{***}p<0.001$ (ANOVA with Bonferroni post-test) represent significant difference of uninfected cells with infected cells.

4.4.3 Loss of TEER under Anaerobic Environment

Effect of *C. difficile* strains on epithelial barrier function under anaerobic conditions was examined by employing the Ussing vertical diffusion chamber system providing an anaerobic environment for the bacteria while supporting 5% CO_2 basolateral conditions. The experiment was conducted by measuring baseline TEER prior to co-incubation with bacteria in the apical compartment, the change in resistance was measured subsequently at 8 h post-infection (Figure 4.13).

Uninfected control cells not only maintained but improved the ''intactness'' of the monolayer during the experimental time-course, as an increase in TEER measurement was observed. At 8 h, 75-90% TEER loss was detected in cells infected with strains R20291, 630, and M68. In contrast, CF5 caused <50% decrease in TEER but it was not statistically significant.

Taken all together, Figures 4.12 and 4.13 showed that strains R20291, 630, and M68 caused greater TEER loss in infected T84 cells; on the contrary strain CF5 exhibited the least effect. It was also noted that anaerobic conditions enhanced epithelial barrier disruption by all four strains.

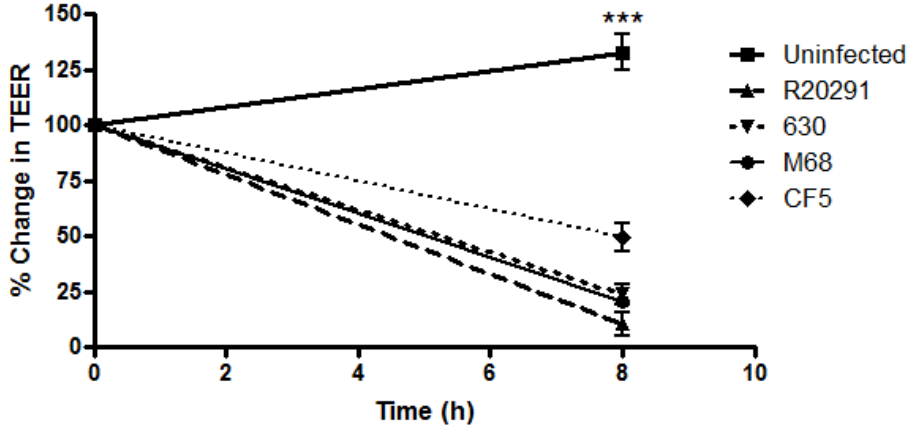

Figure 4.13. *C. difficile* induces a rapid TEER loss in anaerobically infected T84 cells. T84 monolayers were infected with bacterial cultures at an MOI of 250 under an anaerobic environment. Change in resistance was compared at 8 h post-infection to corresponding pre-infected wells. Data represent mean ± SEM, n=3. $^{***}p<0.001$ (ANOVA with Bonferroni post-test) represents significant difference between uninfected and infected cells.

4.4.4 Increased Paracellular Permeability in Response to *C. difficile* infection

Loss of TEER in infected T84 cells was concomitant with increased paracellular permeability, which was measured by apical to basolateral flux of a FITC labelled marker across the cell monolayer.

T84 monolyaers were infected apically with *C. difficile* strains at an MOI of 250, plus FITC-dextran (a paracellular marker) was added to the apical chamber (Figure 4.14). Uninfected control cells showed <10% basal level of FITC-dextran influx although this increased over time. Upon infection, an increase in paracellular permeability was observed as early as 2 h post-infection in response to all four strains (~10%). FITC-dextran flux progressively increased reaching 30% at 8 h and >70% at 24 h post-infection.

Collectively, A^-B^+ *C. difficile* strains caused similar effect as A^+B^+ strains on IEC barrier function leading to TJ disruption and increase in paracellular permeability. CF5 infection led to less occludin redistribution and TEER loss but interestingly showed comparable results with other strains in mediating paracellular permeability.

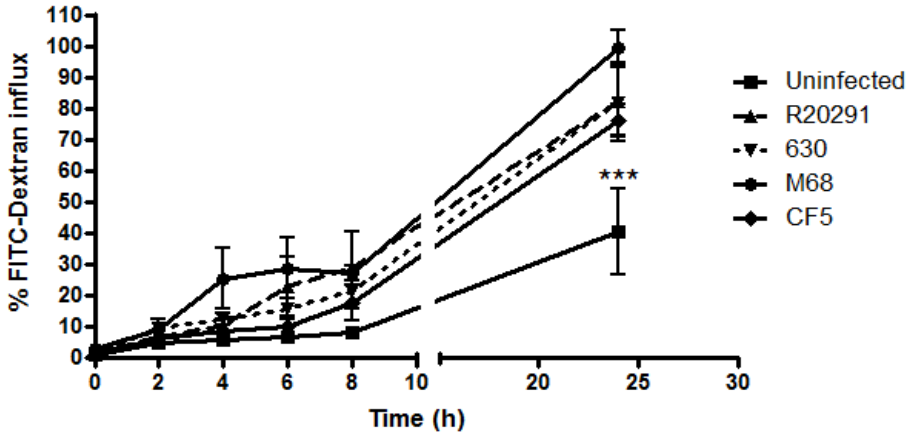

Figure 4.14. Paracellular permeability increases in response to *C. difficile* infection. T84 monolayers were co-cultured with *C. difficile* cultures at an MOI of 250 and FITC-dextran flux from apical to basolateral compartment was measured up to 24 h post-infection. Data represent mean ± SEM, n=3. $^{***}p<0.001$ (ANOVA with Bonferroni post-test) represents significant difference between uninfected and infected cells.

4.5 The *Ex Vivo* Innate Immunity Response(s) of Human Intestinal Mucosa to *C. difficile*

In vitro models of infection using epithelial cell-lines have been used broadly to study host-pathogen interactions; however, cultured cell-lines only indicate how IEC may respond. *In vitro* organ culture (IVOC) is a better alternative that permits studies of host-pathogen interactions under physiologically relevant conditions, where tissues retain their natural architecture and epithelial lining as the host response includes contribution from the underlying lamina propria and the cells it contains rather than just the IEC lining. Thus far, the conventional IVOC method has been used extensively to study *E. coli*, *Salmonella,* and *Campylobacter* pathogenesis (Haque *et al.,* 2004; Schuller *et al.,* 2009; Edwards *et al.,* 2010).

To investigate *C. difficile* interactions with human intestinal mucosa, human paediatric pinch biopsies from healthy area of transverse colon were utilised. Ethical approval to study host-pathogen interactions was obtained (06/Q0508/26). No patient data was collected, therefore tissue usage was anonymous. The explant was co-cultured with 5 x 10^8 bacteria and mucosal cytokine responses were measured 3-6 h post-infection (Figure 4.15 a-f).

IL-8 was measurable in supernatants from uninfected colonic tissue, however *C. difficile* infection enhanced IL-8 secretion by 3 to 4-fold with strain CF5 exhibiting a trend for less response (Figure 4.15 a). IL-6 was detected in uninfected tissues but levels were low compared to IL-8 (median 60 versus ~200 pg/ml) infection increased IL-6 responses to a median ~200 pg/ml (Figure 4.15 b). Although no significant difference was observed between the various strains in mediating IL-6 production, the trend for R20291 being the most potent and CF5 the least effective continued. Infection had a dramatic effect on IL-1β induction when compared to uninfected controls (80 versus 800 pg/ml) (Figure 4.15 c). Strains R20291 and M68 infection led to marked IL-1β release, with significantly less effect of CF5.

The GI mucosal host defence response to *C. difficile* infection was also determined. IFN-γ, IL-17A and IL-22 are the cytokine implicated in this response. Minimal IFN-γ was observed in uninfected biopsies, infection caused marked induction 400-900 pg/ml (Figure 4.15 d) significant difference between R20291 and CF5 response was noted. IL-17A was detected at low levels in uninfected tissue, the induction upon *C. difficile* infection was <60 pg/ml

(Figure 4.15 e), these levels were the lowest amongst the cytokines tested. IL-22 was detectable in uninfected biopsies, this cytokine was significantly induced in response to infection (~300 pg/ml) (Figure 4.15 f).

In summary, *C. difficile* infection led to a significant increase in mucosal inflammatory responses in paediatric colonic biopsies compared to uninfected tissues. No inter-strain difference was observed in IL-8, IL-6, and IL-22 secretions although CF5 induced significantly less IL-1β, IFN-γ, and IL-17A when compared to levels detected with strains R20291, 630, and M68.

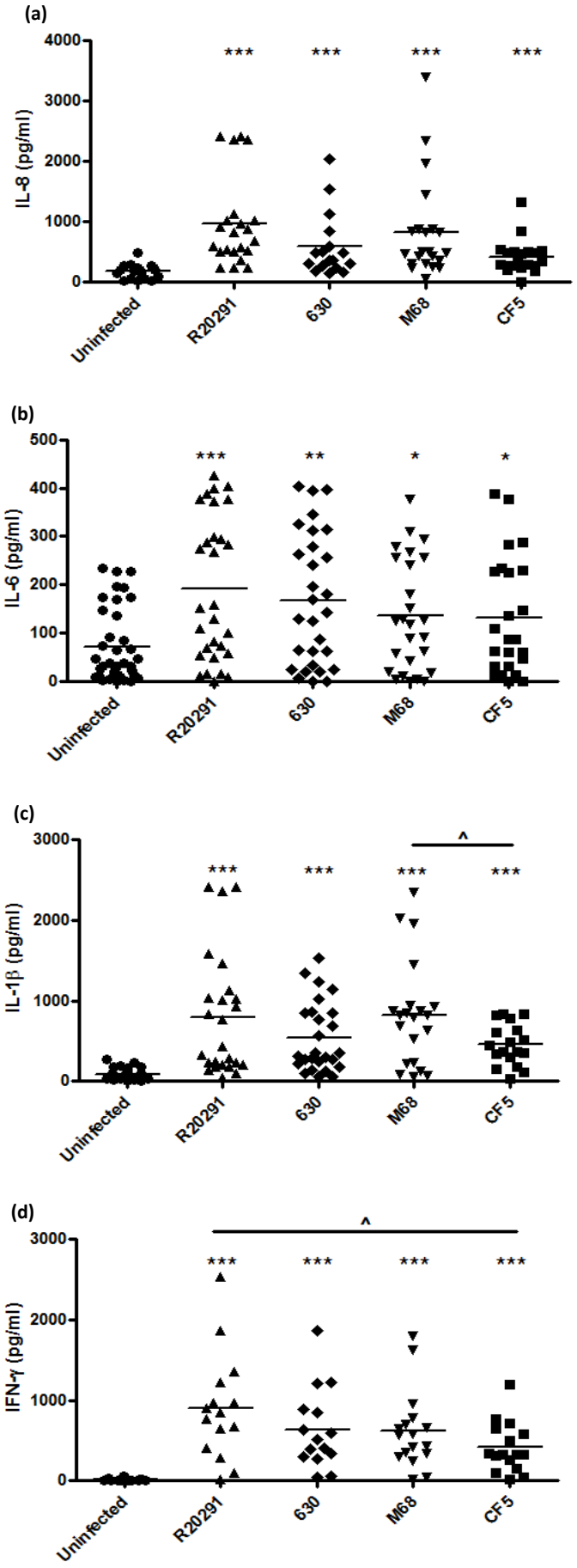
(a)
IL-8 (pg/ml)
4000
3000
2000
1000
0
***
***
***
***
Uninfected
R20291
630
M68
CF5
(b)
IL-6 (pg/ml)
500
400
300
200
100
0
***
**
*
*
Uninfected
R20291
630
M68
CF5
(c)
IL-1β (pg/ml)
3000
2000
1000
0
^
***
***
***
***
Uninfected
R20291
630
M68
CF5
(d)
IFN-γ (pg/ml)
3000
2000
1000
0
^
***
***
***
***
Uninfected
R20291
630
M68
CF5

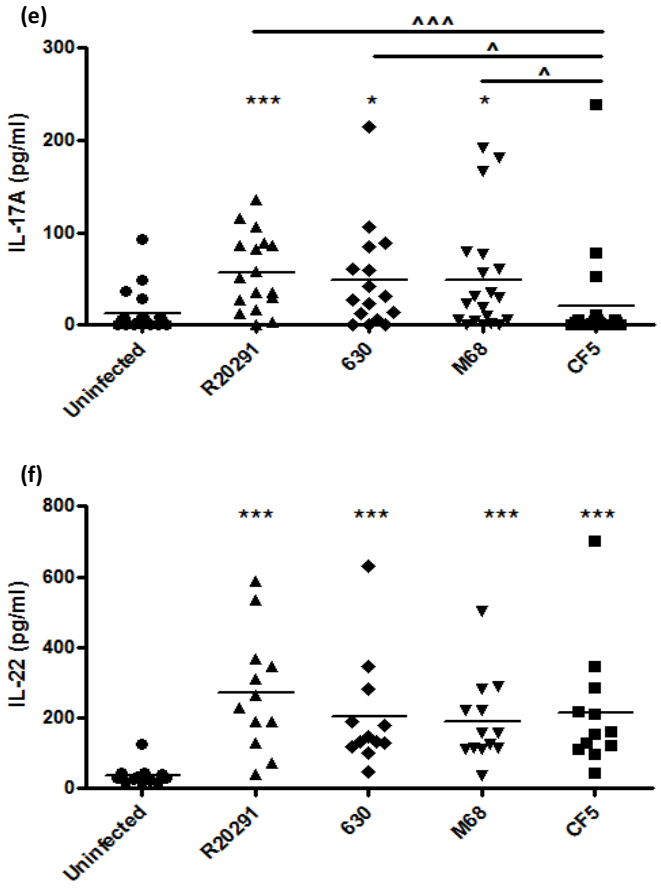

Figure 4.15. *Ex vivo* mucosal cytokine responses to *C. difficile* infection. Macroscopically normal and matched colonic biopsies from paediatric patients (12-30 individuals with mean age of 10.4 ± SD of 4.7) were infected with each *C. difficile* strains (5 x 10^8). Bars represent median levels. Inductions of various cytokines were measured at 3-6 h post-infection. $^{*}p<0.05$, $^{**}p<0.01$ and $^{***}p<0.001$ represent significant difference from uninfected controls, and $^{\wedge}p<0.05$ and $^{\wedge\wedge\wedge}p<0.001$ represent significant inter-strain difference. Data was analysed using a Mann–Whitney U test.

4.6 Conclusions

Cells that line the mucosal surface of the intestine form a critical barrier that divides the host's internal milieu from the external environment and act as a selectively permeable barrier to luminal contents preventing unwanted solutes, microorganisms and antigens from entering the body. In addition to the continuous exposure to dietary and environmental antigens, the intestinal microenvironment forms one of the most densely populated microbial habitats, harbouring an estimated 10^{14} commensal bacteria. Thus, the IECs, which once considered a simple physical barrier not only can directly sense commensal bacteria and pathogens but also play an integral role in discriminating between commensal and pathogenic bacteria, subsequently mounting an appropriate host response(s) (Jung *et al.,* 1995; Hershberg, 2002; Radtke *et al.,* 2005; MacDonald *et al.,* 2005; Artis, 2008; Groschwitz *et al.,* 2009).

In this study IEC cytokine response(s) to *C. difficile* was investigated. For this purpose, various IEC cell-lines including Caco-2, HT-29 and T84 cells were employed. Also cytokine expression in response to *C. difficile* infection was compared under aerobic versus anaerobic co-culture environments. Additionally, mucosal cytokine responses to *C. difficile* were examined in an *ex vivo* model of infection by utilising paediatric colonic biopsies.

Following bacterial adherence, IEC interaction with bacteria, provides early signals for the initiation and maintenance of the mucosal inflammatory response. Several studies have already demonstrated the epithelial response to *C. difficile* toxins and more specifically TcdA contribution to accumulation and activation of inflammatory cells, including neutrophils and monocytes, at the site of infection by establishing a chemotactic gradients such as IL-8 within the underlying mucosa (Mahida *et al.,* 1996; Kim *et al.,* 2002; Johal *et al.,* 2004c; NA *et al.,* 2005; Canny *et al.,* 2006; Kim *et al.,* 2006b; Lee *et al.,* 2007). However, how the *C. difficile* adherence contributes to the up-regulation of pro-inflammatory gene expression in epithelia is uncertain; nonetheless, it may not be an exclusive requirement as epithelial monolayers do respond to bacterial supernatant and toxins (Mahida *et al.,* 1996; Kim *et al.,* 2002; Johal *et al.,* 2004c; Canny *et al.,* 2006; Kim *et al.,* 2006b; Lee *et al.,* 2007).

It was observed that *C. difficile* infection caused an overall 3 to 4-fold increase in mRNA expression of several pro-inflammatory cytokines, the induction that maximum 8 h post-infection. Cytokine mRNA expression was not affected by increasing the MOI from 50 to 100. *C. difficile* strains induced 3 to 4-fold IL-8 gene expression in infected Caco-2 and HT-29

cells; importantly majority of the induction was mediated by bacterial cells, as both supernatant and spores were less potent. To the best of our knowledge the present study is the first to report these responses. Despite similar magnitude of IL-8 mRNA by HT-29 cells, these cells induced 10-15 times more IL-8 protein in response to bacterial cultures and whole cells than that secreted by infected Caco-2 cells. Studies are now forthcoming that suggest Caco-2 cells irrespective of stimuli received remain poor IL-8 producers. This clearly highlights need for caution while interpreting data. Nonetheless, HT-29 cells responded to bacterial supernatants and spores similar to Caco-2 cells.

Gene and/or protein expression of IL-6, TNF-α, beta defensins hBD-1 and hBD-2 was investigated during *C. difficile* infection. Both Caco-2 and HT-29 showed increase in cytokine and antimicrobial responses, indicating activation of multiple host signalling pathways leading to enhancing IEC innate immunity to *C. difficile*. Although *C. difficile* induced IL-1β mRNA expression, no protein was detected by ELISA.

Analysis of GI mucosal responses revealed that *C. difficile* strains caused a robust inflammatory cytokine response in colonic tissues as early as 3h post-infection. It was noted that *C. difficile* infection caused a strong induction of IL-8 and comparatively weak IL-17A, suggesting that IL-8 may play a more crucial role in mediating early neutrophil recruitment necessary for containment of the infection. Interestingly, *C. difficile* infection caused robust induction of IL-22 compared to IL-17A. The role of IL-17A in IEC is both pro-inflammatory and antimicrobial. In contrast, IL-22 has a more regenerative and protective role on IEC. *C. difficile* infection also caused strong pro-inflammatory IL-1β and IFN-γ responses.

As *C. difficile* is an anaerobe, induction of IL-8, TNF-α, and hBD-2 proteins by T84 cells in aerobic co-cultures were compared with cells infected with anaerobically-grown bacteria. Anaerobic conditions induced significant increase in cytokine secretion and more rapid TEER loss. These observations need to be investigated further to clarify whether increased cytokine response was due to optimal conditions for bacterial growth and/or subsequent enhancement of bacterial adherence.

Studies have shown that *C. difficile* toxins alter the barrier function of polarised IEC such as Caco-2 and T84 cells by increasing paracellular permeability (Hecht *et al.,* 1988, 1992; Johal *et al.,* 2004c; Sutton *et al.,* 2008). Johal and co-workers (2004c) demonstrated that TEER loss in T84 cells in response to TcdA is dose dependent and exposure to >10 ng/ml TcdA leads to complete and irreversible loss of TEER. Concomitant with the permeability increase, toxins disrupt apical and basal actin filaments leading to disorganisation of

junctional complexes and redistribution of ZO-1, ZO-2, occludin, and claudin within TJs. TcdB decreases actin-ZO-1 association and disperse ZO-1 and occludin from membrane, without occludin phosphorylation (Nusrat *et al.,* 2001; Chen *et al.,* 2002). Since Rho plays an important role in TJ assembly, it was presumed that the effects of TcdA and TcdB on TJs result from Rho glucosylation (Jou *et al.,* 1998; Popoff and Geny, 2009). Furthermore, disruption of the actin cytoskeleton has been shown to be involved in IL-8 secretion in HT-29 and Caco-2 cells (Nemeth *et al.,* 2004). In the current study, strains R20291, 630, and M68 caused an extensive occludin disruption at 8 h, increased TEER loss and enhanced FITC-dextran flux at 24 h in aerobically infected T84 cells, indicating disruption of epithelial barrier function and increased permeability. Although CF5 also caused disruption of the epithelium and increased permeability it did so to a lesser degree compared to other strains.

Taken all together, IEC cell-lines and human colonic biopsy tissue bear the capacity to distinguish the various *C. difficile* strains as irrespective of the biological parameter measured, strain R20291 was consistently more potent than strain 630 suggesting the presence of CDT maybe partly responsible for the observed greater potency. Also amongst the two A^-B^+ strains M68 and CF5, the latter was consistently less potent compared to M68 suggesting virulence differences between the two strains which at present uncharacterised. Marked induction of GI mucosal responses within 3 h of bacterial infection highlighted players that are most likely involved not only in early immunity but in a susceptible person the same players may also play a role in initiating disease pathogenesis.

4.6.1 Summary

This chapter showed that:

- *C. difficile* whole bacterial cells induced a significant IL-8 secretion compared to supernatants and spores.
- The magnitude of inflammatory cytokine gene expression in response to A^+B^+ strains versus A^-B^+ strains was not significantly different.
- Strain R20291 was detected to cause greater inflammatory cytokine protein expression in both intestinal epithelial cell-lines and human colonic tissues when compared with 630 and M68, whilst CF5 induced the least response.
- Under an anaerobic condition *C. difficile* strains mediated significantly more inflammatory cytokine response(s) and TEER loss.
- Strains R20291, 630 and M68 caused significant epithelial barrier function disruption and enhanced paracellular permeability.
- Although epithelial disruption was detected in response to CF5 infection but it was to a lesser extent compared to other strains.

Chapter 5

Potential Crosstalk between *Clostridium difficile* and Host Toll-Like Receptors

5.1 Introduction

In the GI tract tissue homeostasis is maintained by a harmonious relationship between the mucosal immune system and the environment. This coexistence occurs in the presence of a diverse range of bacterial species. There is no doubt that multiple mechanism(s) are likely to be involved in maintaining homeostasis however at present our understanding of these are limited. In the last decade the role of host Toll-like receptors (TLRs) in GI health and in disease has begun to emerge (Mumy & McCormick, 2005; Tapping, 2009). TLRs are the most studied group of host pattern recognition molecules. Their expression is ubiquitous as they are found on non-immune (epithelial, fibroblast) innate and adaptive (T, B and Treg) cell types. TLRs recognise conserved structural components (MAMPs) of microbes triggering signals leading to protective, tolerant responses or inflammation (Vora *et al.,* 2004; Li *et al.,* 2010).

There is currently limited information regarding the recognition of *C. difficile* by the immune system. Two studies have reported a potential role of TLRs in *C. difficile* infection. Jarchum *et al.* demonstrated that flagellin-mediated TLR5 stimulation protected mice from death during *C. difficile* colitis by delaying *C. difficile* growth and toxin production. TLR5 stimulation improved pathological changes in the cecum and colon of infected mice and reduced epithelial cell loss and apoptosis, thereby protecting the integrity of the intestinal barrier during the infection (Jarchum *et al.,* 2011). In another study, Ryan *et al.* suggested a role for TLR4 in recognition of SLPs and subsequent initiation of the immune response necessary for clearance of *C. difficile* (Ryan *et al.,* 2011). Although these studies implicate TLR5 in protection during *C. difficile* infection and TLR4 in recognising SLPs, the role of other TLR members and details of effector pathways yielding protective immunity to *C. difficile* is unknown.

5.2 The Role of Toll-Like Receptors in *C. difficile* Infection

In the present study, the potential role of TLR family in the recognition of *C. difficile* was investigated by employing TLR-transfected-HEK293, a human embryonic kidney cell-line. Stably transfected HEK293 cells with one or two TLR genes were infected with bacterial culture, supernatant and PFA-fixed *C. difficile* strains of R20291, 630, M68, and CF5 at an MOI of 10. IL-8 secretion was measured as the biological readout of TLR activation. Specific ligands known to activate each TLR, TNF-α (125 ng/ml); *Lactobacillus rhamnosus* GG (LGG), a Gram-positive facultative anaerobe; 630 Δerm *tcdA tcdB* (A^-B^-), an isogenic mutant of strain 630, and CD37, a non-toxigenic *C. difficile* strain (MOI 10) were used as controls.

5.2.1 IL-8 Response to *C. difficile* Infection by HEK293 Cells

As non-transfected HEK293 cells are likely to express endogenous TLRs, it was critical to determine the contribution of these receptors in providing basal IL-8 secretion levels in response to *C. difficile*. Each individual TLR ligand was also tested as the magnitude of response may reflect the degree of corresponding TLR expression (Figure 5.1 a).

Uninfected HEK293 cells spontaneously secreted IL-8 in the range of ~25 pg/ml. Upon *C. difficile* infection, only strains 630 and CD37 showed a modest induction. Amongst the TLR ligands tested, FLA-ST (*S. typhimurium* Flagellin, TLR5 receptor ligand) was the only agonist to yield significant IL-8. TNF-α was included as an independent indicator of the ability of HEK293 cells to produce IL-8. The observations obtained from this study complemented available information as HEK293 cells naturally express TLR5 (Rhee *et al.,* 2009) and TNF-α promotes an inflammatory response (Figure 5.1 a).

Non-transfected cells were also stimulated with bacterial supernatant and PFA-fixed bacteria (Figure 5.1 b). Strains CD37 and 630 Δerm *tcdA tcdB* supernatants caused greater induction amongst the strains tested, interestingly upon PFA fixation, all strains induced more IL-8 compared to their non-fixed counterpart but PFA-fixed strains 630 and 630 Δerm *tcdA tcdB* caused elevated levels of IL-8 secretion. Overall, cells stimulated with PFA-fixed bacteria induced greater level of IL-8 than cells infected with bacterial culture or supernatant.

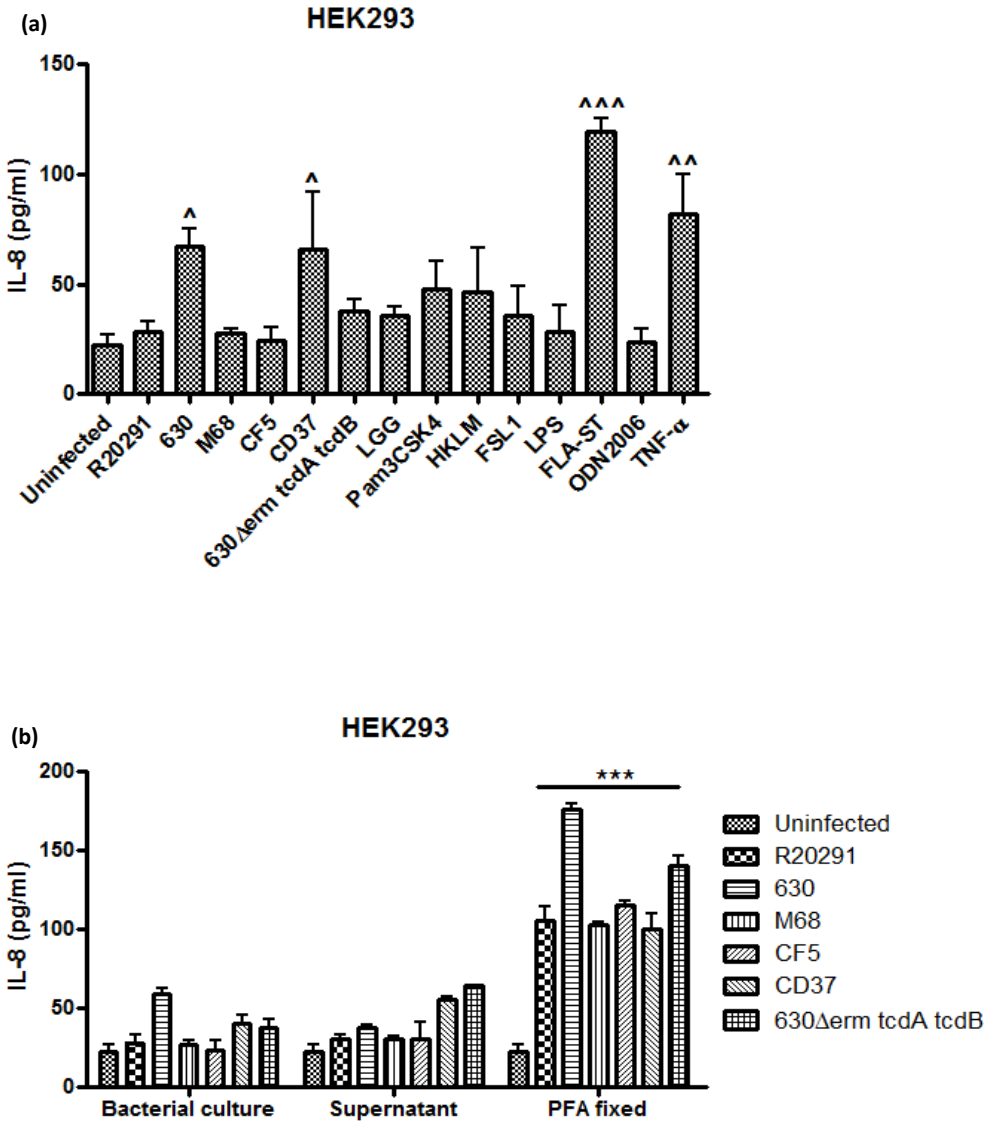

Figure 5.1. IL-8 response of non-transfected HEK293 cells to *C. difficile* infection and TLR ligands. Non- transfected HEK293 cells were infected with *C. difficile* bacterial culture at an MOI of 10, and stimulated with TLR ligands to for 8 h. Strains CD37, 630 Δerm *tcdA tcdB*, and LGG and TNF-α (125 ng/ml) were positive controls (a). Cells were also infected with bacterial culture, supernatant, and PFA-fixed bacteria at an MOI of 10 and IL-8 secretion was measured at 8 h post-infection (b). Data represent mean ± SEM, n=3. $^{\wedge}p<0.05$, $^{\wedge\wedge}p<0.01$ and $^{\wedge\wedge\wedge}p<0.001$ represent significant difference from uninfected control cells and $^{***}p<0.001$ represents significant PFA-fixed difference from bacterial culture and supernatant. *P* values were obtained using ANOVA with Bonferroni post-test analysis.

5.2.2 Recognition of *C. difficile* by TLR2/6-transfected HEK293 Cells

TLR2 is involved in the recognition of a wide range of MAMPs including lipopeptides, peptidoglycan, and lipoteichoic acid. TLR2 generally forms heterodimers with TLR1 or TLR6. Specifically, TLR2/1 heterodimer recognises triacylated lipopetides from Gram-negative bacteria, whereas the TLR2/6 heterodimer recognises diacylated lipopeptides from Gram-positive bacteria (Kawai *et al.,* 2010).

As *C. difficile* is a Gram-positive bacterium, an initial study was performed using TLR2/6-transfected cells to assess bacterial recognition. Cells were infected with bacterial culture, supernatant, and PFA-fixed bacteria and IL-8 was quantified (Figure 5.2). Uninfected TLR2/6 cells secreted <30 pg/ml IL-8 in a spontaneous manner. Bacterial culture and PFA-fixed bacteria caused significant induction with strain M68 being the most potent inducer (Figure 5.2 a). Interestingly, the difference between non-fixed and PFA-fixed bacteria was no longer significant. These preliminary observations indicated that MAMPs involved in *C. difficile* interaction(s) with TLR2 are variable amongst the strains tested to an extent that a differential IL-8 response could be documented. Bacterial supernatants remained poor inducers of IL-8 (Figure 5.2 b). The TLR2/6 agonist FSL 1, induced >1500 pg/ml IL-8, indicating experiments conducted at an MOI of 10 did not completely saturate TLR2 receptor occupancy (Figure 5.2 c).

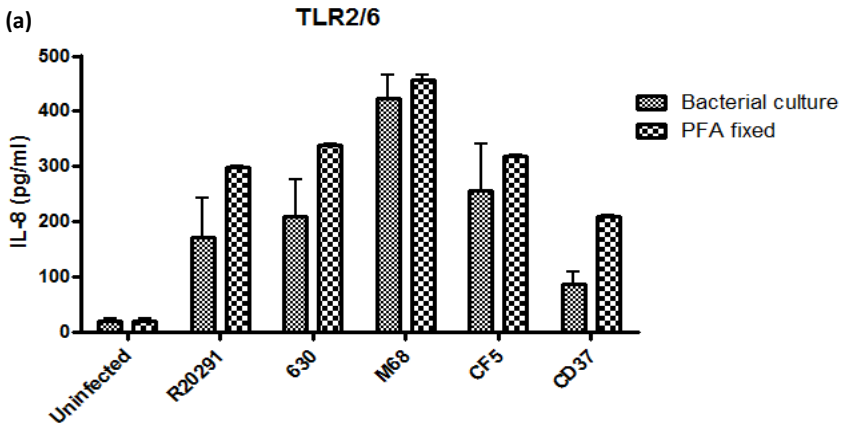

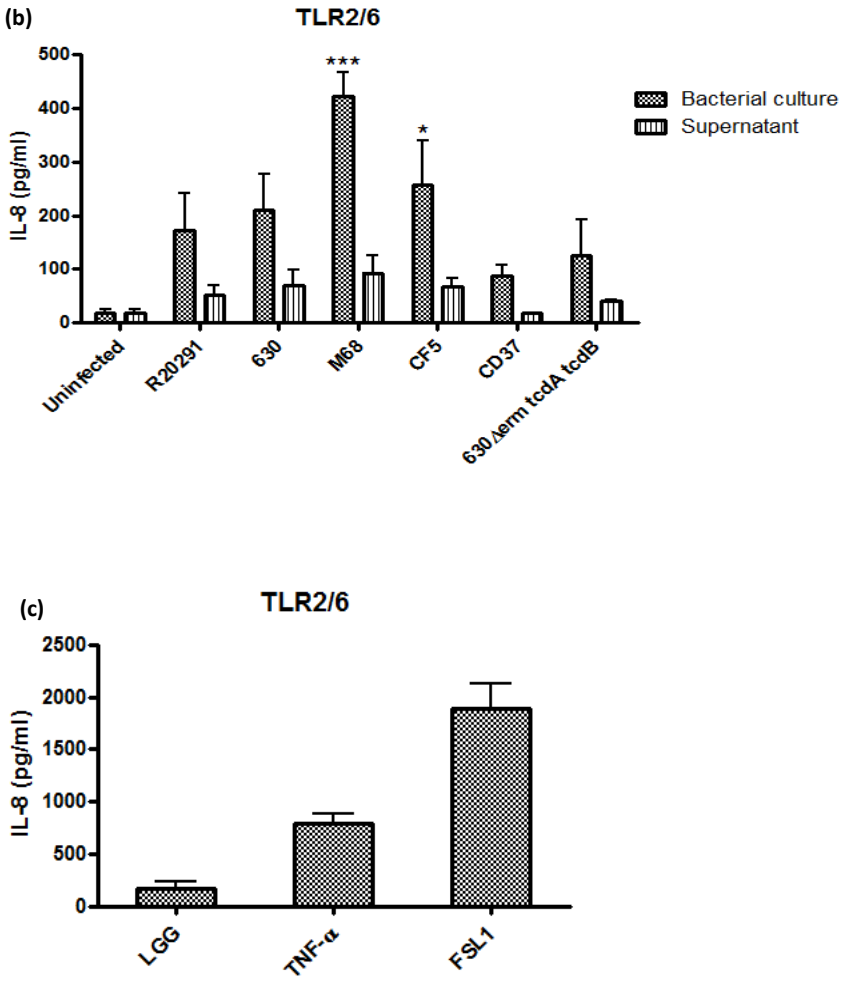

Figure 5.2. *C. difficile*-mediated IL-8 response in TLR2/6-transfected HEK293 cells. Cells were infected with bacterial culture and PFA-fixed bacteria and IL-8 secretion was measured at 8 h (a). Comparison of bacterial culture and corresponding supernatant in mediating IL-8 (b). Stimulated cells with TLR2/6 receptor ligand, FSL 1 showed an IL-8 induction of >1500 pg/ml (c). Data represent mean ± SEM, n=3. $^{*}p<0.05$ and $^{***}p<0.001$ (ANOVA with Bonferroni post-test) represent significant bacterial culture difference from supernatant.

5.2.3 IL-8 Response to *C. difficile* Infection by TLR5-transfected HEK293 Cells

TLR5 recognises bacterial flagellin, it was important to determine whether *C. difficile* flagellin was able to activate TLR5. In this study TLR5-transfected HEK293 cells were co-cultured with bacterial culture, supernatant, and PFA-fixed bacteria at an MOI of 10 and IL-8 induction was measured at 8 h post-infection.

Uninfected TLR5-transfected cells secreted ~15 pg/ml IL-8. It was noted that *C. difficile* strains ranged in their ability to activate TLR5 as IL-8 levels varied between 100-400 pg/ml. Also as observed previuosly, PFA-fixed bacteria induced significantly higher levels of IL-8 (Figure 5.3 a). Infected cells with *C. difficile* supernatants secreted <100 pg/ml IL-8, while 630 Δerm *tcdA tcdB* bacterial culture and supernatant caused ~1000 pg/ml IL-8 induction (Figure 5.3 b). Cells stimulated with TLR5 receptor ligand, FLA-ST expressed 1000 pg/ml IL-8 (Figure 5.3 c).

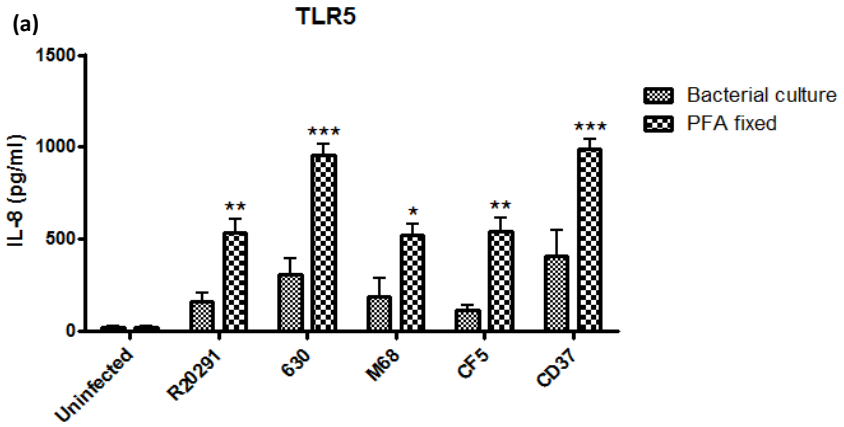

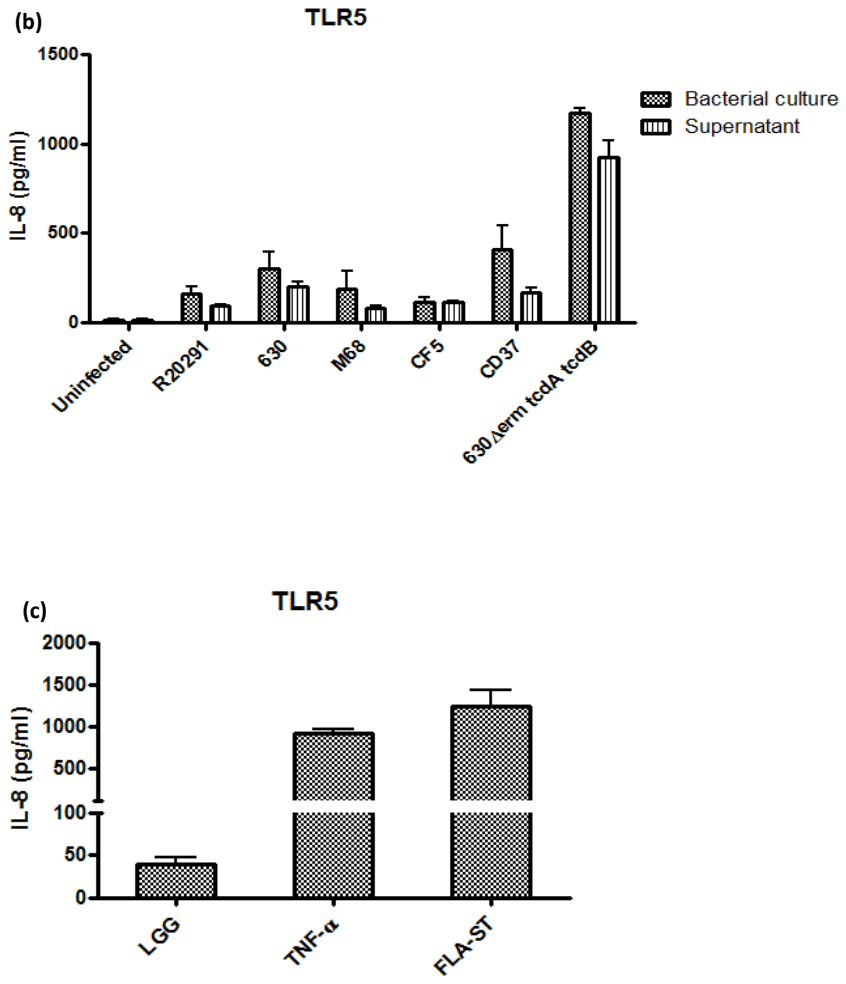

Figure 5.3. IL-8 secretion in response to TLR5 activation by *C. difficile.* TLR5-transfected cells were infected with bacterial culture and PFA-fixed *C. difficile* at an MOI of 10, and IL-8 expression was measured at 8 h (a). IL-8 release in response to bacterial culture and corresponding supernatant (b). IL-8 expression detected in cells stimulated with TLR5 agonist FLA-ST (c). Data represent mean ± SEM, n=3. $^{*}p<0.05$, $^{**}p<0.01$ and $^{***}p<0.001$ represent significant PFA-fixed difference from bacterial culture. *P* values were obtained using ANOVA with Bonferroni post-test analysis.

5.2.4 Role of TLR2-CD14 and TLR4-CD14 HEK293 Transfected Cells in Recognising *C. difficile* Strains

CD14 is a glycosylphosphatidylinositol (GPI)-anchored receptor, which is a component of TLR2 and TLR4 complexes that facilitates ligand binding and signalling efficacy (Kawai *et al.,* 2010). It is known that HEK293 cells lack endogenous CD14 expression therefore, it was important to observe whether CD14 transfection of HEK293 cells increased levels of IL-8 secretion.

CD14-transfected cells were infected with bacterial culture, supernatant, and PFA-fixed *C. difficile* strains (Figure 5.4). Uninfected cells showed <40 pg/ml IL-8 expression. Bacterial culture-infected cells showed an induction of IL-8 between 200-300 pg/ml and co-cultured cells with supernatant secreted 100-200 pg/ml IL-8. A considerable elevation in IL-8 induction was detected in cells infected with PFA-fixed bacteria ranging from 700-900 pg/ml.

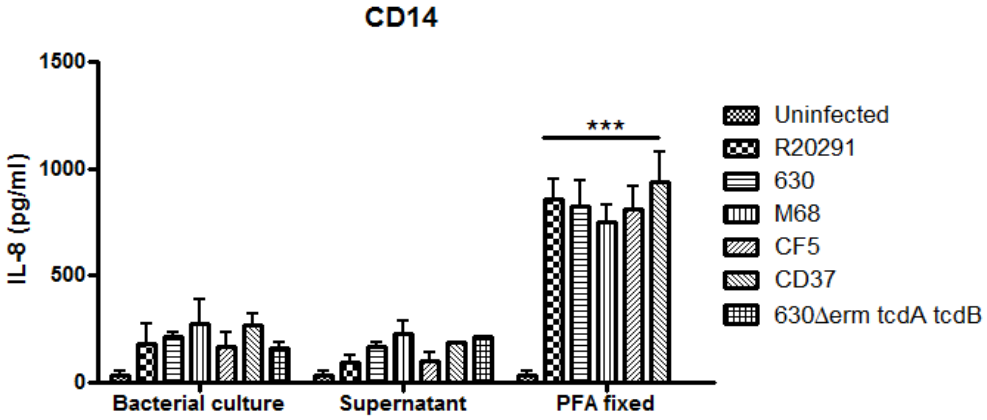

Figure 5.4. *C. difficile*-induced IL-8 secretion by CD14-transfected HEK293 cells. HEK293-CD14 transfected cells were infected with MOI 10 of bacterial culture, supernatant, and PFA-fixed and IL-8 secretion was measured at 8 h. Data represent mean ± SEM, n=3. $^{***}p<0.001$ (ANOVA with Bonferroni post-test) represents significant PFA-fixed difference from bacterial culture and supernatant.

After confirming the basal level of IL-8 secretion in CD14-transfected cells, HEK293 transfected cells with TLR2-CD14, and TLR4-CD14 receptors were utilised to investigate *C. difficile* recognition by these complexes.

TLR2-CD14-transfected HEK293 cells were stimulated with *C. difficile* bacterial culture, supernatant, and PFA-fixed. Uninfected cells showed an induction <40 pg/ml, upon bacterial culture stimulation 200-500 pg/ml IL-8 expression was detected, while PFA-fixed bacteria induced a considerable amount of IL-8 (1500-2000 pg/ml) (Figure 5.5 a). Cells co-cultured with bacterial supernatant secreted 150-300 pg/ml IL-8 (Figure 5.5 b).

Evidently, PFA-fixed bacteria caused a significant amount of IL-8 expression compared to bacterial culture, on the other hand, no significant difference was observed in cells infected with supernatant compared to bacterial culture.

Similar infection was conducted to examine the role of TLR4-CD14 complex in recognition of *C. difficile* strains, although this series of experiments were performed in the absence of MD-2 a co-receptor. Less than 40 pg/ml IL-8 was detected in uninfected cells, while bacterial culture caused 100-300 pg/ml and PFA-fixed 400-800 pg/ml IL-8 expression (Figure 5.6 a). Bacterial supernatant stimulation caused an induction of 50-100 pg/ml IL-8 (Figure 5.6 b). HKLM and LPS were used respectively as TLR2-CD14 and TLR4-CD14 agonist, showed IL-8 secretion more than 1000 pg/ml (Figure 5.6 c).

Notably, IL-8 induction upon PFA-fixed stimulation was significantly higher than bacterial culture, while no significant difference was detected between bacterial culture and supernatant.

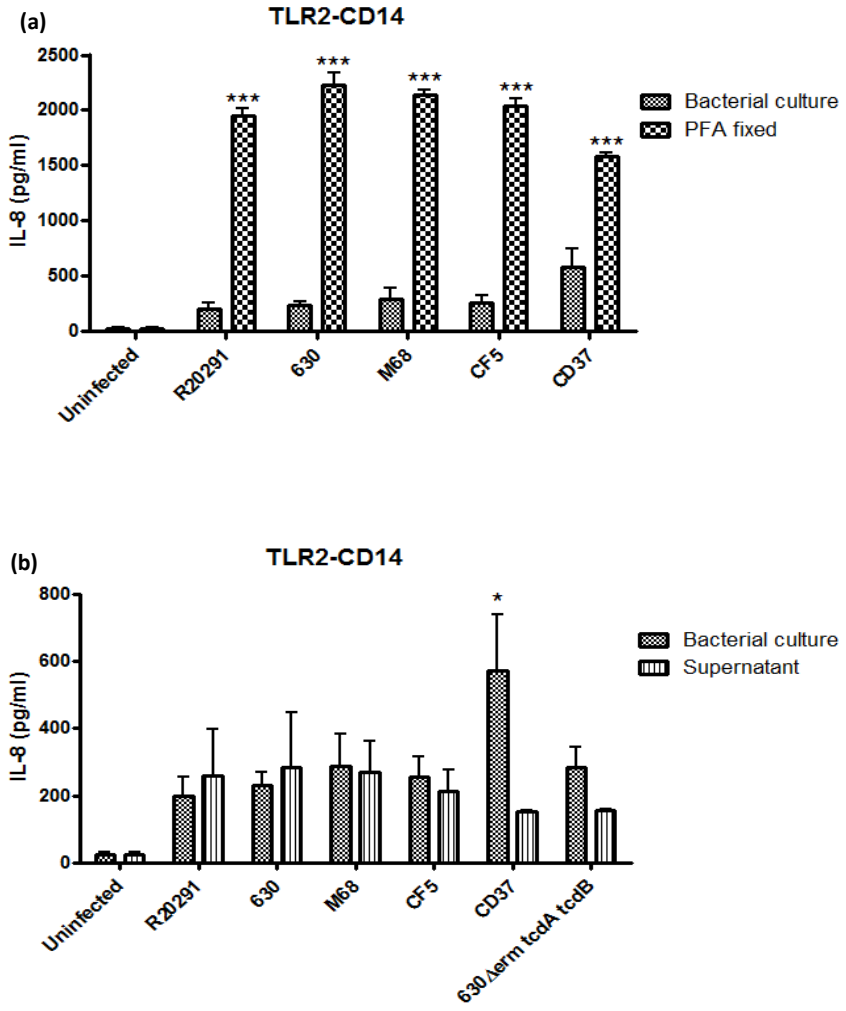

Figure 5.5. IL-8 secretion by TLR2-CD14 complex in response to *C. difficile* stimulation. TLR2-CD14-transfected cells were infected with bacterial culture and PFA-fixed *C. difficile* (MOI 10) and IL-8 expression was measured at 8 h (a). Bacterial culture and supernatant mediated IL-8 release (b). Data represent mean ± SEM, n=3. $^{*}p<0.05$ and $^{***}p<0.001$ represent significant PFA-fixed difference from bacterial culture, and significant difference of bacterial culture from supernatant. *P* values were obtained using ANOVA with Bonferroni post-test analysis.

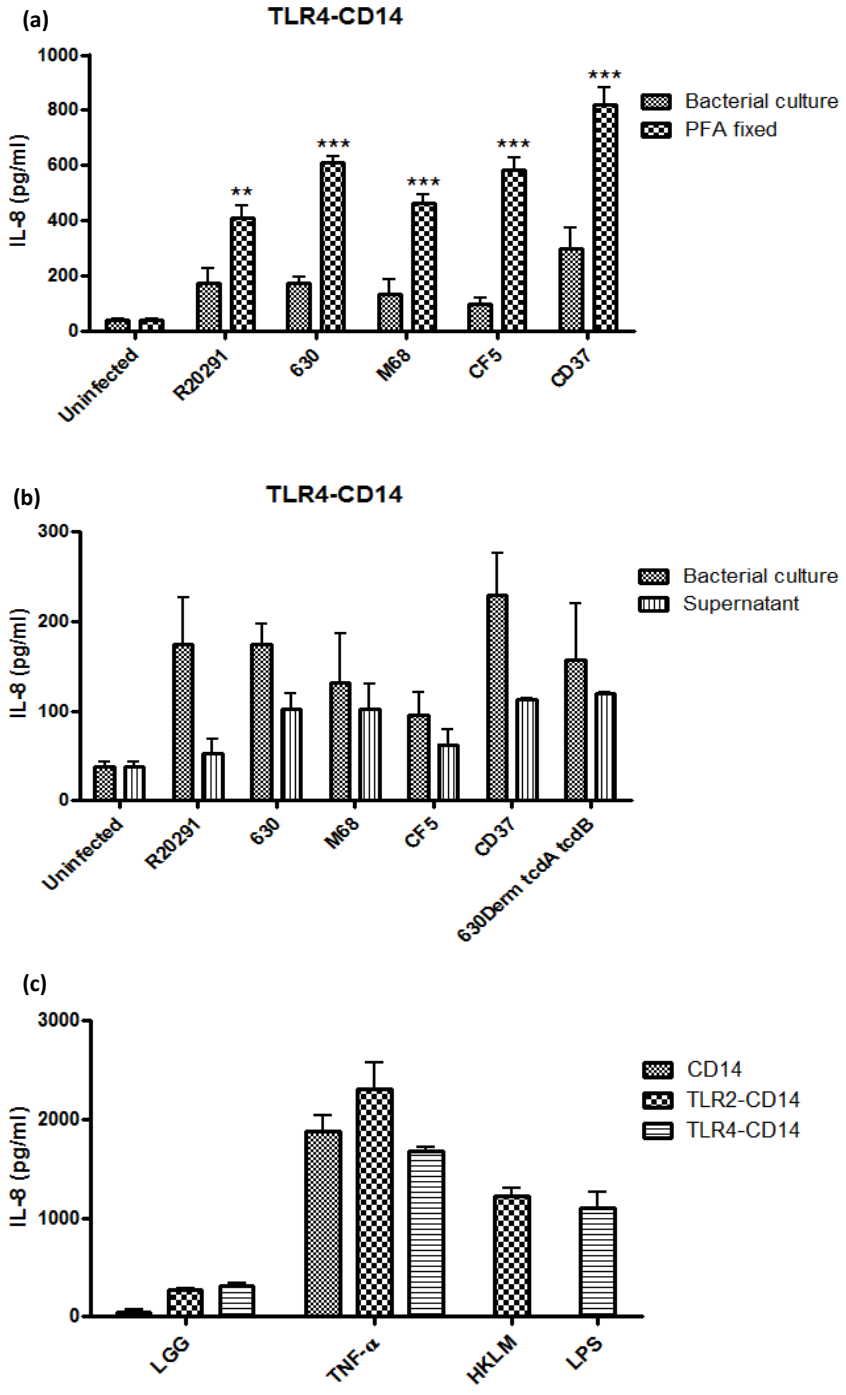

Figure 5.6. *C. difficile*-induced IL-8 secretion by TLR4-CD14 complex. Deficient MD-2 TLR4-CD14 cells were infected with MOI 10 of *C. difficile* bacterial culture and PFA-fixed (a). Cells stimulated with bacterial culture and supernatant (b). IL-8 expression in response to TLR2-CD14 and TLR4-CD14 ligands respectively, HKLM and LPS (c). Data represent mean ± SEM, n=3. $^{**}p<0.01$ and $^{***}p<0.001$ (ANOVA with Bonferroni post-test) represent significant PFA-fixed difference from bacterial culture.

5.2.5 TLR2/1 Heterodimer Activation in Response to *C. difficile* Stimulation

As mentioned previously, TLR2/1 heterodimer recognises bacterial triacyl lipopeptide in order to trigger an inflammatory response. TLR2/1-transfected HEK293 cells were infected with *C. difficile* strains as described before and IL-8 secretion was measured after 8 h infection. TLR2/1 uninfected cells showed <10 pg/ml IL-8 and 30-50 pg/ml was detected in cells infected with bacterial culture. Cells stimulated with PFA-fixed bacteria secreted 60-130 pg/ml IL-8 (Figure 5.7 a). 10-20 pg/ml IL-8 expression was measured as a result of stimulation with bacterial supernatant (Figure 5.7 b). TLR2/1 receptor ligand, Pam3CSK4 caused ~150 pg/ml IL-8 (Figure 5.7 c).

In comparison between different stimuli, PFA-fixed bacteria caused a significant induction of IL-8 compared to bacterial culture. On the other hand, only strains M68, CF5, and CD37 showed a significant difference with bacterial supernatant.

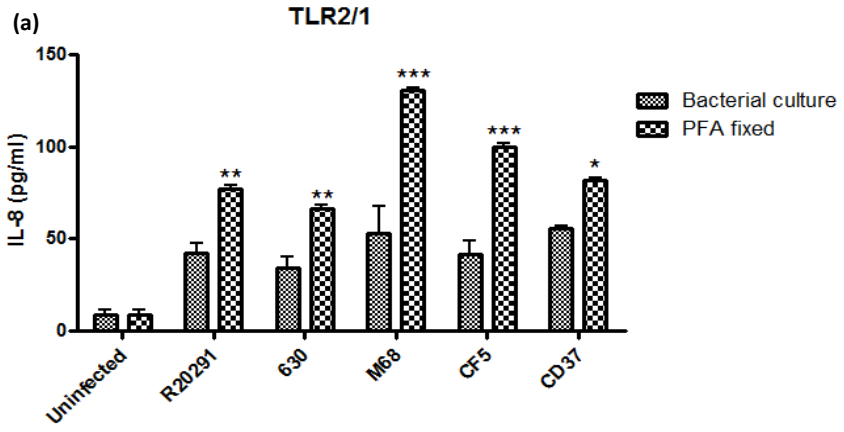

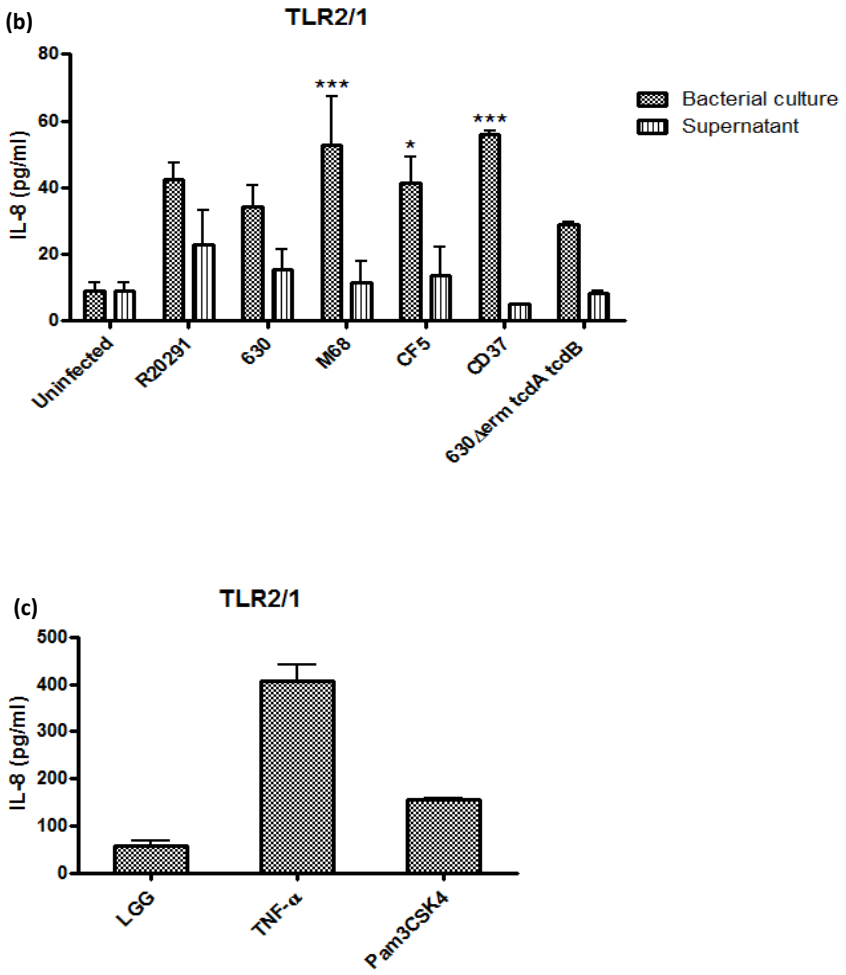

Figure 5.7. *C. difficile*-induced IL-8 response by TLR2/1-transfected HEK293 cells. Cells were co-cultured with bacterial culture and PFA-fixed bacteria at an MOI of 10 (a). IL-8 secretion in response to bacteria culture and supernatant (b). Stimulated cells with TLR2/1 receptor ligand Pam3CSK4 and TNF-α showed an IL-8 induction ranging from 150-400 pg/ml (c). Data represent mean ± SEM, n=3. $^{*}p<0.05$, $^{**}p<0.01$ and $^{***}p<0.001$ represent significant PFA-fixed difference from bacterial culture and significant bacterial culture difference from supernatant. *P* values were obtained using ANOVA with Bonferroni post-test analysis.

5.2.6 Role of TLR9-transfected Cells in Recognition of *C. difficile*

TLR9 has shown to respond to bacterial CpG DNA. To verify whether *C. difficile* is recognised by TLR9, transfected cells were infected with *C. difficile* strains as described. Uninfected TLR9-transfected cells showed a secretion <30 pg/ml, expression increased to 40 pg/ml in response to infection with bacterial culture and <50 pg/ml IL-8 was detected upon PFA-fixed bacteria (Figure 5.8 a), while bacterial supernatant caused 5-25 pg/ml IL-8 induction (Figure 5.8 b). Cells stimulated with ODN2006, a TLR9 agonist and TNF-α showed 150-200 pg/ml IL-8 secretion (Figure 5.8 c).

No significant difference in IL-8 secretion was observed between bacterial culture and PFA-fixed bacteria. Although R20291, 630, and M68 bacterial cultures showed a significant increase in IL-8 compared to bacterial supernatant but the responses were not significantly higher than uninfected cells.

Taken all together, PFA-fixed *C. difficile* was the most significant activator of TLR-transfected HEK293 cells, excluding TLR9. Further, *C. difficile* strains caused considerable activation of TLR2/6, TLR5, and TLR2-CD14, as detected by IL-8 induction compared to TLR4-CD14, TLR1/2, and TLR9.

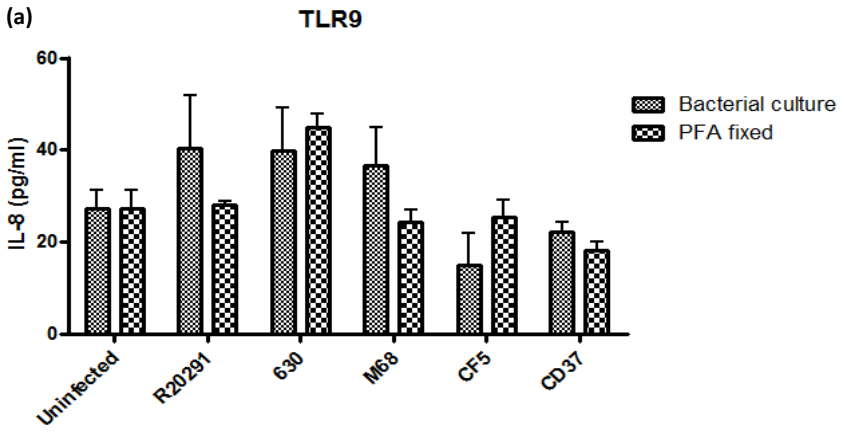

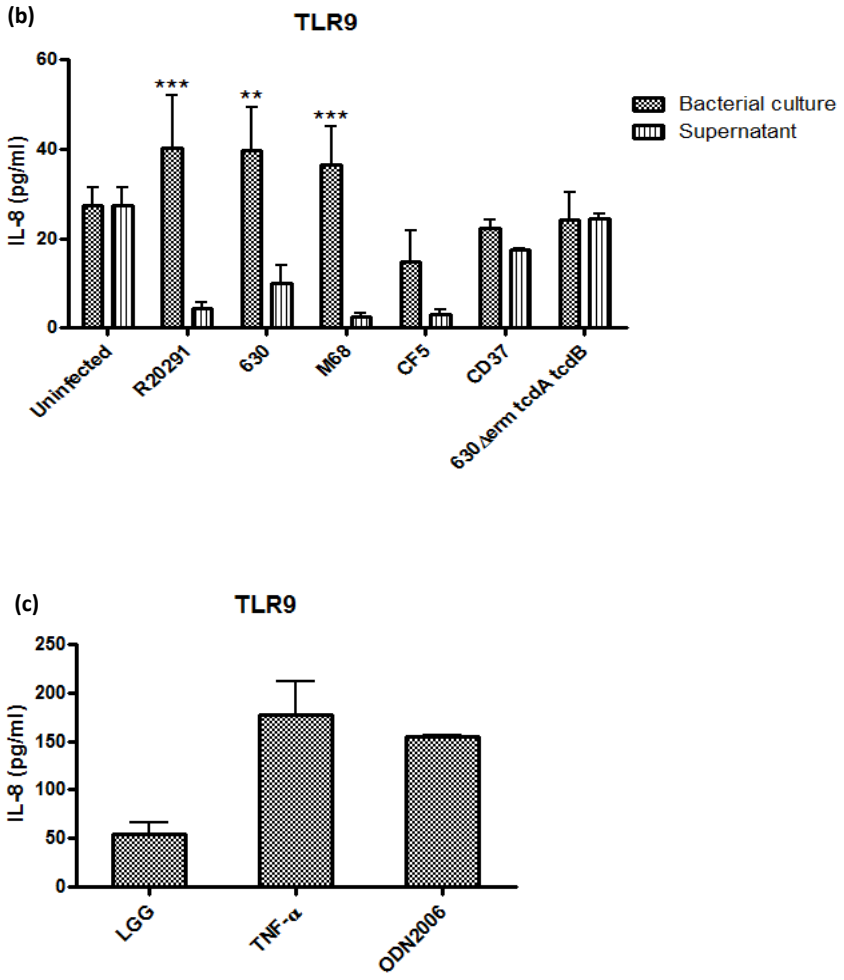

Figure 5.8. IL-8 secretion in response to *C. difficile* stimulation by TLR9. *C. difficile* bacterial culture and PFA-fixed were used at an MOI of 10 to infect TLR9-transfected cells (a). IL-8 secretion in response to bacterial culture and supernatant (b). IL-8 expression detected in cells stimulated with TLR9 agonist ODN2006 (c). Data represent mean ± SEM, n=3. $^{**}p<0.01$ and $^{***}p<0.001$ (ANOVA with Bonferroni post-test) represent significant bacterial culture difference from supernatant.

5.3 Conclusions

The detection of pathogens by the host is achieved through the families of PRRs that recognise conserved molecular structures of microbes and induce production of innate effector molecules. TLRs are one of the major receptors, which have been proven to be crucial for recognition of microbes by the innate immune system and for bridging the innate and acquired immune response (Netea *et al.,* 2004; Wells *et al.,* 2011).

In the current study, recognition of *C. difficile* by a specific TLR was investigated using HEK293 cells, which were stably transfected with one or two TLR genes. Bacterial-induced IL-8 was measured as the biological readout of TLR stimulation.

Bacterial cultures and supernatants of *C. difficile* strains caused a minimum induction of IL-8 by untransfected HEK293 cells, while PFA-treated bacteria were able to trigger a better activation and significant release of IL-8; whether or not secreted toxins by live bacteria have a role in suppressing TLR signalling remains to be determined. Interestingly, no significant difference was observed in recognition of *C. difficile* bacterial culture and PFA-fixed by TLR2/6, signifying that TLR2 is likely involved in recognition of *C. difficile* peptidoglycan-related molecules.

TLR5 appeared to respond to PFA-fixed bacteria more strongly than bacterial culture, while no significant difference was detected between TLR5 cells infected with bacterial culture and supernatant indicating that the supernatant may contain shed flagellin triggering similar responses to bacterial culture. Further, cells stimulated with 630 Δerm *tcdA tcdB* bacterial culture and supernatant showed increased IL-8 secretion compared to other strains. Although the reason for this phenomenon at present is unknown, one may speculate that as strain 630 Δerm was produced by continues subculturing it might influence expressed phenotypes consequently affecting its recognition by TLR5.

C. difficile bacterial culture and supernatant stimulated TLR2-CD14 and TLR4-CD14 complexes in a similar extent. On the other hand, PFA-fixed bacteria stimulated TLR2-CD14 2-3 times more than it stimulated TLR4-CD14. Although TLR2/1 heterodimer exhibited a significant level of IL-8 release in response to PFA-fixed bacteria and bacterial culture nevertheless showed a weak recognition of *C. difficile* strains compared to TLR2/6. Finally, TLR9 stimulation with *C. difficile* showed that TLR9 had no role in recognition of this bacterium and its components.

5.3.1 Summary

Overall, it was observed that:

- PFA-fixed bacteria were able to trigger a significant activation of examined TLRs compared to bacterial culture and supernatant.
- *C. difficile* was recognised specifically with TLR2/6 and TLR5.
- TLR2-CD14 complex may play a role in *C. difficile* recognition, while the role of TLR4-CD14 was not conclusive due to lack of MD-2 co-receptor.

Chapter 6

Clostridium difficile-mediated Dendritic Cell Activation

6.1 Introduction

The GI mucosa is in constant interaction with the luminal micro-environment and is monitored by a highly adaptable host defence system in which sentinels such as DCs, macrophages and IECs together monitor the microbial environment and coordinate immune responses to danger signals (Niess & Reinecker, 2005; Kelsall, 2008). In the intestinal mucosa, DCs are located in the PPs and lamina propria. DCs in PPs perform two important task; uptake of antigen after its transcytosis across the FAE, this is mediated by immature DCs, and T and B cells activation by mature DCs in T cell areas. Furthermore, PP DCs promote the differentiation of B cells into IgA-secreting cells (Iliev *et al.,* 2007; Kelsall, 2008).

DCs can produce an array of cytokines such as IL-10, IL-6, IL-12 and its family members IL-23 and IL-27. The IL-12 family of cytokines have a central role in Th1 responses. IL-12 is a heterodimer formed by two subunits; p35 and p40. Although IL-12 was identified as a unique heterodimeric cytokine, it was recognised that the IL-12p35 subunit is homologous to type I cytokines, such as IL-6, and that the IL-12p40 is structurally related to the soluble IL-6 receptor (IL-6Rα) (Trinchieri, 2003). IL-23 and IL-27 are two other IL-12 family members. IL-23 is composed of two covalently linked subunits: IL-23p19, which was identified on the basis of its homology with IL-6 and the p35 chain, and is distantly related to IL-12p40. IL-23 enhances Th17 cell activity by acting on differentiated Th17 cells, which express the IL-23 receptor chain. IL-27 is a heterdimeric cytokine composed of an IL-27p28 (p28) and Epstein Barr virus induced gene 3 (EBI3) subunits. The p28 subunit is homologous to IL-12p35 and IL-6, whereas EBI3 structurally resembles the IL-12p40 subunit and shares homology with IL-6Rα. Although, IL-27 is similar to IL-12 and IL-23 it is unique in that the p28 and EBI3 subunits are not held together by disulphide bonds. IL-27 promotes early commitment of naive T cells to the Th1 cell-lineage and also modulates pro- and anti-inflammatory activities (Hunter, 2005; Goriely *et al.,* 2008; Gee *et al.,* 2009).

To date, a limited number of studies have examined the role of *C. difficile* in DC activation and maturation, and subsequent initiation of acquired immunity. In 2006, Ausiello *et al.* showed that *C. difficile* SLPs from clinical isolates were able to induce the release of significant amounts of IL-1β and IL-6, and maturation of human DCs. The authors showed that SLPs caused Th1/Th2 polarisation as evidenced by comparable levels of IFN-γ and IL-5 induction. They concluded that SLPs by perturbing the fine balance of inflammatory and regulatory cytokines may play a role in the pathogenicity of *C. difficile*. The same group in a

recent study compared the immunomodulatory activities of purified SLPs from hypervirulent-epidemic strains (ribotype 027 and 001) versus non-hypervirulent-epidemic strains (ribotype 012). They detected high levels of IL-1β and IL-6 secretion, and also IL-10 but not IL-12p70, while in the previous study they reported higher amounts of IL-12p70 than IL-10. Overall, the results suggested that SLPs from hypervirulent-epidemic strains trigger similar inflammatory responses as to non-hypervirulent-epidemic strains, thus, SLP-mediated immunity is not ribotype specific (Bianco *et al.,* 2011).

So far, no studies have shown the impact of *C. difficile* itself on DC activation and subsequent T cell immunity, thus, the aim of this study was to investigate the ability of *C. difficile* strains to modulate the function of human and murine DCs in the induction of pro- or anti-inflammatory cytokines and to evaluate T cell response in *C. difficile*-primed murine DCs. Studies have begun to highlight how *C. difficile* toxins mediate excess IL-1β secretion leading to tissue damage, these studies have mainly been investigated in macrophages. In the present study how *C. difficile* may modulate DC inflammasome activation and subsequent IL-1β was assessed.

6.2 Murine Bone-marrow-derived Dendritic Cell (BMDC) Immune Response(s) to *C. difficile* Strains

Dendritic cells are key elements linking innate and adaptive immune responses to infection. Immature DCs respond to pathogen-derived products by initiating a maturation program that induces their migration to lymphoid organs and ultimately leads to the presentation of antigens associated with MHC molecules, the expression of co-stimulatory molecules and the secretion of cytokines that activate antigen-specific T cells (Niedergang & Kweon, 2005).

In this study, *C. difficile*-mediated effects on DCs and subsequent DC driven-T cell immunity was initially investigated in the murine model as it provides a genetically homogenous model system to decipher host-pathogen interactions. BMDCs were harvested from C57BL/6 mice and stimulated with *C. difficile* strains R20291 (Hypervirulent), 630 (A^+B^+) and M68 and CF5 (A^-B^+). In these series of experiments LPS from *E. coli* was utilised as a reference stimulus.

6.2.1 Dendritic Cell Maturation Induced by *C. difficile* Strains

DCs can broadly exist in two main states of maturation; immature and mature or activated, with respect to their function as APCs and capacity to induce a primary immune response. Maturation or activation of DCs occurs after exposure to pathogens, when DCs migrate to secondary lymphoid organs and express molecules such as, MHC-peptide complexes, co-stimulatory molecules, chemokines, and inflammatory cytokines, which enable DCs to interact with T cells so as to initiate an acquired immune response (Wilson & O'Neill, 2003).

To investigate whether *C. difficile* can influence the expression of cell surface markers, BMDCs were infected with *C. difficile* bacterial cultures at an MOI of 10. At 8 h post-infection, expression of co-stimulatory molecules CD80, CD86, MHC class II and CD40 was investigated by flow cytometry and presented as the mean fluorescence intensity (MFI) fold increase of the marker-specific antibody (Figures 6.1 a-d).

Cells infected with strain R20291 and M68 showed an approximate 1.5-fold increase in CD80 up-regulation, with CF5 causing a modest ≥ 1-fold increase. In comparison, 630-mediated CD80 up-regulation was significantly higher than that observed with the other strains (Figure 6.1 a).

Strains R20291 and 630 caused ≥ 1.5-fold up-regulation of CD86 molecule, whilst M68 showed <1.5-fold CD86 change. Once more, CF5 caused significantly less CD86 up-regulation exhibiting ≥ 1-fold increase (Figure 6.1 b).

MHCII, a mature DC marker was up-regulated <2-fold in response to R20291 and ≥ 1-fold to strain 630. M68 and CF5 caused similar MHCII fold increase (2-fold), while CF5 showed a significant increase compared to strain 630 (Figure 6.1 c).

CD40 was modulated less than 2-fold in response to stimulation with strain R20291, strain 630 showed ≥ 1-fold increase. Strain M68 caused similar CD40 fold change as R20291 (≤ 2), while CD40 was enhanced 3-fold in response to CF5 (Figure 6.1 d).

In summary, this data suggested that *C. difficile* strains caused a moderate up-regulation of co-stimulatory molecules CD80 and CD86, as well as surface expression of MHC class II and accessory cell molecule CD40. While, strain CF5 showed the least modulation of CD80 and CD86, it induced comparatively higher up-regulation of MHCII and CD40.

(a)

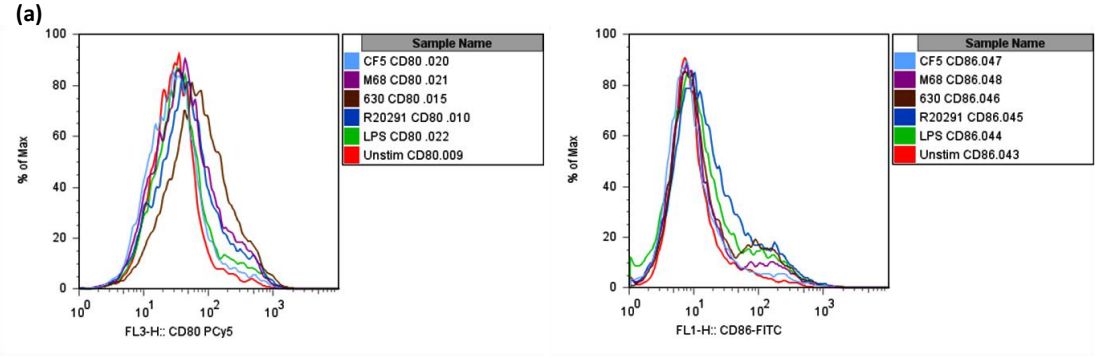

CD80 CD86

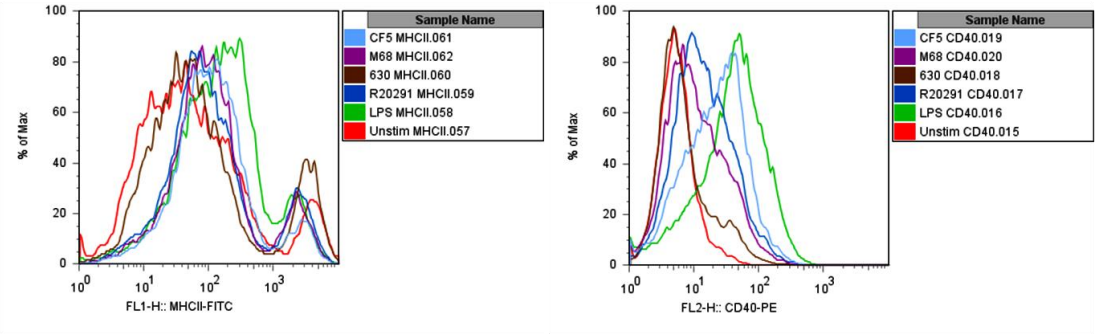

MHCII CD40

(b)

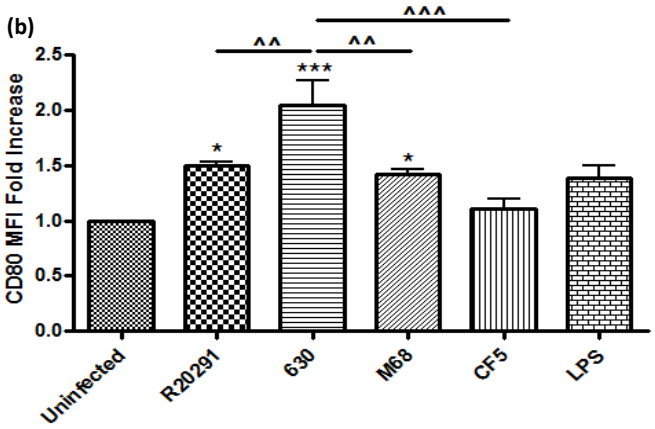

(c)

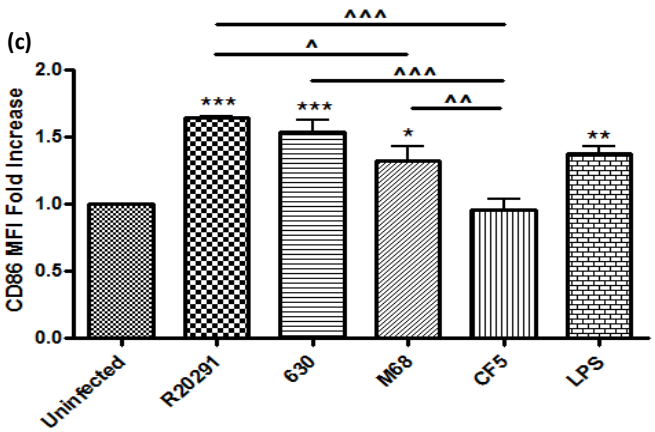

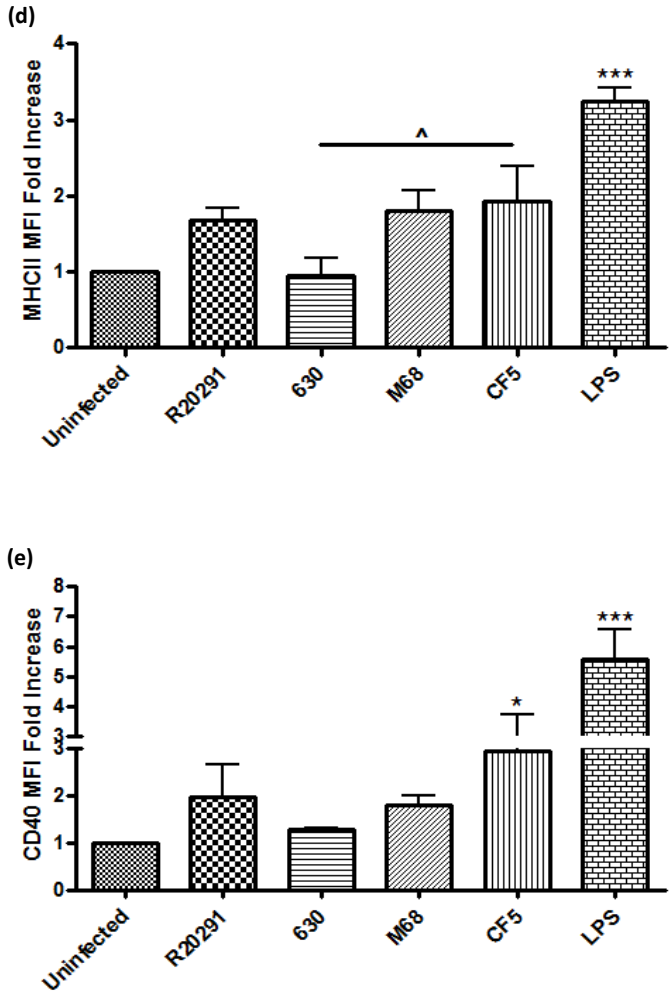

Figure 6.1. *C. difficile* induces maturation of BMDCs by modulating cell surface markers. BMDCs were infected with *C. difficile* bacterial cultures at an MOI of 10. At 8 h post-stimulation, cells were labelled with mouse CD80, CD86, MHCII and CD40 antibodies and analysed by flow cytometry (a). The level of surface expression was quantified and presented as MFI fold increase (b-e). 1 µg/µl LPS was utilised as a reference stimulus. Data represent mean ± SEM, n=3. $^{*}p<0.05$, $^{**}p<0.01$ and $^{***}p<0.001$ represent significant difference from uninfected cells and $^{\wedge}p<0.05$, $^{\wedge\wedge}p<0.01$ and $^{\wedge\wedge\wedge}p<0.001$ represent significant inter-strain difference. *P* values were obtained using ANOVA with Bonferroni post-test analysis.

6.2.2 *C. difficile*-mediated Cytokine Gene Expression in BMDC

The interaction between DCs and pathogens are of prime importance in establishing an appropriate immune response. To investigate *C. difficile*-mediated inflammatory cytokine mRNA expression, BMDCs were infected with *C. difficile* bacterial cultures at an MOI of 10. Gene expression of IL-12 family (IL-12, IL-23, and IL-27) subunits (IL-12: p35/p40; IL-23: p19/p40; IL-27: EBI3/p28), IL-10, IL-6, and IL-1β was measured by quantitative real-time PCR at 2, 4, 6, and 8 h post-infection and presented as a fold increase relative to uninfected control cells (Figure 6.2 a-h).

Infected cells were examined for expression of IL-12 subunits; p35/p40. All strains induced p35 expression in a time-dependent manner (Figure 6.2 a). The expression increased progressively peaking at 6 h post-infection although magnitude of expression varied between strains. Strains R20291 and CF5 caused a significant p35 modulation at 6 and 8 h compared to 630 and M68 (Figure 6.2 a).

P40 subunit, which is shared by IL-12 and IL-23 cytokines, exhibited a 3-fold increase in response to bacterial infection at 2 h (Figure 6.2 b). P40 expression also increased progressively and reached its peak at 6 h thus following the same profile as p35 expression. At 8 h a moderate decrease was observed with all four strains. Interestingly, as seen for p35, R20291 and CF5 showed a significant increase in p40 at 6 and 8 h post-infection compared to strain 630 and M68 (Figure 6.2 b).

Expression of p19, a subunit unique to IL-23 showed 25-fold increase at 2 h and was enhanced further reaching maximum levels at 4 h (Figure 6.2 c). It is worth noting that p19 exhibited the highest fold-induction in this family of cytokines. Between 4 and 6 h, unlike the increase observed for p35 and p40, the expression profile varied amongst the various strains. The expression levels decreased in all four strains at 8 h post-infection. R20291 caused significant p19 mRNA expression at 4, 6, and 8 h post-infection when compared with the other strains (Figure 6.2 c).

Expression of EBI3 and p28, IL-27 subunits were observed in *C. difficile* infected cells. A very modest induction in EBI3 was noted at 2 h, expression reached its maximum at 6 h with a moderate increase ranging between 2.5 to 4-fold. At 8 h, EBI3 mRNA level declined in cells infected with R20291 and 630. R20291 was statistically significant at 6 and 8 h compared to strain 630, while CF showed a significant increase at 8 h compared to 630 (Figure 6.2 d).

In contrast, infected cells showed a better response to p28 induction (Figure 6.2 e). A 4.5-fold increase was observed at 2 h, mRNA expression increased gradually and reached its peak at 6 h, the increase measured ranged between 40 and 220-fold. At 8 h p28 mRNA expression declined in all four strains. Yet again, R20291 showed significant gene expression at 4, 6, and 8 h, while CF5 was statistically significant at 6 and 8 h compared to strains 630 and M68 (Figure 6.2 e).

C. difficile infection modulated DC anti-inflammatory response as measured by IL-10 production (Figure 6.2 f). A marked increase in IL-10 mRNA expression was detected as early as 2 h. At 4 h, IL-10 expression increased further and this continued till 8 h. At 8 h, all strains showed an increase in IL-10, while CF5 caused statistically significant mRNA expression compared to 630 (Figure 6.2 f).

C. difficile Infected cells showed increase in IL-6 expression at 2 h (Figure 6.2 g) mRNA expression increased steadily up to 6 h post-infection. At 8 h, IL-6 mRNA levels showed a moderate decline in all four strains; furthermore, no significant inter-strain difference was detected at any examined time-points (Figure 6.2 g).

Measurement of IL-1β gene expression showed ~20-fold increase in *C. difficile* infected cells at 2 h (Figure 6.2 h). IL-1β expression was up-regulated further at 4 h. At 6 h, strains R20291, 630, and M68 showed increased modulation, whereas CF5 remained unchanged. No significant inter-strain difference was detected in IL-1β gene expression at any time-points measured (Figure 6.2 h).

Taken all together, this data indicated that *C. difficile* strains mediated changes in pro-inflammatory mRNA expression which showed maximal response between 4 and 6 h post-infection, and declined by 8 h. In contrast, IL-10 gene expression continued to show a significant increase at 8 h. Strains R20291 and CF5 were statistically significant in modulating p35, p40, and p28 gene expression at 6 and 8 h compared to strains 630 and M68.

(a)

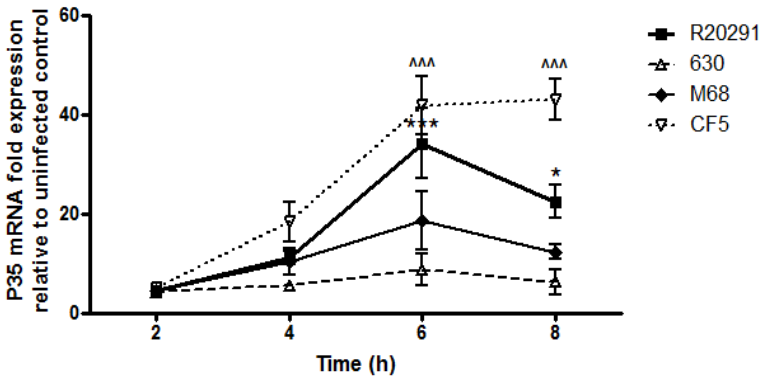
P35 mRNA fold expression relative to uninfected control
60
40
20
0
2
4
6
8
Time (h)
^^^
^^^
***
*
R20291
630
M68
CF5

(b)

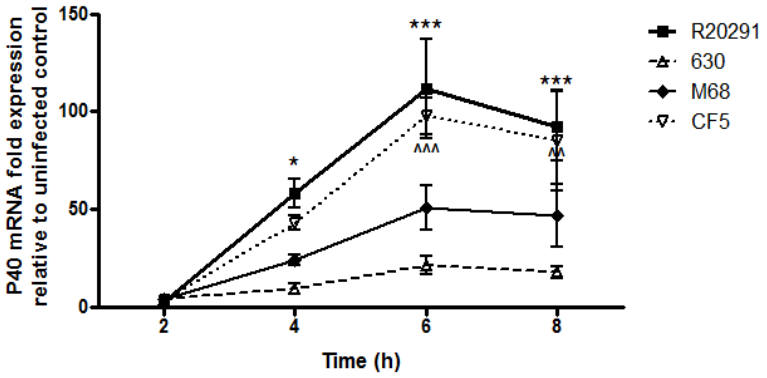
P40 mRNA fold expression relative to uninfected control
150
100
50
0
2
4
6
8
Time (h)
***
***
*
^^^
^^
R20291
630
M68
CF5

(c)

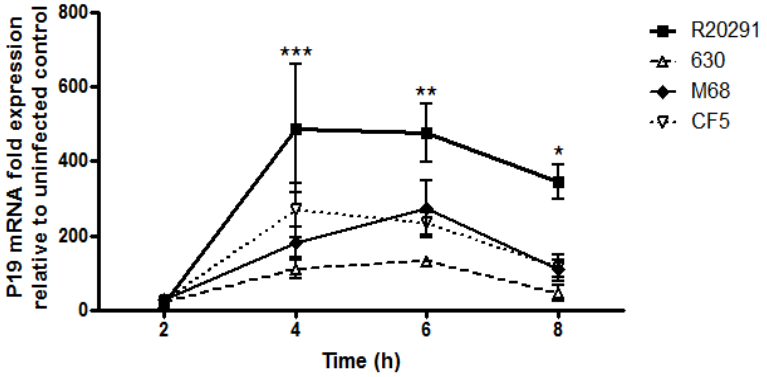
P19 mRNA fold expression relative to uninfected control
800
600
400
200
0
2
4
6
8
Time (h)
***
**
*
R20291
630
M68
CF5

(d)

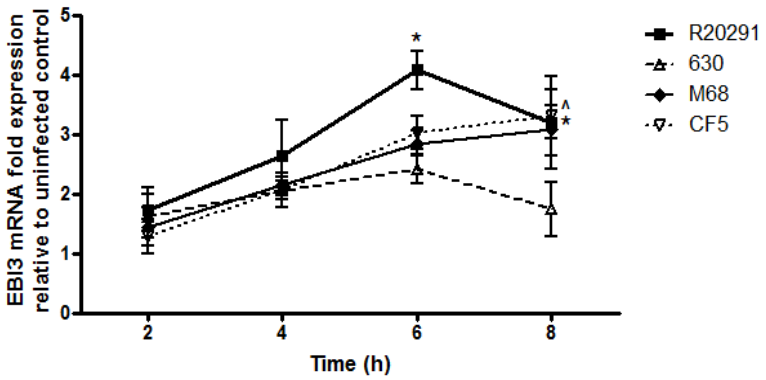
EBI3 mRNA fold expression relative to uninfected control
0
1
2
3
4
5
2
4
6
8
Time (h)
*
*
^
R20291
630
M68
CF5

(e)

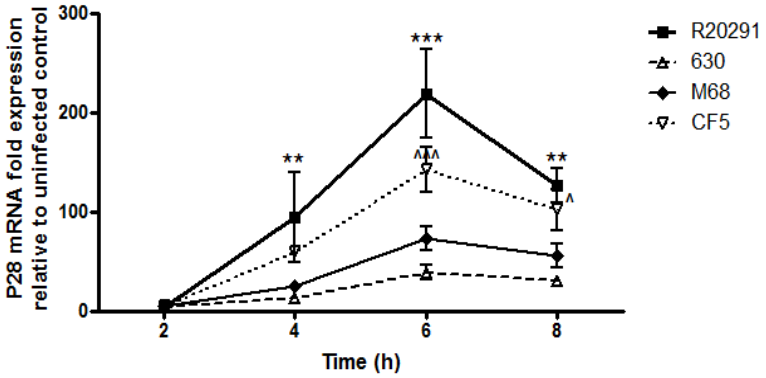
P28 mRNA fold expression relative to uninfected control
0
100
200
300
2
4
6
8
Time (h)
**
***
**
^^^
^
R20291
630
M68
CF5

(f)

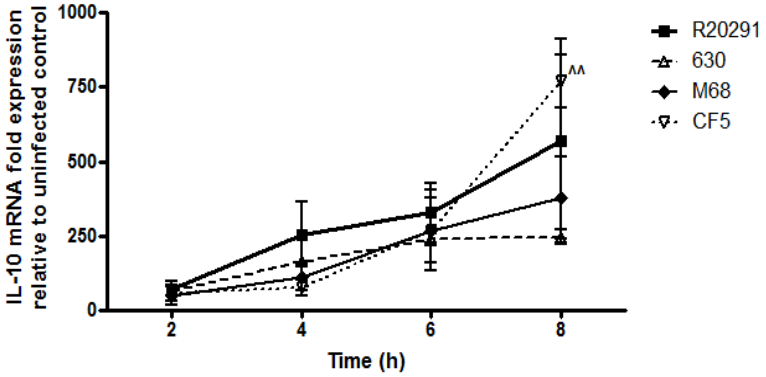
IL-10 mRNA fold expression relative to uninfected control
0
250
500
750
1000
2
4
6
8
Time (h)
^^
R20291
630
M68
CF5

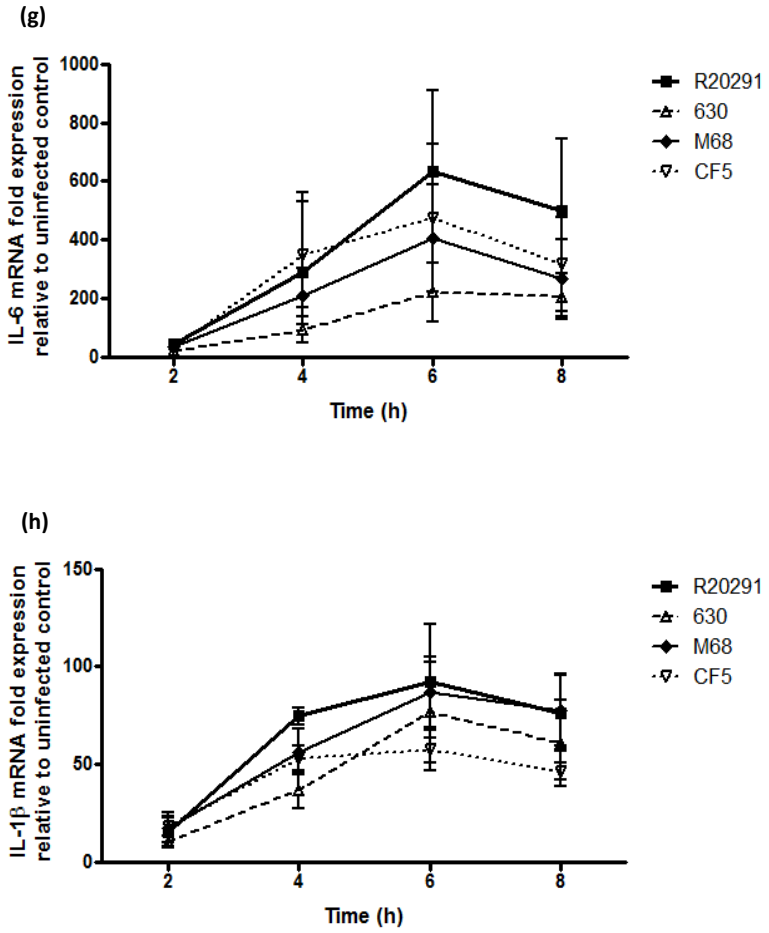

Figure 6.2. Cytokine mRNA expression in response to *C. difficile* infection in BMDCs. BMDCs were infected with *C. difficile* cultures at an MOI of 10. Gene modulation of IL-12 family subunits; p35 (a), p40 (b), p19 (c), EBI3 (d), and p28 (e), as well as IL-10 (f), IL-6 (g) and IL-1β (h) were measured by real-time PCR and normalised to uninfected control cells and presented as a fold increase. Reactions for each sample were conducted in duplicate. Data represent mean ± SEM, n=3. $^{*/\wedge}p<0.05$, $^{**/\wedge\wedge}p<0.001$, and $^{***/\wedge\wedge\wedge}p<0.001$ represent significant inter-strain difference. *P* values were obtained using ANOVA with Bonferroni post-test analysis.

6.2.3 *C. difficile*-induced Cytokine Production by BMDC

Dendritic cells upon interaction with bacteria characteristically release a range of both pro- and anti-inflammatory cytokines. Following assessment of cytokine gene expression in response to *C. difficile* infection, cytokine protein secretion was investigated. BMDCs were infected with *C. difficile* cultures at an MOI of 10 and induction of IL-12 family (IL-12, IL-23, and IL-27), IL-10, TNF-α, and IL-1β cytokines was measured 8 h post-infection (Figures 6.3 a-f).

IL-12 was detected at a basal level of ~10 pg/ml in uninfected control cells. R20291 enhanced IL-12 secretion up to 80 pg/ml, while strain 630 caused ~35 pg/ml induction. Strain M68 mediated intermediate levels, whereas CF5 exhibited significant IL-12 release (>200 pg/ml) compared to the other strains (Figure 6.3 a).

IL-23 was almost undetectable in uninfected control cells. Upon infection with R20291 significant increase in IL-23 was observed, whilst 630 caused more modest increase. M68 and CF5 induced between 300 and 400 pg/ml of IL-23. This data clearly showed the differential capacity of the various *C. difficile* strains to modulate IL-23 (Figure 6.3 b).

IL-27 release in uninfected control BMDC was low (~6 pg/ml). R20291 showed greater ability to induce IL-27 when compared to the 630 (180 versus 50 pg/ml). M68 was as equipotent as R20291, while CF5 enhanced IL-27 secretion to ~350 pg/ml. CF5 showed a significant IL-27 release compared to the other strains (Figure 6.3 c).

Uninfected control BMDCs did exhibit spontaneous IL-10 secretion. Infection with R20291 caused a 7 to 8-fold increase in IL-10 protein levels with a 3 to 4-fold seen in response to strain 630. Strain M68 showed similar ability as R20291, while strain CF5 caused significantly marked increase in IL-10 compared to other strains (Figure 6.3 d).

Uninfected BMDCs secrete TNF-α, this level increased upon infection with strain R20291 to a significant level (7000 pg/ml). Strain 630 was less potent (~6000 pg/ml) while M68 and CF5 induced similar levels to strain R20291 (Figure 6.3 e).

Low levels (~15 pg/ml) of IL-1β were measured in uninfected BMDC. Upon infection with strain R20291, IL-1β secretion increased to >3000 pg/ml, whilst 630 caused less. Strain M68 exhibited similar IL-1β induction as R20291 (>3000 pg/ml) while CF5 showed significantly less ability to modulate IL-1β. Amongst the various cytokines tested, IL-1β was the first

cytokine where the examined bacterial strains showed marked variation in their ability to modulate a pro-inflammatory cytokine (Figure 6.3 f).

In summary, strain CF5 induced significant amounts of IL-12 family and IL-10 compared to the other strains and yet, at the same time was least inducer of IL-1β. The APCs such as BMDCs clearly have the ability to detect and mount differential responses to individual *C. difficile* strains, thus fine tuning their response(s) to each stimulus.

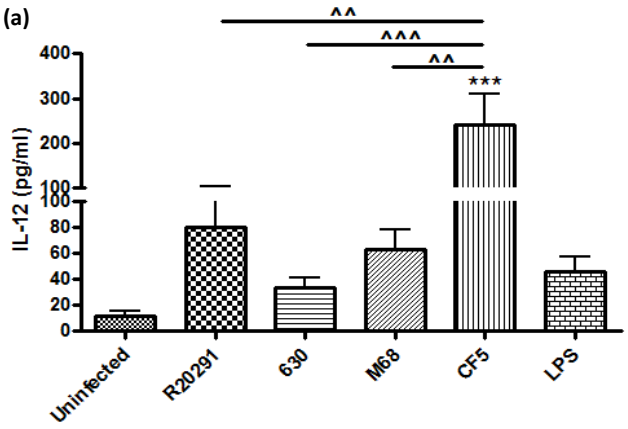
(a)
IL-12 (pg/ml)
400
300
200
100
100
80
60
40
20
0
^^
^^^
^^
***
Uninfected
R20291
630
M68
CF5
LPS

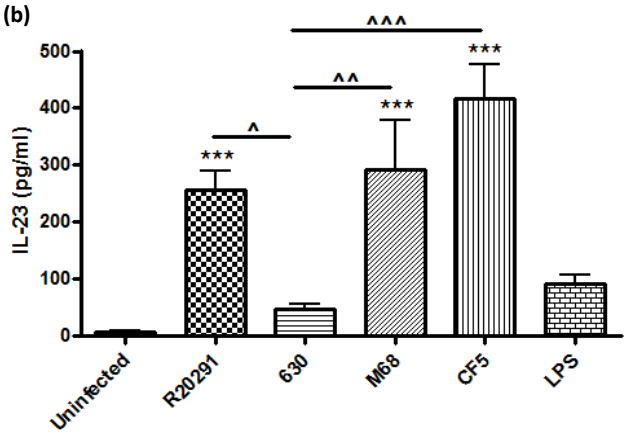
(b)
IL-23 (pg/ml)
500
400
300
200
100
0
^^^
***
^^
***
^
***
Uninfected
R20291
630
M68
CF5
LPS

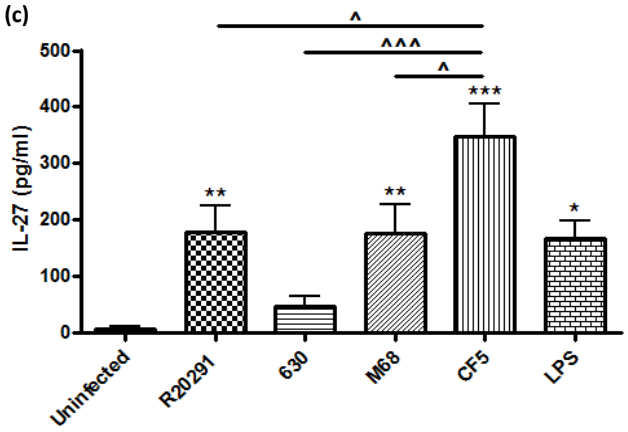
(c)
IL-27 (pg/ml)
500
400
300
200
100
0
^
^^^
^
***
**
**
*
Uninfected
R20291
630
M68
CF5
LPS

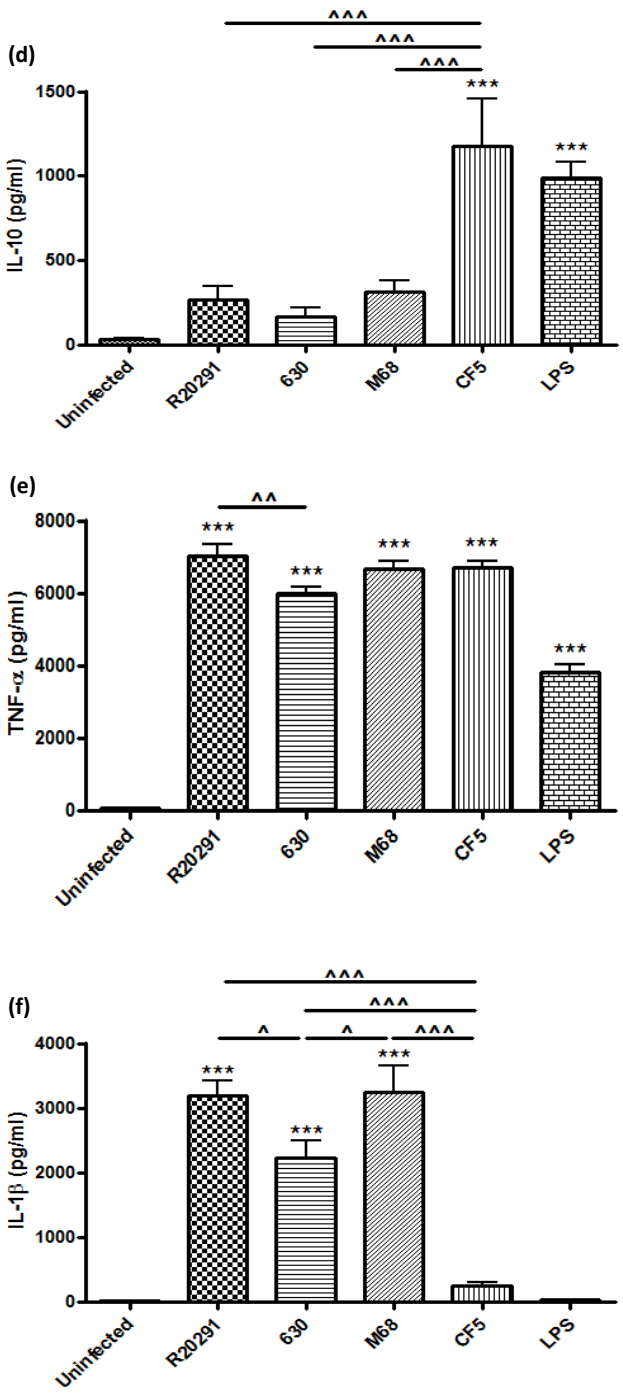

Figure 6.3. Cytokine induction by BMDCs in response to *C. difficile* infection. BMDCs were infected with *C. difficile* cultures at an MOI of 10. IL-12 (a), IL-23 (b), IL-27 (c), IL-10 (d), TNF-α (e), and IL-1β (f) were measured by ELISA at 8 h post-infection. 1 µg/µl LPS was utilised as a reference stimulus. Data represent mean ± SEM of duplicate samples and are representative of three individual experiments. $^{*/\wedge}p<0.05$, $^{**/\wedge\wedge}p<0.01$ and $^{***/\wedge\wedge\wedge}p<0.001$ represent significant difference from uninfected cells and significant inter-strain difference. *P* values were obtained using ANOVA with Bonferroni post-test analysis.

6.3 The Inflammasome Activation Mediated by *C. difficile*

The inflammasome is a caspase-activating complex that mediates the activation of caspase-1, which is the enzyme responsible for cleaving inactive pro-IL-1β and IL-18 into their bioactive form. This process is linked with secretion of the bioactive form. The molecular platform for caspase-1 activation includes NLR family members such as; NLRP1, NLRP3 (NALP3) and NLRC4 (IPAF) and AIM2 (absent in melanoma 2). All four proteins recognise microbial products and upon engagement each can trigger initiation of inflammasome formation in an independent manner. An adaptor protein, ASC (apoptosis-associated speck-like protein containing a CARD domain) is common to all these inflammasome platforms. ASC contains an N-terminal pyrin domain and a C-terminal CARD domain, both enabling ASC to recruit other pyrin- and CARD-containing domains through protein-protein interactions linking NLRs to caspase-1 (Yu & Finlay, 2008; Franchi *et al.,* 2009).

Caspase-1 is present in the cytosol of phagocytic cells as an inactive zymogen. Caspase-1 is activated by auto-proteolytic cleavage leading to the generation of two subunits (10 and 20 kDa). Mature IL-1β and IL-18 have been linked to many immune reactions, including the recruitment of inflammatory cells to the site of infection, production of IFN-γ and enhancement of the cytolytic activity of natural killer cells (Lamkanfi *et al.,* 2007; Yu & Finlay, 2008; Franchi *et al.,* 2009).

Recently, Ng *et al.* reported that *C. difficile* toxins (40 μg/ml TcdA and 2.5 μg/ml TcdB) trigger inflammasome-dependent release of IL-1β. They showed that inhibition of inflammasome signalling through deletion of ASC, completely abrogated caspase-1 activation and IL-1β processing *in vitro*, and significantly reduced toxin-induced intestinal injury *in vivo*, concluding an ASC-dependent activation of the inflammasome by *C. difficile* toxins (Ng *et al.,* 2010).

Although toxins clearly activate the inflammasome complex, what is unclear is whether the bacterial cell itself participates in these reactions. Also the individual components involved during *C. difficile*-mediated IL-β release are not defined yet. The aim of this study was to investigate the potential role of *C. difficile* bacterial components in triggering the activation of the inflammasome.

6.3.1 Caspase-1 Activation in Response to *C. difficile* Strains

To assess whether *C. difficile*-induced IL-1β processing was caspase-1 dependent, BMDCs from wild-type (WT) C57BL/6 (genetically Nlrp1 deficient), Nod2$^{-/-}$, Ipaf$^{-/-}$, Nlrp3$^{-/-}$, and ASC$^{-/-}$ mice were infected with *C. difficile* cultures at an MOI of 10. At 8 h post-infection cell extracts were analysed for the extent of caspase-1 activation and IL-1β release (Figure 6.4 a-k). Pro-caspase-1 was detected as a 45 kDa propeptide and active caspase-1 as a 10 kDa subunit, while pro-IL-1β and IL-1β are 31 kDa and 17 kDa size proteins respectively. In these experiments ATP was used as a positive control to activate the inflammasome (Figure 6.4 a-k).

Pro-caspase-1 and pro-IL-1β were detected in uninfected control WT and knock-out (KO) BMDCs (Figure 6.4 a-j). Infection with *C. difficile* strains caused release of active caspase-1 (Figure 6.4 a), and mature IL-β in WT BMDCs (Figure 6.4 b).

Similar results, detecting pro- and active caspase-1 were observed in Nod2$^{-/-}$ (Figure 6.4 c), Ipaf$^{-/-}$ (Figure 6.4 e), and Nlrp3$^{-/-}$ (Figure 6.4 g) infected BMDCs, followed by the detection of pro-IL-1β and release of mature IL-1β in Nod2$^{-/-}$ (Figure 6.4 d), Ipaf$^{-/-}$ (Figure 6.4 f), and Nlrp3$^{-/-}$ (Figure 6.4 h).

Pro-caspase-1 and pro-IL-1β were detected in ASC$^{-/-}$ uninfected control and *C. difficile* infected BMDCs. In contrast, caspase-1 activation and IL-1β production were completely absent in infected ASC$^{-/-}$ cells (Figure 6.4 i & j).

Taken all together, this data suggested that *C. difficile* strains induced mature IL-1β in a caspase- and ASC-dependent manner consistent with inflammasome activation.

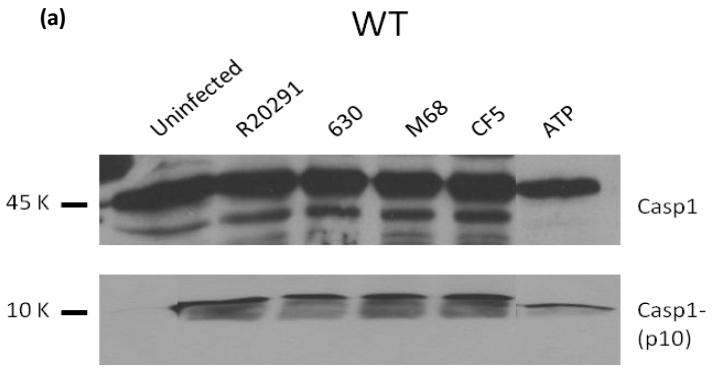
(a)
WT
Uninfected
R20291
630
M68
CF5
ATP
45 K
Casp1
10 K
Casp1-
(p10)

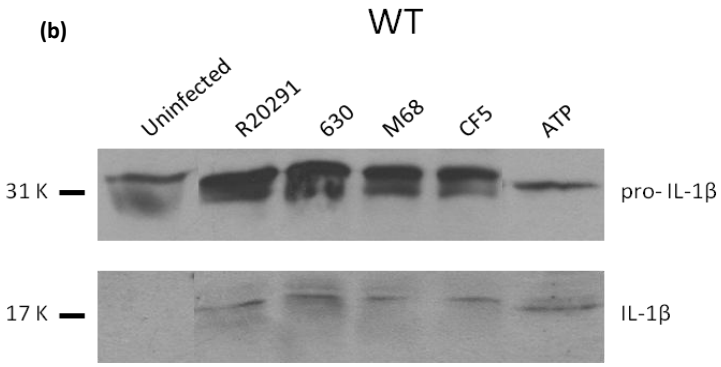
(b)
WT
Uninfected
R20291
630
M68
CF5
ATP
31 K
pro- IL-1β
17 K
IL-1β

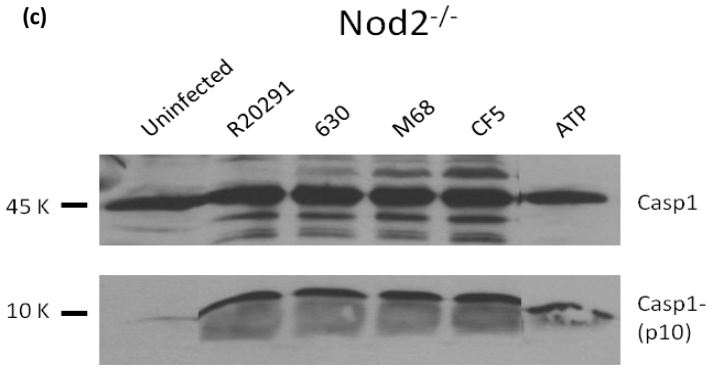
(c)
Nod2-/-
Uninfected
R20291
630
M68
CF5
ATP
45 K
Casp1
10 K
Casp1-
(p10)

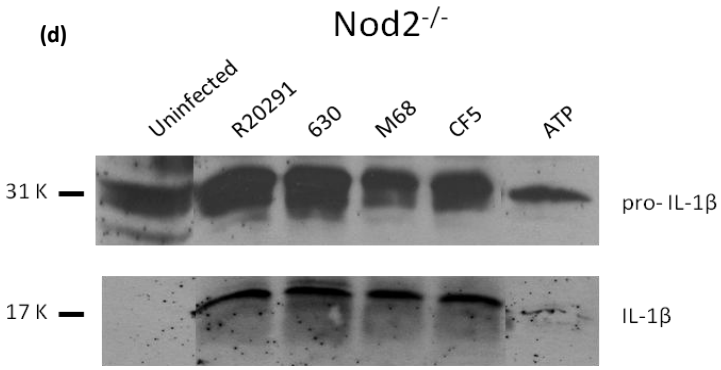
(d)
Nod2-/-
Uninfected
R20291
630
M68
CF5
ATP
31 K
pro- IL-1β
17 K
IL-1β

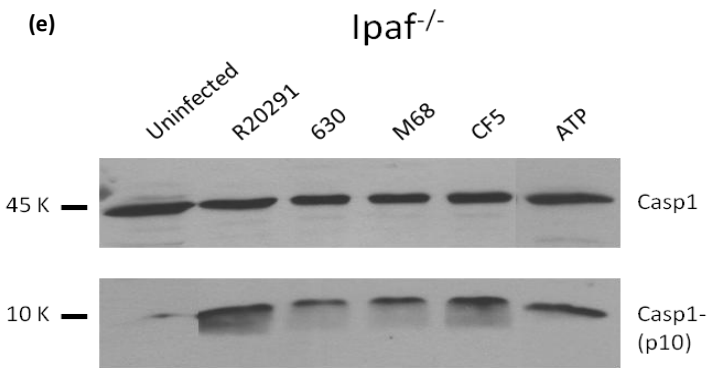
(e)
Ipaf-/-
Uninfected
R20291
630
M68
CF5
ATP
45 K
Casp1
10 K
Casp1-
(p10)

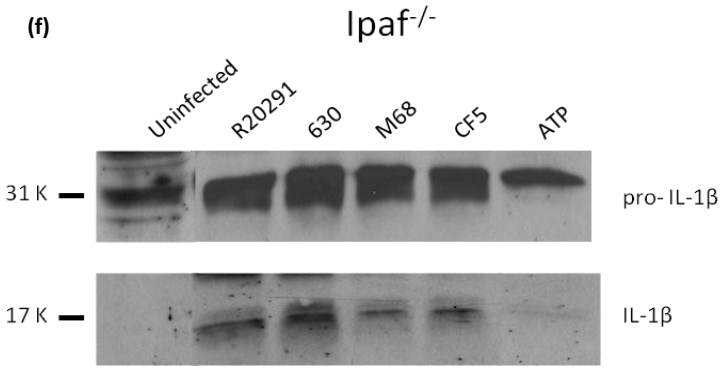
(f)
Ipaf-/-
Uninfected
R20291
630
M68
CF5
ATP
31 K
pro- IL-1β
17 K
IL-1β

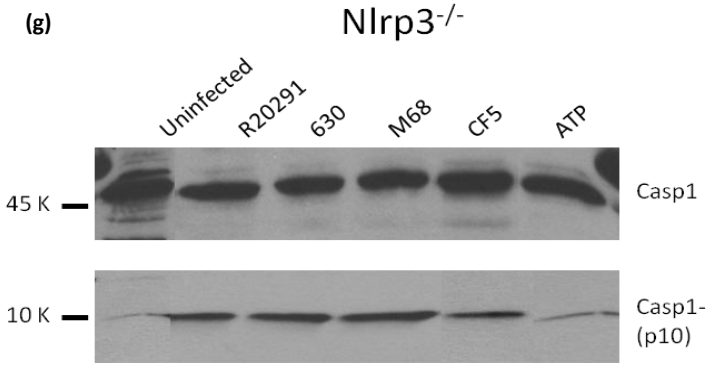
(g)
Nlrp3-/-
Uninfected
R20291
630
M68
CF5
ATP
45 K
Casp1
10 K
Casp1-
(p10)

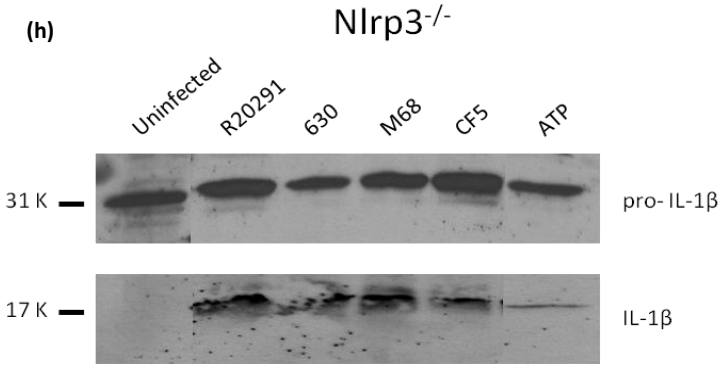
(h)
Nlrp3-/-
Uninfected
R20291
630
M68
CF5
ATP
31 K
pro- IL-1β
17 K
IL-1β

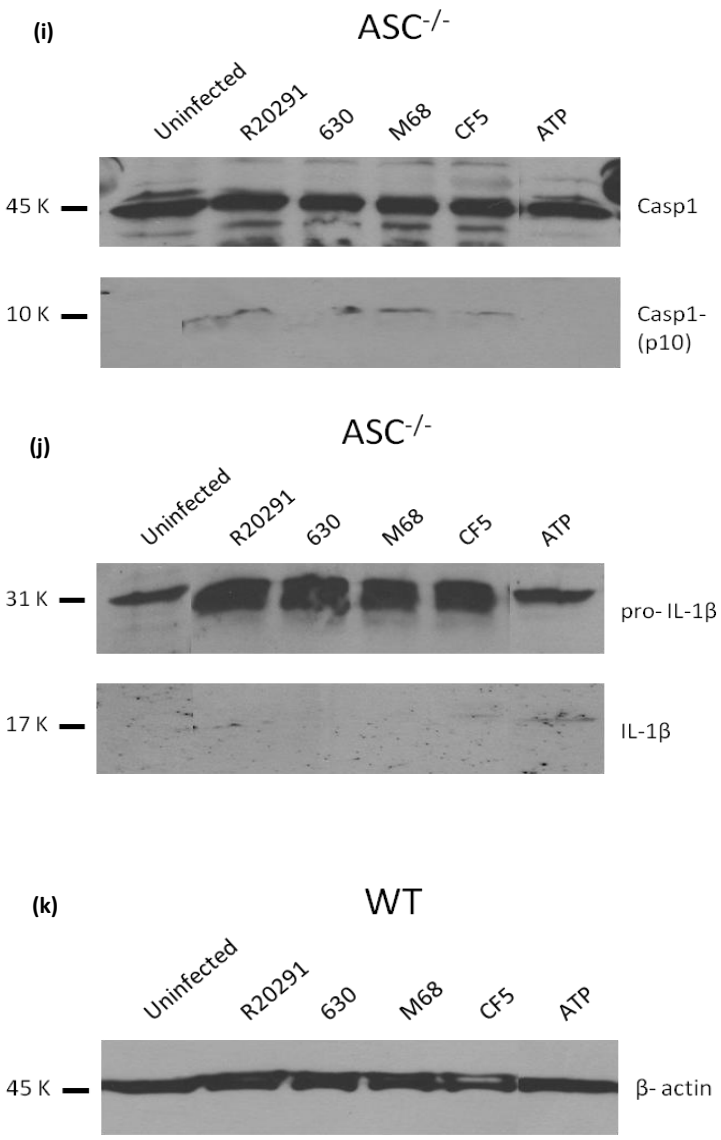

Figure 6.4. *C. difficile* triggers caspase-1 activation and IL-1β secretion. BMDCs from WT mice (a-b) and mice deficient in Nod2 (c-d), Ipaf (e-f), Nlrp3 (g-h) and ASC (i-j) were infected with *C. difficile* bacterial cultures at an MOI of 10. Immunoblotting was used to detect pro- and active caspase-1 (45 & 10 kDa, respectively) and pro- and mature IL-1β (31 & 17 kDa, respectively) release in cell extracts at 8 h post-infection. ATP (5 mM) was used as a stimulator of inflammasome activation. β-actin (45 kDa) was used as a loading control (k).

6.3.2 *C. difficile*-induced IL-1β Secretion

IL-1β, produced by activated macrophages, monocytes, and DCs is a potent pro-inflammatory cytokine and a key immune modulator, controlling both the induction of localised inflammation as well the recruitment and activation of the adaptive immune response. Induction of IL-1β in response to *C. difficile* infection was investigated by utilising BMDCs from WT (C57BL/6, genetically Nlrp1 deficient), Nod2, Ipaf, Nlrp3, and ASC KO mice. Cells were infected with *C. difficile* strains and 017 ribotype strains including: CF2, CF3, CD586, CD636, and CD816 at an MOI of 10 and IL-1β induction in response to infection was measured at 8 h post-infection (Figure 6.5 a-d).

Uninfected WT, Nod2$^{-/-}$, Ipaf$^{-/-}$, Nlrp3$^{-/-}$, and ASC$^{-/-}$ control BMDCs showed a basal level of <20 pg/ml IL-1β (Figure 6.5 a-d). Upon infection with R20291 ≥ 2000 pg/ml IL-1β was secreted in WT, Nod2$^{-/-}$, and Ipaf$^{-/-}$ cells. Similar IL-1β secretion was observed in response to strains 630 and M68. In contrast, CF5 caused significantly less release of IL-1β compared to the other strains. It was originally hypothesised that CF5 causes minimal IL-1β secretion due to lack of caspase-1 activation, however as seen earlier CF5 is equipotent in causing caspase-1 activation when compared to the other strains (Figure 6.5 a), so a molecular explanation of how CF5 infection leads to minimal IL-1β secretion remains unknown. Elevated levels of IL-1β however were observed in Nod2$^{-/-}$ and Ipaf$^{-/-}$ infected cells (450, 600 pg/ml; respectively) compared to WT BMDCs (80 pg/ml), which was not statistically significant (Figure 6.5 a).

The effect of *C. difficile* in the activation of the inflammasome leading to IL-1β release was examined using Nlrp3$^{-/-}$ and ASC$^{-/-}$ BMDCs. Strain R20291 caused release of 1700 pg/ml IL-1β in Nlrp3 KO DCs, while 630 induced >2000 pg/ml and M68 showed ~2600 pg/ml IL-1β secretion. Strain CF5 yet again caused significantly less IL-1β when compared with the other strains (~780 pg/ml). R20291, 630, and M68-induced IL-1β response in ASC deficient BMDCs were significantly less compared to WT and Nlrp3$^{-/-}$ cells (<50 pg/ml) (Figure 6.5 b).

As CF5-induced IL-1β to a significantly less extent, five ribotype 017 strains including CF2, CF3, CD586, CD636, and CD816 were employed to investigate whether ribotype 017 strains shared the property of reduced IL-1β secretion with CF5. WT BMDCs infected with CF5 and ribotype 017 strains showed 40-110 pg/ml IL-1β release, indicating these strains share the ability of being weak inducer of IL-1β compared to R20291, 630 and M68. The induction of IL-1β was increased in infected Nod2$^{-/-}$ cells with ribotype 017 strains (80-280 pg/ml) as was

observed with CF5. This increase in IL-1β responses was not statistically significant. CF5 caused 600 pg/ml IL-1β release in infected Ipaf$^{-/-}$ cells, similar responses were detected in cells infected with ribotype 017 strains (Figure 6.5 c). Stimulation of Nlrp3 deficient BMDCs with ribotype 017 strains and CF5 induced efficient IL-1β secretion (ranging between 150-700 pg/ml) but the responses were markedly attenuated in ASC$^{-/-}$ BMDCs (Figure 6.5 d).

This study showed that *C. difficile* strains triggered the IL-1β release by activating an ASC-containing inflammasome and that they caused IL-1β processing in the examined three cell types Nod2$^{-/-}$, Ipaf$^{-/-}$, and Nlrp3$^{-/-}$, ruling out critical roles for these NLRs in the activation of the inflammasome. Also it was observed that ribotype 017 strains excluding M68, caused the least IL-1β release in infected WT DCs but unexpectedly Nod2, Ipaf and Nlrp3 deficiency enhanced potency of these strains leading to increased levels of IL-1β secretion.

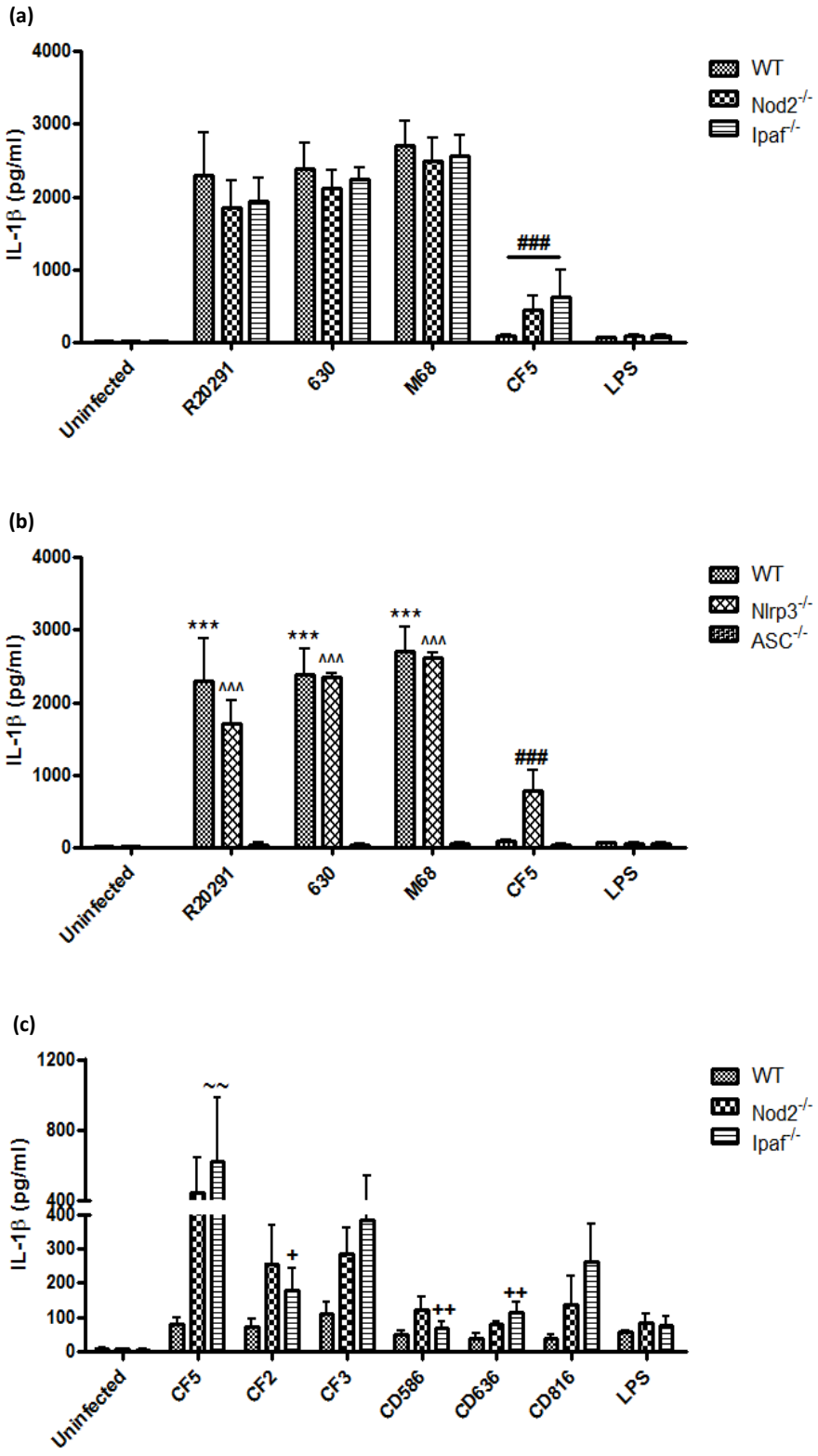
(a)
IL-1β (pg/ml)
4000
3000
2000
1000
0
WT
Nod2-/-
Ipaf-/-
###
Uninfected
R20291
630
M68
CF5
LPS
(b)
IL-1β (pg/ml)
4000
3000
2000
1000
0
WT
Nlrp3-/-
ASC-/-
***
^^^
***
^^^
***
^^^
###
Uninfected
R20291
630
M68
CF5
LPS
(c)
IL-1β (pg/ml)
1200
800
400
400
300
200
100
0
WT
Nod2-/-
Ipaf-/-
~~
+
++
++
Uninfected
CF5
CF2
CF3
CD586
CD636
CD816
LPS

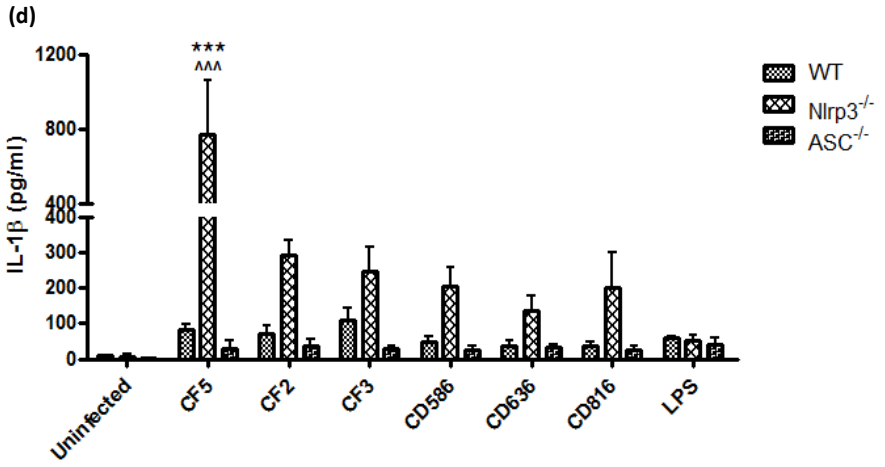

Figure 6.5. *C. difficile* toxins trigger IL-1β release by activating an ASC-containing inflammasome. BMDCs from WT C57BL/6 (genetically Nlrp1 deficient) mice and mice deficient in Nod2, Ipaf (Nlrc4), Nlrp3, and ASC were infected with *C. difficile* strains as well as five ribotype 017 strains at an MOI of 10. IL-1β release was measured by ELISA at 8 h post-infection. 1 µg/µl LPS was utilised as a reference stimulus. Data represent mean ± SEM, n=4. $^{***}p<0.001$ represents significant WT difference from $ASC^{-/-}$, $^{\wedge\wedge\wedge}p<0.001$ represents significant $Nlrp3^{-/-}$ difference from $ASC^{-/-}$, $^{\#\#\#}p<0.001$ represent significant CF5 difference from strains R20291, 630, and M68, $^{\sim\sim}p<0.01$ represents significant WT difference from $Ipaf^{-/-}$, and $^{+}p<0.05$ represents significant strain CF5 difference from ribotype 017 strains. *P* values were obtained using ANOVA with Bonferroni post-test analysis.

6.4 Innate Immune Response of Human Dendritic Cells to *C. difficile* Strains

The murine model of *C. difficile* infection showed that *C. difficile* strains were able to modulated murine BMDC cytokine responses. Human DCs were utilised to determine whether similar mechanisms were at play during *C. difficile*-mediated human DC activation. Human monocyte-derived DCs were infected with *C. difficile* cultures at an MOI of 10 and induction of IL-12, IL-10, and IL-1β cytokines were measured at 8 h post-infection (Figures 6.6 a-c).

Cells infected with R20291 showed <400 pg/ml IL-12 secretion, while strains 630 and M68 showed median induction of ~140 pg/ml. CF5-induced IL-12 was similar to that observed with R20291 (~400 pg/ml) showing significant IL-12 increase compared to uninfected cells, however, no significant inter-strain difference was observed (Figure 6.6 a). Although, strains 630, M68 and CF5 showed similar trend of IL-12 secretion with that observed in BMDC data, R20291 caused significantly high levels of IL-12 in human DCs compared to murine DCs.

Infected cells were also examined for induction of anti-inflammatory IL-10 (Figure 6.6 b). IL-10 expression was increased in response to infection with R20291 reaching to median 500 pg/ml. Similar IL-10 induction was detected in DCs infected with 630, M68 and CF5. All strains were statistically significant compared to uninfected control cells and no inter-strain difference was detected (Figure 6.6 b). Comparatively, strain CF5 caused significantly higher secretion of IL-10 in BMDC compared to the other strains ($p<0.001$) while human DCs showed similar IL-10 response to all four strains.

Furthermore, *C.difficile*-induced IL-1β was measured in infected cells (Figure 6.6 c). Minimum level of IL-1β detected in uninfected control cells was 18 pg/ml. IL-1β induction was increased significantly in response to R20291 infection (750 pg/ml) while cells infected with 630 and M68 showed similar level of IL-1β secretion (380 pg/ml). In comparison, strain CF5 caused the least expression of IL-1β (150 pg/ml) (Figure 6.6 c). Although no significant inter-strain difference in IL-1β response was observed in human DCs, CF5 showed the least secretion, the same results were also detected in BMDC showing CF5 caused significantly less IL-1β compared to other strains ($p<0.001$).

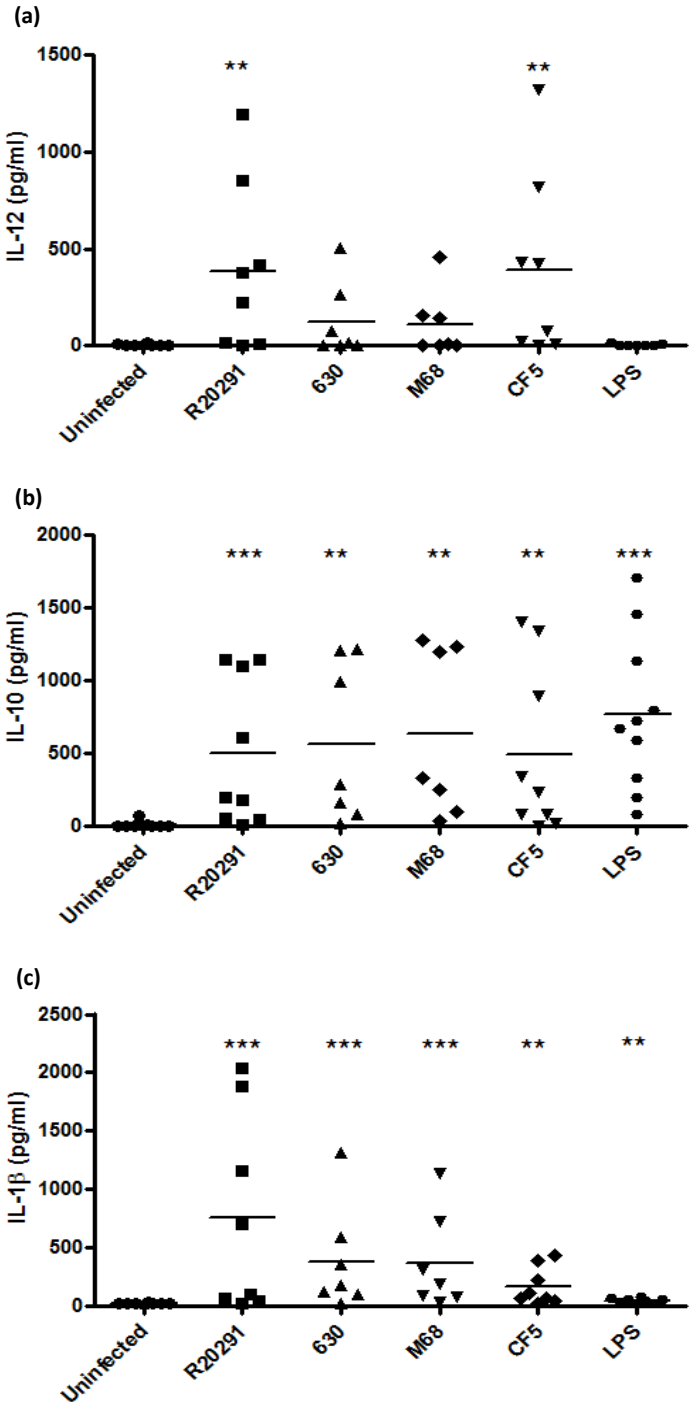

Figure 6.6. Effect of *C. difficile* strains on IL-12, IL-10, and IL-1β production by human DC. Human DCs obtained from nine healthy donors were stimulated with *C. difficile* bacterial cultures at an MOI of 10. IL-12 (a), IL-10 (b) and IL-1β (c) induction was measured by ELISA at 8 h post-infection. 1 µg/µl LPS was utilised as a reference stimulus. $^{**}p<0.01$ and $^{***}p<0.001$ represent significant difference from uninfected control cells. Data was analysed using Mann-Whitney U test.

6.5 Role of *C. difficile*-stimulated Dendritic Cells on T Cell Activation

The generation of adaptive immunity begins with DCs capturing microbial antigens in the peripheral tissues. Subsequently, DCs migrate to the draining lymph nodes to present the processed peptides to naive T lymphocytes in the context of MHC molecules. In transit, DCs also undergo a maturation program that enables the cells to stimulate naive T cells. Once inside the lymph nodes, DCs migrate to the T cell areas, seek out antigen-specific T cells and induce their activation and differentiation into effector cells. Depending on the density of the presented peptides, types of expressed co-stimulatory molecules, and secreted cytokines by the DCs, naive $CD4^+$ T cells differentiate into either Th1 or Th2 cells (Iwasaki & Medzhitov, 2004). Th1 cells can release the signature cytokine IFN-γ and activate macrophages, whereas Th2 cells produce IL-4 and drive the immunoglobulin isotype switching of B cells to IgG1 and IgE (Rescigno, 2002; Reiner, 2007).

One of the most critical cytokines produced by DCs for the induction and growth factor of polarised Th1 responses is IL-12 insofar as it represses expression of the transcription factor GATA-3, a key regulator of Th2 commitment. IL-23, another IL-12 family member, which shares use of the p40 subunit of IL-12, drive T cells to express the signature cytokines of the IL-17 family members, resulted in the term Th17 cells, but it is now known that they also secrete IL-22 (Reiner, 2007). IL-27 is homologous to IL-12 and has a role in the development of Th1-cell responses; however, the evidence from *in vivo* models of parasitic infection has revealed the anti-inflammatory properties of IL-27 (Hunter, 2005).

To date, limited numbers of studies have investigated T cell activation and differentiation in response to *C. difficile*-matured DCs and their cytokine production profile, which are the determinants of the balance between Th1/Th2 responses, by utilising primarily *C. difficile* SLPs (Ausiello *et al.,* 2006) or direct interaction of *C. difficile* toxins with T cells (Daubener *et al.,* 1988; Mahida *et al.,* 1998; Solomon *et al.,* 2005; Wanahita *et al.,* 2006). Thus, the aim of this study was to investigate the cross-talk of whole bacterial cell activated DCs with T cells.

6.5.1 T cell Proliferation in Response to *C. difficile*-stimulated Dendritic Cells

To investigate the proliferative response of T cells to *C. difficile*-stimulated DCs from WT mice, BMDCs were infected with PFA fixed *C. difficile* strains at an MOI of 50. At 24 h post-infection *C. difficile*-stimulated DCs were co-cultured with CFSE-labelled splenocytes of WT mice in the presence of anti-CD3/CD28. Co-cultures were analysed after 72-96 h post-infection by flow cytometry gated on $CD4^+$ cells (Figure 6.7 a), then quantified and presented as percentage of divided and undivided cells (Figure 6.7 b).

CFSE-labelled splenocytes in the absence of DCs (media only), showed no cell division. Co-cultured splenocytes with DCs in the presence of anti-CD3/CD28 initiated a cell proliferation (Figure 6.7 a). No more than 1.5% of cells were proliferated in the absence of DCs (media only). Cell division increased to 60% in the presence of uninfected DCs. *C. difficile*-stimulated DCs caused 74% cell proliferation; however, cell division resulted by uninfected DCs was not statistically different from proliferated cells caused by infected DCs; moreover, there was no significant inter-strain difference (Figure 6.7 b).

Same experiments were performed stimulating BMDCs from WT mice with PFA fixed *C. difficile* strains at an MOI of 50. At 24 h post-infection CFSE-labelled naive $CD4^+$ T cells from OT-II transgenic mice were co-cultured with *C. difficile*-stimulated DCs in the presence of $OVA_{323-339}$. Co-cultures were analysed by flow cytometry after 72-96 h (Figure 6.8 a), then results were quantified and presented as percentage of proliferated and un-proliferated cells (Figure 6.8 b).

No cell division was observed in CFSE-labelled naive $CD4^+$ T cells in the absence of DCs (media only), however, $CD4^+$ T cells co-cultured with BMDCs initiated a cell division (Figure 6.8 a). $CD4^+$ T cells in the absence of DCs showed <1% cell division, this percentage was enhanced to 68% in the presence of uninfected DCs. $CD4^+$ T cells co-cultured with R20291, 630, and M68 stimulated DCs proliferated >80%, which was statistically significant compared to uninfected DCs ($p<0.01$). On the other hand, CF5 infected DCs caused 72% division that was not significantly different from uninfected DCs (Figure 6.8 b).

Taken all together, this data suggested that *C. difficile*-stimulated DCs were able to induce T cell proliferation.

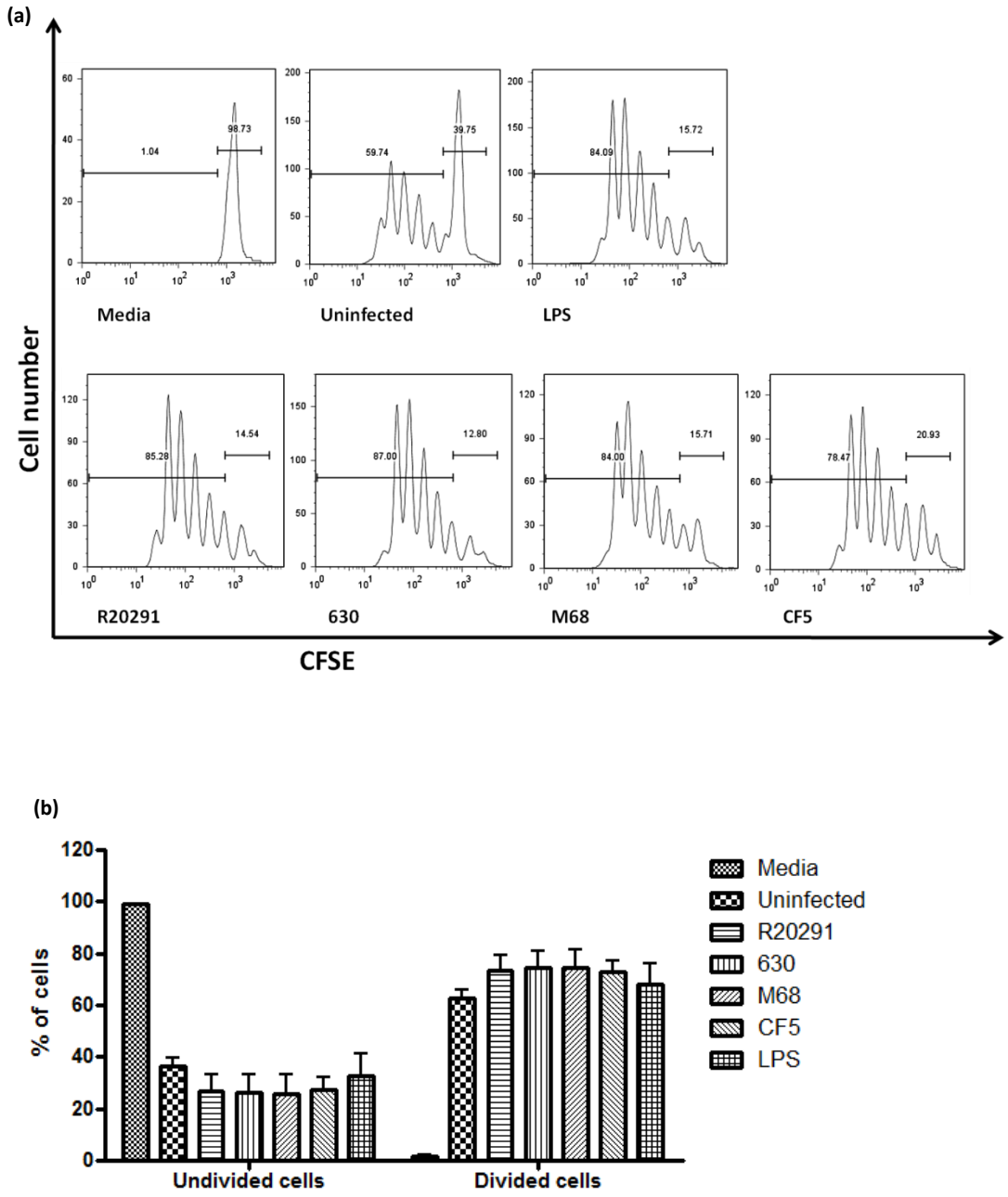

Figure 6.7. *In vitro* proliferation of splenocytes in response to *C. difficile*-stimulated BMDCs. BMDCs from WT mice were infected with PFA fixed *C. difficile* strains at an MOI of 50. At 24 h post-infection *C. difficile*-stimulated DCs were co-cultured with CFSE-labelled splenocytes of WT mice in the presence of anti-CD3/CD28. 1 µg/µl LPS was utilised as a reference stimulus. Co-cultures were analysed after 72-96 h post-infection by flow cytometry gated on $CD4^+$ cells, then quantified and presented as percentage of divided and undivided cells. Data was analysed using ANOVA with Bonferroni post-test.

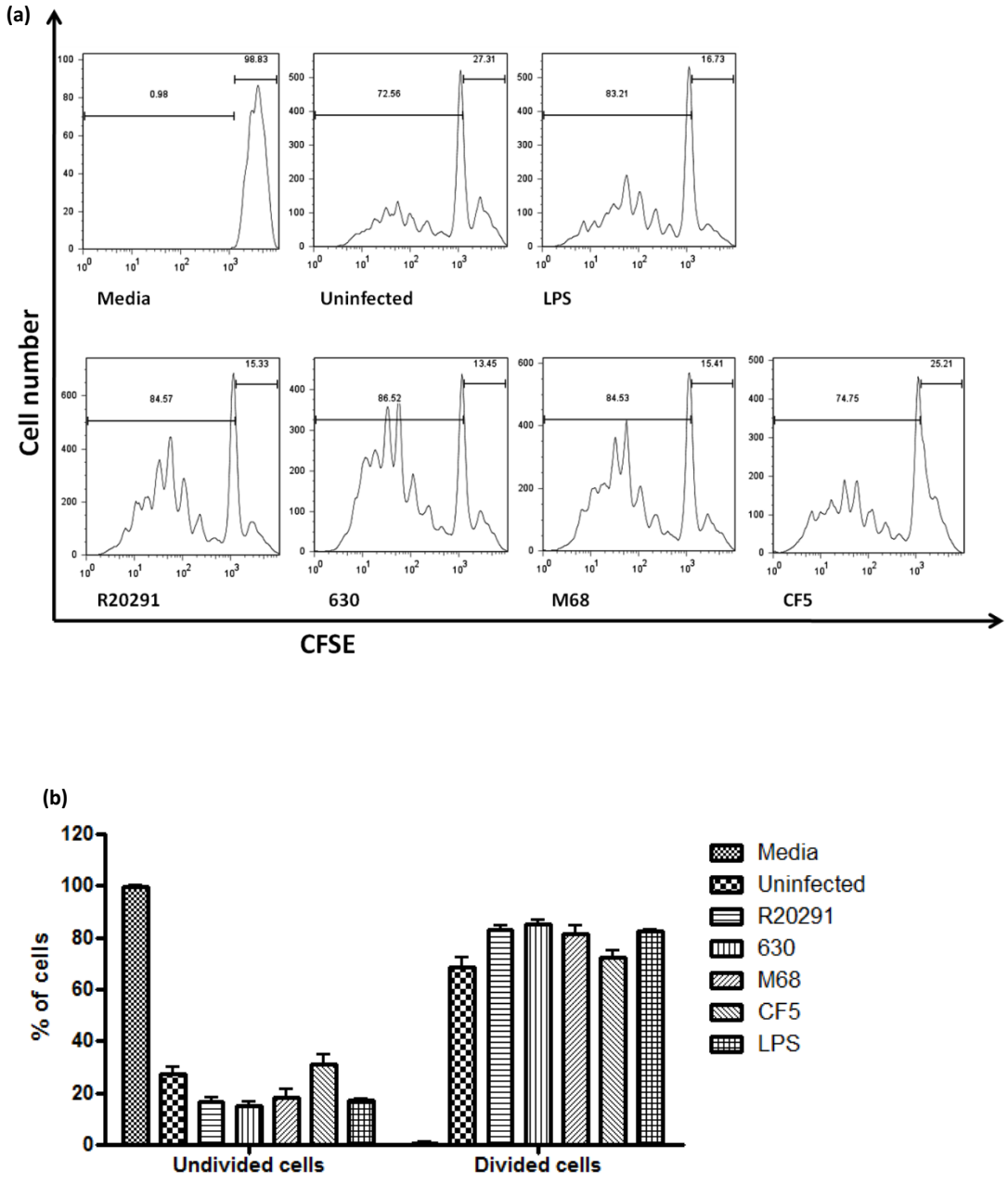

Figure 6.8. Naive CD4$^+$ T cell proliferation in response to *C. difficile*-stimulated BMDCs. BMDCs from WT mice were infected with PFA fixed *C. difficile* strains at an MOI of 50. At 24 h post-infection CFSE-labelled naive CD4$^+$ T cells from OT-II transgenic mice were co-cultured with *C. difficile*-stimulated DCs in the presence of $OVA_{323-339}$. 1 µg/µl LPS was utilised as a reference stimulus. Co-cultures were analysed by flow cytometry after 72-96 h. Results were quantified and presented as percentage of proliferated and un-proliferated cells. Data was analysed using ANOVA with Bonferroni post-test.

6.5.2 Naive CD4+ T Cell Cytokine Response(s) to *C. difficile*-stimulated BMDC

To investigate the ability of *C. difficile*-stimulated BMDCs to induce a T cell response, naive OT-II $CD4^+$ T cells were co-cultured with bacterial-stimulated BMDCs in the presence of $OVA_{323-339}$ for 96 h. Cells were stained for cell surface expression of CD4 and intracellular expression of IFN-γ and IL-17. Stained cells were analysed by flow cytometry gated on $CD4^+$ cells (Figure 6.9 a). Results were quantified and presented as percentage of cells that released intracellular IFN-γ and IL-17 (Figure 6.9 b & c).

Cells gated on $CD4^+$ cells were displayed in IFN-γ and IL-17 axis. In each graph $CD4^+$ cells were shown on the bottom left panel, and IFN-γ^+ cells on the top left panel. Cells that were positive for IL-17 were shown on the bottom right panel, while cells positive for both IFN-γ and IL-17 showed on top right panel (Figure 6.9 a). Figures 5.9 b and c shows percentage of IFN-γ^+ and IL-17^+ cells.

Less than 3% of T cells co-cultured with uninfected DCs expressed IFN-γ. Upon co-culturing with R20291-stimulated BMDCs, IFN-γ induction was increased to 13%. Strain 630 caused 5% secretion, while 10% IFN-γ release was detected in T cells co-cultured with M68 and CF5-stimulated DCs (Figure 6.9 b).

Approximately 0.5% of T cells expressed IL-17 in response to co-culture with uninfected DCs. R20291 and 630 caused <1.5% of cells to induce IL-17, while M68 showed 1.7% of T cells to secrete IL-17, which was significantly higher than that observed with CF5 (1%) (Figure 6.9 c).

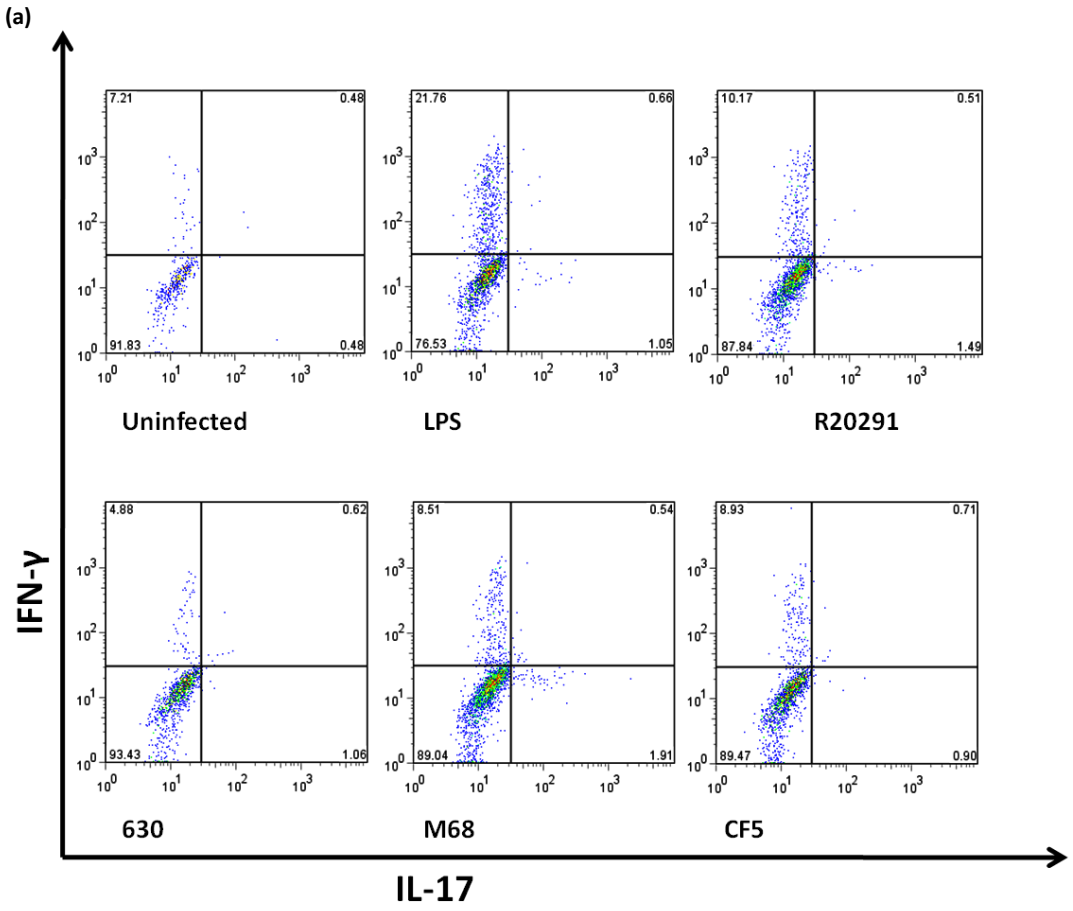
(a)
7.21
0.48
91.83
0.48
Uninfected
21.76
0.66
76.53
1.05
LPS
10.17
0.51
87.84
1.49
R20291
4.88
0.62
93.43
1.06
630
8.51
0.54
89.04
1.91
M68
8.93
0.71
89.47
0.90
CF5
IFN-γ
IL-17

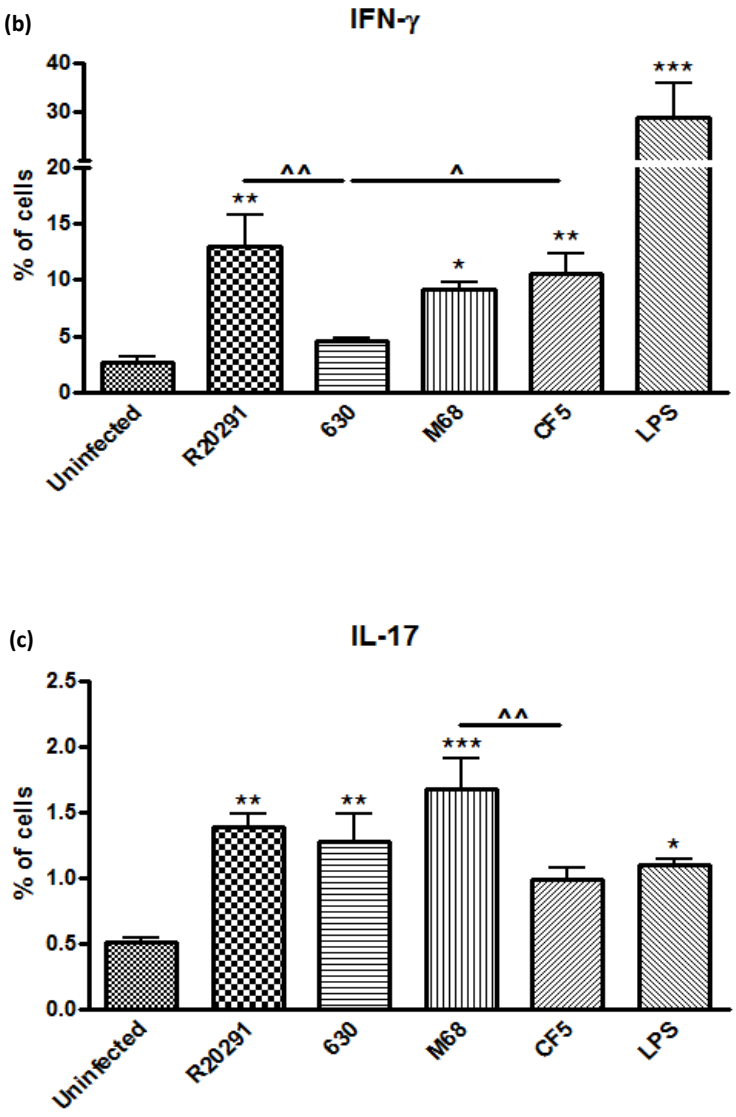

Figure 6.9. Intracellular IFN-γ and IL-17 staining in CD4$^+$ naive T cells stimulated with *C. difficile* infected BMDC. Naive OT-II CD4$^+$ T cells were co-cultured with *C. difficile*-stimulated BMDCs in the presence of $OVA_{323-339}$ for 96 h. Cells were stained for cell surface expression of CD4 and intracellular expression of IFN-γ and IL-17, then analysed by flow cytometry gated on CD4$^+$ cells and displayed in IFN-γ and IL-17 axis. In each graph CD4$^+$ cells were shown on the bottom left panel, and IFN-γ$^+$ cells on the top left panel. Cells that were positive for IL-17 were shown on the bottom right panel, and cells positive for both IFN-γ and IL-17 showed on top right panel (a). 1 µg/µl LPS was utilised as a reference stimulus. Quantified results were presented as percentage of IFN-γ$^+$ (b) and IL-17$^+$ (c) cells. Data represent mean ± SEM, n=3. $^{*/\wedge}p<0.5$, $^{**/\wedge\wedge}p<0.01$ and $^{***/\wedge\wedge\wedge}p<0.001$ represent significant difference from uninfected controls and significant inter-strain difference. *P* values were obtained using ANOVA with Bonferroni post-test analysis.

6.5.3 Splenocytes Cytokine Response(s) to *C. difficile*-stimulated BMDC

To investigate the cytokine production, splenocytes from WT mice were co-cultured with WT BMDCs (stimulated with PFA fixed *C. difficile* strains for 24 h) in the presence of anti-CD3/CD28. At 96 h post-co-culture, supernatants were collected to detect IFN-γ, IL10, IL-17A, IL-2, and IL-4 levels (Figure 6.10 a-e).

Uninfected DCs showed 60 pg/ml IFN-γ secretion. Levels increased to 1000 pg/ml in response to R20291-stimulated BMDCs, which was significantly higher than that observed with strain 630 (400 pg/ml). Strain M68 showed >700 pg/ml IFN-γ release, while CF5 induced 1000 pg/ml IFN-γ secretion (Figure 6.10 a).

Approximately 200 pg/ml of IL-10 was detected in uninfected cells. Upon co-culture with R20291-stimulated BMDCs IL-10 secretion was increased to 2000 pg/ml. Strains 630, M68, and CF5 induced similar levels. No significant inter-strain difference in IL-10 induction was observed (Figure 6.10 b).

IL-17A was detectable (145 pg/ml) in uninfected cells. The induction was increased to ~1800 pg/ml in response to R20291 and 630-stimulated BMDCs. M68 showed 1500 pg/ml IL-17A release, whilst CF5 caused 520 pg/ml. It was detected that CF5-induced IL-17A was significantly less than strains R20291 and 630 (Figure 6.10 c).

Detected IL-2 in uninfected cells was <40 pg/ml. Strains R20291 and M68 caused ~100 pg/ml IL-2 secretion. Strain 630 showed a significant IL-2 induction compared to R20291 and M68. Further, IL-2 secretion was significantly increased in response to CF5 when compared with the other strains (1000 pg/ml) (Figure 6.10 d).

Splenocytes co-cultured with uninfected cells showed <20 pg/ml IL-4. Similar levels of IL-4 secretion was detected in response to R20291, 630, and M68 ranging between 35-70 pg/ml. Strain CF5 caused the highest IL-4 release (~100 pg/ml), which was statistically significant compared to the other strains (Figure 6.10 e).

This data suggested that *C. difficile* can stimulate BMDCs to mount a strong IFN-γ, IL-10 and IL-17 cytokine responses in murine splenocytes. Interestingly, strain CF5 showed greater propensity for IL-2 and IL-4 production compared to other strains, adding weight to the suggestion that crosstalk between *C. difficile* and the host immune outcome is finely tuned at the molecular level.

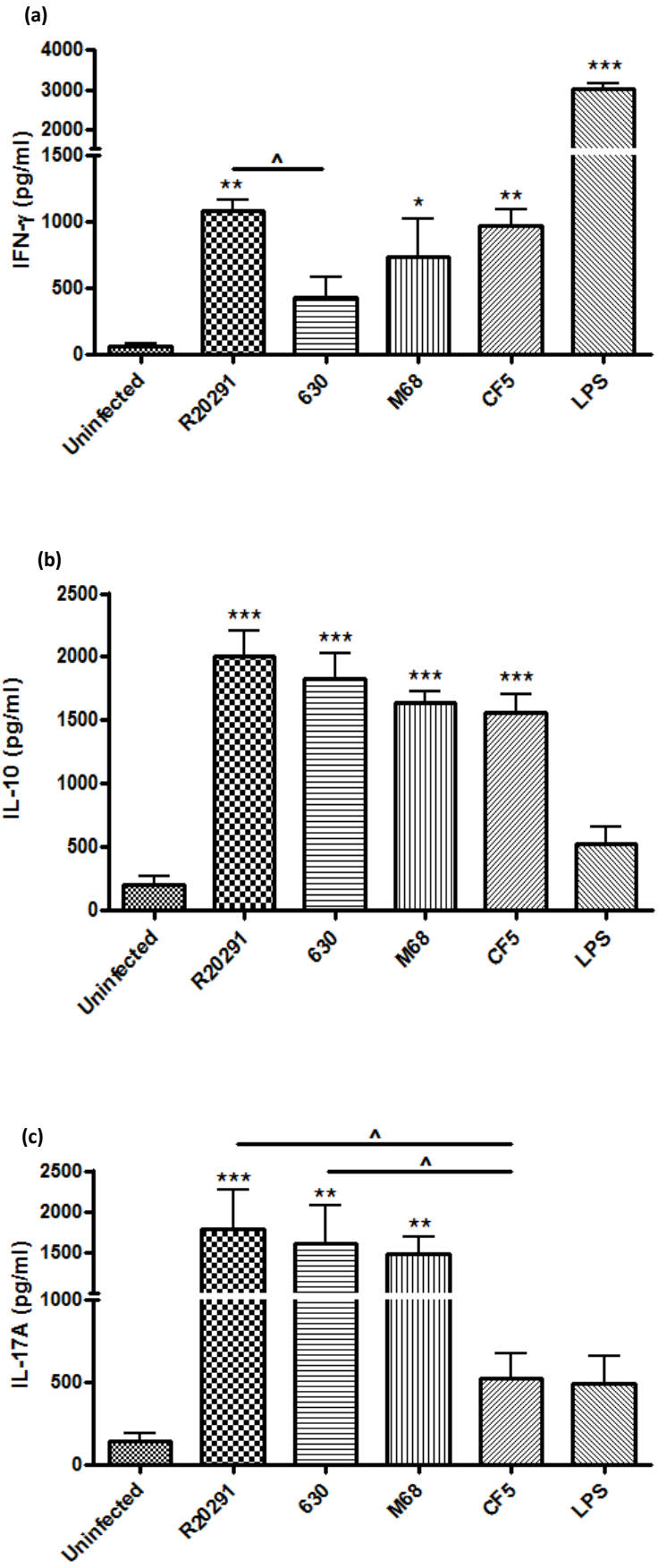
(a)
IFN-γ (pg/ml)
4000
3000
2000
1500
1000
500
0
**
^
*
**
***
Uninfected
R20291
630
M68
CF5
LPS
(b)
IL-10 (pg/ml)
2500
2000
1500
1000
500
0
***
***
***
***
Uninfected
R20291
630
M68
CF5
LPS
(c)
IL-17A (pg/ml)
2500
2000
1500
1000
500
0
^
^
***
**
**
Uninfected
R20291
630
M68
CF5
LPS

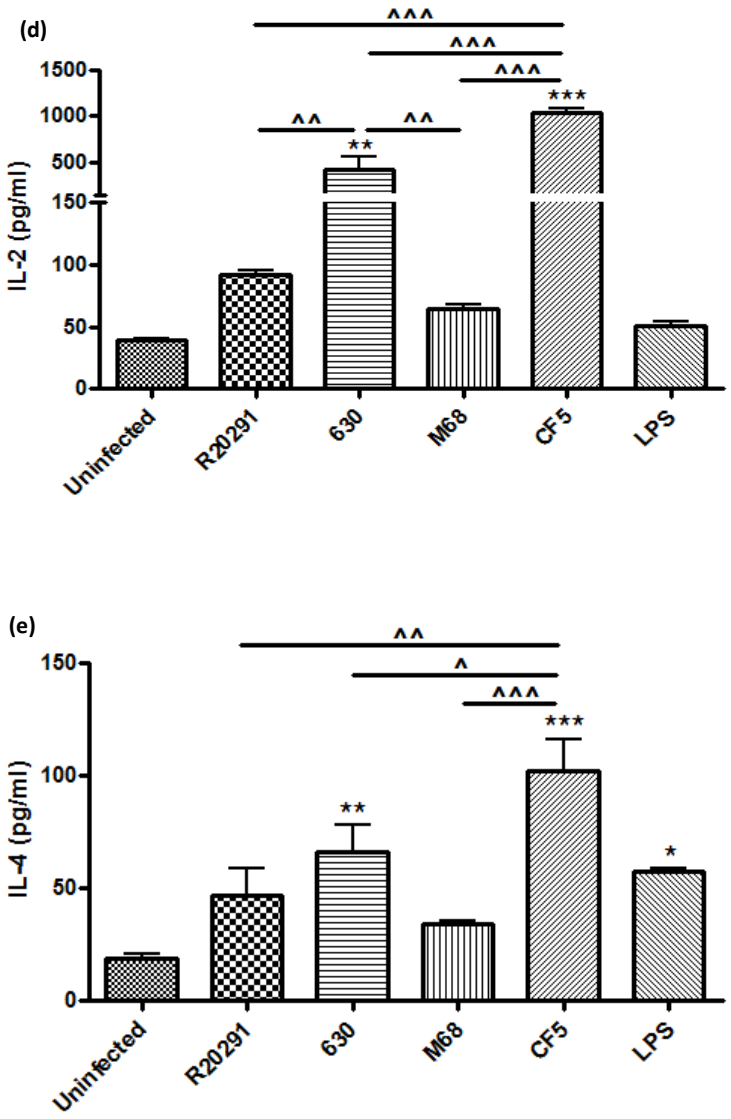

Figure 6.10. Cytokine response of splenocytes stimulated with *C. difficile* infected BMDC. BMDCs from WT mice were infected with PFA fixed *C. difficile* strains at an MOI of 50. At 24 post-infection, stimulated DCs were co-cultured with splenocytes from WT mice in the presence of anti-CD3/CD28. Supernatants were collected after 96 h co-culture and measured by ELISA for IFN-γ (a), IL-10 (b), IL-17A (c), IL-2 (d), and IL-4 (e) induction. 1 µg/µl LPS was utilised as a reference stimulus. Data represent mean ± SEM, n=3. $^{*/\wedge}p<0.05$, $^{**/\wedge\wedge}p<0.01$ and $^{***/\wedge\wedge\wedge}p<0.001$ represent significant difference from uninfected cells and significant inter-strain difference. *P* values were obtained using ANOVA with Bonferroni post-test analysis.

6.6 Conclusions

Dendritic cells are hematopoietic cells that belong to the APC family, which have a central role in both the priming of adaptive immune responses and the induction of self-tolerance. The mechanisms that are used by DCs to translate their environment so that facilitate lymphocytes activation, are represented in the concept of DC maturation. DC exists in two functional states, immature and mature, with only a mature DC having the ability to prime an immune response (Reis e Sousa, 2006). DCs can take up an array of antigens, process and present them in the form of peptides bound to both MHC class I and class II molecules. DCs undergo a process of maturation and migrate to secondary lymphoid organs where they stimulate naive T cells (Rescigno, 2002). Depending on the conditions, DCs can stimulate the outgrowth and activation of a variety of T cells, which affect the immune response differently. DCs are able to influence $CD4^+$ naive T cells to differentiate into IFN-γ-producing Th1 cells, or into IL-4-expressing Th2 cells (Banchereau & Steinman, 1998).

In this study, *C. difficile*-mediated DC activation was established in murine model system. The maturation of murine BMDCs in response to infection with *C. difficile* was examined. Also the gene expression of IL-12 family subunits, IL-10, IL-6, and IL-1β was determined in a time-dependent-manner. The role of *C. difficile* strains in cytokine protein induction was examined in murine and human DCs. *C. difficile*-mediated activation of the inflammasome was determined by detecting active caspase-1 and mature IL-1β in infected BMDCs from WT, $Nod2^{-/-}$, $Ipaf^{-/-}$, $ASC^{-/-}$, and $Nlrp3^{-/-}$ mice. IL-1β protein secretion was further investigated in response to *C. difficile* and ribotype 017 strains. Finally, T cell activation and proliferation was examined in response to stimulated murine BMDCs with PFA fixed *C. difficile* strains.

It was observed that stimulation of BMDCs with *C. difficile* strains caused differential up-regulation of the co-stimulatory molecules CD80, CD86 and cell surface markers MHCII and CD40. Compared to uninfected cells, strains R20291, 630, and M68 caused statistically significant up-regulation of co-stimulatory molecules CD80 and CD86. In contrast, CF5 showed the highest CD40 fold increase. Lee *et al.* (2009) have shown that the expression of cell surface molecules CD80, CD86, MHCII, and CD40 on immature murine DCs were increased after exposure to 100 ng/ml purified TcdA and postulated that *C. difficile* TcdA can promote the maturation of DCs. However, in the current study strain M68 caused comparatively same levels of cell surface markers up-regulation to that observed with R20291 and 630. Furthermore, CF5 showed similar potential to R20291 and M68 in modulation of MHCII and CD40. Moreover, it has been shown that SLPs (35 μg/ml) from *C.*

difficile are able to induce maturation of human DCs by up-regulation of MHCII, CD83, and CD80 (Ausiello *et al.,* 2006) therefore, it can be hypothesised that multiple factors are at play in *C. difficile*-mediated DC maturation.

DCs produce various cytokines and chemokines upon interaction with bacteria. Cells infected with *C. difficile* strains showed maximal gene expression of IL-12p35, IL-12/IL-23p40, IL-23p19, IL-27p28 & EBI3, IL-6, and IL-1β between 4 and 6 h post-infection indicating early sensing of *C. difficile* by DCs. On the contrast, IL-10 mRNA expression showed a significant up-regulation only at 8 h post-infection. It was also noted that strains R20291 and CF5 caused a significant gene modulation compared to strains 630 and M68. In addition, CF5 showed the highest IL-10 and the least IL-1β gene expression at 8 h correspondent to that observed with their protein secretion suggesting that CF5 mediates more anti-inflammatory response than pro-inflammatory compared to other strains.

Gene expression analysis of the IL-12 cytokine family subunits revealed that *C. difficile* strains caused a significant IL-23p19 up-regulation compared to IL-12 and IL-27 subunits. Further on this note, it was detected that *C. difficile* infection caused a significant IL-23 cytokine induction compared to the other IL-12 family members in BMDCs, hence the increased gene expression of IL-23p19 might be accountable for the predominant IL-23 secretion leading to potent Th17 immunity.

It was also noted that strains R20291 and M68 caused comparable protein expression of IL-12 family, whilst CF5 showed the highest secretion; strain 630 was the least inducer of IL-12 family cytokines. Further, infected BMDCs released larger amount of IL-23 and IL-27 compared to IL-12 highlighting that *C. difficile* strains exhibit differential ability in modulating DC IL-12 family members which is likely to impact on downstream T cell immunity. The splenocytes co-cultured with stimulated BMDCs showed significant IFN-γ response compared to IL-4 induction, indicating that *C. difficile* promotes a shift in Th1/Th2 balance toward Th1-dominant immunity. Also significant IL-17A secretion indicated that *C. difficile* infection mediates strong Th17 immunity as well as Th1, although the magnitude of the responses maybe strain-specific.

Direct interaction between *C. difficile* toxins and T cells however has been controversial, while some studies argue that toxins only interact with monocytes and not with T cells (Daubener *et al.,* 1988; Wanahita *et al.,* 2006), there are investigations linking occurrence of T cell apoptosis following exposure to TcdA as a consequence of a direct interaction (Mahida *et al.,* 1998; Solomon *et al.,* 2005).

The current study showed that human and murine DCs released comparatively more IL-10 in response to *C. difficile* infection than IL-12. In contrary, Ausiello and co-workers (2006) showed that *C. difficile* SLP-treated human monocyte-derived DCs secreted greater amounts of IL-12p70 than IL-10 and induced a mixed Th1/Th2 orientation of immune response in naive CD4 T cells. Thus, one may suggest that *C. difficile* cellular components may contribute differentially to the pathogenicity of the bacteria by perturbing the fine balance of pro- and anti-inflammatory responses.

Ng *et al.* (2010) have previously highlighted the toxin-dependent release of IL-1β due to activation of the inflammasome in response to purified TcdA and TcdB. A study by Ausiello and colleagues has also suggested that *C. difficile* SLPs can cause IL-1β secretion from human DC. Taken together, one may speculate that several immunogenic structural determinants of *C. difficile* likely activate this pathway. Results gathered from human and murine DCs in this study clearly showed that strains R20291, 630, and M68 elicited a significant IL-1β release. In contrast, strain CF5 caused the least pro-inflammatory IL-1β response.

Further investigation revealed that *C. difficile* strains activated caspase-1 and triggered IL-1β release in infected DCs from WT mice as well as DCs deficient in Nod2, Ipaf, and Nlrp3. Hasegawa and co-workers have already shown that Nod1 deficient mice are more susceptible to *C. difficile* infection than Nod2 deficient mice. They suggested that Nod1 directly recognises *C. difficile* and induces the recruitment of neutrophils to the site of the infection in order to clear the bacteria consequently triggering pro-inflammatory responses and in particular IL-1β (Hasegawa *et al.,* 2011).

Although strain CF5 consistently caused minimal IL-1β responses, western blot results showed that this strain is as equipotent as other strains in activating caspase-1, thus it remains to be answered how CF5 elicits the least IL-β secretion. Further examination of five additional ribotype 017 strains also showed that these strains share the ability of being a weak inducer of IL-1β. However it is unknown how strain M68 exhibits a potent IL-1β response; furthermore it is not clear why Nod2, Ipaf and Nlrp3 deficiency enhanced potency of CF5 and 017 ribotype strains leading to increased levels of IL-1β secretion.

Inhibition of the inflammasome signals through genetic deletion of ASC markedly decreased active caspase-1 expression and mature IL-1β secretion in all four strains indicating that *C. difficile* infection leads to an ASC-dependent inflammasome activation. Although it has been reported that caspase-1 activation and IL-1β secretion in response to *C. difficile* toxins

from Nlrp3$^{-/-}$ macrophages show reduction by 50% compared to WT cells (Ng *et al.,* 2010) the current study showed no significant difference in caspase-1 activation or IL-β release from Nlrp3 deficient DCs compared to WT BMDCs.

Taken all together, *C. difficile* strains caused up-regulation of co-stimulatory molecules of BMDCs leading to a predominant IL-10 secretion compared to IL-12 family cytokines. It was also shown that *C. difficile* strains may promote more Th1/Th17 responses, despite a significant IL-10 secretion known to suppress IL-12 and IL-23 induction. Additionally, *C. difficile* strains activated the inflammasome in an ASC-dependent manner.

6.6.1 Summary

The work presented in this chapter showed that:

- *C. difficile* strains caused differential up-regulation of the co-stimulatory molecules CD80, CD86, MHCII and CD40.
- BMDCs infected with *C. difficile* strains showed maximal IL-12, IL-23 and IL-27 subunits, IL-6 and IL-1β gene expression between 4-6 h post-infection, while IL-10 mRNA expression was significantly up-regulated only at 8 h.
- Infected BMDCs released greater amount of IL-23 and IL-27 compared to IL-12.
- Strain CF5 showed the highest IL-10 and the least IL-1β gene and protein expression amongst the strains.
- *C. difficile* infected human DCs showed similar trend in IL-12, IL-10 and IL-1β secretion to that observed with BMDCs.
- Significant IFN-γ and IL-17A responses by stimulated splenocytes indicated that *C. difficile* infection mediates Th1/Th17 immunity.
- *C. difficile* strains triggered the inflammasome in an ASC-dependent manner leading to caspase-1 activation and IL-1β release.

Chapter 7

Clostridium difficile Toxin-dependent and Independent Effects on Dendritic Cell Function

7.1 Introduction

Dendritic cells play important roles in innate and adaptive immune responses (Steinman, 1991) by performing functions such as phagocytosis and antigen presentation. Furthermore, a subset of intestinal LP DCs has been identified, which are capable of taking up bacterial antigens by transepithelial dendrites. This DC subset, most likely activates innate immune pathway(s) involved in protecting the mucosa from luminal microorganisms (Niess *et al.,* 2005). Additionally, mucosal DCs have a unique ability to induce T cell differentiation in the gut (Bilsborough & Viney, 2004) thus regulating the degree of inflammation and preserving gut immune homeostasis (Rimoldi *et al.,* 2005; Ausiello *et al.,* 2006).

The interactions between *C. difficile* and DCs leading to toxin-induced inflammation have not yet been fully identified. Lee and co-workers demonstrated that the exposure of immature mouse BMDCs to *C. difficile* purified TcdA (100 ng/ml) results in rapid chronological activation of p38 MAPK, IKK and NF-κB pathways leading to DC maturation and up-regulation of neutrophil-attracting chemokine CXCL2 gene expression (Lee *et al.,* 2009).

As *C. difficile* toxin mutants have only recently become available, the aim of this study was to delineate the role of toxins in *C. difficile*-driven murine and human DCs innate immune responses and also examine the hypothesis that *C. difficile* toxins are the major drivers of inflammasome activation. In these series of experiments R20291 and 630 toxin mutant strains (kindly provided by Prof. Minton, University of Nottingham) were utilised comprising of R20291 *tcdA* (A^-B^+, CDT^+), R20291 *tcdB* (A^+B^-, CDT^+), R20291 *cdtA* and R20291 *cdtB* (A^+B^+ with mutation in one of the *cdtA*/*cdtB* binary toxin gene subunit) (unpublished data). Strain 630 isogenic mutants were constructed using 630 Δerm (erythromycin sensitive derivative of strain 630, Hussain *et al.,* 2005) as the parent strain by the ClosTron system targeting intron insertions to *tcdA* and *tcdB* at nucleotide positions 1584 and 1511, respectively (Kuehne *et al.,* 2010). Toxin mutant stains included 630 Δerm *tcdA* (A^-B^+), 630 Δerm *tcdB* (A^+B^-), and 630 Δerm *tcdA tcdB* (A^-B^-).

7.2 Cytotoxicity of *C. difficile* Toxin Mutants

Prior to co-culture studies, all toxin mutants were examined for their cytotoxicity potential by utilising HT-29 and Vero cell-lines as described previously (Chapter 3). HT-29 and Vero cells are susceptible to both TcdA and TcdB; however, HT-29 cells are known to be more sensitive to TcdA, while Vero cells are more sensitive to TcdB (Torres *et al.,* 1992).

The cytopathic effect (CPE) of TcdA on HT-29 cells was quantified by infecting semi-confluent HT-29 cells with 2-fold dilutions of filter-sterilised bacterial supernatants at starting MOI of 500 (Figure 7.1). Minimum cytotoxic activity was detected in uninfected control cells. Cells infected with R20291 *tcdA* and R20291 *tcdB* caused a modest cytotoxicity, showing significantly less cell toxicity when compared to the parental strain R20291. In contrast, R20291 *cdtA* exhibited the highest cell intoxication, while strain R20291 *cdtB* showed similar cell toxicity to the parental strain R20291; however, no significant difference in cytotoxicity was observed amongst strain R20291 and its binary toxin mutants (Figure 7.1 a).

Cells infected with strain 630 Δerm showed an increase in cytotoxicity compared to uninfected control cells, although this was not statistically significant (Figure 7.1 b). Strain 630 Δerm *tcdA* caused an enhanced level of cell intoxication, while 630 Δerm *tcdB* exhibited comparable cell toxicity to strain 630 Δerm. Cells infected with the A^-B^- double-toxin mutant (630 Δerm *tcdA tcdB*) caused minimum cytotoxicity. No significant inter-strain difference in cytotoxicity was observed amongst 630 isogenic mutants (Figure 7.1 b).

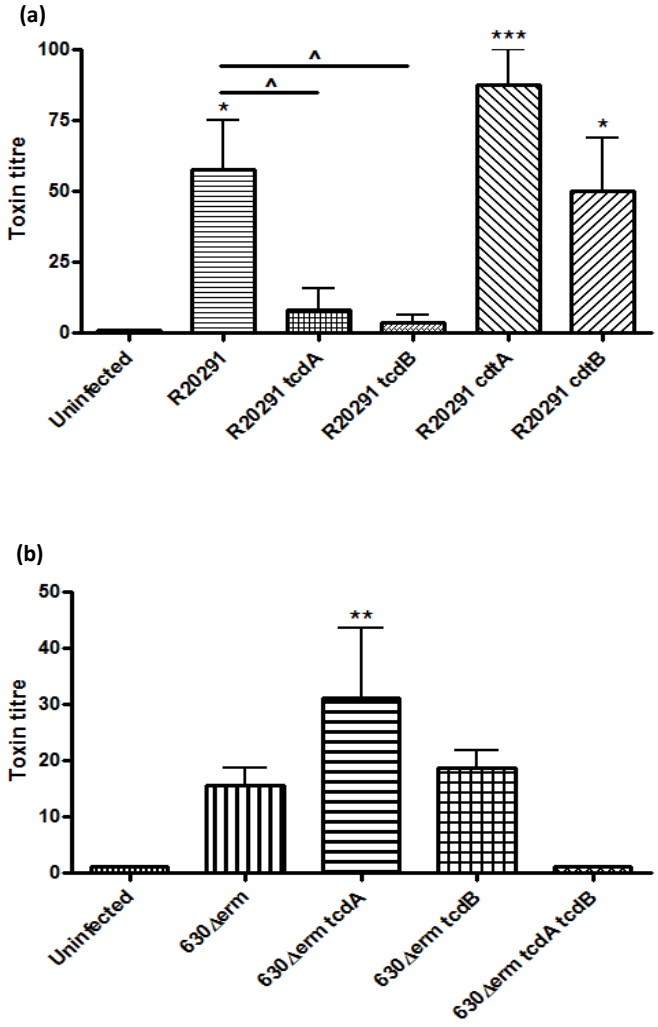

Figure 7.1. *C. difficile* secreted toxins exert varying cytotoxic potential on HT-29 cells. Semi-confluent HT-29 cells were co-cultured with 2-fold dilutions of filter-sterilised bacterial culture supernatants of R20291 (a) and 630 (b) toxin mutants. The end-point titre of each dilution series was scored at 8 h post-infection. Data presented as the mean ± SEM, n=3. $^{*}p<0.05$, $^{**}p<0.01$ and $^{***}p<0.001$ represent significant difference from uninfected control cells, and $^{\wedge}p<0.05$ represents significant difference from the parental strain. *P* values were obtained using ANOVA with Bonferroni post-test analysis.

Role of TcdB in cell intoxication was investigated by conducting similar co-culture experiments using Vero cells. Confluent monolayers were infected with 2-fold dilutions of filter-sterilised supernatants of stationary phase bacterial cultures at starting MOI of 500, CPE was scored at 8 h post-infection (Figure 7.2). Compared to the parental strain R20291, R20291 *tcdA* exhibited an enhanced level of cytotoxicity; however, this was not statistically significant. On the contrary, significantly less cell intoxication was observed with R20291 *tcdB* when compared to the parental strain. Elevated levels of cytotoxicity were also detected in cells infected with strains R20291 *cdtA*, and R20291 *cdtB*, which were not statistically different from the WT strain R20291 (Figure 7.2 a).

Cells infected with 630 Δerm showed significant cell intoxication compared to uninfected control cells. Similar cytotoxicity to the A^+B^+ parental strain was observed with A^-B^+ mutant strain (630 Δerm *tcdA*). The A^+B^- mutant strain (630 Δerm *tcdB*) showed statistically reduced cell toxicity compared to the parental strain. Also, compared to the 630 Δerm, a significantly less cytotoxicity was detected with the double-toxin mutant strain (630 Δerm *tcdA tcdB*) (Figure 7.2 b).

Taken all together, HT-29 cells showed no particular sensitivity to TcdA, and A^-B^+ strains showed similar cell toxicity to A^+B^- strains. On the other hand, TcdB sensitive Vero cells showed the least cytotoxicity when infected with A^+B^- strains. While R20291 binary toxin mutants caused significant cytotoxicity in both cell-lines, the least cell toxicity was detected with the double-toxin mutants.

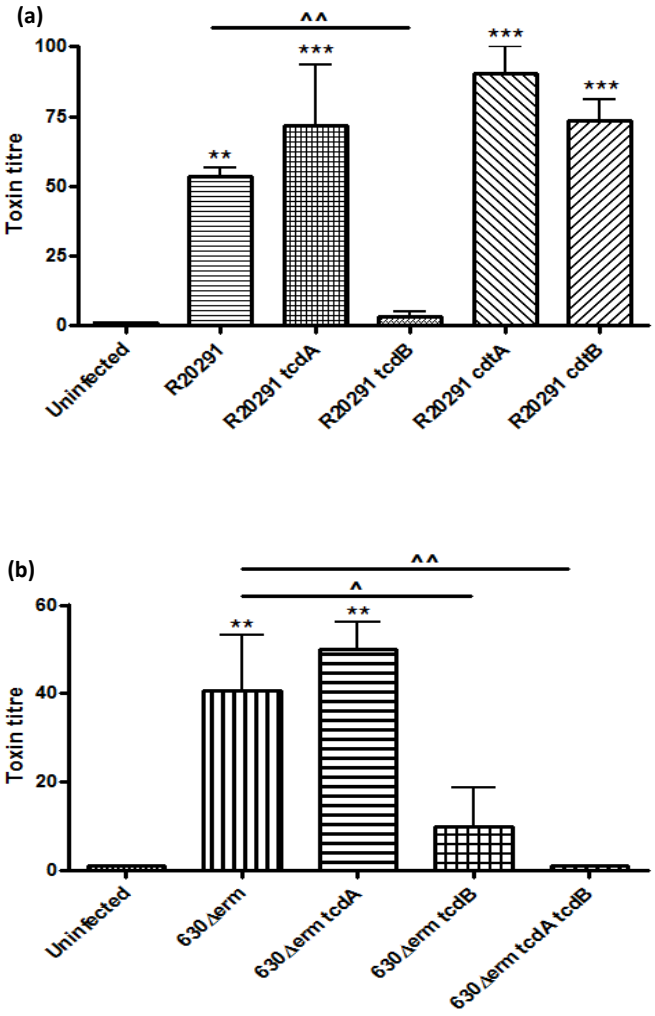

Figure 7.2. *C. difficile* secreted toxins exert varying cytotoxic potential on Vero cells. Vero cell monolayers were co-cultured with 2-fold dilutions of filter-sterilised bacterial culture supernatants of R20291 (a) and 630 (b) toxin mutants. The end-point titre of each dilution series was scored at 8 h post-infection. Data presented as the mean ± SEM, n=3. $^{**}p<0.01$ and $^{***}p<0.001$ represent significant difference from uninfected control cells, and $^{\wedge}p<0.05$ and $^{\wedge\wedge}p<0.01$ represent significant difference from the parental strain. *P* values were obtained using ANOVA with Bonferroni post-test analysis.

7.3 Adherence of *C. difficile* Toxin Mutants to Human Intestinal Epithelial Cells (IECs)

To investigate the contribution of toxins to the process of bacterial adherence to IEC, R20291 and 630 toxin mutants were labelled with FITC and analysed by flow cytometry (Figure 7.3 & 7.5). FITC-labelled bacteria were co-cultured with Caco-2 cells at an MOI of 250. Bacterial adherence was analysed by flow cytometry at 6 h post-infection (Figure 7.4 a & 7.6 a), and presented as change in MFI (Figure 7.4 b & 7.6 b).

Uninfected control cells showed a minimum MFI value (~5), which was similar to that observed with unlabelled bacterial infected cells (Figure 7.4 b). R20291 toxin mutants adhered to Caco-2 cells at the same level as the parental strain R20291 (MFI ~150), exhibiting no significant inter-strain difference (Figure 7.4 b).

Similar experiments were also conducted to investigate the adherence of strain 630 isogenic mutants to Caco-2 cells. Uninfected control cells showed a minimum MFI value (~5), similar to that observed with unlabelled bacterial infected Caco-2 cells (Figure 7.6 b). Toxin mutant strains showed similar adherence levels to the parental strain 630 Δerm and no significant difference was detected amongst the individual (A^-B^+, A^+B^-) and the double toxin (A^-B^-) mutant strains (MFI ~100-125) (Figure 7.6 b).

Collectively, this data suggested that bacterial adherence to Caco-2 cells was toxin independent.

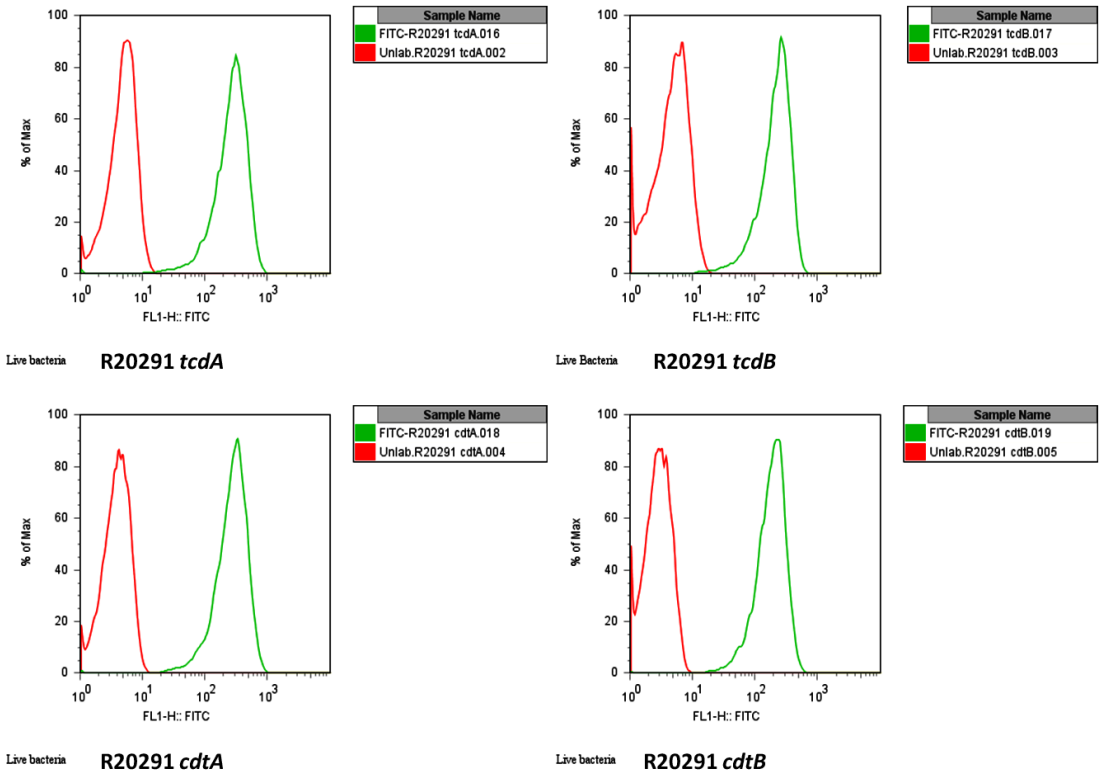

Figure 7.3. *C. difficile* R20291 toxin mutant strains show similar distribution of unlabelled and FITC-labelled bacteria. The FITC-labelling of the bacteria was seen as a shift of the bacteria along the FL1 axis in the histogram display mode, showing unlabelled (left peak) and FITC-labelled *C. difficile* (right peak). The fluorescence signal of the labelled population showed no overlap with unlabelled population indicating that the whole population was labelled. This data is the representative of three individual experiments.

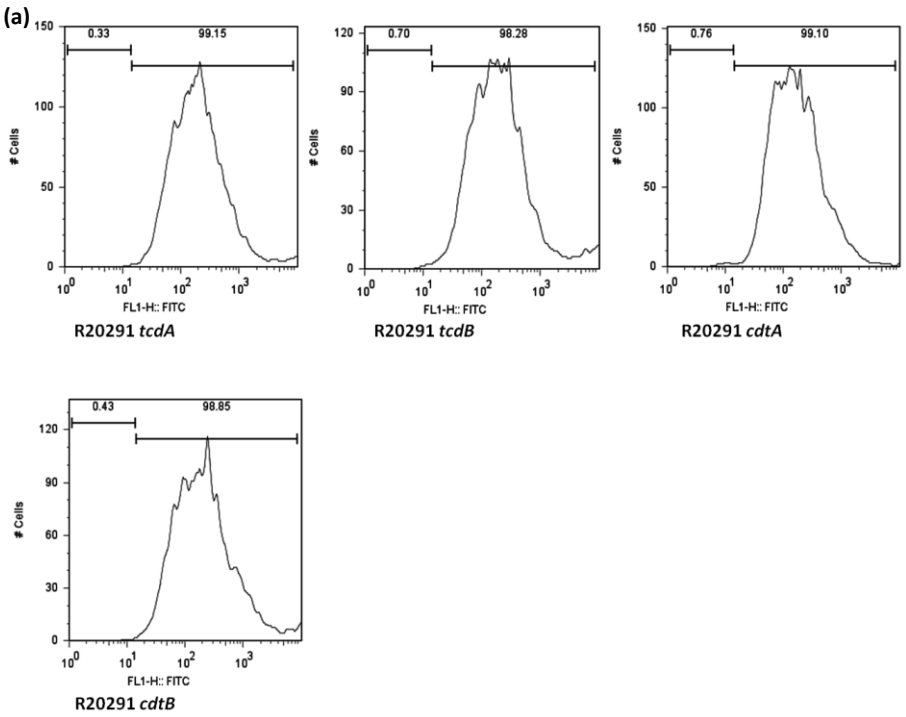

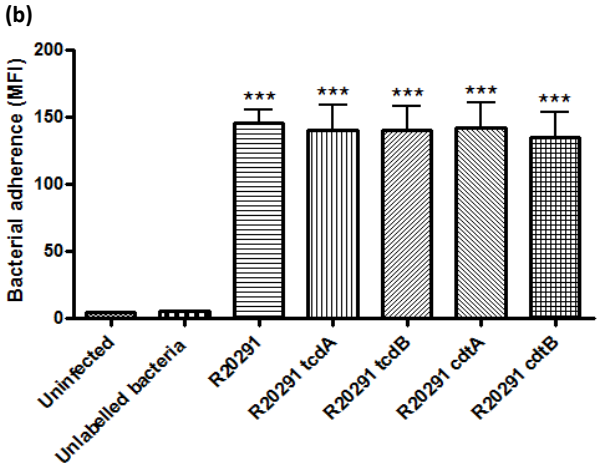

Figure 7.4. *C. difficile* toxins do not contribute to *C. difficile* adherence to Caco-2 cells. FITC-labelled bacteria were co-cultured with Caco-2 cells at an MOI of 250. Flow cytometric analysis of Caco-2 cells alone and after incubation with FITC-labelled *C. difficile* toxin mutant strains showed bacterial association as a shift of adhered bacteria to Caco-2 cells along the FL1 axis in the histogram display. Data is representative of three separate experiments (a). Results were quantified as change in MFI. Data represent mean ± SEM, n=3. $^{***}p<0.001$ (ANOVA with Bonferroni post-test) represents significant difference from uninfected cells (b).

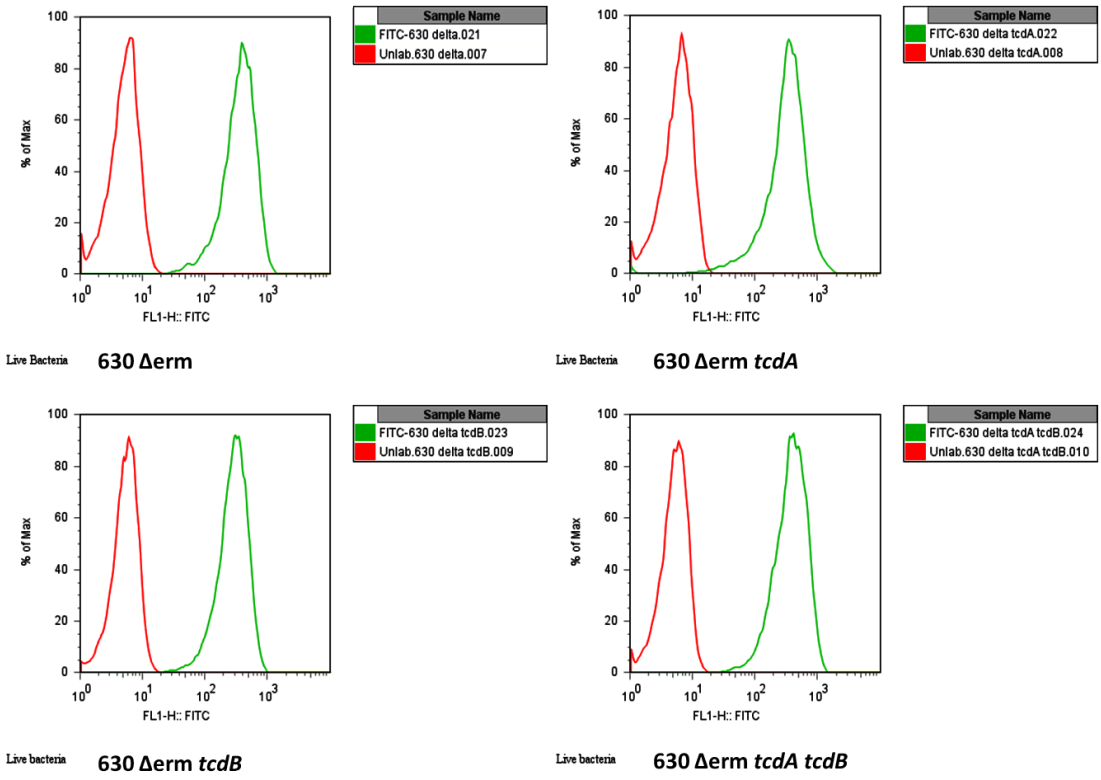

Figure 7.5. *C. difficile* 630 toxin mutant strains show similar distribution of unlabelled and FITC-labelled bacteria. The FITC-labelling of the bacteria was seen as a shift of the bacteria along the FL1 axis in the histogram display mode, showing unlabelled (left peak) and FITC-labelled *C. difficile* (right peak). The fluorescence signal of the labelled population showed no overlap with unlabelled population indicating that the whole population was labelled. This data is the representative of three individual experiments.

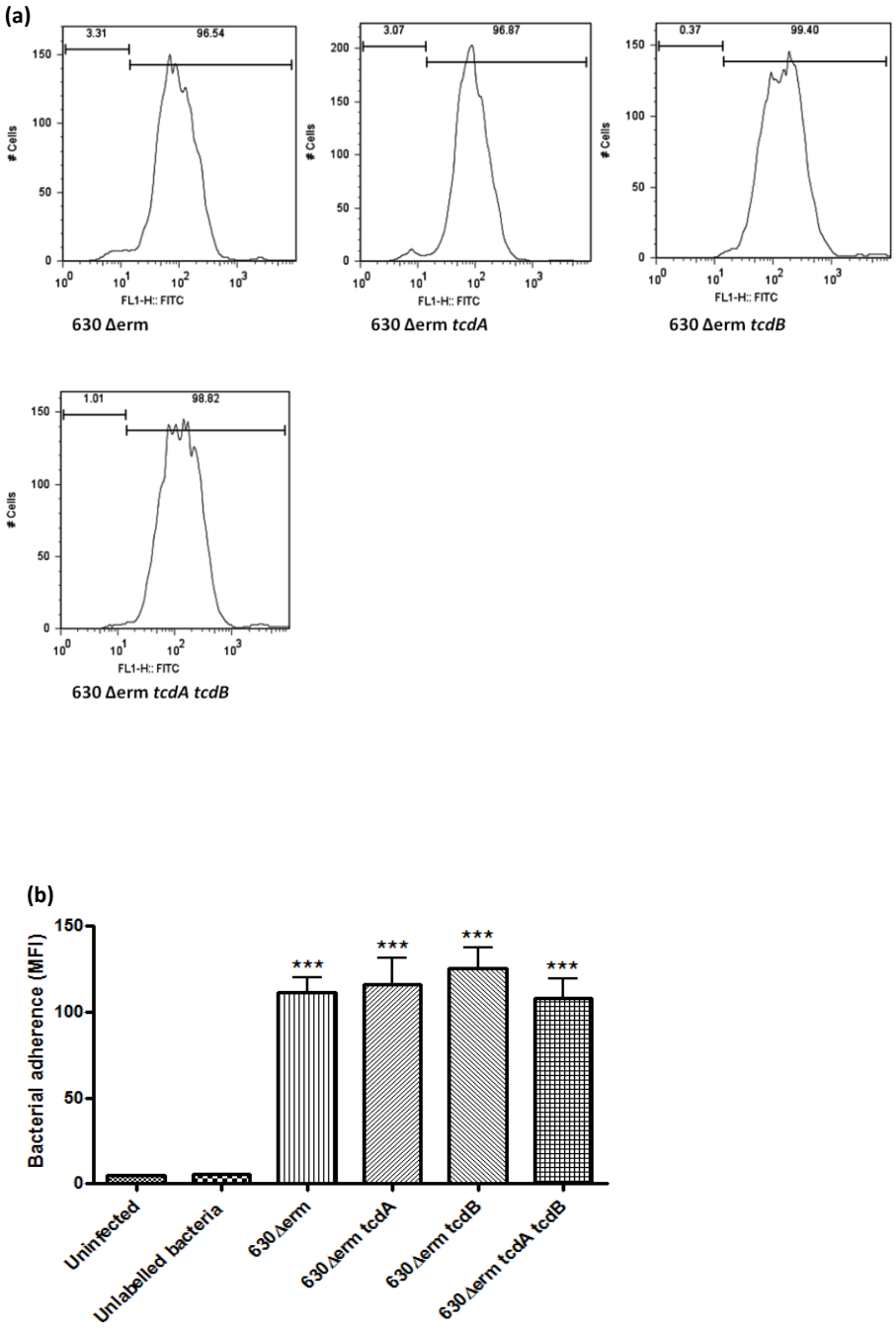

Figure 7.6. Strain 630 TcdA and TcdB do not affect bacterial adherence levels to Caco-2 cells. FITC-labelled bacteria were co-cultured with Caco-2 cells at an MOI of 250. Flow cytometric analysis of Caco-2 cells alone and after incubation with FITC-labelled *C. difficile* toxin mutants showed bacterial association as a shift of adhered bacteria to Caco-2 cells along the FL1 axis in the histogram display. Data is representative of three separate experiments (a). Data represent mean ± SEM, n=3. $^{***}p<0.001$ (ANOVA with Bonferroni post-test) represents significant difference from uninfected cells (b).

7.4 Regulation of BMDC Immune Response(s) by *C. difficile* Toxin Mutant Strains

To determine *C. difficile* toxin-mediated effects BMDCs were harvested from C57BL/6 mice and stimulated with bacterial cultures of R20291 WT and toxin mutants R20291 *tcdA* (A^-B^+), R20291 *tcdB* (A^+B^-), R20291 *cdtA* (A^+B^+, $CDTa^-$), R20291 *cdtB* (A^+B^+, $CDTb^-$), and isogenic mutants of 630 Δerm included 630 Δerm *tcdA* (A^-B^+), 630 Δerm *tcdB* (A^+B^-), 630 Δerm *tcdA tcdB* (A^-B^-). All co-culture studies were conducted at an MOI of 10.

7.4.1 Dendritic Cell Maturation in Response to Infection with *C. difficile* Toxin Mutant Strains

Dendritic cells are known to up-regulate co-stimulatory molecules upon contact with bacterial components. To investigate whether *C. difficile* toxins can influence DC maturation, the expression of co-stimulatory molecules CD80, CD86, as well as MHC class II and CD40 was investigated by flow cytometry (Figures 7.7-7.10).

Cells infected with R20291 showed 1.5-fold increase in CD80. R20291 toxin mutants caused similar levels of CD80 modulation (≥ 1.5-fold) (Figure 7.7 a). Strain 630 Δerm showed 1.5-fold change in CD80 and 630 Δerm *tcdA* caused <1.5-fold increase, while 630 Δerm *tcdB* up-regulated CD80 ~2-fold. The double toxin mutant 630 Δerm *tcdA tcdB* showed <1.5-fold CD80 modulation. Strain 630 Δerm toxin mutant strains were not significantly different from the parental strain; however, strain 630 Δerm *tcdB* showed a significant difference from 630 Δerm *tcdA* ($p<0.05$) and 630 Δerm *tcdA tcdB* ($p<0.01$) (Figure 7.7 b).

Strains R20291 and R20291 *tcdA* both caused ≥ 1.5-fold modulation in CD86. CD86 was up-regulated ≥ 2-fold with R20291 *tcdB* and the binary toxin mutants, which were statistically different from the parental strain (Figure 7.8 a). Strain 630 Δerm showed ~2-fold increase, while CD86 showed minimal impact in response to 630 Δerm *tcdA* (<1.5-fold). 630 Δerm *tcdB* showed similar level of CD86 up-regulation as the parental strain, whereas 630 Δerm *tcdA tcdB* exhibited >1-fold CD86 modulation. The TcdA and the double toxin mutant strains were significantly different from the parental strain, furthermore, 630 Δerm *tcdB* showed a higher CD86 fold increase when compared with 630 Δerm *tcdA* ($p<0.01$) and 630

Δerm *tcdA tcdB* ($p<0.001$), also 630 Δerm *tcdA* up-regulated CD86 significantly more than the double toxin mutant ($p<0.01$) (Figure 7.8 b).

MHCII, a mature DC marker increased <2-fold in response to WT R20291 and toxin mutants showed no significant difference compared to the parental strain (Figure 7.9 a). Strain 630 Δerm caused >1.5-fold MHCII modulation, which was not changed in response to TcdA toxin mutant strain. The TcdB toxin mutant showed <1.5 fold increase, whilst the double toxin mutant up-regulated the MHCII ~2-fold. Strain 630 Δerm toxin mutants were not significantly different from the parental strain and also no significant inter-strain difference was observed (Figure 7.9 b).

A 2-fold increase in CD40 was detected in response to R20291. A similar response was observed with R20291 toxin mutant strains, showing no significant difference from the parental strain and also no inter-strain difference was detected (Figure 7.10 a). Approximately 2-fold increase of CD40 was seen with strain 630 Δerm and >1.5-fold in response to 630 Δerm *tcdA*. CD40 expression was significantly less in response to TcdB mutant compared to the parental strain, whilst the double toxin mutant showed >1.5-fold CD40 up-regulation (Figure 7.10 b).

This data suggested that R20291 toxin mutants showed similar CD80, MHCII, and CD40 up-regulation, while 630 Δerm *tcdB* caused significant modulation of CD80 and CD86 compared to the TcdA and the double toxin mutants. On the other hand, the 630 Δerm toxin mutants showed similar up-regulation of MHCII and CD40.

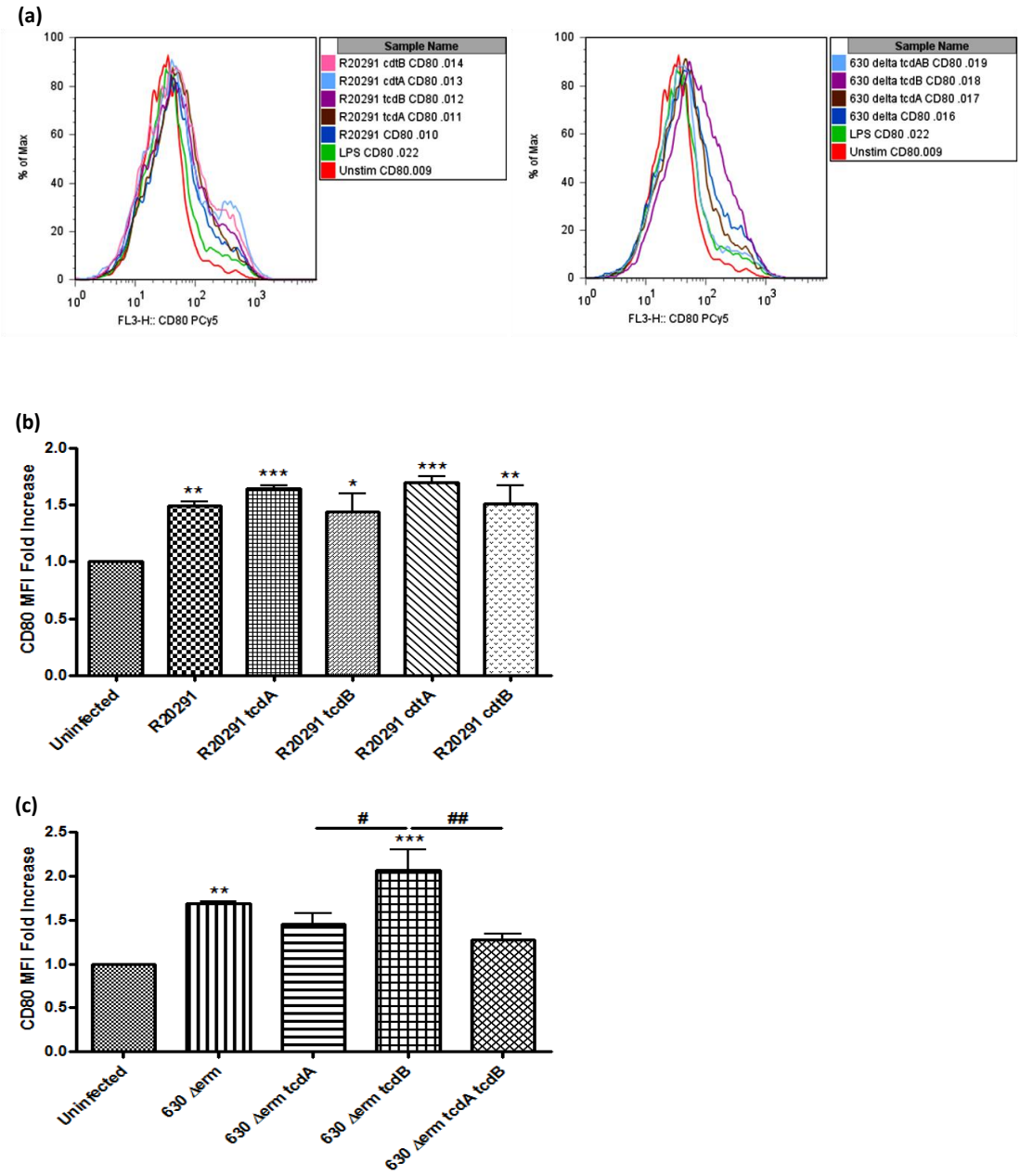

Figure 7.7. *C. difficile* up-regulates DC surface marker CD80. BMDCs were infected with R20291 and 630 Δerm isogenic mutants at an MOI of 10. After 8 h stimulation, cells were labelled with mouse CD80 antibody and analysed by flow cytometry (a). The level of surface expression was quantified and presented as MFI fold increase (b-c). Data represent mean ± SEM, n=3. $^{*}p<0.05$, $^{**}p<0.01$ and $^{***}p<0.001$ represent significant difference from uninfected cells and $^{\#}p<0.05$ and $^{\#\#}p<0.01$ represent significant inter-strain difference. *P* values were obtained using ANOVA with Bonferroni post-test analysis.

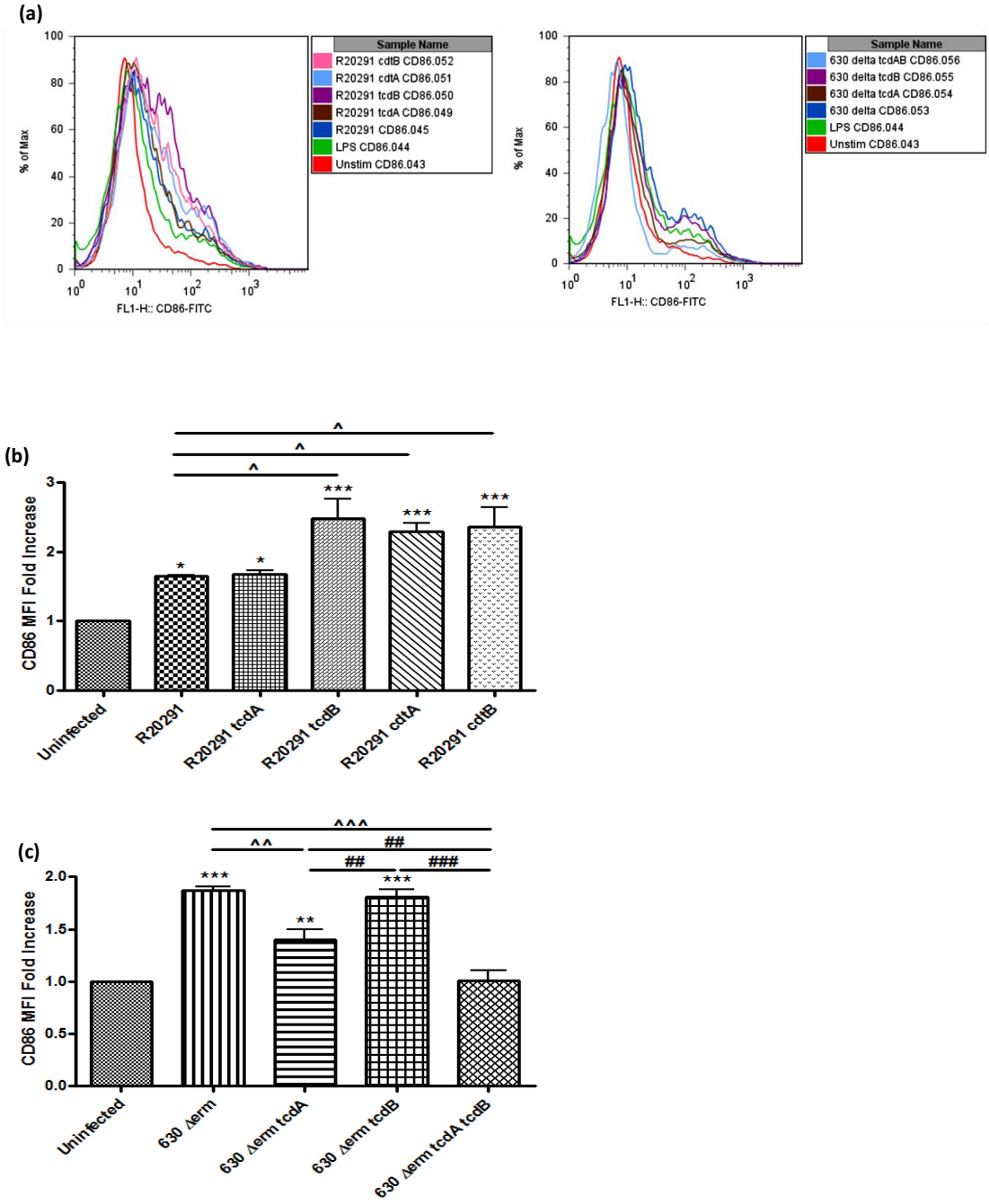

Figure 7.8. *C. difficile* induces maturation of DCs by modulating CD86. BMDCs were infected with toxin mutants of R20291 and 630 Δerm at an MOI of 10. At 8 h post-stimulation, cells were labelled with mouse CD86 antibody and analysed by flow cytometry (a). The level of surface expression was quantified and presented as MFI fold increase (b-c). Data represent mean ± SEM, n=3. $^{*}p<0.05$, $^{**}p<0.01$ and $^{***}p<0.001$ represent significant difference from uninfected cells, $^{\wedge}p<0.05$, $^{\wedge\wedge}p<0.01$ and $^{\wedge\wedge\wedge}p<0.001$ represent significant difference from the parental strain, and $^{\#\#}p<0.01$ and $^{\#\#\#}p<0.001$ represent significant inter-strain difference. *P* values were obtained using ANOVA with Bonferroni post-test analysis.

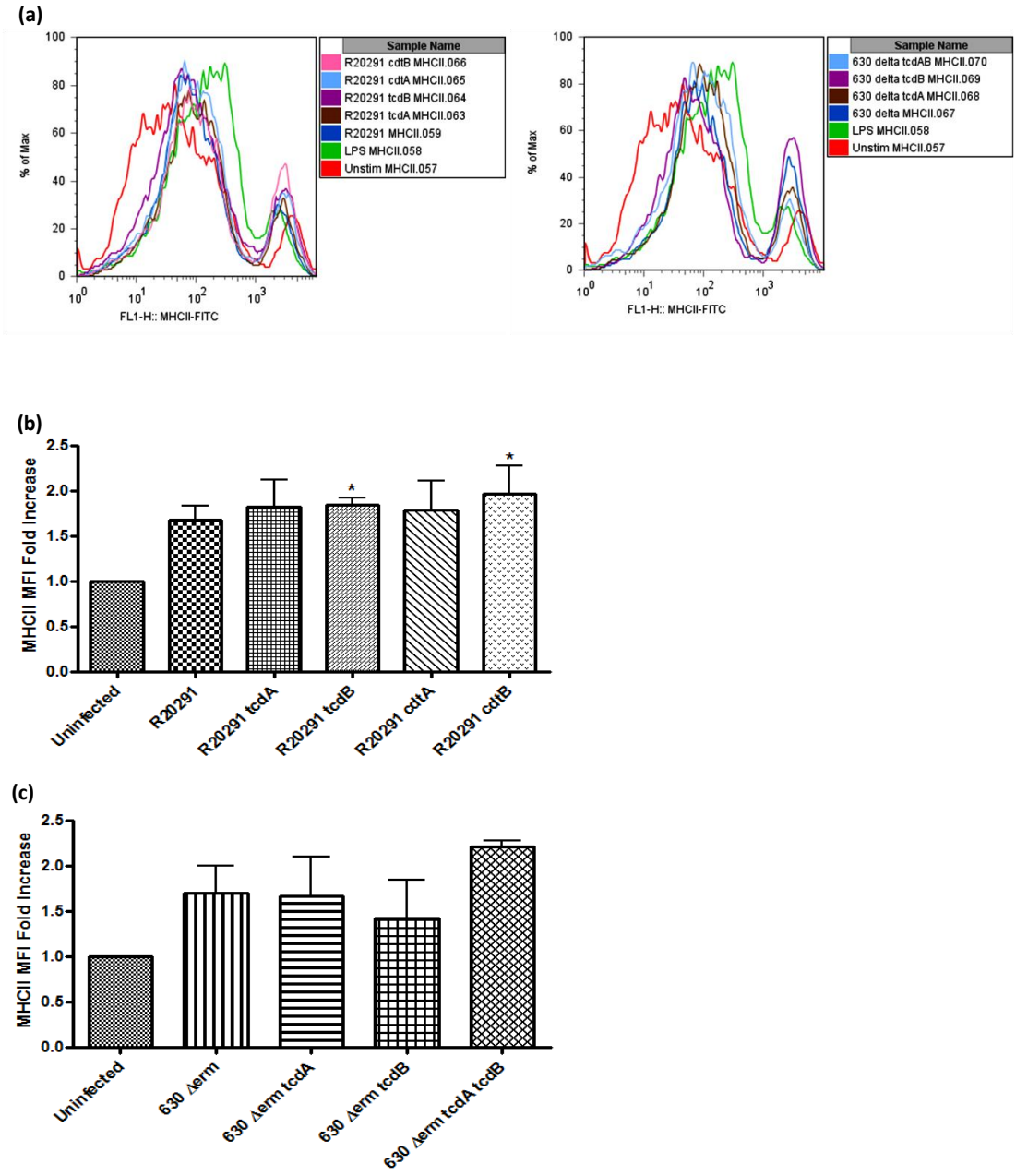

Figure 7.9. *C. difficile* up-regulates co-stimulatory molecule MHCII. BMDCs were infected with R20291 and 630 Δerm isogenic mutants at an MOI of 10. After 8 h stimulation, cells were labelled with mouse MHCII antibody and analysed by flow cytometry (a). The level of surface expression was quantified and presented as MFI fold increase (b-c). Data represent mean ± SEM, n=3. $^{*}p<0.05$ (ANOVA with Bonferroni post-test) represents significant difference from uninfected cells.

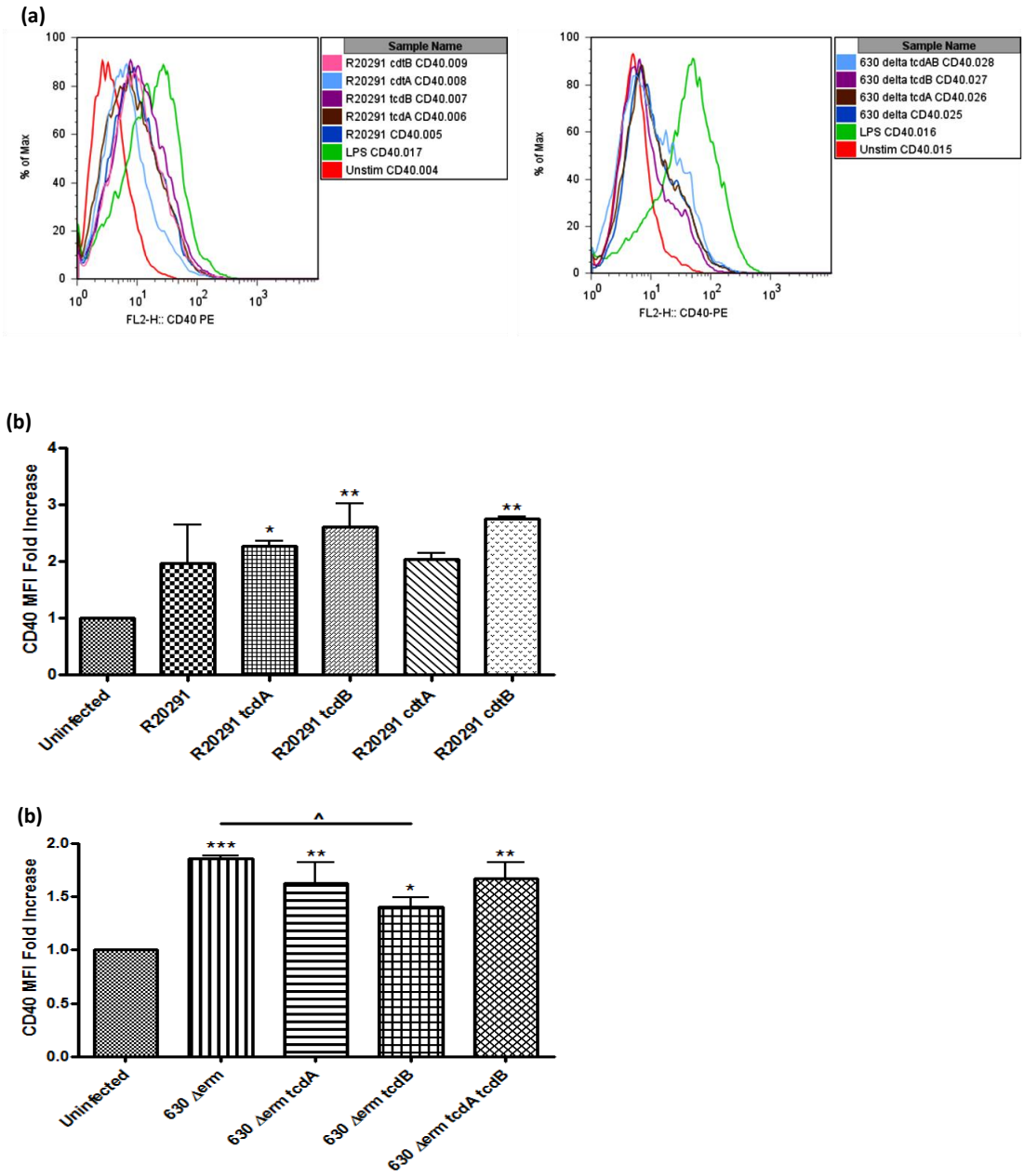

Figure 7.10. *C. difficile* up-regulates CD40 a DC surface marker. BMDCs were infected with toxin mutants of R20291 and 630 Δerm at an MOI of 10. At 8 h post-stimulation, cells were labelled with mouse CD40 antibody and analysed by flow cytometry (a). The level of surface expression was quantified and presented as MFI fold increase (b-c). Data represent mean ± SEM, n=3. $^{*}p<0.05$, $^{**}p<0.01$ and $^{***}p<0.001$ represent significant difference from uninfected cells and $^{\wedge}p<0.05$ represents significant difference from the parental strain. *P* values were obtained using ANOVA with Bonferroni post-test analysis.

7.4.2 Cytokine Production by Dendritic Cells in Response to *C. difficile* Toxin Mutant Strains

To assess the potential role of *C. difficile* toxins in modulating DC innate immune response BMDCs were infected with R20291 and 630 Δerm toxin mutant strains at an MOI of 10. IL-12 family (IL-12, IL-23, and IL-27), IL-10, TNF-α, and IL-1β cytokines were measured at 8 h post-infection (Figures 7.11-7.16).

Basal IL-12 levels were ~10 pg/ml in uninfected control cells. Infection with strain R20291 enhanced IL-12 secretion to ~80 pg/ml. Cells infected with R20291 toxin mutants showed induction which was not statistically different from the parental strain (Figure 7.11 a). Induction in response to strain 630 Δerm was less potent when compared to R20291. Strain 630 Δerm toxin mutants were not significantly different from the parental strain (Figure 7.11 b).

Uninfected control DCs secreted very low levels of IL-23. Upon infection with R20291, marked induction in IL-23 was noted (Figure 7.12 a). R20291 isogenic mutant strains secreted IL-23 to a similar extent. 630 Δerm caused IL-23 release which was 4 to 5-fold less than that observed with R20291, the toxin mutant strains again had minimal impact (Figure 7.12 b).

The basal level of IL-27, another IL-12 family member, in uninfected control cells was <10pg/ml. Infection with R20291 increased IL-27 to ~180 pg/ml. Toxin mutant strains increased IL-27 to a similar extent as seen with the parental strain (Figure 7.13 a). Very modest increase in IL-27 was noted in response to 630 Δerm, again toxin mutant strains were not statistically different from the parental strain (Figure 7.13 b).

Taken together, *C. difficile* strains R20291 and 630 showed distinct abilities in modulating IL-12 family members. Strains R20291 and 630 caused marked increase in IL-23, with an intermediate effect on IL-27. Interestingly, the least induction was noted for IL-12. Importantly, the absence of individual toxins had no significant effect on this family of cytokines.

Infection with strain R20291 showed ~5-fold increase in IL-10 release. The toxin mutant strains showed IL-10 responses in a similar range (Figure 7.14 a). Similar data was noted in response to strain 630 Δerm (Figure 7.14 b). The toxin mutant strains of both R20291 and 630 Δerm did not show any significant difference from the parental strains. Interestingly,

unlike the differential IL-12 family response observed above, both R20291 and 630 Δerm induced IL-10 to a similar extent.

A basal level of <60 pg/ml TNF-α was detected in uninfected control cells. The level was increased upon infection with R20291 to ~7000 pg/ml. Similar responses were detected with R20291 isogenic mutants (Figure 7.15 a). Cells infected with 630 Δerm caused >4000 pg/ml TNF-α secretion. The TcdA toxin mutant showed a significantly reduced level of TNF-α induction compared to the 630 Δerm, while the level of TNF-α released by the TcdB toxin mutant was similar to the parental strain (~4000 pg/ml). On the other hand, a significantly low expression of TNF-α was detected in response to the double toxin mutant (~1850 pg/ml) when compared to the parental strain. It was also observed that the induction of TNF-α by 630 Δerm *tcdB* was significantly higher than 630 Δerm *tcdA* ($p<0.01$) and 630 Δerm *tcdA tcdB* ($p<0.001$) (Figure 7.15 b).

IL-1β secretion was also investigated in response to *C. difficile* toxins. A basal level of ~15 pg/ml IL-1β was detected in uninfected control BMDCs. Upon infection with R20291, IL-1β release markedly increased. Similar responses were detected with R20291 toxin mutant strains (Figure 7.16 a). Cells infected with 630 Δerm showed 1300 pg/ml IL-1β secretion, infection with the TcdA toxin mutant strain caused significantly less release, in contrast 630 Δerm *tcdB* showed IL-1β secretion similar to the parental strain. Importantly, the double toxin mutant was a very poor agonist for IL-1β secretion ($p<0.01$) (Figure 7.16 b).

In summary, studies investigating *C. difficile*-BMDC interactions suggested that BMDC IL-12 and IL-10 responses to *C. difficile* infection were not modulated by the individual toxins. R20291 consistently induced greater cytokine responses compared to strain 630. TNF-α and IL-1β levels were not affected by the absence of individual R20291 toxins. The absence of TcdA and TcdB in the 630 Δerm double toxin mutant had the biggest impact on IL-1β secretion, thus highlighting a major role for the toxins in modulating this specific cytokine.

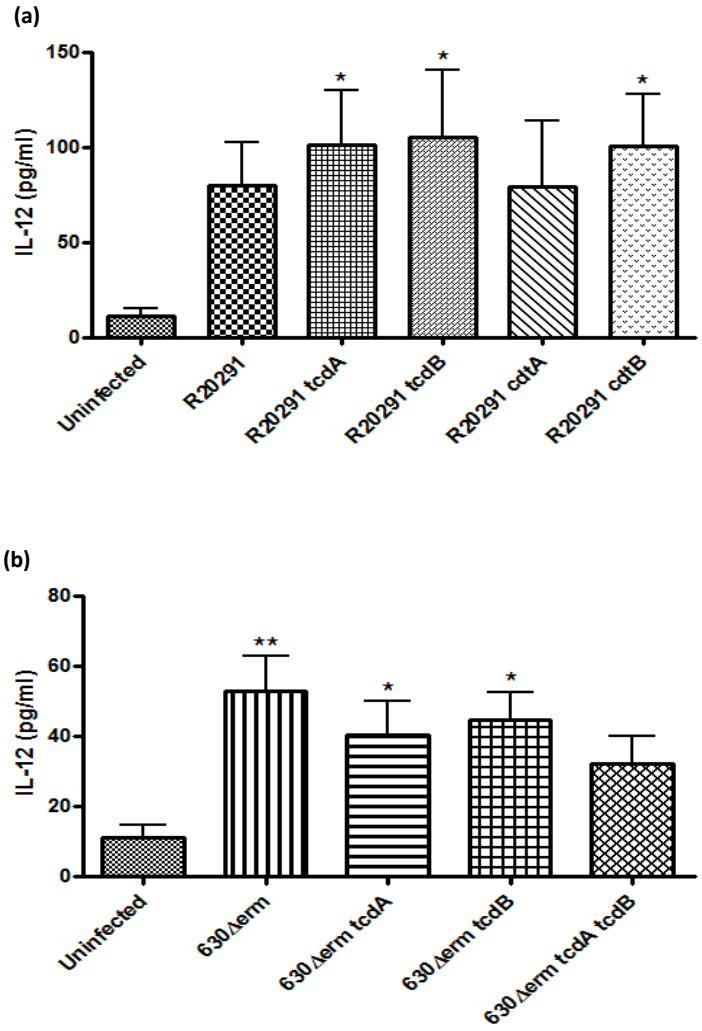

Figure 7.11. BMDCs IL-12 induction in response to *C. difficile* infection. BMDCs were infected with R20291 and 630 Δerm isogenic mutant strains at an MOI of 10. Secretion of IL-12 was measured by ELISA at 8 h post-infection. Data represent mean ± SEM of duplicate samples and are representative of three individual experiments. $^{*}p<0.05$ and $^{**}p<0.01$ represent significant difference from uninfected cells. *p* values were obtained using ANOVA with Bonferroni post-test analysis.

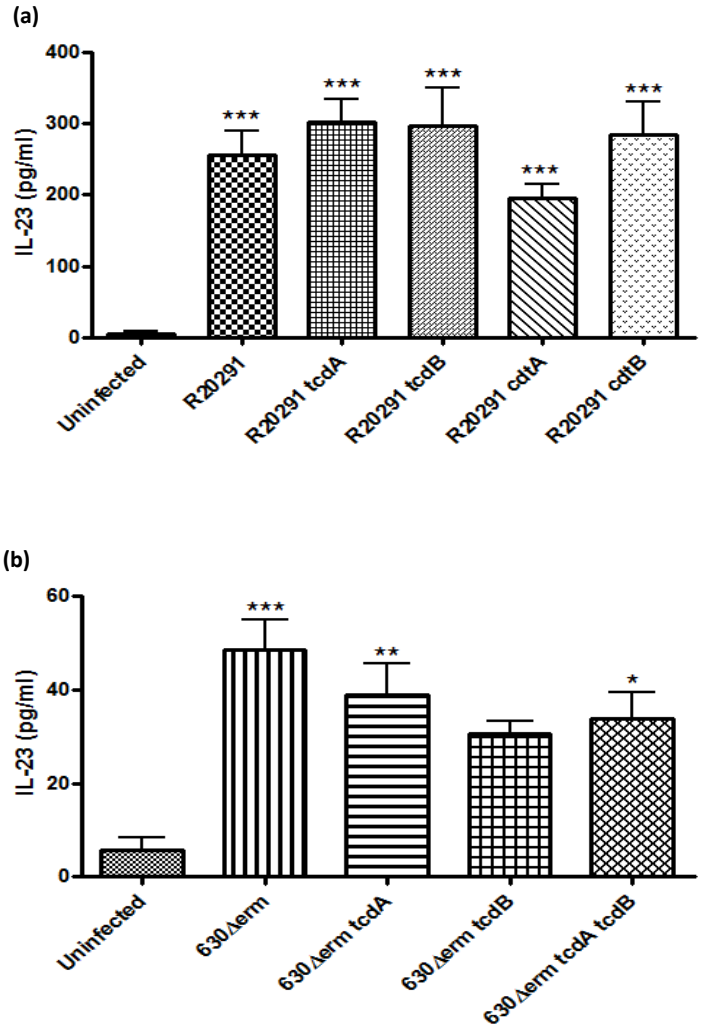

Figure 7.12. IL-23 release in response to *C. difficile* infection by BMDCs. Murine DCs were infected with R20291 and 630 Δerm toxin mutants at an MOI of 10. Secretion of IL-23 was measured by ELISA after 8 h infection. Data represent mean ± SEM of duplicate samples and are representative of three individual experiments. $^{*}p<0.05$, $^{**}p<0.01$ and $^{***}p<0.001$ represent significant difference from uninfected cells. *P* values were obtained using ANOVA with Bonferroni post-test analysis.

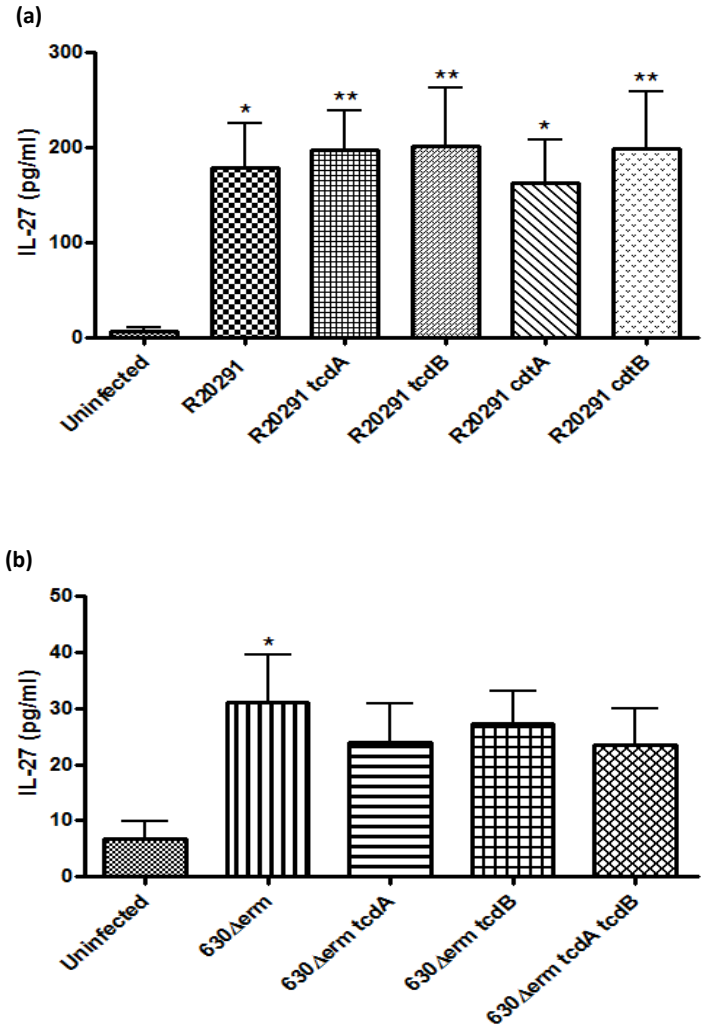

Figure 7.13. IL-27 secretion by BMDCs in response to *C. difficile* infection. Murine DCs were infected with isogenic mutants of R20291 and 630 Δerm at an MOI of 10. Release of IL-27 was measured by ELISA at 8 h post-infection. Data represent mean ± SEM of duplicate samples and are representative of three individual experiments. $^{*}p<0.05$ and $^{**}p<0.1$ represent significant difference from uninfected cells. *P* values were obtained using ANOVA with Bonferroni post-test analysis.

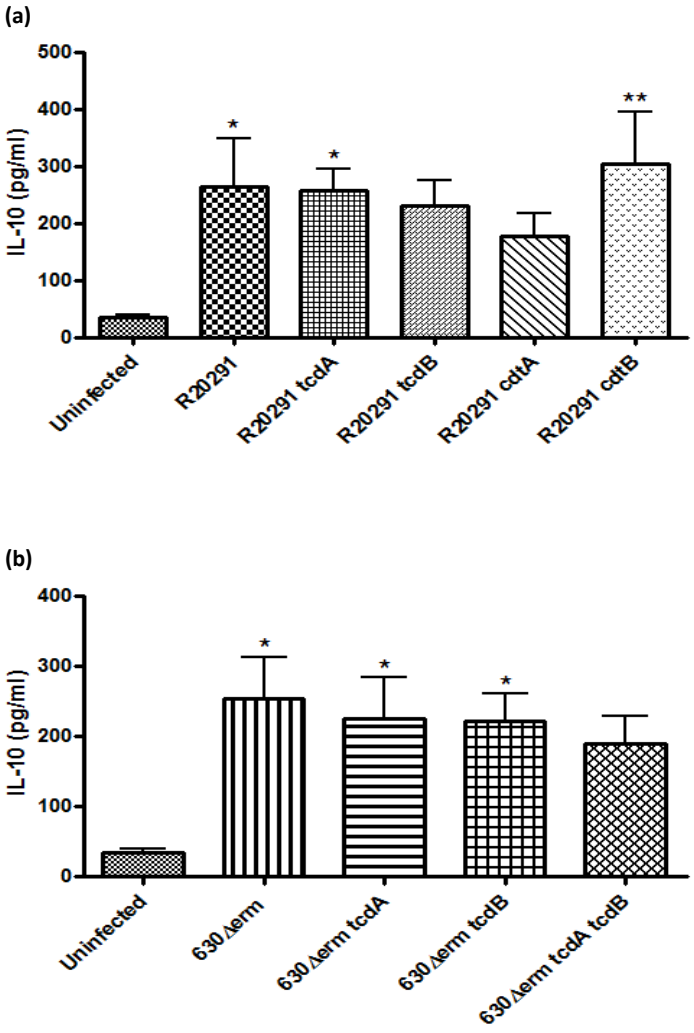

Figure 7.14. IL-10 release in response to *C. difficile* infection by murine DCs. BMDCs were infected with R20291 and 630 Δerm toxin mutants at an MOI of 10. Production of IL-10 was measured by ELISA after 8 h infection. Data represent mean ± SEM of duplicate samples and are representative of three individual experiments. $^{*}p<0.05$ and $^{**}p<0.01$ represent significant difference from uninfected cells. *P* values were obtained using ANOVA with Bonferroni post-test analysis.

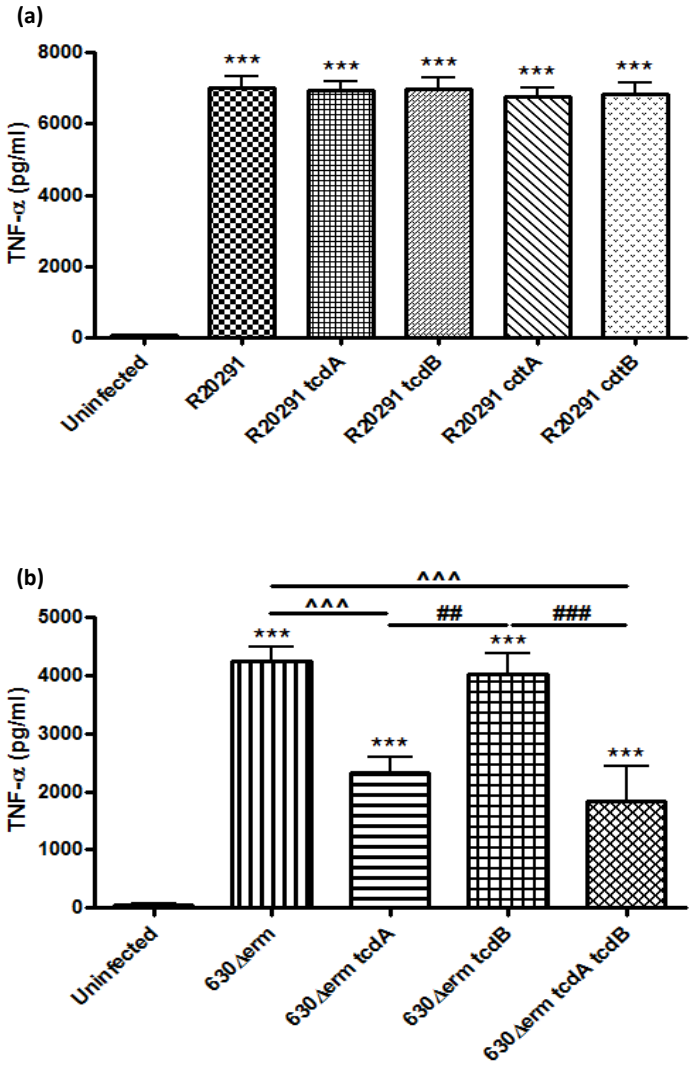

Figure 7.15. TNF-α production in response to *C. difficile* infection. Murine DCs were infected with toxin mutant strains of R20291 and 630 Δerm at an MOI of 10. Release of TNF-α was measured by ELISA after 8 h infection. Data represent mean ± SEM of duplicate samples and are representative of three individual experiments. $^{***}p<0.001$ represents significant difference from uninfected cells, $^{\wedge\wedge\wedge}p<0.001$ represents significant difference from the parental strain, and $^{\#\#}p<0.01$ and $^{\#\#\#}p<0.001$ represent significant inter-strain difference. *P* values were obtained using ANOVA with Bonferroni post-test analysis.

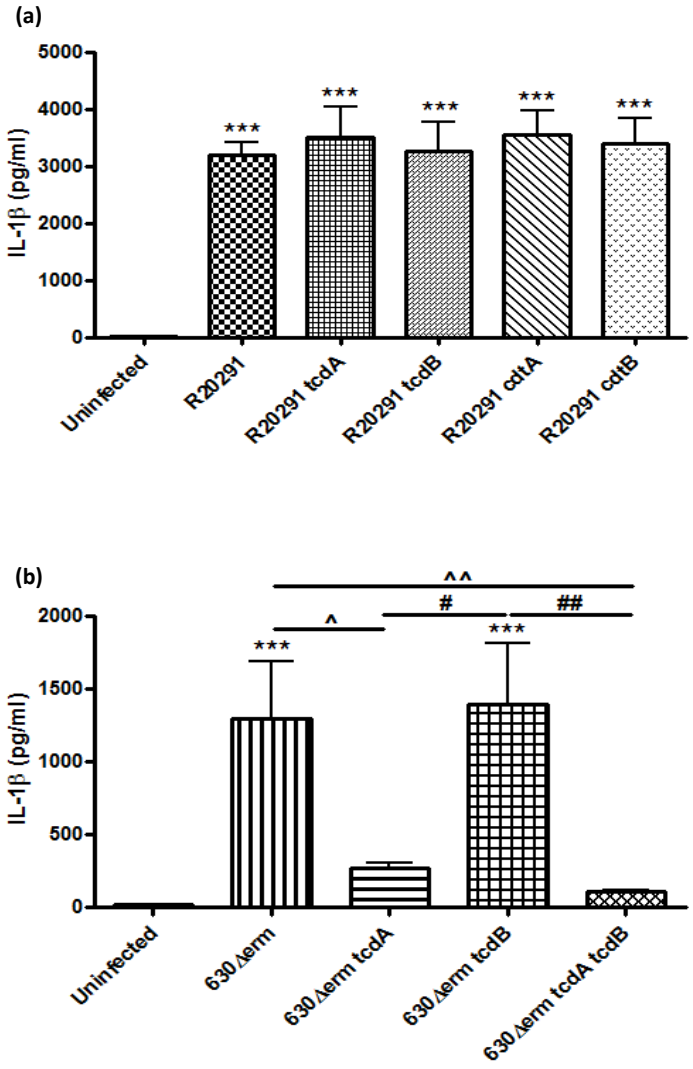

Figure 7.16. IL-1β release in response to *C. difficile* infection. BMDCs were infected with R20291 and 630 Δerm toxin mutant strains at an MOI of 10. Secretion of IL-1β was measured by ELISA after 8 h infection. Data represent mean ± SEM of duplicate samples and are representative of three individual experiments. $^{***}p<0.001$ represents significant difference from uninfected cells, $^{\wedge}p<0.05$ and $^{\wedge\wedge}p<0.01$ represent significant difference from the parental strain, and $^{\#}p<0.05$ and $^{\#\#}p<0.01$ represent significant inter-strain difference. *P* values were obtained using ANOVA with Bonferroni post-test analysis.

7.4.3 *C. difficile* Toxin-mediated IL-1β Secretion

C. difficile strains activate the inflammasome and cause the induction of mature IL-1β in a caspase- and ASC-dependent manner (Chapter 6). Here, the role of individual toxins in mediating IL-1β secretion was further investigated in BMDCs by utilising mutant strain that lacked individual toxins (Figure 7.16). Since no difference was noted in R20291 toxin mutant strains, one may conclude that as the mutant strains lacked only one toxin, presence of the remaining two toxins was sufficient to release bioactive IL-1β. This suggestion is likely to hold, as the deletion of both toxins as seen in the 630 Δerm double toxin mutant did indeed lose the ability to mediate IL-1β release. Although all three *C. difficile* toxins (TcdA, TcdB and CDT) are likely to activate the inflammasome resulting in IL-1β release in an independent manner, how each toxin may engage the various components of the inflammasome is not known. To gain better insight into these mechanism(s) BMDCs from WT (C57BL/6, genetically Nlrp1 deficient), Nod2, Ipaf, Nlrp3, and ASC deficient mice were infected with R20291 and 630 Δerm toxin mutant strains at an MOI of 10 and IL-1β response was measured at 8 h post-infection (Figure 7.17 a-d).

Uninfected WT, Nod2$^{-/-}$, Ipaf$^{-/-}$, Nlrp3$^{-/-}$, and ASC$^{-/-}$ control BMDCs showed a basal level of <20 pg/ml IL-1β (Figure 7.17 a-d). Infection with WT R20291 caused IL-1β secretion to increase to ~2000 pg/ml in WT, Nod2$^{-/-}$, and Ipaf$^{-/-}$ BMDCs (Figure 7.17 a). The IL-1β levels from Nod2$^{-/-}$and Ipaf$^{-/-}$ cells in response to R20291 isogenic mutants were not statistically different from the WT BMDC (Figure 7.17 a).

The Nlrp3 KO cells infected with strain R20291 showed 1700 pg/ml IL-1β secretion, whilst its isogenic mutants caused ~2500 pg/ml. The ASC deficient cells released <60 pg/ml IL-1β in response to R20291 and the toxin mutants exhibited significantly reduced levels of IL-1β when compared with WT and Nlrp3$^{-/-}$ cells (Figure 7.17 b).

The WT, Nod2$^{-/-}$ and Ipaf$^{-/-}$ DCs infected with 630 Δerm released ~1800-2200 pg/ml IL-1β. The Nod2 KO BMDCs infected with the TcdA toxin showed marked reduction compared to the parental strain, whereas the TcdB toxin mutant strain was similar to WT. Infection with the double toxin mutant had minimal effect. The Ipaf deficient BMDC showed reduced IL-1β in response to the TcdA toxin mutant, while the TcdB mutant was similar to WT. Statistically, no significant difference in IL-1β expression from Nod2 and Ipaf KO cells in response to 630 Δerm and its isogenic mutants was detected when compared with the WT BMDCs (Figure 7.17 c).

The Nlrp3 KO cells infected with 630 Δerm showed >2000 pg/ml IL-1β release, while similar IL-1β secretion was detected in response to the TcdA and TcdB toxin mutants. The IL-1β expression from ASC deficient BMDC in response to 630 Δerm, 630 Δerm *tcdA*, and 630 Δerm *tcdB* was significantly reduced (<40 pg/ml) compared to WT and Nlrp3$^{-/-}$ cells. Furthermore, the double toxin mutant mediated minimal IL-1β release in Nlrp3$^{-/-}$ and ASC deficient BMDCs (Figure 7.17 d).

This data indicated that *C. difficile* toxins trigger the release of mature IL-1β as the secretion of IL-1β was completely abrogated with the double toxin mutant. Activation of the inflammasome and release of IL-1β was ASC dependent ruling out a potential role for Nod2, Ipaf and Nlrp3 NLRs in *C. difficile*-mediated inflammasome activation.

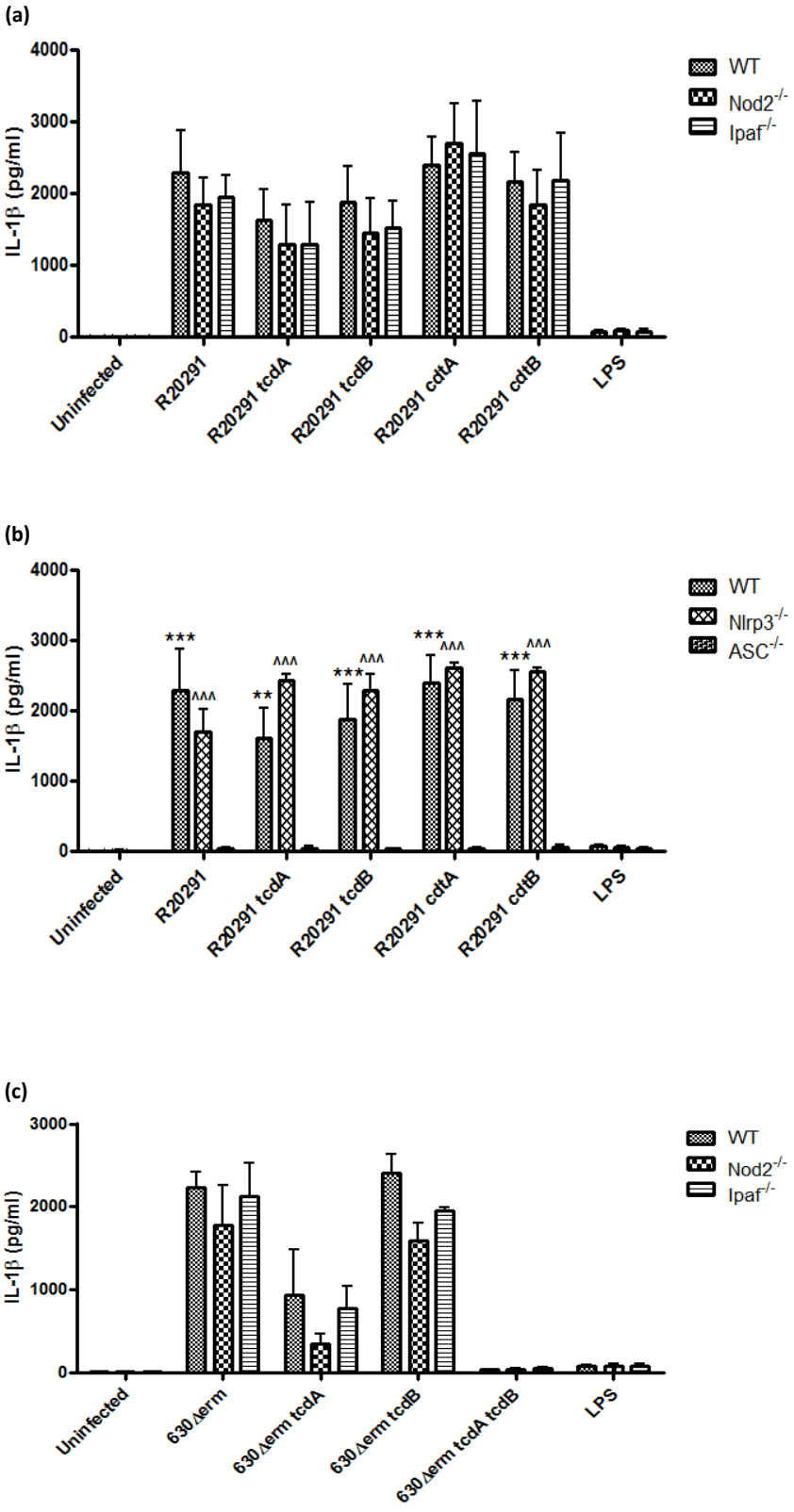
(a)
IL-1β (pg/ml)
4000
3000
2000
1000
0
WT
Nod2-/-
Ipaf-/-
Uninfected
R20291
R20291 tcdA
R20291 tcdB
R20291 cdtA
R20291 cdtB
LPS
(b)
IL-1β (pg/ml)
WT
Nlrp3-/-
ASC-/-
***
^^^
**
Uninfected
R20291
R20291 tcdA
R20291 tcdB
R20291 cdtA
R20291 cdtB
LPS
(c)
IL-1β (pg/ml)
3000
2000
1000
0
WT
Nod2-/-
Ipaf-/-
Uninfected
630Δerm
630Δerm tcdA
630Δerm tcdB
630Δerm tcdA tcdB
LPS

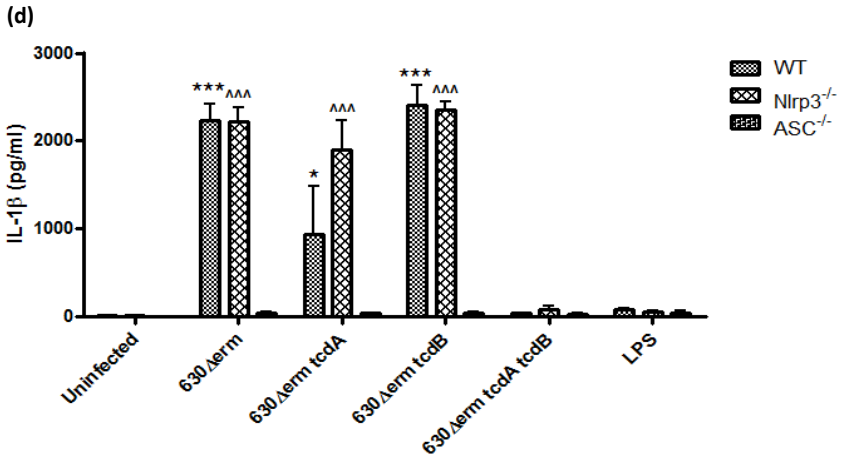

Figure 7.17. *C. difficile* toxins trigger IL-1β release by activating an ASC-containing inflammasome. BMDCs from WT (C57BL/6 genetically Nlrp1 deficient) mice and mice deficient in Nod2, Ipaf (Nlrc4), Nlrp3, and ASC were infected with R20291 and 630 Δerm toxin mutants at an MOI of 10. IL-1β release was measured by ELISA at 8 h post-infection. 1 µg/µl LPS was utilised as a reference stimulus. Data represent mean ± SEM, n=4. $^{*}p<0.05$, $^{**}p<0.01$ and $^{***}p<0.001$ represent significant WT difference from $ASC^{-/-}$ and $^{\wedge\wedge\wedge}p<0.001$ represents significant $Nlrp3^{-/-}$ difference from $ASC^{-/-}$. *P* values were obtained using ANOVA with Bonferroni post-test analysis.

7.5 Human Dendritic Cell Innate Immune Response(s) to *C. difficile* Toxin Mutant Strains

The murine model of *C. difficile* infection showed that *C. difficile* toxins modulated BMDC cytokine responses in a toxin-dependent and independent way. Next we wished to know if similar mechanism(s) were at play during *C. difficile* mediated human DC activation. Human monocyte-derived DCs were infected with strains R20291 and 630 Δerm toxin mutants at an MOI of 10 and induction of IL-12, IL-10, and IL-1β cytokines were measured at 8 h post-infection (Figures 7.18-7.20).

Cells infected with strain R20291 showed <400 pg/ml IL-12 induction (Figure 7.18 a). DCs infected with R20291 toxin mutant strains showed IL-12 median induction in the range of 100-250 pg/ml (Figure 7.18 a). Strain 630 Δerm caused ~75 pg/ml IL-12, while its isogenic mutants induced 110-240 pg/ml (Figure 7.18 b). No significant difference was detected in IL-12 expression in response to both R20291 and 630 Δerm toxin mutants when compared with the parental strains, thus mirroring the response seen in BMDC.

Uninfected control human DCs can spontaneously secrete IL-10. The expression increased in response to WT R20291 and the toxin mutant strains (Figure 7.19 a). Cells infected with 630 Δerm showed less induction compared to WT R20291 (Figure 7.19 b). Human DC IL-10 expression in response to *C. difficile* infection showed a similar trend to that observed in BMDCs. The toxin mutant strains did not show any significant difference in IL-10 release compared to their WT counterparts.

Infection with strain R20291 caused marked IL-1β release, whilst the isogenic mutants showed a range of responses (Figure 7.20 a). The lack of TcdA or TcdB did not significantly affect IL-1β secretion. Interestingly, unlike the data generated in BMDC, human DC showed a trend for less IL-1β release in response to CdtA and CdtB mutants suggesting a potentially greater role for CDT in *C. difficile*-mediated inflammasome activation. Infection with strain 630 Δerm caused 200 pg/ml IL-1β secretion and ~120-210 pg/ml in response to 630 Δerm toxin mutants. Further, unlike the data obtained with BMDC significant reduction of IL-1β was not detected in response to the double toxin mutant strain (Figure 7.20 b). Both R20291 and 630 Δerm toxin mutant strains showed no significant difference in IL-1β response compared to the parental strains.

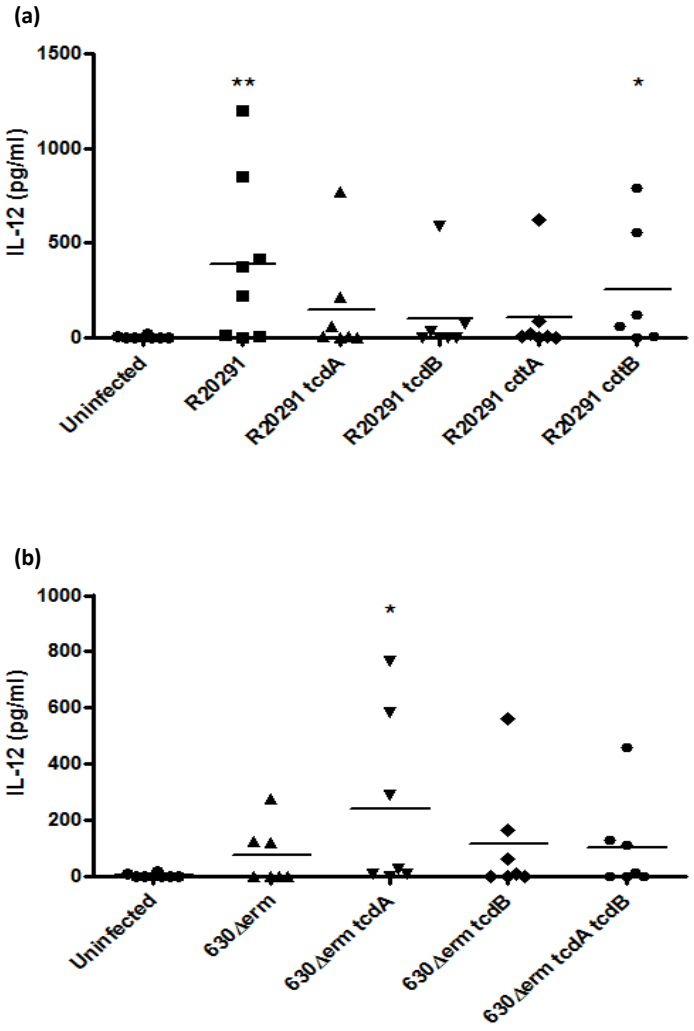

Figure 7.18. Effect of *C. difficile* toxins on IL-12 production by human DC. Human monocyte-derived DCs obtained from nine healthy donors were stimulated with R20291 (a) and 630 Δerm (b) toxin mutants at an MOI of 10. IL-12 secretion was measured by ELISA at 8 h post-infection. $^{*}p<0.05$ and $^{**}p<0.01$ represent significant difference from uninfected control cells. Data was analysed using Mann-Whitney U test.

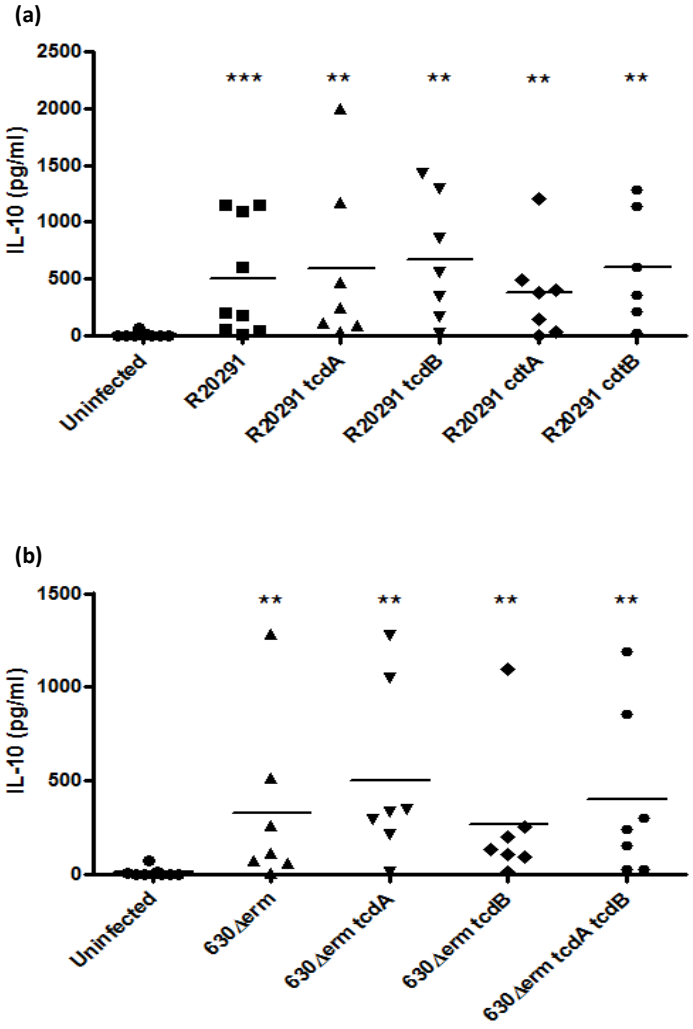

Figure 7.19. Effect of *C. difficile* toxins on IL-10 synthesis by human DC. Human monocyte-derived DCs obtained from nine healthy donors were stimulated with R20291 (a) and 630 Δerm (b) isogenic mutants at an MOI of 10. IL-10 production was measured by ELISA at 8 h post-infection. $^{**}p<0.01$ and $^{***}p<0.001$ represent significant difference from uninfected cells. Data was analysed using Mann-Whitney U test.

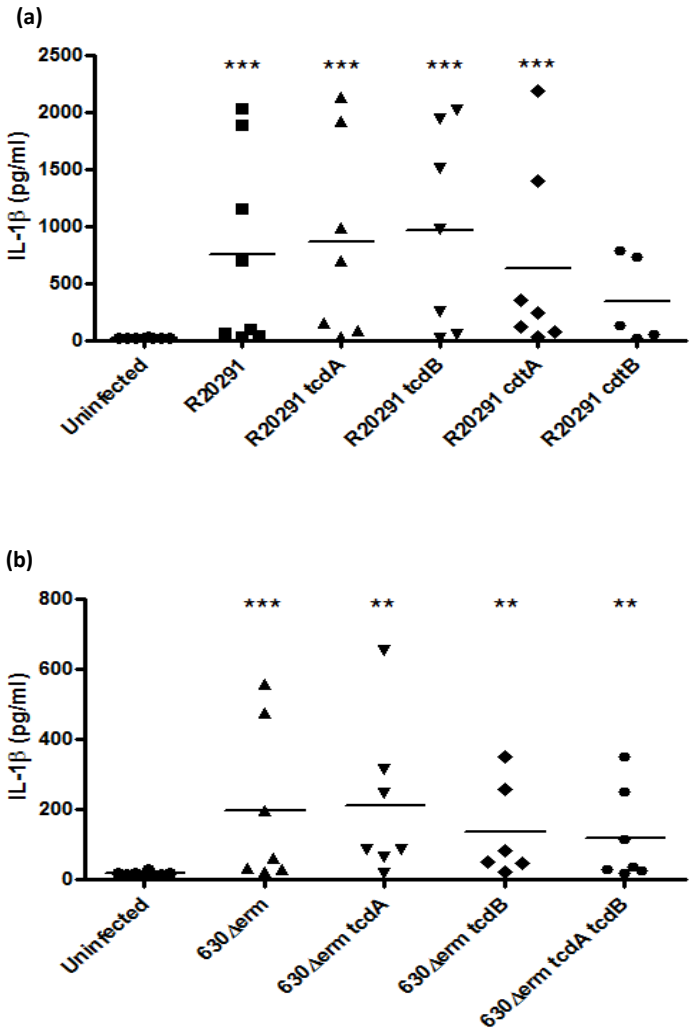

Figure 7.20. Effect of *C. difficile* toxins on human DC IL-1β secretion. Human monocyte-derived DCs obtained from nine healthy donors were stimulated with R20291 (a) and 630 Δerm (b) toxin mutants at an MOI of 10. IL-1β release was measured by ELISA at 8 h post-infection. $^{**}p<0.01$ and $^{***}p<0.001$ represent significant difference from uninfected control cells. Data was analysed using Mann-Whitney U test.

7.6 Conclusions

Immature DCs found in all peripheral tissues are able to efficiently capture microbial antigens (Steinman, 2007). In the gut, exposed DCs to bacterial products are known to mature and migrate to T cell areas of secondary lymphoid organs, where they activate naive T cells (Niess & Reinecker, 2006). Although the process of DC maturation is important to the pathogenesis of CDI, the role of *C. difficile* toxins in mediating disease through DC maturation is less defined.

In the current study, *in vitro* cell cytotoxicity assays were conducted by utilising the R20291 and 630 Δerm toxin mutants then the role of *C. difficile* toxins in bacterial adherence to IEC was investigated. Toxin-mediated DC activation and maturation was examined in murine model system. The induction of IL-12 family members, anti-inflammatory IL-10, pro-inflammatory TNF-α and IL-1β cytokines were measured. Toxin-mediated inflammasome activation and IL-1β secretion was determined in infected BMDCs from WT, $Nod2^{-/-}$, $Ipaf^{-/-}$, $ASC^{-/-}$, and $Nlrp3^{-/-}$ mice and finally, human monocyte-derived DCs were utilised to evaluate the cytokine production in response to *C. difficile* toxins.

In this study, the cytotoxicity assay showed that compared to the parental strain R20291, both R20291 *tcdA* and R20291 *tcdB* caused similar and significantly low cytotoxicity in infected HT-29 cells. HT-29 cells infected with 630 Δerm *tcdA* and *tcdB* showed relatively higher cell toxicity compared to R20291 *tcdA* and *tcdB*, although same trend was observed detecting A^-B^+ strains being potentially more toxic than A^+B^- strains in HT-29 cells, even though 630 Δerm toxin mutants were not significantly different from the parental strain in causing cell toxicity. These findings were unexpected as HT-29 cells are known to be more sensitive to TcdA moreover it was not clear why R20291 *tcdB* exhibited significantly reduced cell toxicity.

Furthermore, HT-29 cells infected with R20291 *cdtA* showed an enhanced but not significantly different cytotoxicity effects compared to the parental strain, while R20291 *cdtB* caused similar cell intoxication to the parental strain. It was not anticipated that deletion of the enzymatic compartment (CDTa) may cause enhanced cell toxicity. This matter requires further investigation and obtaining the triple toxin mutant will elucidate this phenomenon.

Expectedly, 630 Δerm double toxin mutant showed the least cytotoxicity in HT-29 cells.

On the other hand, more sensitivity to TcdB was detected with Vero cell cytotoxicity assay. Cells infected with R20291 *tcdA* showed increased cell toxicity, similar effect was also detected with both R20291 *cdtA* and *cdtB* mutants however the enhanced cytotoxicity levels were not statistically significant to the parental strain. Whereas, R20291 *tcdB* showed significantly reduced cell toxicity compared to R20291. Furthermore, 630 Δerm *tcdA* showed more cytotoxicity but not statistically significant compared to the parental strain. Considerably less cell intoxication was detected with TcdB mutant strain, while the double toxin mutant showed the least cell toxicity when compared to 630 Δerm.

In 2009, Lyras *et al.* in a cytotoxicity assay using HT-29 showed that 630 Δerm *tcdA* mutants were significantly less toxic than the WT strain (630 Δerm). Vero cell cytotoxicity assay also showed that detected cytotoxic activity was predominantly TcdB-mediated, hence the *tcdA* mutants showed the same cytotoxic phenotype as the WT strain. In 2010, Kuehne and co-workers successfully constructed the first double toxin mutant strain of *C. difficile*, which showed no cytotoxic activity towards either HT-29 or Vero cells. They reported that compared to the parental strain (630 Δerm), *tcdA* mutant caused reduced toxicity in HT-29 cells, although the difference was not significant. Similar degree of cytotoxicity in Vero cells was also seen with this mutant. On the other hand, they detected that compared to the parental strain, the *tcdB* mutant showed increased toxicity in HT-29 cells, which was not statistically significant, and a similar level of toxicity in Vero cells. Both authors reasoned that the observed increased TcdA expression in $A^{+}B^{-}$ mutant strains was due to the mutation of *tcdB*. They showed by quantitative RT-PCR that the expression of TcdA was increased 3.3-fold compared to the WT/parental strain however the basis for this increased expression of TcdA is not known.

Moreover, these two studies showed very contradictory results. While Lyras *et al*. detected a significant decrease in HT-29 cell toxicity with *tcdA* mutants compared to the parental strain, Kuehne *et al.* observed reduced but not statistically different outcome. The same discrepancy was also seen in Vero cell cytotoxicity assay. In an article in 2011, Kuehne and co-workers discussed a number of factors that needed to be considered in comparing these two studies, the most important difference was related to the employed strains. Whilst the parent strain employed in both studies was strain 630, the mutants were generated using different isolates. As generation of mutants relies on the ability to select resistance to erythromycin, a requirement that disqualifies the use of strain 630 as it carries a functional copy of *ermB*. Therefore, both studies employed independently isolated derivative strain of 630, which was sensitive to this antibiotic. While Kuehne *et al.* utilised strain 630 Δerm

generated after 30 repeated subculture of strain 630 in non-selective media leading to specific deletion of *ermB*, Lyras *et al.* isolated another erythromycin sensitive strain, through an undisclosed number of subcultures of strain 630 and designated the strain 630E. A preliminary comparison showed that the 630 Δerm and 630E have clear phenotypic differences such as; strain 630E is non-motile, lacks flagella, and has a more severe glucose response, affecting the level of produced toxin in the presence of this carbon source.

The current study is the first one to employ the R20291 toxin mutants, thus the reason why the *tcdB* mutant that has been shown to produce 3.3-fold more TcdA caused significantly less cell toxicity compared to the parental strain is not known. Moreover, although in this study the same 630 Δerm toxin mutants was utilised as those of Kuehne and co-workers, 630 Δerm *tcdA* mutant showed increased cell toxicity in HT-29 and 630 Δerm *tcdB* exhibited a significantly reduced cytotoxicity in Vero cells, which were not observed in the study by Kuehne *et al.* The answer may reside with the *in vitro* model, either employed cell culture conditions or cell confluence could influence the outcome. Also in the current study the cytotoxic activity was not confirmed using toxin neutralisation assay.

In 1988, Borriello *et al*. reported that in a clindamycin-induced disease in the Syrian hamster model there was a correlation between variable efficiencies of gut colonisation by different *C. difficile* strains and their abilities to associate with regions of the GI tract, spanning the jejunum to the colon. They suggested that it might be partly due to strains differential ability to produce toxins however they explored the idea that factors other than toxin production might be responsible too. Later Drudy *et al.* (2001) in a flow cytometric analysis of *C. difficile* adherence showed that toxigenic and non-toxigenic strains adhere equally to primary colonic epithelial cells and intestinal cell-lines nevertheless binding to primary cells were significantly greater than adherence to Caco-2 or HT-29 cells. In the current study, similar *in vitro* results were also observed with R20291 and 630 isogenic mutants. Compared to the parental strain R20291, toxin mutants exhibited similar levels of adherence to Caco-2 cells and no inter-strain difference was detected (Figure 7.4). Toxin mutants of 630 Δerm, single or the double toxin mutants also showed comparable adherence levels to the parental strain 630 Δerm, indicating additional bacterial factors involved in binding to the intestinal epithelia other than toxins (Figure 7.6).

The role of toxins was further investigated by examining their effects on DC activation. Strain R20291 toxin mutants caused up-regulation of cell surface markers CD80, MHCII, and CD40 in similar levels compared to the parental strain. However, R20291 *tcdB*, and binary toxin mutants showed a significant increase in CD86 modulation when compared to the R20291. On the other hand, 630 Δerm *tcdB* exhibited a significant CD80 and CD86 fold increase compared to 630 Δerm *tcdA* and the double toxin mutant, although this was not statistically significant compared to the parental strain. MHCII was up-regulated in response to all 630 Δerm toxin mutants, while similar result was detected with CD40, 630 Δerm *tcdB* showed a significantly less CD40 modulation compared to the 630 Δerm. It has been already shown that the expression of cell surface molecules such as CD40, CD80, CD86, and MHCII on immature murine DCs were increased in response to 100 ng/ml TcdA leading to hypothesise that *C. difficile* TcdA can promote DC maturation (Lee *et al.,* 2009), although in the current study a strong MHCII and CD40 up-regulation was detected with the double toxin mutant strain indicating that DC surface markers were modulated in a toxin-dependent and independent manner.

Following DC maturation upon interaction with bacteria, DCs release an array of cytokines and chemokines. Cells infected with R20291 toxin mutants showed no significant increase in secretion of IL-12 family cytokine, IL-10, TNF-α, and IL-1β compared to the parental strain signifying a toxin independent induction of these cytokines. Similar outcome was also detected with 630 Δerm isogenic mutants showing no significant difference in expression of IL-12 family cytokine and IL-10 when compared to the WT strain. However, while 630 Δerm *tcdB* caused comparable amounts of pro-inflammatory TNF-α and IL-1β to the parental strain, 630 Δerm *tcdA* and the double toxin mutant strains induced significantly less TNF-α and IL-1β, suggesting that TcdA may possibly be the potent inducer of these pro-inflammatory cytokines. It is not clear why differential TNF-α and IL-1β expression was seen in response to R20291 *tcdA* and 630 Δerm *tcdA*, nevertheless the impact of R20291 binary toxin in host response modulation cannot be disregarded.

Additionally, human monocyte-derived DCs infected with R20291 and 630 Δerm toxin mutants showed no significant difference in induction of IL-12, IL-10 and IL-1β cytokines compared to the parental strains and no inter-strain difference was detected. Although human peripheral blood monocytes are widely used, the *in vitro* generated DCs do not demonstrate the same ability and behaviour as *ex vivo* isolated DCs.

Ng *et al.* (2010) have already shown that *C. difficile* infection leads to the activation of the inflammasome and IL-1β secretion in a toxin-dependent way. In this study, it was also observed that *C. difficile* strains caused differential induction of IL-1β, detecting the least IL-1β expression in response to strain CF5. Therefore, the role of toxins in the release of mature IL-1β caused by the activation of the inflammasome was investigated in DCs infected with R20291 and 630 Δerm isogenic mutants. DCs from Nod2, Ipaf, and Nlrp3 deficient mice, infected with R20291 toxin mutants showed no significant difference in IL-1β response compared to the WT DCs however the secretion of IL-1β was significantly decreased in ASC KO DCs. Similar responses were also detected in Nod2, Ipaf, and Nlrp3 deficient mice infected with 630 Δerm toxin mutants, exhibiting no significant difference in IL-1β secretion compared to that observed with WT DCs and deletion of ASC abrogated the release of IL-1β. Furthermore, the double toxin mutant caused the least induction of IL-1β in all tested cell types.

Collectively, *C. difficile* caused DC activation and cytokine production in a toxin-dependent and independent fashion indicating that multiple bacterial factors may play a role in initiating an innate immune response. Nonetheless, *C. difficile* toxins were clearly responsible for activation of the inflammasome in an ASC-dependent manner.

7.6.1 Summary

This chapter demonstrated that:

- Toxin mutant strains exerted varying cytotoxic potential on HT-29 and Vero cells.
- The double toxin mutant strain showed the least cell cytotoxicity compared to other toxin mutants.
- *C. difficile* adherence to IEC was toxin independent.
- BMDC surface markers were modulated in a toxin-dependent and independent manner.
- BMDCs infected with R20291 and 630 Δerm toxin mutants showed toxin-independent secretion of IL-12 family cytokines and IL-10.
- Strain 630 Δerm *tcdA* and the double toxin mutant induced significantly less pro-inflammatory TNF-α and IL-1β.
- Human DCs infected with toxin mutant strains showed similar trend in IL-12 and IL-10 secretion to that observed with BMDCs however the double toxin mutant caused comparable IL-1β release as the parental strain.
- *C. difficile* toxins activated the inflammasome and triggered IL-1β release in an ASC-dependent manner.

Chapter 8

Discussion

C. difficile is recognised as the primary cause of infectious diarrhoea in hospitalised patients (Kelly & LaMont, 2008). In the last decade, the incidence, severity and recurrences of *C. difficile* infection (CDI) have increased considerably, particularly with the emergence of hypervirulent strains (Stabler *et al.,* 2009; Khanna *et al.,* 2012). CDI is a toxin-mediated disease; the majority of strains express two exotoxins (TcdA & TcdB) which are the most extensively studied virulence factors. The mechanisms by which TcdA and TcdB induce enterotoxicity have been well established by utilising purified/recombinant toxins both *in vitro* in an array of cell types and *in vivo* animal models of infection. Until recently our understanding of *C. difficile* pathogenesis was greatly hindered due to the lack of available tools for the construction of chromosomal mutants as *C. difficile* is difficult to manipulate genetically. At the commencement of the present study no isogenic mutant strains were available, the initial studies were therefore conducted utilising four different *C. difficile* strains including R20291 (hypervirulent strain, $A^+B^+CDT^+$), a fully sequenced strain 630 (A^+B^+) and two variant strains, M68 and CF5 (A^-B^+). This study commenced aiming to elucidate the role of the bacterial cell and its native toxins (in the context of infection) in modulating host immunity; these experiments laid the foundation to improve our understanding of how the host may raise differential immune and non-immune responses to A^+B^+ versus A^-B^+ strains. Nonetheless, availability of R20291 and 630 toxin mutant strains later on in the project, allowed a better understanding of the role toxins play in *C. difficile* infection.

The colonic epithelium is the first target tissue of *C. difficile*. The ability to disrupt tight junctions and to breach the intestinal epithelial barrier is one of the most direct events attributed to TcdA and TcdB in the intestine (Feltis *et al.,* 2000). These toxins are glucosyltransferases that mono-glucosylate Rho GTPases (Just *et al.,* 1995). As Rho proteins play an important role in tight junction (TJ) assembly, their inactivation by the toxins causes the loss of epithelial barrier function and re-organisation of filamentous actin structure (Hecht *et al.,* 1988; Halabi-Cabezon *et al.,* 2008). *C. difficile* toxins also possess apoptogenic properties, which may contribute to the inflammatory process induced by this bacterium (Fiorentini *et al.,* 1998; Brito *et al.,* 2002). Studies have shown that *C. difficile* toxin-induced apoptosis depends on glucosylation of Rho GTPases leading to activation of caspases and is independent of the effect on the actin cytoskeleton (Qa'Dan *et al.,* 2002; Gerhard *et al.,* 2008). Additionally, *C. difficile* may gain access to the underlying lamina propria and submucosa, to act directly on other cell types once the epithelial barrier is breached (Mahida *et al.,* 1998; Solomon *et al.,* 2005).

The current study showed that strains R20291, 630, and M68 caused an extensive TJ disruption in infected T84 cell-lines which was concomitant with increased TEER loss and enhanced barrier permeability, detected as FITC-dextran flux (Figures 4.11-4.14). Co-culture experiments showed that R20291 induced the highest levels of IL-8 compared to the other strains. Whilst, similar amount of IL-8 was detected in response to strains 630 and M68, CF5-infected cells released the lowest quantity. Strains R20291, 630 and M68 also induced significant levels of apoptosis/necrosis in infected Caco-2 cells, although disruption of the epithelium and cell death was detected with CF5, it was to the lesser extent compared to other strains. These series of experiments showed that hypervirulent R20291 was inherently more potent compared to strains 630, M68 and CF5. While, 630 and M68 had the potential to induce comparatively similar responses, strain CF5 initiated the least effect. It was hypothesised that CF5 owes its low potency to differential TcdB glucosylation property, although strain CF5 was observed to produce more toxin than M68 (Figure 3.6). Studies have shown that toxins of some *C. difficile* strains and particularly TcdB have inherent variability (Chaves-Olarte *et al.,* 2003; Stabler *et al.,* 2008; Lanis *et al.,* 2010). Strain M68 significantly glucosylated Rac1 compared to CF5, nonetheless further investigation is required to identify the underlying mechanisms responsible for the differences in activity between the two forms of this toxin. Also comparison of M68 and CF5 completed sequences may shed a light on observing any possible sequence variation.

A severe inflammatory response with a marked neutrophil accumulation is a key characteristic of the clinical pathophysiology of CDI (Johnson & Gerding, 1998; Kelly & LaMont, 1998). Neutrophil recruitment to the site of the infection is a complex and multistep process (Springer, 1994), which is driven by a local production of an array of chemoattractants and activated cytokines that establish a chemotactic gradient. IL-8 is a potent pro-inflammatory chemokine that predominantly exerts its effects on neutrophils (Hoch *et al.,* 1996). Analysis of mucosal responses revealed that *C. difficile* strains evoked a robust inflammatory cytokine response in colonic tissues, eliciting a strong induction of IL-8 and comparatively weak IL-17A (Figure 4.15). This response suggested that IL-8 may play a pivotal role in mediating neutrophil recruitment necessary for containment of the infection. Additionally, *C. difficile* infection caused a strong IL-1β and IFN-γ secretion, release of pro-inflammatory cytokines is a critical activation event in *C. difficile*-mediated inflammation. IL-1β has been reported to increase both IL-8 secretion by TcdA-treated HT-29 cells and promote intercellular adhesion molecule-1 (ICAM-1)-dependent neutrophil adhesion, two molecules that are important in neutrophil chemoattraction, adhesion and subsequent

inflammation (Kelly *et al.,* 1994; Tixier *et al.,* 2005). Furthermore, it has been shown that IFN-γ has an essential role in TcdA-induced enteritis by enhancing TNF-α, MIP (Macrophage inflammatory protein)-1α, MIP-2 and ICAM-1 secretion (Ishida *et al.,* 2004). This data showed that M68 initiated inflammatory responses in infected paediatric colonic biopsies to a similar extent as R20291 and 630, while CF5 caused significantly less pro-inflammatory IL-1β, IFN-γ and inflammatory IL-17A release. This study could be further developed to establish host differential responses to *C. difficile* and its toxins by employing toxin mutant strains and providing an anaerobic environment for bacteria by utilising Ussing chambers.

Although *C. difficile* toxins have been suggested to initiate IL-8 secretion nevertheless the present study demonstrated that bacterial whole cell cultures induced considerably more IL-8 release than bacterial supernatants (potential source of secretory toxins) in Caco-2 and HT-29 cells, indicating that additional, as yet undefined cell-associated bacterial factors may be involved in triggering IEC innate immunity alongside the toxins. Moreover, it was observed that *C. difficile* was recognised by a number of TLRs, specifically with TLR2/6 and TLR5 (Figures 5.2-5.3). In addition to the known effect of *C. difficile* mediated IL-8 secretion via TJ disruption, our observations define a second potential mechanism of how *C. difficile* recognition by host TLRs may mediate IEC IL-8 responses. It is still unclear how *C. difficile* induce chemokine and cytokine production. While several studies have suggested both Rho-dependent and independent cytokine release mechanisms (Warny *et al.,* 2000; Yeh *et al.,* 2008; Sun *et al.,* 2009), others have proposed the involvement of NF-κB or MAPK p38 in the cytokine secretion (Castagliuolo *et al.,* 1998; Jefferson *et al.,* 1999; Kim *et al.,* 2006b). There are reports showing NF-κB not being involved in TcdB-mediated IL-8 production, while it plays an important role in TcdA-mediated IL-8 secretion.

C. difficile is an anaerobic bacterium therefore there are limitations with co-culture studies. This thesis described providing an anaerobic environment for bacteria by employing an Ussing vertical chamber system. This series of experiments showed a significant increase in secretion of pro-inflammatory IL-8 and TNF-α, and antimicrobial hBD-2 accompanied by a rapid TEER loss when strains R20291, 630 and M68 were co-cultured under anaerobic conditions compared to cultures under an aerobic environment. It was hypothesised that observed increase in cytotoxic and cytopathic effects were as a result of optimal condition for bacterial growth. However, it is yet to be determined whether these effects were a result of increased bacterial viable count and/or bacterial adherence. Interestingly, the strain CF5 showed an increase in TEER loss when cultured under anaerobic conditions

however no significant increase in cytokine response was detected compared to cultures under an aerobic environment.

Utilising an i*n vitro* murine model of infection suggested that *C. difficile* had the ability to promote bone-marrow-derived DCs (BMDCs) maturation, which was supported by up-regulation of the co-stimulatory molecules CD80 and CD86, as well as the cell surface markers MHCII and CD40. Further, infected BMDCs released larger amounts of IL-23 and IL-27 compared to IL-12 highlighting that *C. difficile* strains exhibit differential ability in modulating DC IL-12 family members which is likely to impact downstream T cell immunity. BMDCs infected with strains R20291 and M68 expressed similar levels of IL-12 family cytokines, 630 was the least inducer while the highest secretion was observed in response to CF5. Previous studies have shown IL-1β release in response to *C. difficile* toxins and SLPs, in here data obtained from human and murine DCs clearly showed that strains R20291, 630 and M68 elicited a significant IL-1β secretion. In contrast, CF5 caused the least pro-inflammatory IL-1β response. As IL-1β is known to be involved in the neutrophil recruitment during CDI this data could provide potential insights into the pathophysiological mechanisms of these strains. Also a robust anti-inflammatory IL-10 was induced in response to strain CF5 which may indicate why CF5 infected hosts typically remain clinically asymptomatic.

T cell activation was investigated to identify whether *C. difficile*-stimulated mature DCs had the potential to prime and influence T cell responses. *C. difficile* strains induced strong IFN-γ secretion compared to IL-4, indicating the ability of *C. difficile* in promoting a shift in Th1/Th2 balance toward Th1-dominant immunity. Further, a robust IL-17A expression in response to R20291, 630 and M68 indicated that these strains mediate potent Th1/Th17 immunity. Although strain CF5 caused the highest IL-23 protein expression, it showed the least propensity for IL-17A production and caused the highest IL-4 secretion compared to other strains promoting more Th1/Th2 responses. Thus, strain CF5 may tune the fine balance of Th1/Th2 immunity affecting antibody responses and in particular IgG which assists toxin neutralisation.

The process of DC maturation is important to the pathogenesis of CDI however the role of *C. difficile* toxins in mediating disease via DC maturation is less clear. This study showed that R20291 and 630 Δerm toxin mutant strains did not exert a significant impact on BMDC CD80, MHCII and CD40 expression compared to the parental strains although an effect on CD86 was observed. Further, data presented in Figures 7.11 – 7.16 indicated that *C. difficile*

may engage in toxin-independent mechanism(s) to regulate BMDC IL-12 family and IL-10 responses, and yet, toxin-dependent mechanism(s) are likely to be critical regulators of IL-1β secretion. However, the notion why 630 Δerm *tcdA* was less potent in IL-1β induction is still unknown. It could be hypothesised that either TcdB is an essential *C. difficile* virulence factor in triggering CDI or the significantly increased IL-1β secretion in response to 630 Δerm *tcdB* is due to increased TcdA expression attributed to *tcdB* mutation. Therefore, although strains R20291 and 630 toxin mutants provided a unique potential to gain a better understanding of the role of toxins nevertheless, R20291 triple toxin mutant can facilitate comprehensive and comparative investigation of *C. difficile* toxins.

Moreover, *C. difficile* activated the caspase-1 and triggered IL-1β secretion in BMDCs in an ASC-containing inflammasome. The ASC-dependent activation of the inflammasome has been reported by Ng *et al.* (2010) showing contribution of IL-1β to toxin-induced inflammation and intestinal injury *in vivo*. They also observed that TcdA and TcdB not only trigger IL-1β release but also induce ASC-dependent pyroptosis. Caspase-1 dependence is a key feature of pyroptosis, which ultimately results in the release of pro-inflammatory intracellular contents, including IL-1β. They suggested that *C. difficile* triggered NLRP3 inflammasome activation and IL-1β release. However, glibenclamide a NLRP3 inhibitor did not completely abolish the toxin-induced IL-1β release, also they were unable to show a significant role for NLRP1, 2, 6, 12 and Ipaf in the toxin-induced inflammasome activation concluding other NLRs may contribute to activation of the inflammasome. The current study showed strains R20291, 630 and their toxin mutants together with M68 caused IL-1β processing in Nod2, Ipaf and Nlrp3 deficient BMDCs, ruling out critical roles for these NLRs in triggering the inflammsome. Hasegawa and co-workers (2011) have already shown that Nod1 deficient mice are more susceptible to *C. difficile* infection than Nod2 deficient mice suggesting a protective role for Nod1 against *C. difficile* by recruiting neutrophil to clear the bacteria. Therefore, a further investigation is required to identify the NLR(s) responsible for *C. difficile*-induced inflammasome activation in DCs and macrophages.

Also, even though strain CF5 consistently caused minimal IL-1β responses, western blot results (Figure 6.4) showed that this strain is as equipotent as other strains in activating caspase-1, thus it remains to be answered how CF5 elicits the least IL-1β secretion. Furthermore, it is unclear why Nod2, Ipaf and Nlrp3 deficiency enhanced potency of CF5 leading to increased levels of IL-1β compared to WT BMDCs.

Taken all together, *C. difficile* strains have the potential to elicit differential immune responses based on a cell type they encounter. Also distinct toxin-dependent and independent effects on host immunity were observed indicating a potential role for other bacterial virulence factors such as the capsule, SLPs, flagella, pili and hydrolytic enzymes in engaging host-pathogen interactions.

Despite the progress that have been made in understanding the molecular mechanisms of TcdA and TcdB, many fundamental questions remain unanswered regarding the involvement and contribution of the bacteria itself and its virulence factors in the onset and progression of the CDI. The nature of the specific receptors for TcdA, TcdB and binary toxin is still unknown and it is not clear why TcdA and TcdB present such a diverse biological activity while they share high amino acid sequence identity, similar domain structures and act in a similar molecular mode, yet display different enterotoxic potential. Also the respective roles of TcdA, TcdB, and binary toxin in the host inflammatory response(s) and pathogenesis still remain undefined.

Given the increasing emergence of hypervirulent strains and community-acquired CDI, further investigations will improve our understanding of this bacterium, leading to a better containment of the associated disease.

REFERENCES

Abreu, M.T., Fukata, M., & Arditi, M. 2005. TLR signaling in the gut in health and disease. *J.Immunol.*, 174, (8) 4453-4460

Abreu, M.T. 2010. Toll-like receptor signalling in the intestinal epithelium: how bacterial recognition shapes intestinal function. *Nat.Rev.Immunol.*, 10, (2) 131-144

Akerlund, T., Svenungsson, B., Lagergren, A., & Burman, L.G. 2006. Correlation of disease severity with fecal toxin levels in patients with *Clostridium difficile*-associated diarrhea and distribution of PCR ribotypes and toxin yields in vitro of corresponding isolates. *J.Clin.Microbiol.*, 44, (2) 353-358

Akerlund, T., Persson, I., Unemo, M., Noren, T., Svenungsson, B., Wullt, M., & Burman, L.G. 2008. Increased sporulation rate of epidemic *Clostridium difficile* Type 027/NAP1. *J.Clin.Microbiol.*, 46, (4) 1530-1533

Aktories, K., Barmann, M., Ohishi, I., Tsuyama, S., Jakobs, K.H., & Habermann, E. 1986. Botulinum C2 toxin ADP-ribosylates actin. *Nature*, 322, (6077) 390-392

Aktories, K. & Wegner, A. 1992. Mechanisms of the cytopathic action of actin-ADP-ribosylating toxins. *Mol.Microbiol.*, 6, (20) 2905-2908

Albesa-Jove, D., Bertrand, T., Carpenter, E.P., Swain, G.V., Lim, J., Zhang, J., Haire, L.F., Vasisht, N., Braun, V., Lange, A., von Eichel-Streiber, C., Svergun, D.I., Fairweather, N.F., & Brown, K.A. 2010. Four distinct structural domains in *Clostridium difficile* toxin B visualized using SAXS. *J.Mol.Biol.*, 396, (5) 1260-1270

Alcantara, C., Stenson, W.F., Steiner, T.S., & Guerrant, R.L. 2001. Role of inducible cyclooxygenase and prostaglandins in *Clostridium difficile* toxin A-induced secretion and inflammation in an animal model. *J.Infect.Dis*, 184, (5) 648-652

Alfa, M.J., Kabani, A., Lyerly, D., Moncrief, S., Neville, L.M., Al-Barrak, A., Harding, G.K., Dyck, B., Olekson, K., & Embil, J.M. 2000. Characterization of a toxin A-negative, toxin B-positive strain of *Clostridium difficile* responsible for a nosocomial outbreak of *Clostridium difficile*-associated diarrhea. *J.Clin.Microbiol.*, 38, (7) 2706-2714

Ardavin, C. 2003. Origin, precursors and differentiation of mouse dendritic cells. *Nat.Rev.Immunol.*, 3, (7) 582-590

Artis, D. 2008. Epithelial-cell recognition of commensal bacteria and maintenance of immune homeostasis in the gut. *Nat.Rev.Immunol.*, 8, (6) 411-420

Ausiello, C.M., Cerquetti, M., Fedele, G., Spensieri, F., Palazzo, R., Nasso, M., Frezza, S., & Mastrantonio, P. 2006. Surface layer proteins from *Clostridium difficile* induce inflammatory and regulatory cytokines in human monocytes and dendritic cells. *Microbes.Infect.*, 8, (11) 2640-2646

Baker, S.S., Faden, H., Sayej, W., Patel, R., & Baker, R.D. 2010. Increasing incidence of community-associated atypical *Clostridium difficile* disease in children. *Clin.Pediatr.(Phila)*, 49, (7) 644-647

Balda, M.S. & Matter, K. 2008. Tight junctions at a glance. *J.Cell Sci.*, 121, (Pt 22) 3677-3682

Banchereau, J. & Steinman, R.M. 1998. Dendritic cells and the control of immunity. *Nature*, 392, (6673) 245-252

Barker, N., van de Wetering, M., & Clevers, H. 2008. The intestinal stem cell. *Genes Dev.*, 22, (14) 1856-1864

Bartlett, J.G., Moon, N., Chang, T.W., Taylor, N., & Onderdonk, A.B. 1978. Role of *Clostridium difficile* in antibiotic-associated pseudomembranous colitis. *Gastroenterology*, 75, (5) 778-782

Bartlett, J.G. 2006. Narrative review: the new epidemic of *Clostridium difficile*-associated enteric disease. *Ann.Intern.Med.*, 145, (10) 758-764

Baumgart, D.C. & Dignass, A.U. 2002. Intestinal barrier function. *Curr.Opin.Clin.Nutr.Metab Care*, 5, (6) 685-694

Beaugerie, L. & Petit, J.C. 2004. Microbial-gut interactions in health and disease. Antibiotic-associated diarrhoea. *Best.Pract.Res.Clin.Gastroenterol.*, 18, (2) 337-352

Belkaid, Y. & Tarbell, K. 2009. Regulatory T cells in the control of host-microorganism interactions. *Annu.Rev.Immunol.*, 27, 551-589

Bergsbaken, T., Fink, S.L., & Cookson, B.T. 2009. Pyroptosis: host cell death and inflammation. *Nat.Rev.Microbiol.*, 7, (2) 99-109

Bianco, M., Fedele, G., Quattrini, A., Spigaglia, P., Barbanti, F., Mastrantonio, P., & Ausiello, C.M. 2011. Immunomodulatory activities of surface-layer proteins obtained from epidemic and hypervirulent *Clostridium difficile* strains. *J.Med.Microbiol.*, 60, (Pt 8) 1162-1167

Bilsborough, J. & Viney, J.L. 2004. Gastrointestinal dendritic cells play a role in immunity, tolerance, and disease. *Gastroenterology*, 127, (1) 300-309

Blasius, A.L. & Beutler, B. 2010. Intracellular toll-like receptors. *Immunity.*, 32, (3) 305-315

Bongaerts, G.P. & Lyerly, D.M. 1994. Role of toxins A and B in the pathogenesis of *Clostridium difficile* disease. *Microb.Pathog.*, 17, (1) 1-12

Borriello, S.P., Welch, A.R., Barclay, F.E., & Davies, H.A. 1988. Mucosal association by *Clostridium difficile* in the hamster gastrointestinal tract. *J.Med.Microbiol.*, 25, (3) 191-196

Borriello, S.P., Davies, H.A., Kamiya, S., Reed, P.J., & Seddon, S. 1990. Virulence factors of *Clostridium difficile*. *Rev.Infect.Dis.*, 12 Suppl 2, S185-S191

Borriello, S.P., Wren, B.W., Hyde, S., Seddon, S.V., Sibbons, P., Krishna, M.M., Tabaqchali, S., Manek, S., & Price, A.B. 1992. Molecular, immunological, and biological characterization of a toxin A-negative, toxin B-positive strain of *Clostridium difficile*. *Infect.Immun.*, 60, (10) 4192-4199

Borriello, S.P. 1998. Pathogenesis of *Clostridium difficile* infection. *J.Antimicrob.Chemother.*, 41 Suppl C, 13-19

Branka, J.E., Vallette, G., Jarry, A., Bou-Hanna, C., Lemarre, P., Van, P.N., & Laboisse, C.L. 1997. Early functional effects of *Clostridium difficile* toxin A on human colonocytes. *Gastroenterology*, 112, (6) 1887-1894

Brito, G.A., Fujji, J., Carneiro-Filho, B.A., Lima, A.A., Obrig, T., & Guerrant, R.L. 2002. Mechanism of *Clostridium difficile* toxin A-induced apoptosis in T84 cells. *J.Infect.Dis.*, 186, (10) 1438-1447

Brombacher, F., Kastelein, R.A., & Alber, G. 2003. Novel IL-12 family members shed light on the orchestration of Th1 responses. *Trends Immunol.*, 24, (4) 207-212

Bruggemann, H. 2005. Genomics of clostridial pathogens: implication of extrachromosomal elements in pathogenicity. *Curr.Opin.Microbiol.*, 8, (5) 601-605

Buckley, A.M., Spencer, J., Candlish, D., Irvine, J.J., & Douce, G.R. 2011. Infection of hamsters with the UK *Clostridium difficile* ribotype 027 outbreak strain R20291. *J.Med.Microbiol.*, 60, (Pt 8) 1174-1180

Burckhardt, F., Friedrich, A., Beier, D., & Eckmanns, T. 2008. *Clostridium difficile* surveillance trends, Saxony, Germany. *Emerg.Infect.Dis*, 14, (4) 691-692

Burns, D.A., Heap, J.T., & Minton, N.P. 2010. *Clostridium difficile* spore germination: an update. *Res.Microbiol.*, 161, (9) 730-734

Burns, D.A. & Minton, N.P. 2011. Sporulation studies in *Clostridium difficile*. *J.Microbiol.Methods*

Calabi, E., Ward, S., Wren, B., Paxton, T., Panico, M., Morris, H., Dell, A., Dougan, G., & Fairweather, N. 2001. Molecular characterization of the surface layer proteins from *Clostridium difficile*. *Mol.Microbiol.*, 40, (5) 1187-1199

Calabi, E., Calabi, F., Phillips, A.D., & Fairweather, N.F. 2002. Binding of *Clostridium difficile* surface layer proteins to gastrointestinal tissues. *Infect.Immun.*, 70, (10) 5770-5778

Campbell, D.J. & Koch, M.A. 2011. Phenotypical and functional specialization of FOXP3+ regulatory T cells. *Nat.Rev.Immunol.*, 11, (2) 119-130

Canny, G., Drudy, D., Macmathuna, P., O'Farrelly, C., & Baird, A.W. 2006. Toxigenic *C. difficile* induced inflammatory marker expression by human intestinal epithelial cells is asymmetrical. *Life Sci.*, 78, (9) 920-925

Carroll, K.C. & Bartlett, J.G. 2010. Biology of *Clostridium difficile*: Implications for Epidemiology and Diagnosis. *Annu.Rev.Microbiol.*

Carter, G.P., Lyras, D., Allen, D.L., Mackin, K.E., Howarth, P.M., O'Connor, J.R., & Rood, J.I. 2007. Binary toxin production in *Clostridium difficile* is regulated by CdtR, a LytTR family response regulator. *J.Bacteriol.*, 189, (20) 7290-7301

Cartman, S.T., Heap, J.T., Kuehne, S.A., Cockayne, A., & Minton, N.P. 2010. The emergence of 'hypervirulence' in *Clostridium difficile*. *Int.J.Med.Microbiol.*, 300, (6) 387-395

Castagliuolo, I., Keates, A.C., Wang, C.C., Pasha, A., Valenick, L., Kelly, C.P., Nikulasson, S.T., LaMont, J.T., & Pothoulakis, C. 1998. *Clostridium difficile* toxin A stimulates macrophage-inflammatory protein-2 production in rat intestinal epithelial cells. *J.Immunol.*, 160, (12) 6039-6045

Cederlund, A., Gudmundsson, G.H., & Agerberth, B. 2011. Antimicrobial peptides important in innate immunity. *FEBS J.*, 278, (20) 3942-3951

Cerquetti, M., Molinari, A., Sebastianelli, A., Diociaiuti, M., Petruzzelli, R., Capo, C., & Mastrantonio, P. 2000. Characterization of surface layer proteins from different *Clostridium difficile* clinical isolates. *Microb.Pathog.*, 28, (6) 363-372

Cerquetti, M., Serafino, A., Sebastianelli, A., & Mastrantonio, P. 2002. Binding of *Clostridium difficile* to Caco-2 epithelial cell line and to extracellular matrix proteins. *FEMS Immunol.Med.Microbiol.*, 32, (3) 211-218

Cerutti, A. & Rescigno, M. 2008. The biology of intestinal immunoglobulin A responses. *Immunity.*, 28, (6) 740-750

Cerutti, A., Chen, K., & Chorny, A. 2011a. Immunoglobulin responses at the mucosal interface. *Annu.Rev.Immunol.*, 29, 273-293

Cerutti, A., Puga, I., & Cols, M. 2011b. Innate control of B cell responses. *Trends Immunol.*, 32, (5) 202-211

Chaves-Olarte, E., Low, P., Freer, E., Norlin, T., Weidmann, M., von Eichel-Streiber, C., & Thelestam, M. 1999. A novel cytotoxin from *Clostridium difficile* serogroup F is a functional hybrid between two other large clostridial cytotoxins. *J.Biol.Chem.*, 274, (16) 11046-11052

Chaves-Olarte, E., Freer, E., Parra, A., Guzman-Verri, C., Moreno, E., & Thelestam, M. 2003. R-Ras glucosylation and transient RhoA activation determine the cytopathic effect produced by toxin B variants from toxin A-negative strains of *Clostridium difficile*. *J.Biol.Chem.*, 278, (10) 7956-7963

Cheknis, A.K., Sambol, S.P., Davidson, D.M., Nagaro, K.J., Mancini, M.C., Hidalgo-Arroyo, G.A., Brazier, J.S., Johnson, S., & Gerding, D.N. 2009. Distribution of *Clostridium difficile* strains from a North American, European and Australian trial of treatment for *C. difficile* infections: 2005-2007. *Anaerobe.*, 15, (6) 230-233

Chen, M.L., Pothoulakis, C., & LaMont, J.T. 2002. Protein kinase C signaling regulates ZO-1 translocation and increased paracellular flux of T84 colonocytes exposed to *Clostridium difficile* toxin A. *J.Biol.Chem.*, 277, (6) 4247-4254

Chen, X., Katchar, K., Goldsmith, J.D., Nanthakumar, N., Cheknis, A., Gerding, D.N., & Kelly, C.P. 2008. A mouse model of *Clostridium difficile*-associated disease. *Gastroenterology*, 135, (6) 1984-1992

Cloud, J. & Kelly, C.P. 2007. Update on *Clostridium difficile* associated disease. *Curr.Opin.Gastroenterol.*, 23, (1) 4-9

Colbere-Garapin, F., Martin-Latil, S., Blondel, B., Mousson, L., Pelletier, I., Autret, A., Francois, A., Niborski, V., Grompone, G., Catonnet, G., & van de Moer, A. 2007. Prevention and treatment of enteric viral infections: possible benefits of probiotic bacteria. *Microbes.Infect.*, 9, (14-15) 1623-1631

Cunliffe, R.N. & Mahida, Y.R. 2004. Expression and regulation of antimicrobial peptides in the gastrointestinal tract. *J.Leukoc.Biol.*, 75, (1) 49-58

Curry, S.R., Marsh, J.W., Muto, C.A., O'Leary, M.M., Pasculle, A.W., & Harrison, L.H. 2007. tcdC genotypes associated with severe TcdC truncation in an epidemic clone and other strains of *Clostridium difficile*. *J.Clin.Microbiol.*, 45, (1) 215-221

Dallal, R.M., Harbrecht, B.G., Boujoukas, A.J., Sirio, C.A., Farkas, L.M., Lee, K.K., & Simmons, R.L. 2002. Fulminant *Clostridium difficile*: an underappreciated and increasing cause of death and complications. *Ann.Surg.*, 235, (3) 363-372

Daubener, W., Leiser, E., von Eichel-Streiber, C., & Hadding, U. 1988. *Clostridium difficile* toxins A and B inhibit human immune response in vitro. *Infect.Immun.*, 56, (5) 1107-1112

Davies, H.A. & Borriello, S.P. 1990. Detection of capsule in strains of *Clostridium difficile* of varying virulence and toxigenicity. *Microb.Pathog.*, 9, (2) 141-146

Dawson, L.F., Stabler, R.A., & Wren, B.W. 2008. Assessing the role of *p-cresol* tolerance in *Clostridium difficile*. *J.Med.Microbiol.*, 57, (Pt 6) 745-749

Dawson, L.F., Valiente, E., & Wren, B.W. 2009. *Clostridium difficile*-a continually evolving and problematic pathogen. *Infect.Genet.Evol.*, 9, (6) 1410-1417

Delaney, J.A., Dial, S., Barkun, A., & Suissa, S. 2007. Antimicrobial drugs and community-acquired *Clostridium difficile*-associated disease, UK. *Emerg.Infect.Dis*, 13, (5) 761-763

Delmee, M. & Avesani, V. 1990. Virulence of ten serogroups of *Clostridium difficile* in hamsters. *J.Med.Microbiol.*, 33, (2) 85-90

Deneve, C., Janoir, C., Poilane, I., Fantinato, C., & Collignon, A. 2009. New trends in *Clostridium difficile* virulence and pathogenesis. *Int.J.Antimicrob.Agents*, 33 Suppl 1, S24-S28

Depitre, C., Delmee, M., Avesani, V., L'Haridon, R., Roels, A., Popoff, M., & Corthier, G. 1993. Serogroup F strains of *Clostridium difficile* produce toxin B but not toxin A. *J.Med.Microbiol.*, 38, (6) 434-441

Dial, S., Delaney, J.A., Barkun, A.N., & Suissa, S. 2005. Use of gastric acid-suppressive agents and the risk of community-acquired *Clostridium difficile*-associated disease. *JAMA*, 294, (23) 2989-2995

Dineen, S.S., Villapakkam, A.C., Nordman, J.T., & Sonenshein, A.L. 2007. Repression of *Clostridium difficile* toxin gene expression by CodY. *Mol.Microbiol.*, 66, (1) 206-219

Dodson, A.P. & Borriello, S.P. 1996. *Clostridium difficile* infection of the gut. *J.Clin.Pathol.*, 49, (7) 529-532

Drudy, D., O'Donoghue, D.P., Baird, A., Fenelon, L., & O'Farrelly, C. 2001. Flow cytometric analysis of *Clostridium difficile* adherence to human intestinal epithelial cells. *J.Med.Microbiol.*, 50, (6) 526-534

Drudy, D., Calabi, E., Kyne, L., Sougioultzis, S., Kelly, E., Fairweather, N., & Kelly, C.P. 2004. Human antibody response to surface layer proteins in *Clostridium difficile* infection. *FEMS Immunol.Med.Microbiol.*, 41, (3) 237-242

Drudy, D., Fanning, S., & Kyne, L. 2007. Toxin A-negative, toxin B-positive *Clostridium difficile*. *Int.J.Infect.Dis.*, 11, (1) 5-10

Du, D., Xu, F., Yu, L., Zhang, C., Lu, X., Yuan, H., Huang, Q., Zhang, F., Bao, H., Jia, L., Wu, X., Zhu, X., Zhang, X., Zhang, Z., & Chen, Z. 2010. The tight junction protein, occludin, regulates the directional migration of epithelial cells. *Dev.Cell*, 18, (1) 52-63

Duerden, B.I. 2011. Contribution of a government target to controlling *Clostridium difficile* in the NHS in England. *Anaerobe.*, 17, (4) 175-179

Dupuy, B., Govind, R., Antunes, A., & Matamouros, S. 2008. *Clostridium difficile* toxin synthesis is negatively regulated by TcdC. *J.Med.Microbiol.*, 57, (Pt 6) 685-689

Eckmann, L., Kagnoff, M.F., & Fierer, J. 1995. Intestinal epithelial cells as watchdogs for the natural immune system. *Trends Microbiol.*, 3, (3) 118-120

Eckmann, L. 2005. Defence molecules in intestinal innate immunity against bacterial infections. *Curr.Opin.Gastroenterol.*, 21, (2) 147-151

Edwards, L.A., Nistala, K., Mills, D.C., Stephenson, H.N., Zilbauer, M., Wren, B.W., Dorrell, N., Lindley, K.J., Wedderburn, L.R., & Bajaj-Elliott, M. 2010. Delineation of the innate and adaptive T-cell immune outcome in the human host in response to *Campylobacter jejuni* infection. *PLoS.One.*, 5, (11) e15398

Egerer, M., Giesemann, T., Jank, T., Satchell, K.J., & Aktories, K. 2007. Auto-catalytic cleavage of *Clostridium difficile* toxins A and B depends on cysteine protease activity. *J.Biol.Chem.*, 282, (35) 25314-25321

Eveillard, M., Fourel, V., Barc, M.C., Kerneis, S., Coconnier, M.H., Karjalainen, T., Bourlioux, P., & Servin, A.L. 1993. Identification and characterization of adhesive factors of *Clostridium difficile* involved in adhesion to human colonic enterocyte-like Caco-2 and mucus-secreting HT29 cells in culture. *Mol.Microbiol.*, 7, (3) 371-381

Fagan, R.P., Albesa-Jove, D., Qazi, O., Svergun, D.I., Brown, K.A., & Fairweather, N.F. 2009. Structural insights into the molecular organization of the S-layer from *Clostridium difficile*. *Mol.Microbiol.*, 71, (5) 1308-1322

Feltis, B.A., Wiesner, S.M., Kim, A.S., Erlandsen, S.L., Lyerly, D.L., Wilkins, T.D., & Wells, C.L. 2000. *Clostridium difficile* toxins A and B can alter epithelial permeability and promote bacterial paracellular migration through HT-29 enterocytes. *Shock*, 14, (6) 629-634

Fiorentini, C., Fabbri, A., Falzano, L., Fattorossi, A., Matarrese, P., Rivabene, R., & Donelli, G. 1998. *Clostridium difficile* toxin B induces apoptosis in intestinal cultured cells. *Infect.Immun.*, 66, (6) 2660-2665

Flegel, W.A., Muller, F., Daubener, W., Fischer, H.G., Hadding, U., & Northoff, H. 1991. Cytokine response by human monocytes to *Clostridium difficile* toxin A and toxin B. *Infect.Immun.*, 59, (10) 3659-3666

Fordtran, J.S. 2006. Colitis due to *Clostridium difficile* toxins: underdiagnosed, highly virulent, and nosocomial. *Proc.(Bayl.Univ Med.Cent.)*, 19, (1) 3-12

Franchi, L., Eigenbrod, T., Munoz-Planillo, R., & Nunez, G. 2009. The inflammasome: a caspase-1-activation platform that regulates immune responses and disease pathogenesis. *Nat.Immunol.*, 10, (3) 241-247

Freeman, J., Bauer, M.P., Baines, S.D., Corver, J., Fawley, W.N., Goorhuis, B., Kuijper, E.J., & Wilcox, M.H. 2010. The changing epidemiology of *Clostridium difficile* infections. *Clin.Microbiol.Rev.*, 23, (3) 529-549

Gee, K., Guzzo, C., Che Mat, N.F., Ma, W., & Kumar, A. 2009. The IL-12 family of cytokines in infection, inflammation and autoimmune disorders. *Inflamm Allergy Drug Targets.*, 8, (1) 40-52

Genth, H., Huelsenbeck, J., Hartmann, B., Hofmann, F., Just, I., & Gerhard, R. 2006. Cellular stability of Rho-GTPases glucosylated by *Clostridium difficile* toxin B. *FEBS Lett.*, 580, (14) 3565-3569

Genth, H., Dreger, S.C., Huelsenbeck, J., & Just, I. 2008. *Clostridium difficile* toxins: more than mere inhibitors of Rho proteins. *Int.J.Biochem.Cell Biol.*, 40, (4) 592-597

George, R.H., Symonds, J.M., Dimock, F., Brown, J.D., Arabi, Y., Shinagawa, N., Keighley, M.R., Alexander-Williams, J., & Burdon, D.W. 1978. Identification of *Clostridium difficile* as a cause of pseudomembranous colitis. *Br.Med.J.*, 1, (6114) 695

Gerhard, R., Nottrott, S., Schoentaube, J., Tatge, H., Olling, A., & Just, I. 2008. Glucosylation of Rho GTPases by *Clostridium difficile* toxin A triggers apoptosis in intestinal epithelial cells. *J.Med.Microbiol.*, 57, (Pt 6) 765-770

Ghantoji, S.S., Sail, K., Lairson, D.R., DuPont, H.L., & Garey, K.W. 2010. Economic healthcare costs of *Clostridium difficile* infection: a systematic review. *J.Hosp.Infect.*, 74, (4) 309-318

Giesemann, T., Guttenberg, G., & Aktories, K. 2008. Human alpha-defensins inhibit *Clostridium difficile* toxin B. *Gastroenterology*, 134, (7) 2049-2058

Goorhuis, A., Bakker, D., Corver, J., Debast, S.B., Harmanus, C., Notermans, D.W., Bergwerff, A.A., Dekker, F.W., & Kuijper, E.J. 2008. Emergence of *Clostridium difficile* infection due to a new hypervirulent strain, polymerase chain reaction ribotype 078. *Clin.Infect.Dis.*, 47, (9) 1162-1170

Goriely, S., Neurath, M.F., & Goldman, M. 2008. How microorganisms tip the balance between interleukin-12 family members. *Nat.Rev.Immunol.*, 8, (1) 81-86

Groschwitz, K.R. & Hogan, S.P. 2009. Intestinal barrier function: molecular regulation and disease pathogenesis. *J.Allergy Clin.Immunol.*, 124, (1) 3-20

Guarner, F. & Malagelada, J.R. 2003. Gut flora in health and disease. *Lancet*, 361, (9356) 512-519

Guttman, J.A. & Finlay, B.B. 2009. Tight junctions as targets of infectious agents. *Biochim.Biophys.Acta*, 1788, (4) 832-841

Halabi-Cabezon, I., Huelsenbeck, J., May, M., Ladwein, M., Rottner, K., Just, I., & Genth, H. 2008. Prevention of the cytopathic effect induced by *Clostridium difficile* Toxin B by active Rac1. *FEBS Lett.*, 582, (27) 3751-3756

Hamouda, T., Shih, A.Y., & Baker, J.R., Jr. 2002. A rapid staining technique for the detection of the initiation of germination of bacterial spores. *Lett.Appl.Microbiol.*, 34, (2) 86-90

Haque, A., Bowe, F., Fitzhenry, R.J., Frankel, G., Thomson, M., Heuschkel, R., Murch, S., Stevens, M.P., Wallis, T.S., Phillips, A.D., & Dougan, G. 2004. Early interactions of *Salmonella enterica serovar typhimurium* with human small intestinal epithelial explants. *Gut*, 53, (10) 1424-1430

Harwood, N.E. & Batista, F.D. 2010. Early events in B cell activation. *Annu.Rev.Immunol.*, 28, 185-210

Hasegawa, M., Yamazaki, T., Kamada, N., Tawaratsumida, K., Kim, Y.G., Nunez, G., & Inohara, N. 2011. Nucleotide-binding oligomerization domain 1 mediates recognition of *Clostridium difficile* and induces neutrophil recruitment and protection against the pathogen. *J.Immunol.*, 186, (8) 4872-4880

HC, 2006. Investigation into outbreaks on *Clostridium difficile* at Stoke Mandeville Hospital, Buckinghamshire Hospitals NHS Trust, http://www.buckinghamshirehospitals.nhs.uk/healthcarecommision/HCC-Investigation-into-the-Outbreak-of-Clostridium-Difficile.pdf

He, M., Sebaihia, M., Lawley, T.D., Stabler, R.A., Dawson, L.F., Martin, M.J., Holt, K.E., Seth-Smith, H.M., Quail, M.A., Rance, R., Brooks, K., Churcher, C., Harris, D., Bentley, S.D., Burrows, C., Clark, L., Corton, C., Murray, V., Rose, G., Thurston, S., van, T.A., Walker, D., Wren, B.W., Dougan, G., & Parkhill, J. 2010. Evolutionary dynamics of *Clostridium difficile* over short and long time scales. *Proc.Natl.Acad.Sci.U.S.A*, 107, (16) 7527-7532

Hecht, G., Pothoulakis, C., LaMont, J.T., & Madara, J.L. 1988. *Clostridium difficile* toxin A perturbs cytoskeletal structure and tight junction permeability of cultured human intestinal epithelial monolayers. *J.Clin.Invest*, 82, (5) 1516-1524

Hecht, G., Koutsouris, A., Pothoulakis, C., LaMont, J.T., & Madara, J.L. 1992. *Clostridium difficile* toxin B disrupts the barrier function of T84 monolayers. *Gastroenterology*, 102, (2) 416-423

Hecht, G. 1999. Innate mechanisms of epithelial host defense: spotlight on intestine. *Am.J.Physiol*, 277, (3 Pt 1) C351-C358

Heinlen, L. & Ballard, J.D. 2010. *Clostridium difficile* infection. *Am.J.Med.Sci.*, 340, (3) 247-252

Hennequin, C., Porcheray, F., Waligora-Dupriet, A., Collignon, A., Barc, M., Bourlioux, P., & Karjalainen, T. 2001. GroEL (Hsp60) of *Clostridium difficile* is involved in cell adherence. *Microbiology*, 147, (Pt 1) 87-96

Hennequin, C., Janoir, C., Barc, M.C., Collignon, A., & Karjalainen, T. 2003. Identification and characterization of a fibronectin-binding protein from *Clostridium difficile*. *Microbiology*, 149, (Pt 10) 2779-2787

Hershberg, R.M. 2002. The epithelial cell cytoskeleton and intracellular trafficking. V. Polarized compartmentalization of antigen processing and Toll-like receptor signaling in intestinal epithelial cells. *Am.J.Physiol Gastrointest.Liver Physiol*, 283, (4) G833-G839

Hicks, S., Candy, D.C., & Phillips, A.D. 1996. Adhesion of enteroaggregative *Escherichia coli* to pediatric intestinal mucosa in vitro. *Infect.Immun.*, 64, (11) 4751-4760

Hoch, R.C., Schraufstatter, I.U., & Cochrane, C.G. 1996. In vivo, in vitro, and molecular aspects of interleukin-8 and the interleukin-8 receptors. *J.Lab Clin.Med.*, 128, (2) 134-145

Hunter, C.A. 2005. New IL-12-family members: IL-23 and IL-27, cytokines with divergent functions. *Nat.Rev.Immunol.*, 5, (7) 521-531

Hussain, H.A., Roberts, A.P., & Mullany, P. 2005. Generation of an erythromycin-sensitive derivative of *Clostridium difficile* strain 630 (630Δerm) and demonstration that the conjugative transposon Tn916ΔE enters the genome of this strain at multiple sites. *J.Med.Microbiol.* , 54, (Pt 2) 137-141

Iliev, I.D., Matteoli, G., & Rescigno, M. 2007. The yin and yang of intestinal epithelial cells in controlling dendritic cell function. *J.Exp.Med.*, 204, (10) 2253-2257

Ishida, Y., Maegawa, T., Kondo, T., Kimura, A., Iwakura, Y., Nakamura, S., & Mukaida, N. 2004. Essential involvement of IFN-gamma in *Clostridium difficile* toxin A-induced enteritis. *J.Immunol.*, 172, (5) 3018-3025

Iwasaki, A. & Medzhitov, R. 2004. Toll-like receptor control of the adaptive immune responses. *Nat.Immunol.*, 5, (10) 987-995

Jank, T. & Aktories, K. 2008. Structure and mode of action of clostridial glucosylating toxins: the ABCD model. *Trends Microbiol.*, 16, (5) 222-229

Janoir, C., Pechine, S., Grosdidier, C., & Collignon, A. 2007. Cwp84, a surface-associated protein of *Clostridium difficile*, is a cysteine protease with degrading activity on extracellular matrix proteins. *J.Bacteriol.*, 189, (20) 7174-7180

Jarchum, I., Liu, M., Lipuma, L., & Pamer, E.G. 2011. Toll-like receptor 5 stimulation protects mice from acute *Clostridium difficile* colitis. *Infect.Immun.*, 79, (4) 1498-1503

Jefferson, K.K., Smith, M.F., Jr., & Bobak, D.A. 1999. Roles of intracellular calcium and NF-kappa B in the *Clostridium difficile* toxin A-induced up-regulation and secretion of IL-8 from human monocytes. *J.Immunol.*, 163, (10) 5183-5191

Johal, S.S., Solomon, K., Dodson, S., Borriello, S.P., & Mahida, Y.R. 2004c. Differential effects of varying concentrations of *clostridium difficile* toxin A on epithelial barrier function and expression of cytokines. *J.Infect.Dis.*, 189, (11) 2110-2119

Johal, S.S., Hammond, J., Solomon, K., James, P.D., & Mahida, Y.R. 2004a. *Clostridium difficile* associated diarrhoea in hospitalised patients: onset in the community and hospital and role of flexible sigmoidoscopy. *Gut*, 53, (5) 673-677

Johal, S.S., Lambert, C.P., Hammond, J., James, P.D., Borriello, S.P., & Mahida, Y.R. 2004b. Colonic IgA producing cells and macrophages are reduced in recurrent and non-recurrent *Clostridium difficile* associated diarrhoea. *J.Clin.Pathol.*, 57, (9) 973-979

Johnson, S. & Gerding, D.N. 1998. *Clostridium difficile*-associated diarrhea. *Clin.Infect.Dis*, 26, (5) 1027-1034

Johnson, S., Sambol, S.P., Brazier, J.S., Delmee, M., Avesani, V., Merrigan, M.M., & Gerding, D.N. 2003. International typing study of toxin A-negative, toxin B-positive *Clostridium difficile* variants. *J.Clin.Microbiol.*, 41, (4) 1543-1547

Jou, T.S., Schneeberger, E.E., & Nelson, W.J. 1998. Structural and functional regulation of tight junctions by RhoA and Rac1 small GTPases. *J.Cell Biol.*, 142, (1) 101-115

Jung, H.C., Eckmann, L., Yang, S.K., Panja, A., Fierer, J., Morzycka-Wroblewska, E., & Kagnoff, M.F. 1995. A distinct array of proinflammatory cytokines is expressed in human colon epithelial cells in response to bacterial invasion. *J.Clin.Invest*, 95, (1) 55-65

Just, I., Fritz, G., Aktories, K., Giry, M., Popoff, M.R., Boquet, P., Hegenbarth, S., & von Eichel-Streiber, C. 1994. *Clostridium difficile* toxin B acts on the GTP-binding protein Rho. *J.Biol.Chem.*, 269, (14) 10706-10712

Just, I., Wilm, M., Selzer, J., Rex, G., von Eichel-Streiber, C., Mann, M., & Aktories, K. 1995. The enterotoxin from *Clostridium difficile* (ToxA) monoglucosylates the Rho proteins. *J.Biol.Chem.*, 270, (23) 13932-13936

Just, I. & Gerhard, R. 2004. Large clostridial cytotoxins. *Rev.Physiol Biochem.Pharmacol.*, 152, 23-47

Kachrimanidou, M. & Malisiovas, N. 2011. *Clostridium difficile* infection: a comprehensive review. *Crit Rev.Microbiol.*, 37, (3) 178-187

Kagnoff, M.F. & Eckmann, L. 1997. Epithelial cells as sensors for microbial infection. *J.Clin.Invest*, 100, (1) 6-10

Karjalainen, T., Barc, M.C., Collignon, A., Trolle, S., Boureau, H., Cotte-Laffitte, J., & Bourlioux, P. 1994. Cloning of a genetic determinant from *Clostridium difficile* involved in adherence to tissue culture cells and mucus. *Infect.Immun.*, 62, (10) 4347-4355

Karjalainen, T., Waligora-Dupriet, A.J., Cerquetti, M., Spigaglia, P., Maggioni, A., Mauri, P., & Mastrantonio, P. 2001. Molecular and genomic analysis of genes encoding surface-anchored proteins from *Clostridium difficile*. *Infect.Immun.*, 69, (5) 3442-3446

Kawai, T. & Akira, S. 2010. The role of pattern-recognition receptors in innate immunity: update on Toll-like receptors. *Nat.Immunol.*, 11, (5) 373-384

Keel, M.K. & Songer, J.G. 2006. The comparative pathology of *Clostridium difficile*-associated disease. *Vet.Pathol.*, 43, (3) 225-240

Kelly, C.P., Keates, S., Siegenberg, D., Linevsky, J.K., Pothoulakis, C., & Brady, H.R. 1994. IL-8 secretion and neutrophil activation by HT-29 colonic epithelial cells. *Am.J.Physiol*, 267, (6 Pt 1) G991-G997

Kelly, C.P. & LaMont, J.T. 1998. *Clostridium difficile* infection. *Annu.Rev.Med.*, 49, 375-390

Kelly, C.P. & LaMont, J.T. 2008. *Clostridium difficile*-more difficult than ever. *N.Engl.J.Med.*, 359, (18) 1932-1940

Kelly, D. & Conway, S. 2005. Bacterial modulation of mucosal innate immunity. *Mol.Immunol.*, 42, (8) 895-901

Kelsall, B. 2008. Recent progress in understanding the phenotype and function of intestinal dendritic cells and macrophages. *Mucosal.Immunol.*, 1, (6) 460-469

Khanna, S., Pardi, D.S., Aronson, S.L., Kammer, P.P., Orenstein, R., St Sauver, J.L., Harmsen, W.S., & Zinsmeister, A.R. 2012. The Epidemiology of Community-Acquired *Clostridium difficile* Infection: A Population-Based Study. *Am.J.Gastroenterol.*, 107, (1) 89-95

Kim, C., Gajendran, N., Mittrucker, H.W., Weiwad, M., Song, Y.H., Hurwitz, R., Wilmanns, M., Fischer, G., & Kaufmann, S.H. 2005. Human alpha-defensins neutralize anthrax lethal toxin and protect against its fatal consequences. *Proc.Natl.Acad.Sci.U.S.A*, 102, (13) 4830-4835

Kim, C., Slavinskaya, Z., Merrill, A.R., & Kaufmann, S.H. 2006a. Human alpha-defensins neutralize toxins of the mono-ADP-ribosyltransferase family. *Biochem.J.*, 399, (2) 225-229

Kim, J., Smathers, S.A., Prasad, P., Leckerman, K.H., Coffin, S., & Zaoutis, T. 2008. Epidemiological features of *Clostridium difficile*-associated disease among inpatients at children's hospitals in the United States, 2001-2006. *Pediatrics*, 122, (6) 1266-1270

Kim, J.M., Kim, J.S., Jun, H.C., Oh, Y.K., Song, I.S., & Kim, C.Y. 2002. Differential expression and polarized secretion of CXC and CC chemokines by human intestinal epithelial cancer cell lines in response to *Clostridium difficile* toxin A. *Microbiol.Immunol.*, 46, (5) 333-342

Kim, J.M., Lee, J.Y., Yoon, Y.M., Oh, Y.K., Youn, J., & Kim, Y.J. 2006b. NF-kappa B activation pathway is essential for the chemokine expression in intestinal epithelial cells stimulated with *Clostridium difficile* toxin A. *Scand.J.Immunol.*, 63, (6) 453-460

Knoop, F.C. 1979. Clindamycin-associated enterocolitis in guinea pigs: evidence for a bacterial toxin. *Infect.Immun.*, 23, (1) 31-33

Kraehenbuhl, J.P. & Corbett, M. 2004. Immunology. Keeping the gut microflora at bay. *Science*, 303, (5664) 1624-1625

Kuehne, S.A., Cartman, S.T., Heap, J.T., Kelly, M.L., Cockayne, A., & Minton, N.P. 2010. The role of toxin A and toxin B in *Clostridium difficile* infection. *Nature*, 467, (7316) 711-713

Kuehne, S.A., Cartman, S.T., & Minton, N.P. 2011. Both, toxin A and toxin B, are important in *Clostridium difficile* infection. *Gut Microbes.*, 2, (4)

Kyne, L., Warny, M., Qamar, A., & Kelly, C.P. 2000. Asymptomatic carriage of *Clostridium difficile* and serum levels of IgG antibody against toxin A. *N.Engl.J.Med.*, 342, (6) 390-397

Kyne, L. & Kelly, C.P. 2001. Recurrent *Clostridium difficile* diarrhoea. *Gut*, 49, (1) 152-153

Kyne, L., Warny, M., Qamar, A., & Kelly, C.P. 2001. Association between antibody response to toxin A and protection against recurrent *Clostridium difficile* diarrhoea. *Lancet*, 357, (9251) 189-193

Kyne, L. 2010. *Clostridium difficile*-beyond antibiotics. *N.Engl.J.Med.*, 362, (3) 264-265

Lamkanfi, M., Kanneganti, T.D., Franchi, L., & Nunez, G. 2007. Caspase-1 inflammasomes in infection and inflammation. *J.Leukoc.Biol.*, 82, (2) 220-225

Lanis, J.M., Barua, S., & Ballard, J.D. 2010. Variations in TcdB activity and the hypervirulence of emerging strains of *Clostridium difficile*. *PLoS.Pathog.*, 6, (8) e1001061

Lawley, T.D., Clare, S., Walker, A.W., Goulding, D., Stabler, R.A., Croucher, N., Mastroeni, P., Scott, P., Raisen, C., Mottram, L., Fairweather, N.F., Wren, B.W., Parkhill, J., & Dougan, G. 2009. Antibiotic treatment of *clostridium difficile* carrier mice triggers a supershedder state, spore-mediated transmission, and severe disease in immunocompromised hosts. *Infect.Immun.*, 77, (9) 3661-3669

Lee, J.Y., Park, H.R., Oh, Y.K., Kim, Y.J., Youn, J., Han, J.S., & Kim, J.M. 2007. Effects of transcription factor activator protein-1 on interleukin-8 expression and enteritis in response to *Clostridium difficile* toxin A. *J.Mol.Med.(Berl)*, 85, (12) 1393-1404

Lee, J.Y., Kim, H., Cha, M.Y., Park, H.G., Kim, Y.J., Kim, I.Y., & Kim, J.M. 2009. *Clostridium difficile* toxin A promotes dendritic cell maturation and chemokine CXCL2 expression through p38, IKK, and the NF-kappaB signaling pathway. *J.Mol.Med.(Berl)*, 87, (2) 169-180

Li, X., Jiang, S., & Tapping, R.I. 2010. Toll-like receptor signaling in cell proliferation and survival. *Cytokine*, 49, (1) 1-9

Linevsky, J.K., Pothoulakis, C., Keates, S., Warny, M., Keates, A.C., LaMont, J.T., & Kelly, C.P. 1997. IL-8 release and neutrophil activation by *Clostridium difficile* toxin-exposed human monocytes. *Am.J.Physiol*, 273, (6 Pt 1) G1333-G1340

Lyerly, D.M., Saum, K.E., MacDonald, D.K., & Wilkins, T.D. 1985. Effects of *Clostridium difficile* toxins given intragastrically to animals. *Infect.Immun.*, 47, (2) 349-352

Lyerly, D.M., Krivan, H.C., & Wilkins, T.D. 1988. *Clostridium difficile*: its disease and toxins. *Clin.Microbiol.Rev.*, 1, (1) 1-18

Lyras, D., Adams, V., Lucet, I., & Rood, J.I. 2004. The large resolvase TnpX is the only transposon-encoded protein required for transposition of the Tn4451/3 family of integrative mobilizable elements. *Mol.Microbiol.*, 51, (6) 1787-1800

Lyras, D., O'Connor, J.R., Howarth, P.M., Sambol, S.P., Carter, G.P., Phumoonna, T., Poon, R., Adams, V., Vedantam, G., Johnson, S., Gerding, D.N., & Rood, J.I. 2009. Toxin B is essential for virulence of *Clostridium difficile*. *Nature*, 458, (7242) 1176-1179

Ma, C.S., Tangye, S.G., & Deenick, E.K. 2010. Human Th9 cells: inflammatory cytokines modulate IL-9 production through the induction of IL-21. *Immunol.Cell Biol.*, 88, (6) 621-623

Macdonald, T.T. & Monteleone, G. 2005. Immunity, inflammation, and allergy in the gut. *Science*, 307, (5717) 1920-1925

Mahida, Y.R., Makh, S., Hyde, S., Gray, T., & Borriello, S.P. 1996. Effect of *Clostridium difficile* toxin A on human intestinal epithelial cells: induction of interleukin 8 production and apoptosis after cell detachment. *Gut*, 38, (3) 337-347

Mahida, Y.R., Galvin, A., Makh, S., Hyde, S., Sanfilippo, L., Borriello, S.P., & Sewell, H.F. 1998. Effect of *Clostridium difficile* toxin A on human colonic lamina propria cells: early loss of macrophages followed by T-cell apoptosis. *Infect.Immun.*, 66, (11) 5462-5469

Mahida, Y.R. 2004. Microbial-gut interactions in health and disease. Epithelial cell responses. *Best.Pract.Res.Clin.Gastroenterol.*, 18, (2) 241-253

Malefyt, R.W. 2009. Interleukin-17 kick-starts T helper 1 cell differentiation. *Immunity.*, 31, (5) 700-702

Matamouros, S., England, P., & Dupuy, B. 2007. *Clostridium difficile* toxin expression is inhibited by the novel regulator TcdC. *Mol.Microbiol.*, 64, (5) 1274-1288

Matarrese, P., Falzano, L., Fabbri, A., Gambardella, L., Frank, C., Geny, B., Popoff, M.R., Malorni, W., & Fiorentini, C. 2007. *Clostridium difficile* toxin B causes apoptosis in epithelial cells by thrilling mitochondria. Involvement of ATP-sensitive mitochondrial potassium channels. *J.Biol.Chem.*, 282, (12) 9029-9041

Melo Filho, A.A., Souza, M.H., Lyerly, D.M., Cunha, F.Q., Lima, A.A., & Ribeiro, R.A. 1997. Role of tumor necrosis factor and nitric oxide in the cytotoxic effects of *Clostridium difficile* toxin A and toxin B on macrophages. *Toxicon*, 35, (5) 743-752

Meyer, G.K., Neetz, A., Brandes, G., Tsikas, D., Butterfield, J.H., Just, I., & Gerhard, R. 2007. *Clostridium difficile* toxins A and B directly stimulate human mast cells. *Infect.Immun.*, 75, (8) 3868-3876

Miura, M., Kato, H., & Matsushita, O. 2011. Identification of a novel virulence factor in *clostridium difficile* that modulates toxin sensitivity of cultured epithelial cells. *Infect.Immun.*, 79, (9) 3810-3820

Monaghan, T., Boswell, T., & Mahida, Y.R. 2008. Recent advances in *Clostridium difficile*-associated disease. *Gut*, 57, (6) 850-860

Moran, A.P., Gupta, A., & Joshi, L. 2011. Sweet-talk: role of host glycosylation in bacterial pathogenesis of the gastrointestinal tract. *Gut*, 60, (10) 1412-1425

Mowat, A.M. 2003. Anatomical basis of tolerance and immunity to intestinal antigens. *Nat.Rev.Immunol.*, 3, (4) 331-341

Mumy, K.L. & McCormick, B.A. 2005. Events at the host-microbial interface of the gastrointestinal tract. II. Role of the intestinal epithelium in pathogen-induced inflammation. *Am.J.Physiol Gastrointest.Liver Physiol*, 288, (5) G854-G859

Na, X., Zhao, D., Koon, H.W., Kim, H., Husmark, J., Moyer, M.P., Pothoulakis, C., & LaMont, J.T. 2005. *Clostridium difficile* toxin B activates the EGF receptor and the ERK/MAP kinase pathway in human colonocytes. *Gastroenterology*, 128, (4) 1002-1011

Na, X., Kim, H., Moyer, M.P., Pothoulakis, C., & LaMont, J.T. 2008. gp96 is a human colonocyte plasma membrane binding protein for *Clostridium difficile* toxin A. *Infect.Immun.*, 76, (7) 2862-2871

Nemeth, Z.H., Deitch, E.A., Davidson, M.T., Szabo, C., Vizi, E.S., & Hasko, G. 2004. Disruption of the actin cytoskeleton results in nuclear factor-kappaB activation and inflammatory mediator production in cultured human intestinal epithelial cells. *J.Cell Physiol*, 200, (1) 71-81

Netea, M.G., van der Graaf, C., Van der Meer, J.W., & Kullberg, B.J. 2004. Toll-like receptors and the host defense against microbial pathogens: bringing specificity to the innate-immune system. *J.Leukoc.Biol.*, 75, (5) 749-755

Ng, E.K., Panesar, N., Longo, W.E., Shapiro, M.J., Kaminski, D.L., Tolman, K.C., & Mazuski, J.E. 2003. Human intestinal epithelial and smooth muscle cells are potent producers of IL-6. *Mediators.Inflamm*, 12, (1) 3-8

Ng, J., Hirota, S.A., Gross, O., Li, Y., Ulke-Lemee, A., Potentier, M.S., Schenck, L.P., Vilaysane, A., Seamone, M.E., Feng, H., Armstrong, G.D., Tschopp, J., Macdonald, J.A., Muruve, D.A., & Beck, P.L. 2010. *Clostridium difficile* toxin-induced inflammation and intestinal injury are mediated by the inflammasome. *Gastroenterology*, 139, (2) 542-52, 552

Niedergang, F. & Kweon, M.N. 2005. New trends in antigen uptake in the gut mucosa. *Trends Microbiol.*, 13, (10) 485-490

Niess, J.H., Brand, S., Gu, X., Landsman, L., Jung, S., McCormick, B.A., Vyas, J.M., Boes, M., Ploegh, H.L., Fox, J.G., Littman, D.R., & Reinecker, H.C. 2005. CX3CR1-mediated dendritic cell access to the intestinal lumen and bacterial clearance. *Science*, 307, (5707) 254-258

Niess, J.H. & Reinecker, H.C. 2005. Lamina propria dendritic cells in the physiology and pathology of the gastrointestinal tract. *Curr.Opin.Gastroenterol.*, 21, (6) 687-691

Niess, J.H. & Reinecker, H.C. 2006. Dendritic cells in the recognition of intestinal microbiota. *Cell Microbiol.*, 8, (4) 558-564

Nottrott, S., Schoentaube, J., Genth, H., Just, I., & Gerhard, R. 2007. *Clostridium difficile* toxin A-induced apoptosis is p53-independent but depends on glucosylation of Rho GTPases. *Apoptosis.*, 12, (8) 1443-1453

Nusrat, A., von Eichel-Streiber, C., Turner, J.R., Verkade, P., Madara, J.L., & Parkos, C.A. 2001. *Clostridium difficile* toxins disrupt epithelial barrier function by altering membrane microdomain localization of tight junction proteins. *Infect.Immun.*, 69, (3) 1329-1336

O'Connor, J.R., Johnson, S., & Gerding, D.N. 2009. *Clostridium difficile* infection caused by the epidemic BI/NAP1/027 strain. *Gastroenterology*, 136, (6) 1913-1924

Ochsner, U.A., Bell, S.J., O'Leary, A.L., Hoang, T., Stone, K.C., Young, C.L., Critchley, I.A., & Janjic, N. 2009. Inhibitory effect of REP3123 on toxin and spore formation in *Clostridium difficile*, and in vivo efficacy in a hamster gastrointestinal infection model. *J.Antimicrob.Chemother.*, 63, (5) 964-971

Paredes-Sabja, D., Bond, C., Carman, R.J., Setlow, P., & Sarker, M.R. 2008. Germination of spores of *Clostridium difficile* strains, including isolates from a hospital outbreak of *Clostridium difficile*-associated disease (CDAD). *Microbiology*, 154, (Pt 8) 2241-2250

Paredes, C.J., Alsaker, K.V., & Papoutsakis, E.T. 2005. A comparative genomic view of clostridial sporulation and physiology. *Nat.Rev.Microbiol.*, 3, (12) 969-978

Pastorelli, L., Vecchi, M., Cominelli, F., & Pizarro, T.T. 2008. Genetic regulation of epithelial barrier function: Recent insights into the pathogenesis of inflammatory bowel disease. *Inflamm Bowel Dis Monit*., 8, (4) 124-133

Paul, W.E. & Zhu, J. 2010. How are T(H)2-type immune responses initiated and amplified? *Nat.Rev.Immunol.*, 10, (4) 225-235

Philpott, D.J. & Girardin, S.E. 2010. Nod-like receptors: sentinels at host membranes. *Curr.Opin.Immunol.*, 22, (4) 428-434

Popoff, M.R. & Geny, B. 2009. Multifaceted role of Rho, Rac, Cdc42 and Ras in intercellular junctions, lessons from toxins. *Biochim.Biophys.Acta*, 1788, (4) 797-812

Popoff, M.R. & Geny, B. 2011. Rho/Ras-GTPase-dependent and -independent activity of clostridial glucosylating toxins. *J.Med.Microbiol.*, 60, (Pt 8) 1057-1069

Pothoulakis, C., Castagliuolo, I., LaMont, J.T., Jaffer, A., O'Keane, J.C., Snider, R.M., & Leeman, S.E. 1994. CP-96,345, a substance P antagonist, inhibits rat intestinal responses to *Clostridium difficile* toxin A but not cholera toxin. *Proc.Natl.Acad.Sci.U.S.A*, 91, (3) 947-951

Price, A.B., Larson, H.E., & Crow, J. 1979. Morphology of experimental antibiotic-associated enterocolitis in the hamster: a model for human pseudomembranous colitis and antibiotic-associated diarrhoea. *Gut*, 20, (6) 467-475

Qa'Dan, M., Ramsey, M., Daniel, J., Spyres, L.M., Safiejko-Mroczka, B., Ortiz-Leduc, W., & Ballard, J.D. 2002. *Clostridium difficile* toxin B activates dual caspase-dependent and caspase-independent apoptosis in intoxicated cells. *Cell Microbiol.*, 4, (7) 425-434

Radtke, F. & Clevers, H. 2005. Self-renewal and cancer of the gut: two sides of a coin. *Science*, 307, (5717) 1904-1909

Reineke, J., Tenzer, S., Rupnik, M., Koschinski, A., Hasselmayer, O., Schrattenholz, A., Schild, H., & von Eichel-Streiber, C. 2007. Autocatalytic cleavage of *Clostridium difficile* toxin B. *Nature*, 446, (7134) 415-419

Reiner, S.L. 2007. Development in motion: helper T cells at work. *Cell*, 129, (1) 33-36

Reis e Sousa 2006. Dendritic cells in a mature age. *Nat.Rev.Immunol.*, 6, (6) 476-483

Rescigno, M. 2002. Dendritic cells and the complexity of microbial infection. *Trends Microbiol.*, 10, (9) 425-461

Rhee, K.J., Wu, S., Wu, X., Huso, D.L., Karim, B., Franco, A.A., Rabizadeh, S., Golub, J.E., Mathews, L.E., Shin, J., Sartor, R.B., Golenbock, D., Hamad, A.R., Gan, C.M., Housseau, F., & Sears, C.L. 2009. Induction of persistent colitis by a human commensal, enterotoxigenic Bacteroides fragilis, in wild-type C57BL/6 mice. *Infect.Immun.*, 77, (4) 1708-1718

Riegler, M., Sedivy, R., Pothoulakis, C., Hamilton, G., Zacherl, J., Bischof, G., Cosentini, E., Feil, W., Schiessel, R., LaMont, J.T., & Wenzl, E. 1995. *Clostridium difficile* toxin B is more potent than toxin A in damaging human colonic epithelium in vitro. *J.Clin.Invest*, 95, (5) 2004-2011

Rimoldi, M., Chieppa, M., Salucci, V., Avogadri, F., Sonzogni, A., Sampietro, G.M., Nespoli, A., Viale, G., Allavena, P., & Rescigno, M. 2005. Intestinal immune homeostasis is regulated by the crosstalk between epithelial cells and dendritic cells. *Nat.Immunol.*, 6, (5) 507-514

Rocha, M.F., Maia, M.E., Bezerra, L.R., Lyerly, D.M., Guerrant, R.L., Ribeiro, R.A., & Lima, A.A. 1997. *Clostridium difficile* toxin A induces the release of neutrophil chemotactic factors from rat peritoneal macrophages: role of interleukin-1beta, tumor necrosis factor alpha, and leukotrienes. *Infect.Immun.*, 65, (7) 2740-2746

Rupnik, M., Brazier, J.S., Duerden, B.I., Grabnar, M., & Stubbs, S.L. 2001. Comparison of toxinotyping and PCR ribotyping of *Clostridium difficile* strains and description of novel toxinotypes. *Microbiology*, 147, (Pt 2) 439-447

Rupnik, M., Grabnar, M., & Geric, B. 2003a. Binary toxin producing *Clostridium difficile* strains. *Anaerobe.*, 9, (6) 289-294

Rupnik, M., Kato, N., Grabnar, M., & Kato, H. 2003b. New types of toxin A-negative, toxin B-positive strains among *Clostridium difficile* isolates from Asia. *J.Clin.Microbiol.*, 41, (3) 1118-1125

Rupnik, M., Pabst, S., Rupnik, M., von Eichel-Streiber, C., Urlaub, H., & Soling, H.D. 2005. Characterization of the cleavage site and function of resulting cleavage fragments after limited proteolysis of *Clostridium difficile* toxin B (TcdB) by host cells. *Microbiology*, 151, (Pt 1) 199-208

Rupnik, M. 2007. Is *Clostridium difficile*-associated infection a potentially zoonotic and foodborne disease? *Clin.Microbiol.Infect.*, 13, (5) 457-459

Rupnik, M., Wilcox, M.H., & Gerding, D.N. 2009. *Clostridium difficile* infection: new developments in epidemiology and pathogenesis. *Nat.Rev.Microbiol.*, 7, (7) 526-536

Ryan, A., Lynch, M., Smith, S.M., Amu, S., Nel, H.J., McCoy, C.E., Dowling, J.K., Draper, E., O'Reilly, V., McCarthy, C., O'Brien, J., Ni, E.D., O'Connell, M.J., Keogh, B., Morton, C.O., Rogers, T.R., Fallon, P.G., O'Neill, L.A., Kelleher, D., & Loscher, C.E. 2011. A Role for TLR4 in *Clostridium difficile* Infection and the Recognition of Surface Layer Proteins. *PLoS.Pathog.*, 7, (6) e1002076

Savidge, T.C., Pan, W.H., Newman, P., O'brien, M., Anton, P.M., & Pothoulakis, C. 2003. *Clostridium difficile* toxin B is an inflammatory enterotoxin in human intestine. *Gastroenterology*, 125, (2) 413-420

Schuller, S., Lucas, M., Kaper, J.B., Giron, J.A., & Phillips, A.D. 2009. The *ex vivo* response of human intestinal mucosa to enteropathogenic *Escherichia coli* infection. *Cell Microbiol.*, 11, (3) 521-530

Schuller, S. & Phillips, A.D. 2010. Microaerobic conditions enhance type III secretion and adherence of enterohaemorrhagic *Escherichia coli* to polarized human intestinal epithelial cells. *Environ.Microbiol.*, 12, (9) 2426-2435

Schwan, C., Stecher, B., Tzivelekidis, T., van, H.M., Rohde, M., Hardt, W.D., Wehland, J., & Aktories, K. 2009. *Clostridium difficile* toxin CDT induces formation of microtubule-based protrusions and increases adherence of bacteria. *PLoS.Pathog.*, 5, (10) e1000626

Sears, C.L. 2005. A dynamic partnership: celebrating our gut flora. *Anaerobe.*, 11, (5) 247-251

Sebaihia, M., Wren, B.W., Mullany, P., Fairweather, N.F., Minton, N., Stabler, R., Thomson, N.R., Roberts, A.P., Cerdeno-Tarraga, A.M., Wang, H., Holden, M.T., Wright, A., Churcher, C., Quail, M.A., Baker, S., Bason, N., Brooks, K., Chillingworth, T., Cronin, A., Davis, P., Dowd, L., Fraser, A., Feltwell, T., Hance, Z., Holroyd, S., Jagels, K., Moule, S., Mungall, K., Price, C., Rabbinowitsch, E., Sharp, S., Simmonds, M., Stevens, K., Unwin, L., Whithead, S., Dupuy, B., Dougan, G., Barrell, B., & Parkhill, J. 2006. The multidrug-resistant human pathogen *Clostridium difficile* has a highly mobile, mosaic genome. *Nat.Genet.*, 38, (7) 779-786

Soehn, F., Wagenknecht-Wiesner, A., Leukel, P., Kohl, M., Weidmann, M., von Eichel-Streiber, C., & Braun, V. 1998. Genetic rearrangements in the pathogenicity locus of *Clostridium difficile* strain 8864-implications for transcription, expression and enzymatic activity of toxins A and B. *Mol.Gen.Genet.*, 258, (3) 222-232

Soler, P., Nogareda, F., & Cano, R. 2008. Rates of *Clostridium difficile* infection in patients discharged from Spanish hospitals, 1997-2005. *Infect.Control Hosp.Epidemiol.*, 29, (9) 887-889

Solomon, K., Webb, J., Ali, N., Robins, R.A., & Mahida, Y.R. 2005. Monocytes are highly sensitive to *clostridium difficile* toxin A-induced apoptotic and nonapoptotic cell death. *Infect.Immun.*, 73, (3) 1625-1634

Songer, J.G. & Anderson, M.A. 2006. *Clostridium difficile*: an important pathogen of food animals. *Anaerobe.*, 12, (1) 1-4

Sorg, J.A. & Sonenshein, A.L. 2008. Bile salts and glycine as cogerminants for *Clostridium difficile* spores. *J.Bacteriol.* , 190, (7) 2505-2512

Souza, M.H., Melo-Filho, A.A., Rocha, M.F., Lyerly, D.M., Cunha, F.Q., Lima, A.A., & Ribeiro, R.A. 1997. The involvement of macrophage-derived tumour necrosis factor and lipoxygenase products on the neutrophil recruitment induced by *Clostridium difficile* toxin B. *Immunology*, 91, (2) 281-288

Spencer, J., Barone, F., & Dunn-Walters, D. 2009. Generation of Immunoglobulin diversity in human gut-associated lymphoid tissue. *Semin.Immunol.*, 21, (3) 139-146

Spigaglia, P. & Mastrantonio, P. 2002. Molecular analysis of the pathogenicity locus and polymorphism in the putative negative regulator of toxin production (TcdC) among *Clostridium difficile* clinical isolates. *J.Clin.Microbiol.*, 40, (9) 3470-3475

Spigaglia, P., Barbanti, F., Mastrantonio, P., Brazier, J.S., Barbut, F., Delmee, M., Kuijper, E., & Poxton, I.R. 2008. Fluoroquinolone resistance in *Clostridium difficile* isolates from a prospective study of C. difficile infections in Europe. *J.Med.Microbiol.*, 57, (Pt 6) 784-789

Springer, T.A. 1994. Traffic signals for lymphocyte recirculation and leukocyte emigration: the multistep paradigm. *Cell*, 76, (2) 301-314

Stabler, R.A., Gerding, D.N., Songer, J.G., Drudy, D., Brazier, J.S., Trinh, H.T., Witney, A.A., Hinds, J., & Wren, B.W. 2006. Comparative phylogenomics of *Clostridium difficile* reveals clade specificity and microevolution of hypervirulent strains. *J.Bacteriol.*, 188, (20) 7297-7305

Stabler, R.A., Dawson, L.F., Phua, L.T., & Wren, B.W. 2008. Comparative analysis of BI/NAP1/027 hypervirulent strains reveals novel toxin B-encoding gene (tcdB) sequences. *J.Med.Microbiol.*, 57, (Pt 6) 771-775

Stabler, R.A., He, M., Dawson, L., Martin, M., Valiente, E., Corton, C., Lawley, T.D., Sebaihia, M., Quail, M.A., Rose, G., Gerding, D.N., Gibert, M., Popoff, M.R., Parkhill, J., Dougan, G., & Wren, B.W. 2009. Comparative genome and phenotypic analysis of *Clostridium difficile* 027 strains provides insight into the evolution of a hypervirulent bacterium. *Genome Biol.*, 10, (9) R102

Steele, J., Feng, H., Parry, N., & Tzipori, S. 2010. Piglet models of acute or chronic *Clostridium difficile* illness. *J.Infect.Dis*, 201, (3) 428-434

Steinman, R.M. 1991. The dendritic cell system and its role in immunogenicity. *Annu.Rev.Immunol.*, 9, 271-296

Steinman, R.M. 2007. Dendritic cells: understanding immunogenicity. *Eur.J.Immunol.*, 37 Suppl 1, S53-S60

Stockinger, B. & Veldhoen, M. 2007. Differentiation and function of Th17 T cells. *Curr.Opin.Immunol.*, 19, (3) 281-286

Stockinger, B., Veldhoen, M., & Martin, B. 2007. Th17 T cells: linking innate and adaptive immunity. *Semin.Immunol.*, 19, (6) 353-361

Stoddart, B. & Wilcox, M.H. 2002. *Clostridium difficile*. *Curr.Opin.Infect.Dis*, 15, (5) 513-518

Stubbs, S., Rupnik, M., Gibert, M., Brazier, J., Duerden, B., & Popoff, M. 2000. Production of actin-specific ADP-ribosyltransferase (binary toxin) by strains of *Clostridium difficile*. *FEMS Microbiology Letters*, 186, (2) 307-312

Sun, X., He, X., Tzipori, S., Gerhard, R., & Feng, H. 2009. Essential role of the glucosyltransferase activity in *Clostridium difficile* toxin-induced secretion of TNF-alpha by macrophages. *Microb.Pathog.*, 46, (6) 298-305

Sutton, P.A., Li, S., Webb, J., Solomon, K., Brazier, J., & Mahida, Y.R. 2008. Essential role of toxin A in *C. difficile* 027 and reference strain supernatant-mediated disruption of Caco-2 intestinal epithelial barrier function. *Clin.Exp.Immunol.*, 153, (3) 439-447

Szabo, S.J., Kim, S.T., Costa, G.L., Zhang, X., Fathman, C.G., & Glimcher, L.H. 2000. A novel transcription factor, T-bet, directs Th1 lineage commitment. *Cell*, 100, (6) 655-669

Tan, K.S., Wee, B.Y., & Song, K.P. 2001. Evidence for holin function of tcdE gene in the pathogenicity of *Clostridium difficile*. *J.Med.Microbiol.*, 50, (7) 613-619

Tapping, R.I. 2009. Innate immune sensing and activation of cell surface Toll-like receptors. *Semin.Immunol.*, 21, (4) 175-184

Tasteyre, A., Barc, M.C., Collignon, A., Boureau, H., & Karjalainen, T. 2001. Role of FliC and FliD flagellar proteins of *Clostridium difficile* in adherence and gut colonization. *Infect.Immun.*, 69, (12) 7937-7940

Terry, S., Nie, M., Matter, K., & Balda, M.S. 2010. Rho signaling and tight junction functions. *Physiology.(Bethesda.)*, 25, (1) 16-26

Tixier, E., Lalanne, F., Just, I., Galmiche, J.P., & Neunlist, M. 2005. Human mucosa/submucosa interactions during intestinal inflammation: involvement of the enteric nervous system in interleukin-8 secretion. *Cell Microbiol.*, 7, (12) 1798-1810

Torres, J., Camorlinga-Ponce, M., & Munoz, O. 1992. Sensitivity in culture of epithelial cells from rhesus monkey kidney and human colon carcinoma to toxins A and B from *Clostridium difficile*. *Toxicon*, 30, (4) 419-426

Torres, J.F. 1991. Purification and characterisation of toxin B from a strain of *Clostridium difficile* that does not produce toxin A. *J.Med.Microbiol.*, 35, (1) 40-44

Trinchieri, G. 2003. Interleukin-12 and the regulation of innate resistance and adaptive immunity. *Nat.Rev.Immunol.*, 3, (2) 133-146

Turner, J.R. 2009. Intestinal mucosal barrier function in health and disease. *Nat.Rev.Immunol.*, 9, (11) 799-809

Twine, S.M., Reid, C.W., Aubry, A., McMullin, D.R., Fulton, K.M., Austin, J., & Logan, S.M. 2009. Motility and flagellar glycosylation in *Clostridium difficile*. *J.Bacteriol.*, 191, (22) 7050-7062

Vandekerckhove, J., Schering, B., Barmann, M., & Aktories, K. 1987. *Clostridium perfringens* iota toxin ADP-ribosylates skeletal muscle actin in Arg-177. *FEBS Lett.*, 225, (1-2) 48-52

Vernacchio, L., Vezina, R.M., Mitchell, A.A., Lesko, S.M., Plaut, A.G., & Acheson, D.W. 2006. Diarrhea in American infants and young children in the community setting: incidence, clinical presentation and microbiology. *Pediatr.Infect.Dis.J.*, 25, (1) 2-7

von Eichel-Streiber, C., Zec-Pirnat, I., Grabnar, M., & Rupnik, M. 1999. A nonsense mutation abrogates production of a functional enterotoxin A in *Clostridium difficile* toxinotype VIII strains of serogroups F and X. *FEMS Microbiol.Lett.*, 178, (1) 163-168

Vora, P., Youdim, A., Thomas, L.S., Fukata, M., Tesfay, S.Y., Lukasek, K., Michelsen, K.S., Wada, A., Hirayama, T., Arditi, M., & Abreu, M.T. 2004. Beta-defensin-2 expression is regulated by TLR signaling in intestinal epithelial cells. *J.Immunol.*, 173, (9) 5398-5405

Voth, D.E. & Ballard, J.D. 2005. *Clostridium difficile* toxins: mechanism of action and role in disease. *Clin.Microbiol.Rev.*, 18, (2) 247-263

Waligora, A.J., Hennequin, C., Mullany, P., Bourlioux, P., Collignon, A., & Karjalainen, T. 2001. Characterization of a cell surface protein of *Clostridium difficile* with adhesive properties. *Infect.Immun.*, 69, (4) 2144-2153

Wanahita, A., Davis, B., Hamill, R.J., Goldsmith, E.A., Rodgers, J.R., Cook, R.G., Lamphear, J.G., & Musher, D.M. 2006. *Clostridium difficile* lacks detectable superantigen activity. *FEMS Immunol.Med.Microbiol.*, 47, (2) 275-277

Warny, M., Vaerman, J.P., Avesani, V., & Delmee, M. 1994. Human antibody response to *Clostridium difficile* toxin A in relation to clinical course of infection. *Infect.Immun.*, 62, (2) 384-389

Warny, M., Keates, A.C., Keates, S., Castagliuolo, I., Zacks, J.K., Aboudola, S., Qamar, A., Pothoulakis, C., LaMont, J.T., & Kelly, C.P. 2000. p38 MAP kinase activation by *Clostridium difficile* toxin A mediates monocyte necrosis, IL-8 production, and enteritis. *J.Clin.Invest*, 105, (8) 1147-1156

Warny, M., Pepin, J., Fang, A., Killgore, G., Thompson, A., Brazier, J., Frost, E., & McDonald, L.C. 2005. Toxin production by an emerging strain of *Clostridium difficile* associated with outbreaks of severe disease in North America and Europe. *Lancet*, 366, (9491) 1079-1084

Wegner, A. & Aktories, K. 1988. ADP-ribosylated actin caps the barbed ends of actin filaments. *J.Biol.Chem.*, 263, (27) 13739-13742

Weiner, H.L. 1994. Oral tolerance. *Proc.Natl.Acad.Sci.U.S.A*, 91, (23) 10762-10765

Weiner, H.L., da Cunha, A.P., Quintana, F., & Wu, H. 2011. Oral tolerance. *Immunol.Rev.*, 241, (1) 241-259

Wells, J.M., Rossi, O., Meijerink, M., & van, B.P. 2011. Epithelial crosstalk at the microbiota-mucosal interface. *Proc.Natl.Acad.Sci.U.S.A*, 108 Suppl 1, 4607-4614

Wilson, H.L. & O'Neill, H.C. 2003. Murine dendritic cell development: difficulties associated with subset analysis. *Immunol.Cell Biol.*, 81, (4) 239-246

Wilson, M.E. 2006. *Clostridium difficile* and childhood diarrhea: cause, consequence, or confounder. *Clin.Infect.Dis.*, 43, (7) 814-816

Wright, A., Wait, R., Begum, S., Crossett, B., Nagy, J., Brown, K., & Fairweather, N. 2005. Proteomic analysis of cell surface proteins from *Clostridium difficile*. *Proteomics.*, 5, (9) 2443-2452

Wust, J. & Hardegger, U. 1983. Transferable resistance to clindamycin, erythromycin, and tetracycline in *Clostridium difficile*. *Antimicrob.Agents Chemother.*, 23, (5) 784-786

Yeh, C.Y., Lin, C.N., Chang, C.F., Lin, C.H., Lien, H.T., Chen, J.Y., & Chia, J.S. 2008. C-terminal repeats of *Clostridium difficile* toxin A induce production of chemokine and adhesion molecules in endothelial cells and promote migration of leukocytes. *Infect.Immun.*, 76, (3) 1170-1178

Yu, H.B. & Finlay, B.B. 2008. The caspase-1 inflammasome: a pilot of innate immune responses. *Cell Host.Microbe*, 4, (3) 198-208

Zaalouk, T.K., Bajaj-Elliott, M., George, J.T., & McDonald, V. 2004. Differential regulation of beta-defensin gene expression during Cryptosporidium parvum infection. *Infect.Immun.*, 72, (5) 2772-2779

Zilberberg, M.D., Shorr, A.F., & Kollef, M.H. 2008. Increase in *Clostridium difficile*-related hospitalizations among infants in the United States, 2000-2005. *Pediatr.Infect.Dis.J.*, 27, (12) 1111-1113